Optimisation of expression of recombinant puroindolines and analysis of protein-protein interactions *in planta*

Azadeh Niknejad

This thesis is presented for the degree of
Doctor of Philosophy
June 2014

Department of Chemistry and Biotechnology
Faculty of Science, Engineering and Technology
Swinburne University of Technology
Melbourne, Australia

Abstract

The two puroindoline proteins of wheat (*Triticum aestivum* L.), puroindoline-a (PINA) and puroindoline-b (PINB) are largely responsible for grain texture, a property important in food technology and the wheat trade. Furthermore, it has been suggested that PINs may have an *in vivo* role in seed pathogen defence and antimicrobial properties, which make them very attractive as antimicrobial agents for novel medical, pharmaceutical and food-industry applications. Soft grain texture in wheat grains depends on the presence of both PIN proteins in their wild type and functional form. Variations in either or both genes, or lack of expression of either gene, result in a hard grain texture. Currently, the biochemical basis of the role of PIN proteins in endosperm texture as well as in antimicrobial functions remains unclear. Plant expression systems are being developed to produce recombinant PINA and PINB proteins, with the aim to assess their structure and function. For therapeutic use, production and purification of high quality PIN proteins is important. One aspect of this study focussed on the rapid transient expression of PINs for better yield using the deconstructed tobacco mosaic virus-based 'magnICON®' plant expression system. This system was used to test the subcellular localisation of PINs in different compartments of *Nicotiana benthamiana* cells (cytosol, chloroplast, apoplast and endoplasmic reticulum). The results indicated a profound impact of the cellular compartment on the yield and stability of the PIN proteins. The presence of recombinant PINA and PINB was confirmed using western blot and ELISA analyses. Maximum yields of His-tagged recombinant PINA and PINB occurred when proteins were targeted to the chloroplast. Each PIN protein was shown to occur in both monomeric and oligomeric forms, which addresses some of the observations in the literature related to their functionality in determining wheat grain texture. Affinity purification systems using His-tag and hydrophobic interactions were used to purify the recombinant PINs. The purified proteins exhibited antibacterial and antifungal activities, suggesting they were correctly folded. There is evidence that PINs may interact co-operatively or interdependently to confer the soft grain texture and influence in pathogen protection. Therefore, as a second major focus of this work, interactions between PINs were investigated using the Bimolecular Fluorescence Complementation (BiFC) system in a plant system. Results based on the fluorescence intensity obtained and confirmed *in vivo* interactions between PINA and PINB and also between PINB and PINB *in planta*. In order to investigate the regions involved in the

protein-protein interactions of PINs, clones constructed previously containing deletion of the tryptophan-rich domain (TRD) in PINA and the hydrophobic domain (HD) in both PINs were used for cloning into BiFC vectors. The result indicated that no interaction occurred between the mutant PIN proteins. The finding shows that both the TRD and HD regions may have roles in the interactions of PIN proteins, but may contribute in different ways to their folding and stability.

The work has led to successful expression, purification and characterisation methodology for obtaining PINs of appropriate quality essential for potential infection control in diverse areas. Additionally, the work also confirmed their *in planta* interactions. To our knowledge, this is the first report of functional PINs produced in *N. benthamiana* based on transient expression, and it provides a starting point for investigating a potential role for PINs on grain texture and antimicrobial abilities.

Acknowledgments

All praises to Almighty God for the strength and His blessing in completing this work.

I would like to thank my principal supervisor, Professor Mrinal Bhave for giving me the great opportunity of performing this research and for her support, guidance and patience throughout this project. Thanks particularly for all the time that she has put on the preparation of this thesis. I would also like to express my deepest appreciation and gratitude to Dr Diane Webster for acting as a supervisor and being helpful and supportive from the first day I stepped into the Plant Biotechnology laboratory in Monash University for three years. Thanks for encouragement and generosity of time in all meetings during this study.

I am also grateful to Swinburne University of Technology for awarding me the SUPRA scholarship.

Thanks to Professor Michael Gilding and Dr Elena Verezub for advice and help and Ms Angela McKellar in Swinburne University. I would also like to thank Professor David Smyth and Mr Tezz Quon in Monash University for providing plasmid pNBV and pMLBART. Thanks to Associate Professor Sureshkumar Balasubramanian and his group for always welcoming me in SKB lab in Monash University.

Thank you to all my lab mates and friends in Monash University; Rasika, Kartika, Claire, Robert, Indramohan, David, Vincent and Victor.

Thank you to past and present PhD students in Swinburne University; Dr Peter Gollan and Dr Rebecca Alfred for always sharing their knowledge. Many thanks to Dr Abirami Ramalingam, Dr Runyararo Hove, Dr Shanthi Joseph and Dr Kaylass Poorun for all their help, encouragement and friendship. Thank you to my other friends; Bita, Narges, Farnaz, Saifone, Atul, Yen, Guri, Nadin, Rasika, Jafar, June, Elisa, Dhivya, Snehal, Rashida and Chris.

Dedicated to

The memory of my dear father; Rasoul

and

My beloved mother; Zahra

For her loving support and always believing in me

Declaration

I, **Azadeh Niknejad**, declare that the PhD thesis entitled 'Optimisation of expression of recombinant puroindolines and analysis of protein-protein interactions *in planta*' is no more than 100,000 words in length, exclusive of tables, figures, appendices, references and footnotes. This thesis contains no material that has been submitted previously, in whole or in part, for the award of any other academic degree or diploma, and has not been previously published by another person. Except where otherwise indicated, this thesis is my own work.

Azadeh Niknejad

2014

Abbreviations

BDT	Big Dye Terminator
BiFC	Bimolecular Fluorescence Complementation
bp	Base pair
BSA	Bovine Serum Albumin
C-terminal	Carboxyl terminal (of a protein)
Cys (or C)	Cysteine
DNA	Deoxyribonucleic acid
dNTP	Deoxyribonucleotide (A, T, G or C)
dpi	Days post infiltration
EDTA	Ethylenediaminetetraacetic acid
ELISA	Enzyme linked immunosorbent assay
ER	Endoplasmic Reticulum
g	Centrifuge force
gDNA	Genomic DNA
GFP	Green Fluorescent Protein
GSP-1	Grain Softness Protein-1 (a component of friabilin)
His (or H)	Histidine
IPTG	Isopropyl β-D-1-thiogalactopyranoside
Kb	Kilobase pairs; 1kb= 1000 bp
kDa	KiloDalton
LB	Luria Bertani broth
MALDI-TOF	Matrix-assisted laser desorption ionisation-time of flight
mg	Milligram
mL	Millilitre
MW	Molecular Weight
N-terminal	Amino terminal (of a protein)
OD	Optical Density
ORF	Open Reading Frame
PCR	Polymerase Chain Reaction
Pin	*Puroindoline* genes
Pina	*Puroindoline-a* gene
Pinb	*Puroindoline-b* gene

PIN(s)	Puroindoline protein(s)
PINA	Puroindoline-a protein (wild type)
PINB	Puroindoline-b protein (wild type)
rPINA	Recombinant PINA
rPINB	Recombinant PINB
PPI	Protein-Protein Interaction
RBCs	Red Blood Cells
rpm	Revolutions per minute
SDM	Site-directed mutagenesis
SDS-PAGE	Sodium dodecyl sulphate-poly acrylamide gel electrophoresis
TAE	Tris acetate ethlenediaminetetraacetic acid buffer
TBSV	Tomato Bushy Stunt Virus
Trp (or W)	Tryptophan
TRD	Tryptophan-rich domain
TSP	Total Soluble Protein
UV	Ultra Violet
X-gal	5-bromo-4-chloro-3-indolyl-b-D-galactopyranoside
YFP	Yellow Fluorescent Protein
YC	C-terminal fragment of YFP
YN	N-terminal fragment of YFP
°C	Degree Celsius

List of databases/softwares

ApE	A plasmid Editor
BioEdit	Biological sequence alignment editor
BLAST	Basic Local Alignment Search Tool
COTH	Threading-recombination approach
ExPASY	Expert Protein Analysis System
I-TASSER	Iterative Threading Assembly Refinement
NCBI	National Center for Biotechnology Information
PyMOL	Python-enhanced molecular graphics tool
WoLF PSORT	PSORT II program for protein subcellular location prediction

Table of contents

List of Figures

List of Tables

CHAPTER 1

General introduction and literature review

1. General introduction

The information in this chapter provides an extensive review of the literature on *puroindoline* (*Pin*) genes and puroindoline (PIN) proteins, their specific function in controlling grain texture, as well as their possible biological roles as antimicrobial proteins in wheat seeds.

Following the general overview, the introduction also highlights the importance of:

- Understanding the roles of PIN proteins in lipid binding and impact on grain hardness
- Identifying further PINs or PIN-based peptide structures
- Plants as an alternative system for the expression of proteins in order to study the structure and function of antimicrobial proteins and peptides

1.1 Introduction to wheat

Wheat (*Triticum aestivum* L.) is one of the most widely consumed grain crops in the world. It is no doubt one of the most important cereal crops for humankind, with unique end-use qualities that allow it to be processed into a range of flour-based foods such as bread, biscuit and pastry products; additionally, it also has a role in the production of starch and gluten (Li et al., 2012; Shewry, 2009). Wheat in the form of bread provides essential nutrients like fibre, carbohydrates, protein, B vitamins, iron, calcium, phosphorus, zinc, potassium and magnesium (Painter et al., 2002; Pena et al., 2002; Wrigley, 2009). Wheat ranks third after maize (corn) and rice in terms of worldwide production (Shewry, 2013).

Originating in the Middle East region about 10,000 years ago, wheat is the largest grain crop based on area of cultivation (Dubcovsky and Dvorak, 2007; Matsuoka 2011; Wrigley, 2009). Among agricultural crops, wheat is well adapted to a wide range of soils, climates, and environmental conditions, unlike rice and maize that prefer tropical environments (Gill et al., 2004). Durum wheat (*Triticum turgidum* L. *var. durum)* is more adapted to the dry Mediterranean climate than bread wheat (*Triticum aestivum* L.) (Shewry, 2009). Wheat varieties are categorised into six major classes based on planting and harvesting dates, as well as hardness, shape and the colour of the kernels: (1) hard red spring; (2) hard red winter; (3) soft red winter; (4) hard white wheat; (5) soft white wheat; (6) durum (Rochelle, 2001).

1.1.1 Evolution of wheat species

A detailed understanding for the origin of cultivated wheat has extended our knowledge for improving it genetically. Wheat (genus *Triticum*) belongs to the Poaceae (or Gramineae) family. The genus has three subclasses of ploidy: diploid (2n=2x=14), tetraploid (2n=4x=28) and hexaploid (2n=6x=42) (Eckardt, 2001; Feldman, 1995; Feldman, 2001). Three genomes, designated A, B and D, are involved in the formation of the polyploidy series with seven pairs of chromosomes (Feldmann, 2001). Bread wheat (*Triticum aestivum*), the most widely cultivated wheat today, is hexaploid AABBDD and its origin has most likely occurred through one or more rare hybridisation processes. Wild einkorn *T. urartu* (AA) crossed through natural hybridisation with *Aegilops speltoides* (BB) to produce wild emmer *T. turgidum* L. ssp. *durum* (AABB) (Chantret et al., 2005; Matsuoka, 2011). *T. urartu* is the diploid progenitor of the A genome in tetraploid and hexaploid wheats (Haider, 2013). Another hybridization between the tetraploid *T. turgidum* L. ssp. *dicoccum* (AABB) and the diploid donor of the D genome, *Ae. tauschii* (2n =14, DD) restored the *Hardness* (*Ha*) locus in *T. aestivum* (Chantret et al., 2005; Wrigley, 2009). The D genome is present in *T. aestivum* but not in *T. turgidum* L. ssp. *durum*. Probably as a result of transposable element insertions and two large deletions caused by illegitimate recombination, the *Ha* locus in the D genome of hexaploid wheat (*T. aestivum*) is 29 kb smaller than in the D genome of diploid *Ae. tauschii* (Chantret et al., 2005; Haider, 2013). Numerous studies have attempted and published reports about the origin of the B genome in cultivated wheat; however, the B genome donor remains uncertain. It is believed that the B genome is closely related to the S genome from the *Sitopsis* group of the genus *Ae. speltoides* (Feldman, 2001; Haider, 2013). The formation of tetraploid and hexaploid wheat is summarised in Figure 1.1.

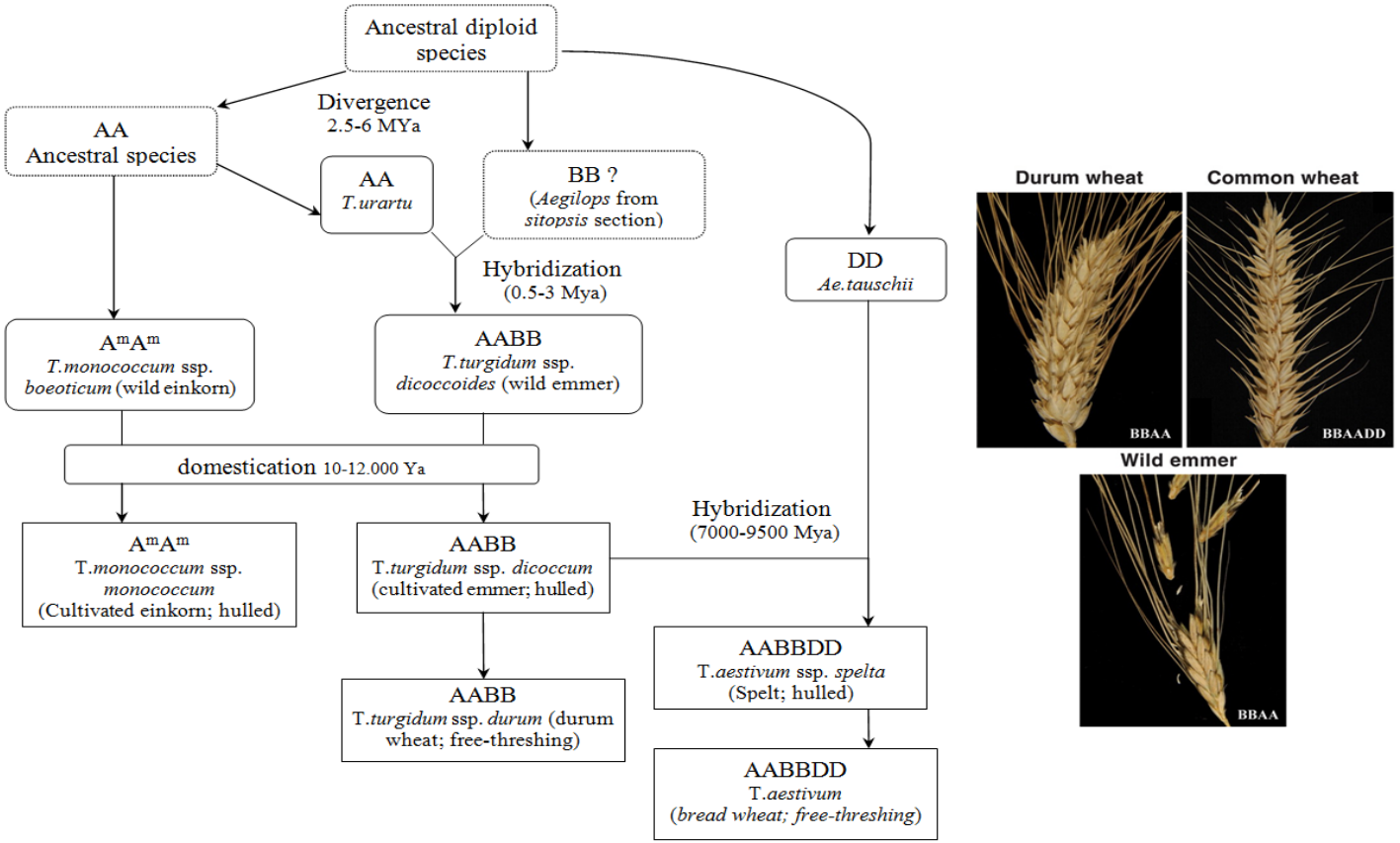

Figure 1.1 Schematic representation of the evolutionary history of wheat species (*Triticum* and *Aegilops*).
Source: modified from Chantret et al. (2005) and Dubcovsky and Dvorak, (2007).

1.1.2 Structure of the wheat grain

Wheat kernels consist of three distinct layers: the endosperm, germ and bran (Shewry, 2013) (Figure 1.2). The major part of wheat grain is endosperm and approximately three-quarters of the endosperm includes starch, which has an important role in determining the end-use of wheat grain. Differences in the endosperm texture of wheat are an extremely important characteristic that have an effect on flour quality and yield for human consumption. White flour contains the starchy endosperm, which contains a high proportion of starch and gluten (Delcour and Hoseney, 2010; Turnbull and Rahman, 2002).

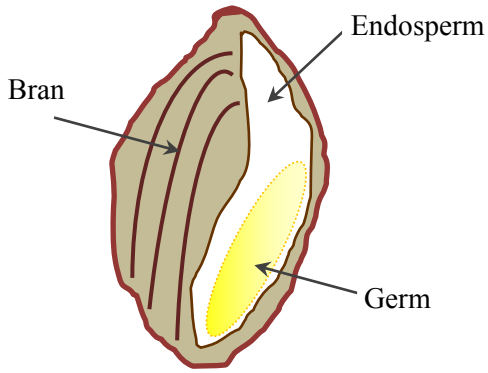

Figure 1.2 Composition of the wheat kernels: the endosperm, germ and bran.

The germ is the embryo of the kernel and comprises only about 2.5% of the weight. Wheat germ contains protein (~25%) and lipids (~8%), and is also an important source of vitamins B and E (Cornell, 2003; Slavin, 2003). The bran layers surrounding the endosperm are rich in vitamins and minerals and contains high-quality protein (19%), as well as large amounts of insoluble dietary fibre (Wrigley et al., 2004). The bran layer accounts for approximately 14.5% of the weight of the kernel. The aleurone layer is the outermost layer of the endosperm and is located between the bran layer and endosperm. The bran and aleurone layers play a role in protecting the embryo and nutrient-rich endosperm against stress and pathogens (Gillies et al., 2012; Jerkovic et al., 2010).

1.2 Grain texture in wheat

Wheat hardness is a major quality trait and is defined as the force needed to crush the kernels, which is required for the marketing and technological utilisation of wheat (Morris, 2002), and also relates to the degree of hardness or softness of the grain. Grain hardness is an essential factor, as it impacts milling and baking in the flour industry (Bettge et al., 1995). Overall flour particle size, shape and flour density, starch damage, water adsorption and milling yield are physical properties affected by hardness (Martin et al., 2001). Grain hardness defines the quantitative variations within and across three qualitative classes: 'soft' hexaploid wheats, 'hard' hexaploid wheats and the 'very hard' durum wheats. Moreover based on intermediate hardness, wheat has been classified as 'medium hard' and 'medium soft' (Morris, 2002). Bread wheat endosperm texture varies from extremely soft to hard, while durum wheat has the hardest kernels of all wheat species. In comparison with hard wheat, soft wheat generally yields flour with a smaller average particle size and lower levels of damaged starch. Differences in endosperm texture between hard and soft wheats are the most important factors for functionality and marketing of wheat (Mikulikova, 2007). Generally, different types of wheat are required by breeders, millers and bakers. Soft wheat flour with low protein content is used to make cakes and pastries while hard wheat flour is suited for bread in addition to other yeast raised products. Durum wheat with unique properties like high protein content and gluten strength is used for pasta products and semolina (Douliez et al., 2000; Morris, 2002).

Wheat endosperm hardness is controlled by genetic factors and biochemical factors such as seed moisture, lipid and pentosan content. However, environmental conditions also affect endosperm hardness (Konopka et al., 2005; Turnbull and Rahman et al., 2002). Grain hardness has been linked to one major and several minor loci (Mattern et al., 1973; Symes, 1965, 1969). The major locus was named *Hardness* (*Ha*) and shown to be located at the distal end of the short arm of chromosome 5D (Doekes and Belderok, 1976; Law et al., 1978; Mattern et al., 1973). Hard wheat has shown stronger adhesion between starch granules and storage protein compared to soft wheat (Simmonds et al., 1973). Studies conducted using scanning electron microscopy have also revealed that more gluten adheres to the surface of starch granules isolated from

hard wheat than to the surface isolated from soft wheat (Barlow et al., 1973; Hoseney and Seib, 1973). It has been suggested that the degree of adhesion between starch and gluten proteins is one of the essential factors for differences in endosperm hardness between hard and soft wheat (Barlow et al., 1973; Hoseney and Seib, 1973; Simmonds et al., 1973; Pauly et al., 2013).

1.2.1 Friabilin

Endosperm hardness is related to the occurrence of a 15 kDa protein complex called 'friabilin' on the surface of water-washed starch granules (Greenwell and Schofield, 1986). The protein was named 'friabilin' as it was observed that soft wheat was more friable than hard wheat, while durum wheat lacked this protein (Morrison et al., 1992; Morris, 2002). The amounts of starch granule associated protein from water washed starch differ in soft and hard wheats (Jolly, 1993; Jolly et al., 1996; Rahman et al., 1994). The occurrence of friabilin on the surface of water-washed starch granules appears to be related to the level of bound polar lipids (glycolipids and phospholipids). Polar lipids are present in high levels on the starch granule surface in soft wheat, but in low levels in hard wheat (Capparelli et al., 2003; Greenblatt et al., 1995). Furthermore, Greenblatt et al. (1995) showed that friabilin can be extracted with a propan-2-ol/water (90:10) mixture, which is effective for removing starch-bound polar lipids. However, with the same buffer, when no lipids are removed earlier, only a very small amount of friabilin can be extracted. Friabilin components associated with starch granules through polar lipids were shown to be involved in ionic and hydrophobic interactions (Greenblatt et al., 1995). Friabilin protein analysis revealed that it is likely a mixture of several polypeptides (Blochet et al., 1993; Morris et al., 1994; Oda and Schofield, 1997). The two major friabilin components are puroindoline-a (PINA) and puroindoline-b (PINB) (Gautier et al., 1994). Grain Softness Protein-1 (GSP-1) and α-amylase inhibitors (Rahman et al., 1994) are the minor components (Blochet et al., 1993; Morris et al 1994). The GSP-1 protein (Figure 1.3) with approximately 164 amino acids long exhibits 40% identity and 60% similarity to the PINs with 10 cysteine backbone and TRD with two tryptophan residues (Bhave and Morris, 2008a; Rahman et al., 1994). Elmorjani et al. (2013) have shown that the GSP-1 protein may undergo different proteolytic cleavages in the N and C-terminal regions of the pre-pro-protein.

Figure 1.3 GSP-1 putative protein sequence from common wheat.
(*T. aestivum*) GenBank accession number: S48186

1.3 *Puroindoline* genes and grain texture

The *Puroindoline* (*Pin*) genes *Pina-D1* and *Pinb-D1*, responsible for encoding the wild type puroindoline proteins, are part of the *Ha* locus on the short arm of chromosome 5D in common wheat (Gautier et al., 1994; Ragupathy and Cloutier, 2008). However, during evolution and after polyploidisation of cultivated polyploid durum wheat, *Pin* genes were deleted from chromosomes 5A and 5B. The *Pin* (*Pina-D1*, *Pinb-D1*) and *Gsp-1* genes are located in a 60 kbp DNA fragment of the *Ha* locus of *Ae. tauschii,* which is the D-genome donor of *T. aestivum* (Pauly et al., 2013). *Pin* genes are located only on the D-genome, while *GSP-1* is present on all three wheat genomes (A, B and D) in diploid, tetraploid and hexaploid wheat (Chantret et al., 2004, Chantret et al., 2005; Morris 2002; Rahman et al., 1994). Without the D genome and thus both *Pin* genes and also PIN proteins, resulting in the very hard durum wheats (Chantret et al., 2005).

1.3.1 Mutations, duplications and deletions in *Pin* genes

The *Puroindoline* genes (*Pina-D1*, *Pinb-D1*) contain 447 base pairs (bp) without introns and both genes are 70.2% identical in the coding regions, but only 53% identical in the 3'-untranslated region (Gautier et al., 1994). The presence of both *Pina-D1* and *Pinb-D1* genes in functional forms results in soft endosperm texture; however, mutations in, or absence of either genes result in low levels of PIN protein(s) and hard endosperm (Giroux and Morris 1998, Wall et al, 2010). The most common form of mutations are single nucleotide polymorphisms (SNPs), which may result in an amino acid substitution, or replacement with a stop codon, or a frame shift caused by a single base

insertion or deletion (INDELs). The first report to show mutations in both *Pin* genes in common wheats was by Chang et al. (2006). The mutations identified to date in *Pina-D1a* and *Pinb-D1a* genes are listed in Table 1.1 (reviewed by Bhave and Morris, 2008a; Nadolska-Orczyk et al., 2009).

1.3.2 Point mutations, duplications and deletions in *Pina-D1* gene

The most common hardness-associated mutation to be reported in *Pina-D1* was a null mutation (*Pina-D1b*) and has a harder texture than other prevalent hardness alleles (Giroux and Morris 1998; Morris, 2002. This results in the absence of *Pina* transcripts and a lack of the PINA proteins in the kernel (Giroux and Morris 1998; Pauly et al., 2013). Point mutations or SNPs have been reported in *Pina-D1* genes (Chen et al., 2006; Gazza et al., 2005; Massa et al., 2004). Chen et al. (2006) described different SNPs in the mature protein sequence, which are: a) premature stop codon replacing tryptophan at position 43 (*Pina-D1n*), b) proline to serine at position 35 (Pro35Ser) (*Pina-D1m*). Mutations of serine in *Pina-D1m* may affect the lipid-binding ability of the TRD due to the location of Ser in a loop between the first helix and the TRD (Bhave and Morris, 2008a). Moreover, in Asian wheat cultivars, two types of deletion mutation in *Pina-D1* which results in PINA-null products have been reported. The 4.4kb deletion mutant was designated *Pina-D1r* and the 10.5kb deletion was designated *Pina-D1s* (Ikeda et al., 2010).

1.3.3 Point mutations, duplications and deletions in *Pinb-D1* gene

Giroux and Morris (1997) were the first to report a single nucleotide change in *Pinb-D1*, leading to the glycine-to-serine change at position 46 in PINB (G46S; *Pinb-D1b*), which was associated with the hard texture in common wheat. This mutation has been discovered widely in wheats around the world (Chen et al., 2006; Lillemo et al., 2006; Pickering and Bhave, 2007; Tanaka et al. 2007; Xia et al., 2005). Wheats possessing *Pinb-D1b* alleles were slightly softer than wheats with the *Pina-D1b*/*Pinb-D1a* (Morris, 2002). It has been suggested that this amino acid change affects lipid binding and starch granule interaction, in addition to altering the tertiary structure of PINB at the TRD (Bhave and Morris, 2008a). The point mutation of *Pinb-D1c* that causes a leucine-to-proline change at position 60 (Leu60Pro) was first reported by Lillemo and Morris,

(2000). Among the point mutations of *Pinb-D1,* mutations frequently occur at position 44 of the mature protein sequence, e.g., a tryptophan to arginine change at position 44 (Trp44Arg; *Pinb-D1d*) (Lillemo and Morris, 2000), tryptophan to early stop codon at position 44 (Trp44stop codon; *Pinb-D1f*) (Morris et al., 2001), as well as a *Pinb-D1q* (Trp44Leu) (Chen et al., 2005).

1.3.4 *Pinb-2* genes

The six alleles of *Pinb-2* gene have been reported and designated *Pinb-2v1* to *Pinb-2v6* (Chen et al., 2010a; Chen et al., 2010c; Ramalingam et al., 2012; Wilkinson et al., 2008), which provide a potential new resource for minor variation in grain texture. Mapping of the *Pinb-2* genes in wheat reported *Pinb-2v1* to be located on chromosome 7D in bread wheat and absent in durum wheat, *Pinb-2v2* and *Pinb-2v3* are located on chromosome 7B and *Pinb-2v4* is located on chromosome 7A (Chen et al., 2010a; Chen et al., 2010c). The reported transcript levels of *Pinb-2* variants suggest they are only expressed at 10% the levels of the *Pinb-D1* genes in common wheat (Wilkinson et al., 2008). Additionally, RNA sequencing has shown that relative to *Pinb, Pinb-2v1* expression was at 1%, and *Pinb-2v2* and *Pinb-2v3* was at ~8% of the expression levels detected, while *Pinb-2v4* was undetectable (Giroux et al., 2013). *Pinb-2* genes appear to have a greater impact on the grain texture of soft wheat than hard wheat and are associated with increased grain texture in soft wheats (Chen et al., 2010b). Moreover, the putative TRD of the PINB-2v1 proteins with two tryptophan residues (Figure 1.4) has shown antimicrobial activity *in vitro* against a number of bacteria and fungi (Ramalingam et al., 2012).

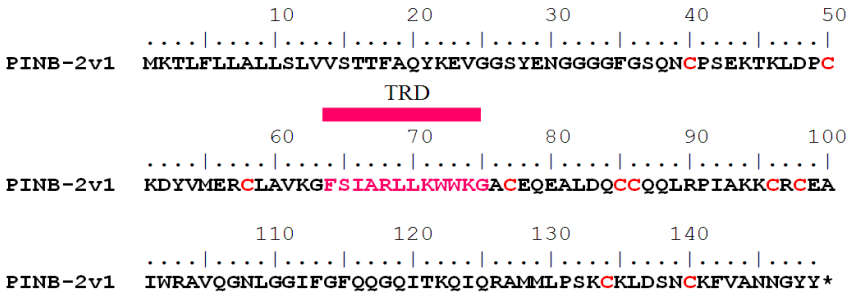

Figure 1.4 PINB-2v1 putative protein sequence.
(*T. aestivum*) GenBank accession number: ADA7764

Table 1.1 The mutations identified in *Pina-D1a* and *Pinb-D1a* alleles in common wheat (*T. aestivum*)

PIN allele	Phenotype	PIN protein	Change to protein sequence*	Reference
Pina-D1a	Soft	Wild-type	-	Gautier et al. (1994)
Pina-D1b	Hard	PINA null	Gene deletion	Giroux and Morris (1998)
Pina-D1f	Hard	PINA	Three SNPs. Arg58Gln and NS Ala19+Leu52	Massa et al. (2004)
Pina-D1k	Hard	PINA null	Gene deletion (Associated with *Pinb* deletion)	Tranquilli et al. (2002) Ikeda et al. (2005)
Pina-D1l	Hard	PINA truncated	Single base deletion, frame shift Gln61Lys, then a premature stop codon at pos120	Gazza et al. (2005)
Pina-D1m	Hard	PINA	Single SNP. Pro35Ser	Chen et al. (2006)
Pina-D1n	Hard	PINA	Single SNP. Trp43stop, premature stop codon	Chen et al. (2006)
Pina-D1p	Hard	PINA truncated	Single base deletion, frame shift Cys110Ala, then premature stop codon	Chang et al. unpublished
Pina-D1q	Hard	PINA	Two SNP. Asn111Lys+lle112Leu	Chang et al. (2006)
Pina-D1r	Hard	PINA null	Gene deletion	Ikeda et al. (2010)
Pina-D1s	Hard	PINA null	Gene deletion	Ikeda et al. (2010)
Pina-D1t	Hard	PIN A truncated	Single SNP. Trp41stop, premature stop codon	Ramalingam et al. (2012)
Pinb-D1a	Soft	Wild-type	-	Gautier et al. (1994)
Pinb-D1b	Hard	PINB	Single SNP. Gly46Ser	Giroux and Morris (1997)
Pinb-D1c	Hard	PINB	Single SNP. Leu60Pro	Lillemo and Morris (2000)
Pinb-D1d	Hard	PINB	Single SNP. Trp44Arg	Lillemo and Morris (2000)
Pinb-D1e	Hard	PINB truncated	Single SNP.Trp39Stop,premature stop codon	Morris et al. (2001)
Pinb-D1f	Hard	PINB truncated	Single SNP.Trp44stop,premature stop codon	Morris et al. (2001)
Pinb-D1g	Hard	PINB truncated	Single SNP.Cys56stop,premature stop codon	Morris et al. (2001)
Pinb-D1l	Hard	PINB	Single SNP.Lys45Glu	Pan et al. (2004)
Pinb-D1p	Hard	PINB truncated	Single base deletion, frame shift Lys42Asn, then a premature stop at pos60	Chang et al. (2006)
Pinb-D1q	Hard	PINB truncated	Single SNP.Trp44Leu	Ikeda et al. (2005) Xia et al. (2005) Chen et al. (2005)
Pinb-D1r	Hard	PINB truncated	Single base deletion, frame shift Glu14Gly, then a premature stop at pos48	Ram et al. (2005)
Pinb-D1s	Hard	PINB truncated	Single base deletion and SNP, frame shift Glu14Gly, then a premature stop at pos48	Ram et al. (2005)
Pinb-D1t	Hard	PINB	Single SNP. Gly47Arg	Chen et al. (2006)
Pinb-D1u	Hard	PINB truncated	Single base deletion, frame shift Glu14Ser, then a premature stop at pos18	Chen et al. (2007)
Pinb-D1v	Hard	PINB	Two SNPs. Ala8Thr+Leu9lle	Chang et al. (2006)
Pinb-D1w	Hard	PINB	Single SNP.Ser115lle	Chang et al. (2006)
Pinb-D1aa	Hard	PINB truncated	Single SNP. Single based deletion, frame shift Lys42Asn, a premature stop codon	Li et al. (2008a)
Pinb-D1ab	Hard	PINB truncated	Single SNP. Gln99stop, premature stop codon	Tanaka et al. (2008)

*SNP: Single nucleotide polymorphism

*NS: Non-synonymous mutation, a change in the nucleotide sequence that does not lead to a change in the amino acid sequence

1.3.5 *Pin*-like genes in related species

Genes encoding puroindoline-like proteins do not occur in rice, maize or sorghum, but are present in cereals related to wheat such as rye, barley and oat (Gautier et al., 2000; Pauly et al., 2013). The PIN homologues in rye (*Secale cereal* L.) and triticale cultivar are named secaloindoline a (SINA) and secaloindoline b (SINB) (Li et al., 2006; Simeone and Lafiandra, 2005) (Figure 1.5). Until now, no relationship between secaloindoline alleles and grain hardness has been reported in rye since rye cultivars have generally soft endosperm texture with very low variation in kernel hardness (Simeone and Lafiandra, 2005). Recently, Gasparis et al. (2013) reported RNAi-based silencing of *Sin* genes resulted in a significant decrease in the level of transcripts and the yield of both secaloindoline proteins but did not affect grain hardness in triticale cultivar Wanad. Furthermore, barley (*Hordeum vulgare* L.) contains the PIN homologues hordoindoline a (HINA) and hordoindoline b (HINB) and have been mapped on the short arm of chromosome 5H (Beecher et al., 2002b). The *Ha* locus in barley has been shown to be associated with variations in endosperm texture (Beecher et al., 2002b). In addition, PIN homologues have been identified in oat (*Avena sativa* L.), designated avenoindoline a and avenoindoline b (Gautier et al., 2000). Immunolocalisation studies using Durotest antifriabilin antibody have detected tryptophanins (TRPs) proteins in oat seed associated with the surface of starch granules (Mohammadi et al., 2007).

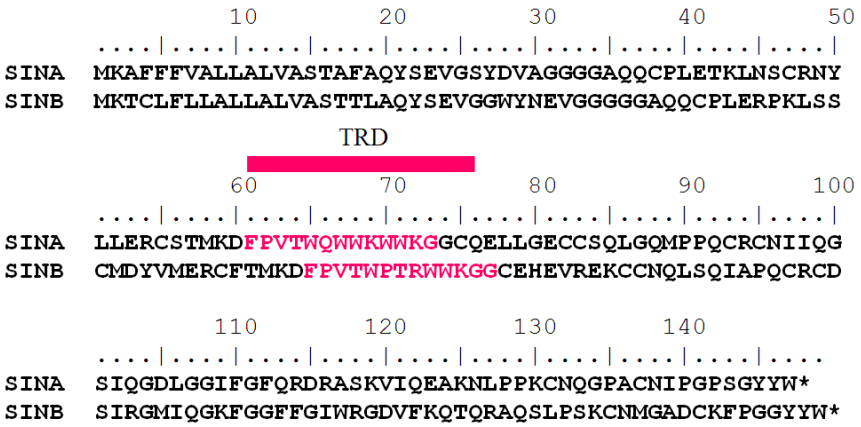

Figure 1.5 Alignment of amino acid sequences of SINA and SINB in triticale.
GenBank accession numbers: AGO65289.1 and AGO65290.1 for SINA and SINB respectively

1.4 Biochemical properties and structure of PIN proteins

N-terminal sequencing identified the basic cysteine-rich proteins Puroindoline-a (PINA) and Puroindoline-b (PINB) as the major components of friabilin (Blochet et al., 1993). The name 'puroindoline' is derived from the Greek word 'puros' for wheat, and 'indoline', referring to the indoline ring of the tryptophan-rich domain (Gautier et al. 1994). The PINs and other proteins (for instance storage proteins and the enzyme granule-bound starch synthase I) with affinity for defatted starch granules were also isolated from wheat endosperm using the nonionic detergent Triton X-114 (Blochet et al., 1993; Bako et al., 2007).

PINA and PINB contain tryptophan residues in the unique tryptophan-rich domain (TRD) and a highly conserved cysteine-rich backbone of 10 cysteine residues (Blochet et al., 1993). The TRD of PINA consists of five tryptophan residues (WRWWKWWK; position without the putative signal paptide: 38 to 45), while in PINB, it consists of three (WPTKWWK; position without the putative signal paptide: 39 to 45) (Blochet et al., 1993; Gautier et al., 1994). The full length PIN proteins consist of 148 amino acids with a similar molecular mass of 13 kDa (Gautier et al., 1994). PIN proteins are highly basic, with a calculated isoelectric point (pI) of 10.5 for PINA and 10.7 for PINB and show 55% similarity at the amino acid level (Gautier et al., 1994). Both PINs are synthesized as pre-pro-proteins containing an N-terminal signal peptide, which comprises the first 28 amino acid residues for PINA and the first 29 amino acid residues for PINB (Gautier et al., 1994) (Figure 1.6). These N-terminal signal peptides may have a role in intracellular targeting (Bhave and Morris, 2008a; Gautier et al., 1994). C-terminal processing has also been suggested for both PINs and can result from slightly different post-translation processing pathways (Day et al., 2006). Raman spectroscopy studies have shown that PINA and PINB have a similar secondary structure at pH 7. Both PINs consist of approximately 30% α-helices, 30% ß-sheets and 40% unordered structures (Le Bihan et al., 1996). Far-UV circular dichroism (CD) measurements have confirmed similarity between PINs in secondary structure (Kooijman et al., 1997).

The 10 cysteine residues form five intramolecular disulphide bonds. Disulphide bonds are essential for stabilizing the α-helical structure and to maintain the native structure and solubility of PINA and PINB (Le Bihan et al., 1996). Eight of the cysteines form a particular pattern known as the "eight cysteine motif" (8CM), which appears widely among plant proteins and has a similar tertiary structure, including four α-helical structures (Figure 1.6) and variable loops (Pauly et al., 2013). Proteins containing this motif show a wide range of functions in storage, enzyme inhibition, lipid transfer, plant defence and cell wall structure (José-Estanyol et al., 2004). The cysteine residues may have an important role in forming a network of disulphide bridges, which are important for the maintenance of the three-dimensional (3D) structure of the molecule, together with the central helical core (José-Estanyol et al., 2004). The TRD is located between two additional cysteine residues. Kooijman et al. (1997) suggested that the TRD of PINs has a role in the stability of the structure. The TRD confers hydrophobicity for strong affinity in PIN interactions with lipids (Douliez et al., 2000; Kooijman et al., 1997).

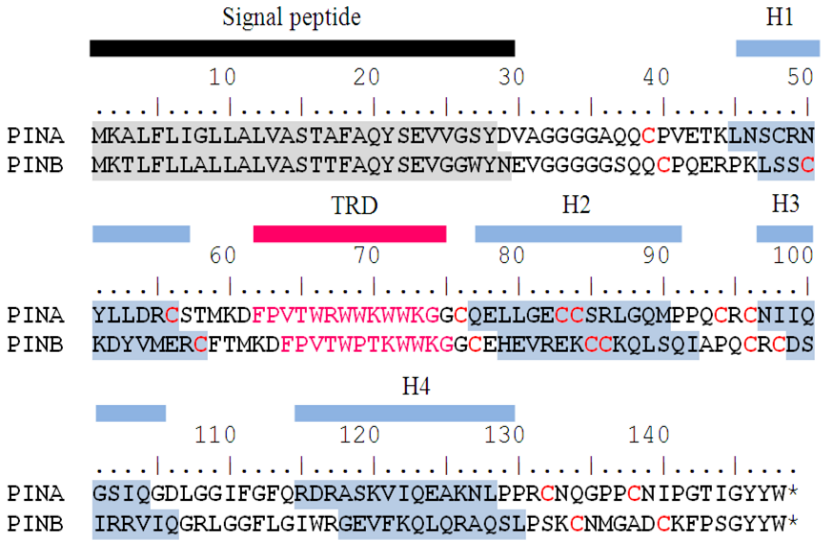

Figure 1.6 Alignment of the primary structure of PINA and PINB.
Signal peptide in both PINs is highlighted before potential N-terminal cleavage sites (after the 28th residue for PINA and after the 29th residue for PINB). The 4-alpha helices are as determined by Le Bihan et al. (1996) with the following locations, respectively for PINA and PINB: residues 17-28 and 18-29 for H1, 49-62 and 50-63 for H2, 69-76 and 70-77 for H3, and 87-100 and 89-101 for H4.

The high resolution structure of PINs has some limitations due to the strong aggregative properties at high protein concentration and difficulties in obtaining a stable non-aggregated solution required for crystallisation and NMR characterisation (Clifton et al., 2011a; Marion et al., 2007). The 3D structure of PINs has not yet been determined. However, a considerable amount of literature has been published on predicted models. The first of these was based on the folding pattern of the eight-cysteine motif in nonspecific lipid transfer proteins (ns-LTP). The eight-cysteine motif, including the Cys-Cys and Cys-arginine-Cys characteristic of both PINs, is also found in nsLTPs. The similarities of the disulphide bonds support the suggestion that nsLTPs and puroindolines are related in their primary and secondary structure, and display similar folding properties (Douliez et al., 2000; Marion et al., 2007) (Figure 1.7). PINs have five disulphide bonds while ns-LTPs have four. The TRD of PINs is located in a loop between the first and second α-helix, outside the protein based on the 3D model for ns-LTP (Doulies et al., 2000; Kooijman et al., 1997; Marion et al., 1994). In addition, the variable loops connected to the α-helices are the functional regions of the eight-cysteine motif proteins (José-Estanyol et al., 2004), which seems appropriate for PINs. There is also a unique tyrosine residue (positions without the putative signal paptide: 23 and 24 for PINA and PINB respectively) in the first α-helix, which may be functionally important. Tyrosine is not bound to a negatively charged carboxylate of the protein, but is hydrogen-bonded to water molecules (Le Bihan et al., 1996).

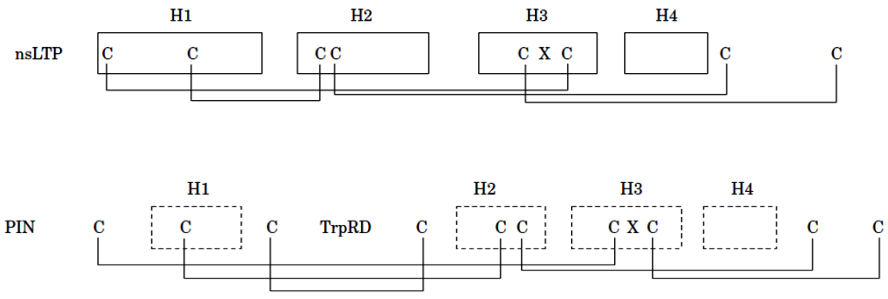

Figure 1.7 Cysteine backbone and α-helix positioning in PINs and nsLTP.
Source: Douliez et al. (2000)

Recently, a different 3D structure model of PINA using iterative threading assembly refinement (I-TASSER) has been revealed for structure prediction by Lesage et al. (2011) (Figure 1.8). The prediction result for PINA displayed the five disulphide bonds: Cys20/Cys55 and Cys56/Cys104 are connected and readily form disulphide bonds; Cys11/Cys66 and Cys68/Cys110 are positioned at close proximity (Lesage et al. 2011) and the TRD is an extension stabilised by a Cys28/Cys48 disulphide bridge in PINA and a Cys29/Cys48 disulphide bridge in PINB (Le Bihan et al., 1996). PINs have several features of membrane proteins, such as high levels of α-helices. In addition, both PIN proteins can be extracted with non-ionic detergent like TX-114; however, none of them contains a typical trans-membrane region. Moreover, after extraction in the absence of detergents, puroindolines are fairly water-soluble, and act differently from membrane proteins (Lesage et al., 2011).

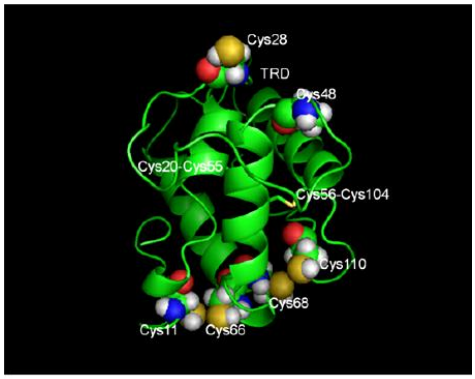

Figure 1.8 Structure prediction of PINA using I-TASSER.
Source: Lesage et al. (2011)

PINA forms aggregate under acidic and high ionic strength conditions and at low temperatures, where the TRD plays an important role in the aggregate formation (Le Bihan et al., 1996). Clifton et al. (2011a) confirmed this observation and has shown that PINA forms monodisperse prolate ellipsoidal micelles in a solution consisting of 38 PINA molecules and is stable in a wide range of pH and temperatures. Self-assembly of PINA is suggested to be driven by intermolecular hydrophobic forces between the tryptophan at the TRD. Although PINB shows more than 50% amino acid similarity with PINA, no self-assembly into micelles has been reported. This may be due to the fewer tryptophan residues in the PINB TRD, resulting in weaker intermolecular hydrophobic interactions (Clifton et al., 2011a). The structure of a PINA section, i.e.,

the peptide PuroA (FPVTWRWWKWWKG) was determined by NMR (Jing et al., 2003) (Figure 1.9) and showed that all positively charged residues are located close to the tryptophan indole rings (Jing et al., 2003). Furthermore, the 3D structure of micelle-bound PuroA shows that all positively charged residues are placed close to the tryptophan indole rings, which have a role in cation-interactions and allow PuroA to penetrate and disrupt bacterial membrane (Chan et al., 2006) (Figure 1.10).

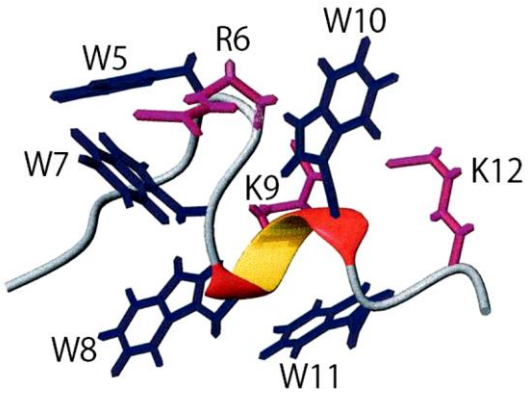

Figure 1.9 NMR solution structure of PuroA.
Source: Jing et al. (2003). 13 amino acids corresponding to the tryptophan-rich domain (TRD) of puroindoline a. tryptophan (W), arginine (R) and lysine (K) residues are numbered based on their position in the PuroA peptide.

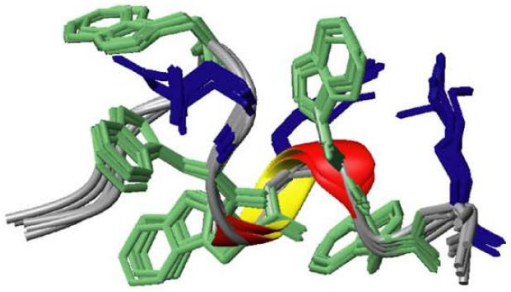

Figure 1.10 Structure of PuroA in the presence of SDS (sodium dodecyl sulfate) micelles.
Source: Chan et al. (2006). The cation–π arrangement between tryptophan and arginine residues on the left side of the peptide are shown; tryptophan residues are highlighted in green, phenylalanine is show red, and lysine and arginine residues are presented in blue colour. The disulphide bridges are shown in yellow stick representation.

A prediction of the tertiary structure of wild type PINA (represented as ABC) and mutants of PINA (contain two (ABBC) or three (ABBBC) copies of TRD) proteins was obtained using the program Protein Homology/analogue Y Recognition Engine v2.0 (Phyre2) (Miao et al., 2012) (Figure 1.11). Furthermore, the secondary structures of the purified recombinant proteins were estimated by Circular dichroism (CD) spectroscopy (Miao et al, 2012).

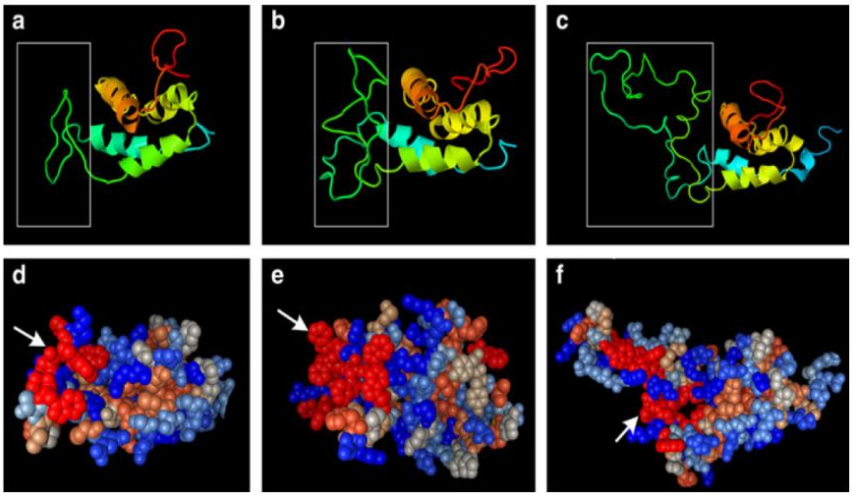

Figure 1.11 The predicted tertiary structures of PINA and mutants of PINA.
Source: Miao et al. (2012). a and d: Wild type PINA (ABC); b and e: mutant of PINA (ABBC); c and f: mutant of PINA (ABBBC). TRD(s) are shown in boxes; arrows point to the hydrophobic tryptophan residues (in red).

1.4.1 Heterologous expression of recombinant PIN proteins

Heterologous expression of PINs is an important strategy for scaling up their production and functional analysis, and has been described by several authors (Capparelli et al., 2006; Capparelli et al., 2007; Issaly et al., 2001; Miao et al., 2012; Sorrentino et al., 2009). The yeast *Pichia pastoris* has been successfully used to express recombinant PINA protein (Issaly et al., 2001). During fermentation the addition of Triton X-114 increased the production yield of the recombinant PINA by 10-fold to 14 mg/L (of which 80% was soluble), compared to concentrations of recombinant PINA previously detected without Triton X-114 (Issaly et al., 2001).

The cysteine-rich PIN proteins fused with an N-terminal His-tag (6 histidine amino acids) were successfully expressed in *Escherichia coli* strains BL21 and BL21pLysS as

18 kDa proteins (Capparelli et al., 2006). Both types of cells expressed His-PINA and His-PINB in the insoluble fraction, while His-PINs did not refold properly. His-protein purification using Ni-NTA spin column under denaturing conditions allowed the proteins to be obtained in purified form. Additionally, both PINs were expressed in *E. coli* strain DH5α with a GST-tag (Glutathione-S-Transferase, known to increase the solubility of the target protein) as 38 kDa proteins and correctly folded. Further, only recombinant GST-PINs could be efficiently purified, refolded and cleaved from their tag (Capparelli et al., 2006).

In summary, 1.5 mg recombinant His and GST tagged PINs were obtained from a 1 L culture (Capparelli et al., 2006). In addition, Capparelli et al. (2007) described the expression of PINA and PINB in the Origami strain of *E. coli*, with yields of the purified proteins at 1.8 and 0.65 mg per litre of culture, respectively, the yield being 2.6 mg per litre of culture for each protein before cleaving the tag. Wild type PINA (ABC) and mutants of PINA (with two (ABBC) or three (ABBBC) copies of TRD) were expressed in *E. coli* strain Rosetta-gami (DE3), with a NusA fusion tag at the N-terminal to promote the solubility. The strain Rosetta-gami (DE3) has trxB and gor mutations, which enhance disulphide bond formation in the *E. coli* cytoplasm and provides rare codon tRNAs, hence it can be assumed that the recombinant PINs expressed in it were folded correctly. A low temperature pre-culture and induction strategy was also used to substantially increase the yield of soluble, functional PINs (Miao et al., 2012). Alongside the use of classical organism systems such as *E. coli* and yeast to express recombinant PIN proteins, molecular farming approaches with plant system have also been used. The mature sequence of PINs (lacking the signal peptide) was fused with an N-terminal 3×FLAG tag (DYKDDDDK) and sub-cloned into a plant expression vector to target both PINs in the apoplast and the PINB in the chloroplast of *Nicotiana tabacum* cv. Bright Yellow 2 (BY-2) cells. PINB targeted to the chloroplast showed a 20 kDa band based on immunoblot analysis using the MαFLAG-M2 monoclonal antibody and yields of 0.35% of the total soluble proteins. Nevertheless, in stable suspension-cell cultures, no positive signals were observed for PINA and PINB targeted to the apoplast in either the cell protein extract or the culture medium (Sorrentino et al., 2009). The reported recombinant PIN proteins are listed in Table 1.2.

Table 1.2 Reported recombinant PIN proteins

Protein	Host	Result	References
PINA and PINB	*Escherichia coli* (BL21, BL21pLysS and DH5α)	Obtained His tagged and GST tagged PINs, 1.5 mg recombinant protein from 1 l culture	Capparelli et al. (2006)
	Escherichia coli (Origami)	Obtained 1.8 mg l^{-1} PINA and 0.65 mg l^{-1} PINB yields of purified protein	Capparelli et al. (2007)
PINA	Yeast (*Pichia pastoris*)	Obtained 80% of soluble recombinant PINA	Issaly et al. (2001)
	Escherichia coli (Rosetta-gami, DE3)	Expressed and purified PINA and two artificial mutants of PINA	Miao et al. (2012)
PINB	Tobacco (*Nicotiana tabacum*)	Expressed recombinant PINB; 0.35% of TSP	Sorrentino et al. (2009)

1.4.2 Evidence of transgenic *Pin* genes altering grain texture

PINs may be synthesised in the aleurone and transported to the endosperm (Gautier et al., 1994). PIN localisation in wheat indicated that both proteins were co-localised in the aleurone layer and the starchy endosperm of rehydrated mature seeds, however, neither PIN could be found in root, leaf, shoot or hypocotyls of seedlings (Capparelli et al., 2005; Digeon et al., 1999; Dubreil et al., 1998). Additionally, immunofluorescent localisation study confirmed the presence of both PINs at the starch granule surface (Feiz et al., 2009c). In transgenic wheat, both *Pin* genes were expressed in the starch endosperm cells (Wiley et al., 2007). However, PINs have been found in protein bodies during endosperm development by Lesage et al. (2011). It is currently hypothesised that PINs determine wheat hardness by stabilising the amyloplast membrane on the surface of starch granules during grain desiccation, thereby preventing total breakdown of the lipids when the wheat kernel ripens resulting in soft genotypes containing more phospholipids and glycolipids than hard textured genotypes (Feiz et al., 2009b; Kim et al., 2012b).

Expression of both wild type *Pin* alleles (*Pina-D1a* and *Pinb-D1a*) in rice, under the control of the maize ubiquitin promoter, resulted in reduced hardness of the transgenic rice seeds texture and decreased levels of damaged starch granules, as well as the average particle size during milling (Krishnamurthy and Giroux, 2001). A softer texture in transgenic Japonica rice was also observed following *Pinb-D1a* gene expression (Wada et al., 2010). Two different transgenic rice lines were also used for histochemical analysis of the endosperm cell and immunodetection of wheat PINA and

PINB using the Durotest anti-friabilin antibody and the results suggest that they were localised between starch granules in the rice endosperm cell (Fujiwara et al., 2014). In transgenic corn, the expression of *Pin* genes (*Pina-D1a* and *Pinb-D1a*), resulted in an increase in germ size, germ yield and seed oil content (Zhang et al., 2010a).

The expression of wild type *Pinb-D1a* in the hard wheat cv. Hi-Line resulted in soft phenotype, increased friabilin yield and decreased damaged starch (Beecher et al., 2002a). Further, in a similar study by Hogg et al. (2004), the transgenic hard wheat cultivar 'Hi-Line' with wild type *Pina-D1a*, *Pinb-D1a* or both showed reduced softness; however, expression of PINB resulted in softer kernel. Swan et al. (2006a) reported that the crossing of the transgenic 'Hi-Line' with a soft wheat resulted in progenies expressing different levels of PINs; those expressing PINB were softer and had more starch-bound PINs compared to those expressing PINA which only had an increase of starch-bound PINA. This work supports the need for both PINs in their wild form for the soft endosperm texture and may indicate that PINB has a role in assisting PINA binding to starch.

The over-expression of foreign *Pina* has been associated with co-suppression of the endogenous *Pina* (silencing of *Pina*), resulting in significantly harder kernels (Xia et al., 2008). The silencing of either *Pin* was found to decrease the expression of the other *Pin* genes and increased grain hardness, based on RNA interference (RNAi) studies in transgenic wheat (Gasparis et al., 2011). The introduction of *Pina-D1a* and *Pinb-D1a* (Gazza et al., 2008) or *Pina-D1a* (Li et al., 2014) into durum wheat significantly reduced its hardness value. *Pin* genes from soft wheat cv. Chinese Spring were transferred through *ph1b*-mediated homoeologous recombination into durum wheat, and these durum lines were stable and could be used in crossing the soft endosperm texture to other durum wheat cultivars (Morris et al., 2011).

1.5 Evidence of *in vitro* antimicrobial activity of PINs

PIN proteins are located in the starchy endosperm and the aleurone cells of wheat seed, and have a possible biological role as antimicrobial proteins. Therefore, a considerable number of studies have been published on the *in vitro* antibacterial and antifungal activities of PIN proteins (Capparelli et al., 2005; Capparelli et al., 2006; Capparelli et al., 2007; Dubreil et al., 1998; Jing et al., 2003). However, the biological function of PINs is not yet clear. PINA and PINB purified from wheat display *in vitro* antifungal activity against *Alternaria brassicola*, *Ascochyta pisi*, *Botrytis cineria*, *Fusarium culmorum* and *Verticillium dahlia*, with the antifungal activity of PINB higher than that of PINA (Dubreil et al., 1998) (Table 1.3). Both wheat PINs show similar antibacterial activity and it appears that synergy between the two proteins may enhance their antimicrobial activity (Capparelli et al., 2005). Further, recombinant PINs expressed and purified from bacterial expression systems (i.e., *E. coli*) folded similarly to the native proteins purified from wheat and revealed the same extent of *in vitro* antibacterial activity (Capparelli et al., 2006) (Table 1.3). Antimicrobial activity against *E. coli* (91% growth inhibition) has been demonstrated for chloroplast targeted PINB in *Nicotiana tabacum* cells (Sorrentino et al., 2009). Mutant forms of recombinant PINA that contain an extra copy of the TRD have shown higher antibacterial activities (70 µg/mL against *E. coli*) than the wild type PINA (90 µg/mL against *E. coli*) (Miao et al., 2012), providing evidence that the TRD has a role in their antimicrobial activity. Other studies have also proposed the TRD of PINs to have a role for their antibacterial and antifungal activities (Evrard et al., 2008; Jing et al., 2003; Phillips et al., 2011). The PIN proteins also seem to be a promising tool in topical antibiotics for bacterial infections. Recombinant PINs have been shown to be effective in ectopic treatments for fungal skin infections caused by *Staphylococcus epidermidis* without exhibiting any haemolytic activity or toxicity to mouse macrophage cells *in vitro*, and ability to kill intracellular *S. epidermidis* (Capparelli et al., 2007). Furthermore, Palumbo et al. (2010) showed potential antibacterial activity against *Listeria monocytogenes* in a mouse model with intravenously injected PIN proteins.

Table 1.3 Reported antibacterial and antifungal activities of PIN proteins

Puroindoline proteins purified from wheat			
Protein	Organism	Antimicrobial activity (μg/mL)	Reference
PINA	*Alternaria brassicicola*	100	Dubreil et al. (1998)
	Ascochyta pisi	200	
	Fusarium culmorum	100	
	Verticillium dahliae	100	
	Escherichia coli	30	Capparelli et al. (2005)
	Staphylococcus aureus	30	
	Agrobacterium tumefaciens	35	
	Pseudomonas syringae	50	
	Erwinia carotovora	50	
	Clavibacter michiganensis	50	
PINB	*Alternaria brassicicola*	20	Dubreil et al. (1998)
	Ascochyta pisi	70	
	Fusarium culmorum	40	
	Verticillium dahliae	30	
	Escherichia coli	30	Capparelli et al. (2005)
	Staphylococcus aureus	30	
	Agrobacterium tumefaciens	35	
	Pseudomonas syringae	50	
	Erwinia carotovora	50	
	Clavibacter michiganensis	50	
Puroindoline proteins expressed in bacterial cells			
Protein	Organism	Antimicrobial activity (μg/mL)	Reference
PINA	*Escherichia coli*	30	Capparelli et al. (2006)
	Staphylococcus aureus	30	
	Staphylococcus epidermidis	30	Capparelli et al. (2007)
	Escherichia coli	90	Miao et al. (2012)
	Staphylococcus aureus	150	
PINB	*Escherichia coli*	30	Capparelli et al. (2006)
	Staphylococcus aureus	30	
	Staphylococcus epidermidis	30	Capparelli et al. (2007)
Puroindoline protein expressed in *Nicotiana tabacum*			
Protein	Organism	Percentage growth inhibition	Reference
PINB	*Escherichia coli*	91%	Sorrentino et al.(2009)

1.5.1 Evidence of *in vivo* antimicrobial activity of PINs

PINs have been shown to induce a significant increase in plant resistance towards microbial pathogens by over-expression and can therefore be applied in the preservation of food products. However, no *in vivo* work had been reported until 2001, when the earliest evidence of *in vivo* antimicrobial activity for PIN expression was reported. Transgenic rice expressing PINA and/or PINB showed *in vivo* antimicrobial activity and higher resistance against two major fungal pathogens in rice, *Magnaportha grisea* and *Rhizoctonia solani*, which are causal agents of rice blast and sheath blight, respectively (Krishnamurthy et al., 2001).

The durum wheat varieties 'Luna' and 'Venusia' which naturally lack *Pina* and *Pinb* genes were transformed with the *Pina-D1a* gene, under the control of the maize ubiquitin promoter, and both varieties showed significantly increased resistance to *Puccinia triticina* (leaf rust fungus) and an increase in harvest yield (Luo et al., 2008). Kim et al. (2012a) compared seed fungal resistance by overexpression of PINA, PINB or both PINs in wheat to near-isogenic lines (NILs) with mutations in PINA or PINB and found that lines expressing both PINs had reduced *Penicillium* sp. fungal infection in seeds and increased germination. Expressing both *Pin* genes into corn was also effective in reducing the symptoms of *Cochliobolus heterostrophus,* the corn southern leaf blight pathogen, by 42% (Zhang et al., 2011).

PINs can also be expressed successfully in dicots. For example, two apple genotypes transformed via *Agrobacterium tumefaciens* with *Pinb-D1a* under the control of the cauliflower mosaic virus 35S promoter (CaMV35S) led to PINB yield to 0.24% of the total soluble proteins. In addition, the expression of *Pinb* alone or in association with a natural resistance gene *Vf*, induced partial resistance to scab, a fungal disease caused by *Venturia inaqualis* (Faize et al., 2004). The *in vitro* antifungal activity of PINB against *V. inaqualis* had previously been shown by Chevreau et al. (2001). The reported *in vivo* antimicrobial activity of PINs is listed in Table 1.4.

Table 1.4 Reported *in vivo* antimicrobial activity of PINs

Gene	Host	Resistance against	Disease	Reference
Pina* and/or *Pinb	Transgenic rice	*Magnaportha grisea* and *Rhizoctonia solani*	rice blast and sheath blight	Krishnamurthy et al. (2001)
	Transgenic wheat lines	*Penicillium* sp.	fungal infection in seeds	Kim et al. (2012a)
Pina* and *Pinb	Transgenic corn	*Cochliobolus heterostrophus*	southern corn leaf blight	Zhang et al. (2011)
Pina	Transgenic tetraploid wheat	*Puccinia triticina*	leaf rust	Luo et al. (2008)
Pinb	Transgenic apple lines	*Venturia inaqualis*	apple scab	Faize et al. (2004)

1.5.2 Evidence of antimicrobial activity of PIN-based peptides

Several studies have utilised chemically synthesised peptides, which have been designated to identify the bioactive domain of the PIN proteins. The PuroA (FPVTWRWWKWWKG-NH_2) and PuroB (FPVTWPTKWWKG-NH_2) peptides were designed based on the TRD of PINA and PINB, respectively, to identify the antimicrobial activity. PuroA showed a bactericidal effect on both Gram positive and Gram negative bacteria; in contrast, PuroB showed no activity even at the highest concentration tested (Jing et al., 2003). Wild type and variant forms of synthetic peptide were tested against bacteria, as well as phyto-pathogenic fungi (Table 1.5). PuroB showed specific activity against *Rhizoctonia* sp., with minimum inhibitory concentrations (MIC) 64 µg/mL, however, PuroA had a much higher antibacterial activity than PuroB. The number of tryptophan and positively charged residues can be a possible explanation for these different functions (Jing et al., 2003; Phillips et al., 2011). Evrard et al. (2008) showed that two tryptophan residues (W41 and W44) in the TRD were essential for PINA to interact with the membrane of *Saccharomyces cerevisiae*, while the lysine residues (K42 and K45) in the TRD of PINB seem to be more important for yeast membrane interaction.

Table 1.5 Reported antibacterial and antifungal activities of PIN-based peptides

Name	Sequence	Organism	Activity (µg/mL)	References
PuroA	FPVTWRWWKWWKG-NH_2	*Escherichia coli*	14	Jing et al. (2003)
		Staphylococcus aureus	33	
		Escherichia coli	16	Phillips et al. (2011)
		Staphylococcus aureus	16	
		Collectotrichum graminicola	250	
		Drechslera brizae	250	
		Rhizoctonia cerealis	64	
		Rhizoctonia solani	32	
PuroB	FPVTWPTKWWKG-NH_2	*Rhizoctonia cerealis*	64	Phillips et al. (2011)
		Rhizoctonia solani	64	

1.5.3 Possible mode of action for PINs as antimicrobial proteins and peptides

Anti-microbial peptides or proteins (AMPs) identified from prokaryotes and eukaryotes are usually less than 100 amino acid residues long and often have a high frequency of positively charged amino acids (Silva et al., 2011). They are strongly cationic (pI: 8.9-10.7) having a net charge of 2+ to 7+, mainly due to the presence of arginine, lysine and

histidine residues, heat-stable (100°C, 15 minutes), and additionally, they have may have 50% hydrophobic amino acids and do not have any lysing/killing effects on eukaryotic cells (Hancock and Chapple 1999; Li et al., 2012b).

AMPs have been shown to be an important and ancient mechanism of natural resistance, a rapid and metabolically inexpensive first line of defence against pathogens (Brokaert et al., 1997; Egorov et al., 2005). The antimicrobial activity of such peptides was observed to involve ionic interactions between their basic residues and the negatively charged bacterial membrane constituents, such as phospholipid head groups (Jenssen et al. 2006; Melo et al., 2009; Shai, 2002). On the other hand, the outermost layer of the eukaryotic membranes is composed of lipids with no net charge and zwitterionic headgroups positioned within the inner layers; membrane-binding is controlled by hydrophobic rather than ionic interactions (Lee et al., 2011a). The simplest models of microbe permeation by antimicrobial peptides involve the formation of transbilayer pores or channels, as shown by the models in Figure 1.12 (Wimley, 2010).

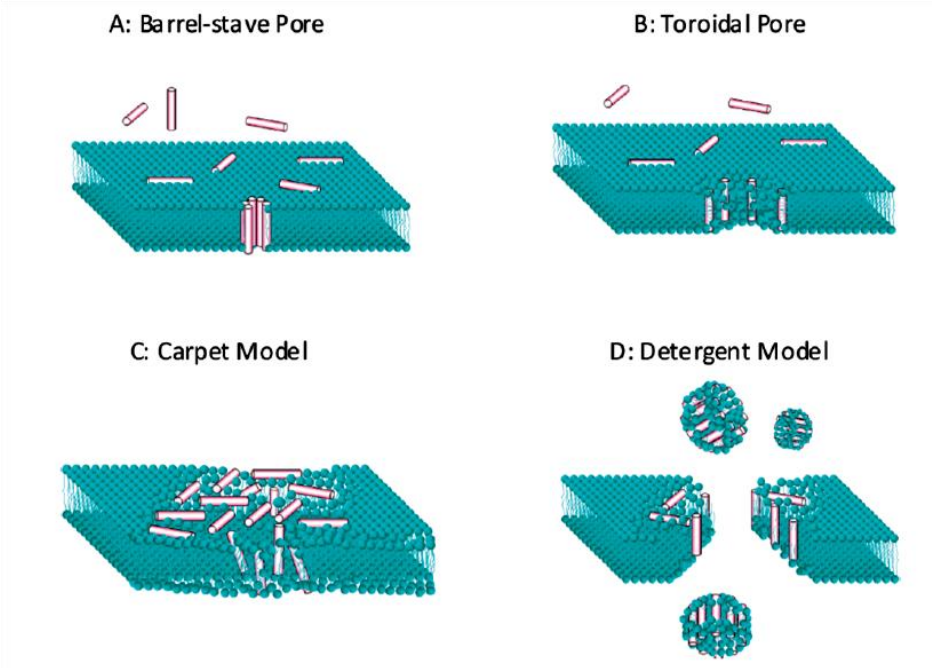

Figure 1.12 Commonly cited models for antimicrobial peptide activity.
Source: Wimley (2010).

During the past 15 years, a wide range of AMPs have been shown to play essential roles in plant defence systems. Their sizes range from 2 to 9 kDa and many of them have a cysteine-rich structure with 6 or 8 cysteine residues involved in disulphide bridges; e.g., thionins, defensins, non-specific lipid transfer proteins (nsLTPs), hevein- and knottin-like peptides, MBP1, IbAMP and snakins (Broekaert et al., 1997; Benko-Iseppon et al., 2010; Egorov et al., 2005; García-Olmedo et al., 1998; Nawrot et al., 2014; Odintsova et al., 2009). Some of the cysteine-rich AMPs, such as defensins, thionins and LTPs, are observed in wheat plants (Egorov et al., 2005). The hevein-like peptide with a 10 cysteine motif isolated from *Triticum kiharae* has been shown to have antifungal and antibacterial activity (Dubovskii et al., 2011; Odintsova et al., 2009).

The wheat puroindoline proteins share properties with other AMPs, e.g., the low molecular weight and the disulphide bond structure (Chan et al., 2006; Schibli et al., 2002). Dubreil et al. (1997) showed that PINA is able to interact tightly with both wheat phospholipids and glycolipids while PINB interacts only with negatively charged phospholipids. However, the integrity of the highly hydrophobic TRD is required for interaction with neutral polar lipids. Using fluorescence emission and circular dichroism (CD) spectroscopy the involvement of the TRD region in lipid binding confers strong affinity for polar lipids to PINs (Kooijman et al., 1997). The TRD in PINA is involved in insertion into the lipid biofilm and interacts with the lipid head group region of anionic phospholipids, mostly due to external hydrophobic residues and cationic side chains at the TRD (Kooijman et al., 1998). The involvement of tryptophan and basic residues in the TRD of PINA has been proposed as important for lipid binding and its insertion into membranes (Kooijman et al., 1997; Le Guerneve et al., 1998). Tryptophan-rich antimicrobial peptides have shown unique amphipathic properties from the side chain of tryptophan (Schiffer et al., 1992).

The *in vitro* antimicrobial properties of cationic peptides based on the TRD of the PINA and/or PINB proteins (Capparelli et al., 2005; Charnet et al., 2003; Jing et al., 2003; Phillips et al., 2011; Ramalingam et al., 2012) have been summarized above. PuroA binds strongly with and penetrates deeper into negatively charged phospholipid head groups of microbial membranes and disrupts the membrane bilayer structure by forming

cation interactions between arginine and lysine and the indole side chains of tryptophan (Jing et al., 2003). Tryptophan and arginine residues play a key role in the antimicrobial action of peptides such as tritrpticin and indolicidin (Chan et al., 2006). However, it has been suggested that the position rather than the number of tryptophans is an important factor (Bi et al., 2013). Membrane interaction studies in yeast have shown that tryptophan-41 and tryptophan-44 at the TRD of PINA may be essential for interaction with fungal plasma membranes. However, for PINB, none of the tryptophan residues were required, whereas the positively charged lysine-42 and lysine-45 were essential for yeast membrane interaction of PINB (Evrard et al., 2008). In addition, single substitution at the TRD of PINB, of a glycine to a more polar serine residue (Gly46Ser) and a tryptophan to a basic arginine residue (Trp44Arg) decreased the selectivity towards anionic phospholipids (Clifton et al., 2007a; Clifton et al., 2007b), which supports the hypothesis that tryptophan may influence membrane selectivity. Further, Phillips et al. (2011) showed the antimicrobial properties of cationic peptides based on the unique TRD of the PIN proteins. They have shown reduced activity of PINA peptide upon substitution of tryptophan residues with phenylalanine within the TRD. For antifungal activity of the PINB-TRD, lysine-45 and tryptophan-39 have indicated important roles, while tryptophan-44 does not appear to be essential and substitution of lysin-45 to glutamic acid in Pinb-L abolished any observable antifungal activity (Phillips et al., 2011). Microbial membrane interaction via the polar lipids and membranes may be required as a mode of action of the PIN proteins (Blochet et al. 1993). Using electrophysiological experiments on *Xenopus oocytes* and artificial planar bilayers, channel formation mechanisms were shown to be important for puroindolines antimicrobial activity (Charnet et al., 2003). Moreover, the PIN proteins appear to act synergistically in combating pathogens not only with α-purothionins but also with one another (Capparelli et al., 2005; Chan et al., 2006). The pore formations by PIN-based peptides appear by a carpet-like model, following the intracellular mechanisms of activity (Alfred et al., 2013b). Recently it has also been suggested that PIN-based peptides may inhibit DNA synthesis (Haney et al., 2013). It is thus clear that further work is required to determine the mechanism(s) of activity of the PIN proteins in membrane interactions, relevant to both their effects on texture and any *in vivo* defence roles

1.5.4 Possible interactions between PINs

A considerable number of studies on comparative genetic and protein expression have suggested some co-operation or interdependence between the two PIN proteins. The presence of both PINs in their functional form at the surface of starch is necessary for the soft phenotype (Hogg et al., 2004) and with a single protein present; the result is an intermediate grain texture (Feiz et al., 2009c; Wanjugi et al., 2007). It is likely that PINA has a primary role in binding to the starch granule surface and also has a co-operative role in stabilising the binding of PINB, as well as mediating its binding to starch granules (Amoroso et al., 2004; Capparelli et al., 2003; Gazza et al., 2005). Furthermore there is a possible minor role for PINB in assisting the binding of PINA to the starch granule surface (Bhave and Morris, 2008b). Supportive roles for PINA and PINB in binding to the starch granules have been hypothesised (Amoroso et al., 2004; Swan et al., 2006b). Ziemann et al. (2008), using the yeast two-hybrid system, provided evidence of physical interactions between PINA and PINB, suggesting that both functional PINA and PINB are essential for soft texture and that interaction between PINA and PINB may occur in the wheat kernel.

The requirement of both PIN proteins in polar lipid binding was shown in transgenic wheat (Feiz et al., 2009c). PIN proteins were independent of each other in localising to the surface of starch granules, but the greater binding to polar lipids was observed only when both PINs were present (Feiz et al., 2009c). The occurrence of both wild type PINs may explain the increase in the equilibrium surface pressure at air/water interphase and the degree of penetration in lipid monolayers (Clifton et al., 2007a). Overall, the different lipid binding behaviours of PIN proteins provide further insight into the impact of hydrophobic and cationic amino acid residues on the functional properties of their antimicrobial activity (Sanders et al., 2013). Based on these reports, the synergism between wild type PINA and PINB seems important for grain hardness and possibly in their antimicrobial activity.

1.6 Plant expression system

Among various expression systems such as bacteria, yeast, mammalian cells and insects, plants are becoming an attractive system for the production of recombinant proteins for pharmaceuticals, industrial proteins, monoclonal antibodies and vaccine antigens due to many advantages including safe usage, rapid scale-up, long-term storage and lower production cost (Daniell et al., 2001, 2009b; Fischer and Emans, 2000; Fischer et al., 2003, 2004, 2013; Horn et al., 2004; Howard and Hood, 2005; Klimyuk et al., 2008; Ma et al., 2003, 2005; Rybicki, 2009; Schmidt, 2004 Thomas et al., 2011). In addition, plant cells have the ability to perform post-translational modifications (PTM) of proteins which are typical of eukaryotic organisms (Gomord and Faye, 2004; Mett et al., 2008; Vitale and Pedrazzini 2005). PTM affects the proteins activities and functions such as folding, stability, and solubility, and dynamic interactions with other molecules, the major type of PTM for plant-made recombinant proteins being glycosylation (Marino, 1991; Stulemeijer and Joosten, 2008; Webster and Thomas, 2012).

A wide variety of promoters have been used for protein expression in plants, including constitutive, inducible and tissue-specific, native and synthetic promoters (reviewed in Egelkrout et al., 2012). The most widely used promoter is the cauliflower mosaic virus 35S promoter (CaMV35S), which promotes high-level of gene expression through the transcriptional terminator of the *Agrobacterium* nopaline synthase gene (*nos*) (Barampuram and Zhang, 2011; Lee et al., 2008). Several molecular events such as gene transcription, mRNA translation and protein accumulation affect overall success of protein expression (Table 1.6).

Table 1.6 Summary of factors affecting gene transcription, mRNA translation and protein accumulation Source: modified from Egelkrout et al. (2012)

Factors affecting transcription rate	**Factors affecting translation rate**
Promoter selection	Post-transcriptional gene silencing
Transcription factor binding (TFB) sites	Codon usage
Upstream regulatory sequences (URS)	mRNA stability
Intron-mediated sequences	Recruitment and retention of translation-ralated protein
Transcriptional gene silencing (TGS)	**Factors affecting protein accumulation**
Pre-mRNA stability	Protein stabilisation
Transgene trait stacking	Protein localisation
The impact of the site of integration	Protein modification
The number of gene copies	Cellular milieu

Successful recombinant protein accumulation in plant systems depends on several key factors including suitable host tissue, sub-cellular location, the nature of the foreign proteins, their possible effect on the host plant, as well as the post-translational modifications and the degree of protein purification required, and based on these factors, there are several options for protein expression in plant systems (Egelkrout et al., 2012; Schiermeyer et al., 2004). These are discussed below.

1.6.1 Host plants

Protein expression platforms have been developed for a variety of host systems including seed crops (corn, canola, soybeans, and rice) and leafy crops (tobacco, alfalfa, lettuce), as well as plant cell cultures (tobacco, carrot, rice), hairy root cultures and aquatic plants (*Lemna minor*), in addition to moss and green algae (Wilken and Nikolov, 2012). One of the major plant systems that is used for the production of recombinant proteins is tobacco, the advantage being high leaf biomass yields as it can be cropped several times a year (Basaran and Rodriguez-Cerezo, 2008; Twyman et al., 2003; Twyman, 2004; Wilken and Nikolov, 2012).

1.6.1.1 *Nicotiana tabacum* (Tobacco)

The genus *Nicotiana* belongs to the family Solanaceae, which includes 76 species originating in North America, South America, Australia and Africa (Chase et al., 2003; Knapp et al., 2004). *Nicotiana tabacum* is an amphidiploid/allotetraploid species with 48 chromosomes, generated from hybridisation between *N. sylvestris* and either *N. tomentosiformis* Goodspeed or *N. otophpra* Grisebach, all of which originate from

South America (Kitamura et al., 2001; Lewis, 2011). *Nicotiana tabacum* as a model plant in research provides many practical advantages for large-scale production of recombinant proteins, including high biomass yield, low maintenance and high seed production (Twyman, 2004). It is a non-food, non-feed crop, hence carries a reduced risk of transgenic material contaminating food chains (Stoger et al., 2005; Twyman et al., 2003; Twyman, 2004). Tobacco cultivars contain a high amount of nicotine and other alkaloids; hence, it is necessary to remove these toxic components (Twyman, 2004). Ma et al. (1995, 1998) reported the first successful expression of the secretory monoclonal antibody in transgenic *N. tabacum*. The two tobacco cell lines, BY-2 (bright yellow 2) and NT-1 (*N. tabacum* 1), are readily available for *Agrobacterium*-mediated genetic transformation and have been optimised for rapid growth (Doran, 2013).

1.6.1.2 *Nicotiana benthamiana*

The non-cultivated tobacco species, *Nicotiana benthamiana,* is a unique Australian native plant that may have resulted from hybridisation between *N. suaveolens* and *N. debneyi* (Goodspeed, 1954; Goodin et al., 2008). It is an amphidiploid with 38 chromosomes (Goodspeed, 1954) and has been used as a host in the production of monoclonal antibodies and vaccines. It is a suitable host species for producing recombinant proteins using viral vectors such as the tobacco mosaic virus (TMV) (Twyman, 2004; Yang et al., 2004). It can be transformed with high efficiency and maintained easily, due to its short stature, short regeneration time and high seed production, and is also useful for transient expression of genes (Goodin et al., 2008).

1.6.2 Transformation method and expression systems

Genetic transformation can be achieved by physical or biological methods. Physical methods are usually used to transfer non-viral vectors by using a gene gun (biolistics) and chemical polyethylene glycol (PEG) transformation or electroporation of protoplasts (Barampuram and Zhang, 2011; Rao et al., 2009). The biological method of genetic transformation of plant cells by *Agrobacterium* involves the transfer and integration of a large tumor-inducing (Ti) or rhizogenic (Ri) plasmid resident in *Agrobacterium* into the plant nuclear genome. Although several species of

Agrobacterium are known, two species are predominantly used for transformation; *Agrobacterium tumefaciens* (T-DNA transfer for generation of transgenic plants) and *Agrobacterium rhizogenes* (Ri-plasmid transfers necessary DNA to generate transgenic hairy roots) (Gelvin, 2003; Gleba et al., 2014; Rao et al., 2009).

The production of recombinant proteins in plants, also known as molecular farming, is classified into two expression systems, i.e., stable or transient. Stable expression involves integration of foreign DNA into the plant genome and transfer to the next generations (Sharma et al., 2005). The storage organs such as seeds have been used for the stable expression of proteins of interest (Scheller and Conrad, 2004). The chloroplast stable transformation requires more than two months and nuclear stable transformation that requires several months (Patiño-Rodríguez et al., 2013).

Transient expression systems include *Agrobacterium*-mediated and viral-based transformation, wherein the foreign gene is not integrated in the genome is expressed only for a few days after being introduced into the plant cell/tissue. The strategy relies on *A. tumefaciens*, which contains transgenes; the bacteria are infiltrated directly into the organs of interest by injection or by using a vacuum chamber (agroinfiltration) (Klimyuk et al., 2014; Leckie and Stewart, 2011; Leuzinger et al., 2013; Vaghchhipawala et al., 2011). Transient expression is generally used to verify the activity of the expression constructs and generate small amounts of recombinant protein for functional analyses (Twyman et al., 2003). Many results have been obtained so far with viral backbones such as those of the RNA viruses, Tobacco mosaic virus (TMV), Potato virus X (PVX) and Cowpea mosaic virus (CPMV) (Gleba et al., 2014; Marillonnet et al., 2005). Transient expression using viral vectors is one of the best and rapid methods for obtaining a high yield of protein expression (Egelkrout et al., 2012).

1.6.2.1 Transient expression using viral vectors

Transient, viral-based systems are amongst the best available systems and have the advantage of being a rapid method for large-scale production of proteins such as antibodies and vaccine antigens (Gleba et al., 2007; Pogue et al., 2002). The viral vector system is based on two strategies: ‘full virus’ vectors used to express long

polypeptides (at least 140 amino acids) and 'deconstructed' virus vectors which rely on *A. tumefaciens* to deliver DNA copies of one or more viral RNA replicons to plant cells (Gleba et al., 2007; Gleba and Giritch, 2012). One main system of deconstructed virus vectors is the 'magnICON®' from ICON genetics, based on the tobacco mosaic virus (TMV), but instead of supplying whole RNA or linear DNA, it is divided in different modules captured between the left and right border of T-plasmid of *A. tumefaciens* (Gleba et al., 2004; Gleba et al., 2014; Marillonnet et al., 2004). Three *A. tumefaciens* cultures deliver different vector modules containing different viral components, targeting and gene sequences and these pro vector 5' and 3' modules assemble within the plant cell in the form of functional viral vector (Marillonnet et al., 2004). After delivery by agroinfiltration, they assembled inside the cell with the help of a site-specific recombinase to create an RNA replicon to produce the desired protein. The advantage of this system is that the desired protein can be produced at high yield, because of viral amplification (Marillonnet et al., 2004). Targeting the proteins into different subcellular compartments can alter protein stability (Gils et al., 2005) e.g., chloroplasts can improve stability (Doran, 2006). The green florescence protein (GFP) has been expressed in different sub cellular compartments of *N. benthamiana* using this system, to produce recombinant protein at up to 80% total soluble protein (Marillonnet et al., 2004; 2005). A considerable amount of research has been published on the use of the magnICON® system (Gleba et al., 2004, 2005, 2007; Gils et al., 2005; Giritch et al., 2006; Huang et al., 2006, 2010; Marillonnet et al., 2004, 2005; Santi et al., 2006, 2008; Webster et al., 2009; Werner et al., 2011).

1.6.3 Subcellular location in a plant system for protein accumulation

The targeting of foreign proteins to the most appropriate subcellular compartment is important for protein accumulation, stability, folding and posttranslational modification (Twyman, 2004). The choice depends on the structural characteristics of the protein and the use of appropriate signals (Benchabane et al., 2008; Faye et al., 2005). Several subcellular compartments have been considered including the cytosol, endoplasmic reticulum (ER), apoplast, vacuole and chloroplast (Benchabane et al., 2008; Ma et al., 2003).

1.6.3.1 Cytosol

Recombinant proteins are retained in the cytosol when no targeting signals are used. Several studies have revealed recombinant proteins that remain stable within the cytosol (De Jaeger et al., 1999; Michaud et al., 1998; Marusic et al., 2007). However, the cytosol may not be the best location for several reasons: high levels of protease and ubiquitin activity, the negative redox potential that may affect the correct folding of proteins with disulphide bonds, and a lack of important co- and post-translational modifications, such as glycosylation, which may affect folding, assembly and the tertiary structural stability (Benchabane et al., 2008; Faye et al., 2005).

1.6.3.2 Endoplasmic Reticulum (ER)

Targeting proteins to the ER can lead to high yields of recombinant proteins *in planta* (Conrad and Fiedler, 1998; Wandelt et al., 1992). Recombinant proteins entering the endoplasmic reticulum (ER) can be retained here by adding (SEK/H/K)DEL retention sequences to the C-terminal (Benchabane et al., 2008; Michaud et al., 1998; Mainieri et al., 2004), in most cases a (K/H)DEL sequence (Benchabane et al., 2008; Ma et al., 2003). The presence of molecular chaperones in the ER can have a role in disulphide bond formation (Benchabane et al., 2008; Faye et al., 2005; Nuttall et al., 2002).

1.6.3.3 Apoplast

Proteins can be targeted into the apoplast via the secretory pathway (Benchabane et al., 2008). The plant apoplast includes the cell wall matrix and intercellular spaces and has a wide range of physiological functions (Witzel et al., 2011). The lack of KDEL in endosperm-expressed protein resulted in targeting to the apoplast, where mostly the recombinant protein accumulates in the space under the cell wall (Christou et al., 2004).

1.6.3.4 Vacuole

The vacuole is one of the alternative destinations for recombinant proteins produced in plants (Benchabane et al., 2008). Additionally, it has several key roles *in planta* e.g., control of cell turgidity, levels of macromolecules, accumulation of toxic secondary metabolites and storage of high-energy compounds in vegetative tissues (Benchabane et al., 2008; Twyman, 2004).

1.6.3.5 Chloroplast

The chloroplast is one of the cellular destinations in a plant expression system, through the addition of an appropriate targeting signal peptide (Daniell and Dhingra, 2002; Hyunjong et al., 2006). The recombinant proteins may be moved to the chloroplast. Chloroplast transformation offers uniform expression rates, a high copy number of the transformed genes (due to hundreds of plastids in a cell), co-expression of multiple genes from the same construct, minimal transgene escape in the environment due to the maternal inheritance of chloroplast DNA and minimal gene silencing (Daniell et al., 2004). Post-translational modifications such as multimerisation and disulphide bridge formation can occur in the stroma (Daniell, 2006; Parachin et al., 2012). The chloroplast can thus be a suitable compartment without needing the cell secretory pathway or modifications such as glycosylation; however, some endogenous proteases can affect the stability and accumulation of recombinant proteins (Adam and Clarke, 2002). However, this may not be relevant issue for proteins expressed at very high yield (Daniell, 2006).

In conclusion, plants can act as 'biofactories' for the production of recombinant proteins, for reducing the production costs due to the low maintenance cost and high quality of the therapeutic protein (Davies, 2010; Gomord and Faye, 2004; Gleba, 2007; Ling et al., 2010; Mett et al., 2008; Melnik and Stoger, 2013). The use of plant systems for production of AMPs is summarised as follows.

1.6.4 Plant systems for heterologous production of antimicrobial peptide

Antimicrobial peptides/proteins (AMPs) are unique biologically active molecules that comprise defence systems against numerous pathogens such as bacteria, fungi, parasites and/or viruses. Heterologous expression systems, including bacteria and fungi as host cells, have been used for production of AMPs with different sizes, folds and complexities (reviewed in Parachin et al., 2012). Plant systems have also been used as a suitable source for the production of AMPs and can be directly used for crop improvement without purifying the peptide or proteins (Desai et al., 2010; Giddings et al., 2000). The heterologous production of radish Rs-AFP2 defensin in tobacco protected the transgenic tobacco from *Alternaria longipes* (Terras et al., 1995), whereas

the alfalfa anti-fungal peptide (alfAPF) defensin reduced the infection in transgenic potato plants against the fungal pathogen *Verticillium dahliae* (Gao et al., 2000).

Several AMPs cannot be produced in microbial systems due to their antimicrobial activity and complex structures. For example, retrocyclin-101 (RC101) and Protegrin-1 (PG1) can be used as therapeutic agents against bacterial and/or viral infections; both have not yet been produced in microbial systems, but have been expressed in the tobacco chloroplast with a yield of around 20% of total soluble protein, and retention of antiviral activity (Lee et al., 2011b). The large scale production of AMPs can be applied in numerous industries such as biotechnology, pharmaceuticals, cosmetics and food. However, the limiting factor is the high production costs of some AMPs due to their molecular mass and protein folding characteristics. The AMP can aggregate or be degraded by endopeptidases, which also limits their bioactivity. Choosing the right system is thus essential for large scale production and functional recombinant AMPs. Plant-based expression systems are a promising platform for further engineering, and production of AMPs (Parachin et al., 2012). All AMPs heterologously produced in *N. tabacum* are listed in Table 1.7.

Table 1.7 AMPs heterologous produced in *Nicotiana tabacum*

AMP transformed	Source	Objective	Resistance against	References
protegrin-1 (PG-1)	Synthesized peptide	Production peptide and antimicrobial activity	*Klebsiella pneumoniae*, *Staphylococcus aureus*, *Escherichia coli*, *Mycobacterium bovis*, *Candida albicans*	Patiño-Rodríguez et al. (2013)
Dermaseptin Lysozyme C4V3	*Phyllomedusa sauvagii, Gallus gallus,* Synthetic	Production and isolation of the peptide and vaccine	Anti-HIV activity, induction of mammalian immune response	Rubio-Infante et al. (2012)
EtMIC2	*Eimeria tenella*	Peptide production	*Eimeria tenella* (chicken coccidiosis)	Sathish et al. (2011)
Retrocyclin-101 and Protegrin-1	Artificial AMP based on rhesus monkey (*Macaca mulatta*) circular minidefensins	Chloroplast genome transformation aiming peptide production	*Erwinia carotovora*, tobacco mosaic virus	Lee et al. (2011b)
NmDEF02	*Nicotiana megalosiphon*	Proof of concept for crop improvement	*Phytophthora parasitica* var. *nicotianae*, *Peronospora hyoscyami* f.sp. *tabacina*, *Alternaria solani, Phytophthora infestans*	Portieles et al. (2010)
Trichokonins	*Trichoderma pseudokoningii*	Proof of concept for crop improvement	Tobacco mosaic virus	Luo et al. (2010)
Pal and Cpl-1	Phages infecting *S.pneumoniae*	Chloroplast genome transformation aiming peptide production	*Streptococcus pneumoniae*	Oey et al. (2009)
MsrA2 (N-methionine-dermaseptin B1)	*Phyllomedusa sauvagei* and *Phyllomedusa bicolor*	Gene stacking for crop improvement	*Fusarium solani*, *Fusarium oxysporum*, *Alternaria alternata*, *Botrytis cinerea*, *Sclerotinia sclerotiorum*, *Pythium aphanidermatum*, *Pectobacterium carotovorum*	Yevtushenko and Misra, (2007)

1.7 Summary of the literature and aims of the research

1.7.1 Summary of the above literature

This chapter provided background information that addressed the basics of puroindoline proteins (PINs) in wheat, one of the most widely used crops worldwide. The relationship between *Pin* genes and grain texture was reviewed. The review also addressed the antimicrobial activity and lipid binding properties of PIN proteins and PIN-based peptides. However, the *in vivo* roles for both PIN proteins in wheat seed and the effect of these hardness mutations in puroindolines on the grain hardness as well as their antimicrobial activity remain unclear. Several studies have reported the co-operative or interdependent interaction binding to the surface of starch granules to confer the soft phenotype, the basis for which is also unclear.

PIN proteins aggregate in the presence of membrane lipids and in the absence of lipids, these proteins can still aggregate, but no precise information is available on the relationship between aggregation and interaction with lipids in the absence of three-dimensional structure of the proteins. The high resolution structure of PINs are yet to be solved, due to problems with their crystallisation and difficulties in obtaining a stable non-aggregated solution required for NMR structural characterisation. It is important to investigate the functionality of the PIN proteins in order to better understanding the biological functions of this family of proteins for their use in biotechnology and therapeutic applications. Plant molecular farming approach can be used for expressing large quantities of proteins or peptide. The characterisation of the two PIN proteins in expressed in such systems will be invaluable for addressing many of the above stated issues.

1.7.2 The aims of the project

The specific aims of this project are as follows:

1. To clone the *Pin* genes encoding the putative mature PINA and PINB in to the magnICON® viral vector system and utilise *A. tumefaciens* infiltrations, to express and optimize their transient expression for high yield in the leaves of *Nicotiana benthamiana*.

2. To test the antibacterial and antifungal activities of recombinant PIN proteins purified with affinity purification using His-tag and hydrophobic interactions systems.

3. To analyse the protein-protein interactions among the PIN proteins *in planta* using the BiFC system based on pNBV vectors and co-expression of the silencing suppressor protein p19.

4. To test the significance of the tryptophan-rich domain (TRD) of PINA and the hydrophobic domain (HD) of both PINs in any interactions between the PINs using the BiFC system.

CHAPTER 2

Materials and methods

Equipment and materials

2.1 Equipment

The instruments and major apparatus used in this work are listed in Table 2.1.

Table 2.1 Instruments and apparatus used

Equipment	Purpose	Manufacturer
MyCycler™	Conducting the Polymerase Chain Reactions (PCR)	Bio-Rad, California, USA
PowerPac™ HC power supply	Nucleic acid and protein gel electrophoresis	
Mini-protean® Tetra cell	Polyacrylamide gel electrophoresis (PAGE or SDS-PAGE)	
Westen blotting Mini-Protein II Trans blot module	Transfer of proteins from gels to membrane	
SmartSpec 3000 Spectrophotometer	Determining bacterial concentration (Optical Density or OD)	
Gene pluser II	Electroporation system for transforming various cell types	
NanoDrop™ 1000 Spectrophotometer	Quantification of nucleic acid concentration	Thermo Fisher, USA
Finnpipette (0.5-10,5-50,20-200 and 100-1000µL)	Dispensing liquid	
Microplate reader	Absorbance detection for ELISA assays and microbial growth turbidity	
Microscope (Axioskop 2 MOT Plus)	Visualizing the bimolecular fluorescence complementation (BiFC) assay results	Carl Zeiss, Germany
Microscope camera (AxioCam HR)	Imaging the BiFC assay results	
SNAP i.d	Blocking, washing and antibody incubations for western blot	Merck Millipore, Australia
Amicon® ultra 0.5 centrifugal filter (3K device - 3,000 NMWL)	Concentrating dilute protein samples	
Spectroline Ultra Violet (UV) transilluminators	Visualisation of green or yellow fluorescent protein (GFP or YFP) expression	Spectroline, USA
Chemidoc system	Visualisation of gel images	UVP,California, USA
End-over-end mixer	Mixing of samples for extractions and purification	Ratek, Australia
Plant growth cabinet	Growth of wheat plants under controlled conditions	Thermoline, Victoria, Australia
Film processor CP1000	Developer for illumination of antibody-HRP labeled western blot	Agfa, Australia
Kodak, BioMax light film	For western blotting analysis	Sigma, USA

2.2 Commercial kits

The commercial kits and reagents used in study are listed in Table 2.2.

Table 2.2 Commercial kits

Kit/material	Purpose	Manufacturer
Biomix™ Red (2×)	PCR	Bioline, Australia
Hyperladder™I (10000bp-200bp)	Molecular weight standard for agarose gel electrophoresis of DNA samples	
Precision Plus Protein Dual Xtra Standards (250 kDa-2 kDa)	Molecular weight sizing on SDS-PAGE gels	Bio-Rad, California, USA
Butyl-Toyopearl	Hydrophobic interaction protein purification	Tosoh Corporation, Japan
HiYield™ Gel/PCR Fragments Extraction Kit	Recover or concentrate DNA fragments from agarose gels, PCR or other enzymatic reactions	Real Biotech Corporation (RBC), Taiwan
HiYield™ Plasmid Mini Kit	Plasmid DNA isolation	
HisPur™ Ni-NTA Resin	Affinity protein purification	Thermo Fisher, USA
KOD Hot Start DNA polymerase	PCR	Novagen, Germany
PlatinumR *Pfx* DNA polymerase	PCR	Life Technologies, Invitrogen, USA
SYBR® Safe DNA gel stain	Staining of DNA in agarose gels	
RNase A	RNA digestion during genomic DNA extraction	Sigma, USA
Restriction endonucleases	DNA digestion	NEB, (Genesearch), Australia
Sheep blood	Haemolysis assay	Amyl Media, Australia
Calf intestinal alkaline phosphatase (CIAP)	Dephosphorylation of DNA ends	Promega, Australia
Wizard® Genomic DNA Purification Kit	Genomic DNA extraction	

2.3 Primary and secondary antibodies

Table 2.3 Antibodies for western blot analysis

Antibody name	Purpose	Specific	Manufacturer and Catalog number
Durotest® S*	To detect friabilin proteins	Monoclonal antibody Host: mouse	R-Biopharm Rhone Ltd., Glasgow, UK; P10
Anti-His	To detect histidine tag containing proteins	Monoclonal antibody Host: mouse	Life Technologies, Invitrogen, USA; 37-2900
Anti-GFP	To detect GFP protein	Monoclonal antibody Host: rabbit	Life Technologies, Invitrogen, USA; G10362
Anti-mouse	Secondary antibody	Polyclonal antibody Host: goat	Sigma, USA; A0168
Anti-Rabbit	Secondary antibody	Polyclonal antibody Host: goat	Sigma, USA; A0545

*The Durotest® S has a monoclonal antibody raised to detect 'friabilin' protein mixture from bread wheat. The kit is detailed later under western blotting section.

2.4 Commonly used buffers, other solutions and media

The common buffers, solutions and media were prepared according to the instructions in Sambrook and Russell (2001). These are listed in Table 2.4. All aqueous buffers and solutions were prepared with MilliQ water (Millipore, Australia) that also autoclaved. Solutions were sterilised by autoclaving (121°C for 20 minutes), or filter sterilizing through a 0.22 μm syringe filter. All glassware and appropriate disposable plastic ware (such as PCR tubes, centrifuge tubes, tips) were also autoclaved before use.

Table 2.4 Composition of general buffers and solutions

Buffer and Solution	Composition
Coomassie Blue staining solution	40% methanol, 10% acetic acid, 0.05% Coomassie Blue R-250
Coating buffer	15 mM Na_2CO_3, 35 mM $NaHCO_3$, (pH 9.6)
De-stain solution	50% methanol, 10% acetic acid
Infiltration buffer for magnICON® system	10 mM 2-(N-Morpholino)ethanesulfonic acid (MES), 10 mM $MgSO_4$ (pH 5.5)
Infiltration buffer for BiFC system	10 mM $MgCl_2$ and acetosyringone to a final concentration of 200 μM
Isopropyl-β-D-thiogalactopyranoside (IPTG)	0.1 M in sterile MilliQ water
Phosphate-buffered saline (PBS)	137 mM NaCl, 2.7 mM KCl, 10 mM Na_2HPO_4, 2 mM KH_2PO_4 (pH 7.4)
PBS containing Tween-20 (PBST)	PBS with 0.1% (v/v) Tween 20
Milk-PBS-Tween 20 (MPBST)	0.5% milk powder, PBS, 0.05% Tween 20

Table 2.4 Composition of general buffers and solutions (continued)

Buffer and Solution	Composition
Native-PAGE loading dye, 2x	125 mM Tris (pH 6.8), 50% glycerol, 0.02% bromophenol blue
SDS-PAGE loading dye, 5x	50 mM Tris-HCl (pH 8.8), 10% sodium dodecyl sulfate (SDS), 30% glycerol, 500 mM ß-mercaptoethanol, 0.02% bromophenol blue
TB buffer	10 mM Hepes, 15 mM $CaCl_2$, 250 mM KCl, (pH 6.7) then add $MnCl_2$ to a final concentration of 55 mM
TE buffer	10 mM Tris, 1 mM EDTA, (pH 8)
Tris acetate EDTA (TAE) buffer, 50x	2 M Tris base, 6.5 M EDTA disodium salt (pH 8)
Tris glycine buffer, 10x	25 mM Tris, 192 mM glycine buffer (pH 8.8)
Transfer buffer, 1x	25 mM Tris, 192 mM glycine buffer, 20% (v/v) methanol
Running buffer, 1x	25 mM Tris, 192 mM glycine buffer, 0.1% SDS
5-bromo-4-chloro-3-indolyl-β-D-galactopyranoside (X-gal)	5% (w/v) in dimethylformamide (DMF)
Composition of buffers and solutions for sequencing	
BDT reaction buffer, 5x	400 mM Tris (pH 9), 10 mM $MgCl_2$
Sequencing reactions clean-up solution	0.2 mM $MgSO_4$ in 70% ethanol
Media Name	**Composition**
Luria Bertani (LB) broth	10 g/L tryptone, 5 g/L yeast extract, 5 g NaCl
Luria Bertani (LB) agar	LB with 15 g/L agar added (for plates)
Luria Bertani (LB) glycerol	LB with 30% glycerol
Mueller-Hinton Broth (MHB)	21 g/L
Potato Dextrose Agar (PDA)	39 g/L
Super Optimal broth (SOB)	0.5% yeast extract, 2% tryptone, 10 mM NaCl, 2.5 mM KCl, 10 mM $MgCl_2$, 10 mM $MgSO_4$
Super Optimal broth with Catabolite repression (SOC)	SOB with 20 mM glucose (filter sterilized)
Antibiotic stock	
Carbenicillin	200 mg/mL in sterile MilliQ water
Ampicillin	50 mg/mL in sterile MilliQ water
Kanamycin	
Rifampicin	
Spectinomycin	

2.4.1 Protein purification buffers

Various buffers were needed to be prepared as per the protein purification protocol and systems applied. These are listed in Table 2.5.

Table 2.5 Composition of protein purification buffers

His-tag purification buffer (Native condition) [Thermo Fisher, USA]
Equilibration buffer 20 mM sodium phosphate, 300 mM sodium chloride with 10 mM imidazole, pH 7.4
Wash buffer 20 mM sodium phosphate, 300 mM sodium chloride with 25 mM imidazole, pH 7.4
Elution buffer 20 mM sodium phosphate, 300 mM sodium chloride with 250 mM imidazole, pH 7.4
His-tag purification buffer (denaturing conditions) [Propur™, Denmark]
Equilibration buffer 20 mM sodium phosphate, 300 mM sodium chloride , 6 M urea with 10 mM imidazole, pH 7.4
Wash buffer 20 mM sodium phosphate, 300 mM sodium chloride, 6 M urea with 25 mM imidazole, pH 7.4
Elution buffer 20 mM sodium phosphate, 300 mM sodium chloride, 6 M urea with 250 mM imidazole, pH 7.4
Hydrophobic Interaction buffer [Lee et al, 2011b]
Extraction buffer Saturated ammonium sulphate, pH 7.8; a final saturation of 60%, 70%, 80%
Equilibration buffer 20% ammonium sulphate in 10 mM Tris–HCl, pH 7.8
Elution buffer 10 mM Tris–HCl, pH 7.8

2.5 Microbial strains

2.5.1 Strains used as hosts for gene cloning

Escherichia coli Mach1 strain was obtained from stock in Monash University and used for general molecular cloning procedures. It was typically used for gene cloning.

Agrobacterium tumefaciens strain GV3101 was also used in transformation of plant expression system vectors which is resistant to rifampicin due to a chromosomal mutation (Lee and Gelvin, 2008).

The gift glycerol stock vectors which are detailed below were cloned in *E. coli* XL1-Blue and *A. tumefaciens* strain LBA4404.

2.5.2 Strains used for testing of antimicrobial activity of recombinant PINs

The bacterial species *Escherichia coli* (ATCC 25922) and *Staphylococcus aureus* (ATCC 25923) and the fungal species, *Collectotrichum graminicola, Drechslera brizae, Fusarium oxysporum, Rhizoctonia cerealis* and *Rhizoctonia solani* were obtained from the culture collection at Swinburne University of Technology. The bacterial cultures were streaked on fresh LB plates and incubated overnight at 37°C and a single colony was used to inoculate overnight cultures. The fungal cultures were maintained on PDA plates (Table 2.4).

2.6 Plant material

2.6.1 Propagation of wheat seedlings

The soft common wheat (*Triticum aestivum* L cv. Rosella) was used for isolation of the wild type alleles of *Puroindoline a* (*Pina-D1a*) and *Puroindoline b* (*Pinb-D1a*) henceforth designated as *Pina* and *Pinb.* The seeds, kindly provided by the Australian Winter Cereals Collection (AWCC, Tamworth, Australia) were soaked in sterile water overnight then sown on a sterilised mixture of potting soil and vermiculite (2:1). The seedlings were grown in a plant growth cabinet (Thermoline, Australia) with 16 hours of light (25ºC) and 70% humidity (Figure 2.1). For DNA extractions, leaf tissue was harvested from 4 week old plants for immediate use or snap-frozen in liquid nitrogen and stored at -80ºC.

2.6.2 Propagation of *Nicotiana benthamiana* seedlings

Nicotiana benthamiana was used for plant transformations. The seeds for the wild type *N. benthamiana* in Australia were kindly provided by Dr Diane Webster, Monash University, Melbourne. The seeds were germinated in jiffy peat pellets. The plantlets (Figure 2.1) were transferred to sterilised mixture of potting soil and vermiculite (2:1) and grown in a greenhouse maintained at 25°C with a 16h light/8h dark photoperiod. Young, fully expanded leaves of 8 week old seedlings were used for infiltration.

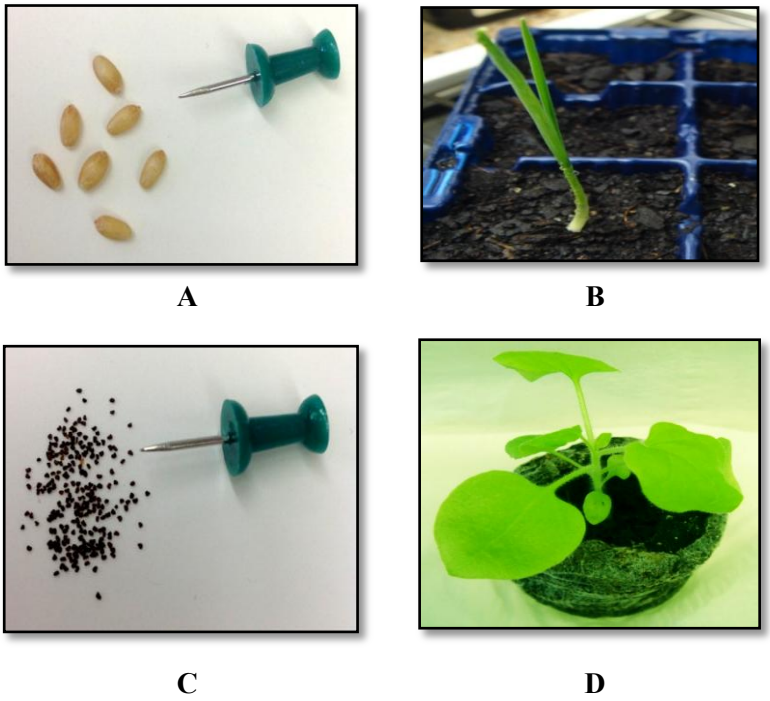

Figure 2.1 Wheat and *N. benthamiana* seeds and plantlets.
A: Wheat seeds (*T. aestivum* L cv. Rosella); B: Wheat plantlet (3 weeks); C: *N. benthamiana* seeds; D: *N. benthamiana* plantlet (3 weeks).

2.7 General molecular methods

2.7.1 Genomic DNA extraction

Genomic DNA (gDNA) was extracted from the leaves of the wheat (*T. aestivum* L cv. Rosella) seedlings (grown as above) using the Wizard® Genomic DNA Purification Kit (Promega, Australia), according to the protocol supplied. Approximately 100 mg of the leaf tissue was snap-frozen in liquid nitrogen, ground to a powder using a mortar and pestle, mixed with 600 µL Nuclei Lysis solution and incubated at 65°C for 15 minutes. Then 3 µL of RNase A (4 mg/mL) was added and the solution incubated at 37°C for 10 minutes. 200 µL Protein Precipitation solution was added and the mixture centrifuged at 10000×g for 5 minutes. The supernatant was carefully mixed with 600 µL isopropanol and centrifuged as above for 5 minutes. The DNA pellet was washed in 400 µL of 70% ethanol and re-spun as above. The DNA pellet was air-dried, dissolved in 70 µL TE buffer and stored at -20°C. Then 5 µL of the DNA solution was run on a 1% agarose gel in TAE buffer to determine quality, any degradation and approximate size.

2.7.2 Plasmid DNA purification

The HiYield™ Plasmid Mini Kit (RBC, Taiwan) and the related instructions were used for all plasmid preparations. A single colony of a bacterial culture was inoculated into 3 mL LB with relevant antibiotics (carbenicillin) and grown overnight at 37°C temperature and 220 rpm. The cultures were pelleted for one minute at 200×g. The cell pellets were resuspended in 200 µL PD1 buffer (Resuspension solution), mixed with 200 µL PD2 buffer (Cell Lysis solution) and incubated at room temperature (RT) for two minutes. Subsequently, 300 µL PD3 buffer (neutralisation) was added to the lysate and the solution centrifuged for three minutes at 200×g. The supernatant was transferred to a spin-column assembly (provided with the kit) and centrifuged at 200×g for one minute. The flow-through was discarded and the column washed twice with diluted W1 and Wash buffers. The plasmid DNA was eluted by addition of 30 µL Elution buffer to the column and centrifugation at 200×g for two minutes. DNA (5 µL) was electrophoresed to check it quality and the DNA concentrations determined using a Spectrophotometer. The methodology detailed above was applied to all non-recombinant or recombinant plasmid preparations from transformants in *E. coli* Mach1 or *E. coli* XL-1 Blue.

2.7.3 Spectrophotometric quantification of DNA

Purified genomic DNAs were diluted 1:50 with sterile MilliQ water to determine the DNA concentrations based on absorbance recorded at 260 nm and 280 nm using the SmartSpec 3000 Spectrophotometer (Bio-Rad, USA), which also reported the concentration based on absorbance of 1 at A_{260}=50 µg/mL of double stranded DNA. The A260/A280 absorbance ratio of 1.8 to 2 was used as an indication of high purity (Sambrook and Russell, 2001). Purified plasmid DNA concentrations were determined with 1 µL of sample using NanoDrop™ 1000 Spectrophotometer.

2.7.4 Agarose gel electrophoresis

Agarose gel electrophoresis was used for multiple purposes such as qualitative examination of the isolated gDNA, its approximate quantification, determining the sizes of PCR products or restriction fragments, and purifying selected bands. Agarose gels were typically prepared as 1% (w/v) gels in 1×TAE buffer with SYBR® Safe DNA gel

stain (0.5 μg/mL; Invitrogen) added to the cooled gel solution. Electrophoresis was typically performed at 100V for 30-90 minutes. The DNA samples were mixed with a 5×loading dye and loaded onto gels. A molecular weight marker such as the Hyperladder™ I (10,000-200bp; Bioline) was used for fragment size estimation and for approximate estimation of DNA concentrations by comparison of the intensity of the test DNA bands with that of the marker fragments. The gels were viewed on a UV transilluminator and photographed using a Chemidoc system (UVP, USA).

2.8 The polymerase chain reaction (PCR) for gene amplifications

2.8.1 Design and synthesis of primers

Primers for gene amplifications by the polymerase chain reaction (PCR) were designed using Netprimer (http://www.premierbiosoft.com/netprimer; last accessed October 2013) with the following criteria: length 18-25 bp (without tag), a 3' G/C clamp, percentage of GC content kept to approximately 50%, minimisation of secondary structures such as dimers, cross-dimers and hairpins and the difference between annealing temperatures of the forward and reverse primers limited to ±5°C. All primers were synthesised commercially by Invitrogen (Australia) and supplied as desalted pellets. The pellets were re-suspended in sterile MilliQ water to a stock concentration of 2 μg/μL and stored at -20°C. The working concentration in standard PCR was 0.1 μg/μL (approximately 10 μM depending on primer length and sequence). The specific primers designed for amplifying the *Pina* and *Pinb* genes and various protein expression strategies are detailed in separate sections below.

2.8.2 Design of primers for amplification of full-length *Pin* genes

Primers *Pina-D1*-Forward and *Pina-D1*-Reverse were designed to amplify the entire coding sequence (start to stop codon) of the wild type (WT) allele *Pina-D1a* of the *Pina* gene (Gautier et al., 1994) (Genbank accession number DQ363911) (Table 2.6).

Likewise, *Pinb-D1*-Forward and *Pinb-D1*-Reverse were designed to amplify the entire coding sequence of the WT allele *Pinb-D1a* (Gautier et al., 1994) (Genbank accession number DQ363913).

Table 2.6 Primer used for the wild type full length *Pina-D1* and *Pinb-D1* amplifications

Amplicons	Primers sequence*	Expected product size
Pina-D1	*Pina-D1*-Forward 5'-**ATG**AAGGCCCTCTTCCTCA-3'	447bp (Genbank: DQ363911)
	Pina-D1-Reverse 5'-**TCA**CCAGTAATAGCCAATAGTG-3'	
Pinb-D1	*Pinb-D1*-Forward 5'-**ATG**AAGACCTTATTCCTCCTA-3'	447bp (Genbank: DQ363913)
	Pinb-D1-Reverse 5'-**TCA**CCAGTAATAGCCACTAGGGAA-3'	

*Start and stop codons are shown in bold

2.8.3 Design of primers for directional cloning into magnICON® and BiFC vectors

These are described in chapter-specific methods sections below.

2.8.4 Typical PCR conditions

Routine amplifications such as those of *Pina* and *Pinb* genes from gDNA or inserts from recombinant plasmids, were generally carried out in 25 µL volumes, consisting 12.5 µL of 2×BioMix™ Red (Bioline, Australia), 5-10 ng plasmid DNA or 100 ng of first-round PCR products as templates, and 0.1 µg of each forward and reverse primer. Negative control reactions were identical except that the template DNA was omitted. All amplifications involved an initial denaturation at 94°C for 5 minutes. This was followed by 35 cycles of denaturation at 94°C (30 seconds), annealing at primer-specific temperature (30 seconds) generally 5°C below the theoretical annealing temperatures for both primers, extension at 72°C (30 seconds) and then a final extension at 72°C for 5 minutes. The extension time was estimated roughly using 2 kb/min as the rate of Taq polymerase activity at 72°C. The BioMix™ Red contains an inert red dye that permits easy visualisation and direct loading onto a gel. Five µL aliquots of the PCR products were examined by gel electrophoresis.

2.8.5 PCR for directional cloning of *Pin* genes into plant expression vectors

The PCRs for amplifying the mature protein-encoding sections of *Pin* genes (i.e., without the putative signal peptides; Gautier et al., 1994) for directional cloning into various expression vector systems (described later) were conducted using KOD Hot Start DNA Polymerase (Novagen, Germany) for increased specificity. For each reaction, the following was assembled in a 0.5 mL PCR tube: 5 µL 10×PCR buffer for KOD Hot Start DNA polymerase, 0.2 mM dNTPs and 1 mM $MgSO_4$, 200 ng gDNA or

5-10 ng plasmid DNA, 0.5 U/μL of KOD Hot Start DNA Polymerase, each primer to a final concentration of 0.3 μM and sterile MilliQ water to a final volume 50 μL. Negative controls (no template) were also included. The polymerase was activated by heating for 2 minutes at 95°C followed by 35 cycles of denaturation at 95°C (20 seconds), annealing at 60°C (10 seconds) and extension at 72°C (15 seconds). The results were assessed by agarose gel electrophoresis using 5 μL of each PCR products.

2.8.6 Purification of PCR products

The PCR products (when of a single size) or DNA bands of interest were purified using HiYield™ gel/PCR fragments extraction kit (RBC, Taiwan). For purification from gels, the desired band was excised and weighed (maximum 300 mg in one tube). The gel slice was mixed with 500 μL of DF buffer and incubated at 55°C for 10 minutes to melt the gel. The mixture was transferred to a spin column assembly (provided with the kit) and centrifuged at 6,000×g for 30 seconds. The column was then washed with 500 μL wash buffer. The assembly was centrifuged for additional 30 seconds at 10,000×g to ensure wash buffer was removed completely. The elution buffer (20 μL) was then added to the centre of the spin column, incubated for 2 minutes at RT and centrifuged at 10,000×g for 2 minutes. The eluted purified DNA was stored at -20°C. The kit was also used for direct clean-up of PCR products, prior to restriction digestion and/or cloning. The reaction (up to 100 μL) was transferred to a microcentrifuge tube. Five volumes of DF buffer were added and mixed, followed by the steps as above. The eluted DNAs were quantified by gel electrophoresis and/or NanoDrop^{TM} 1000 spectrophotometer.

2.9 Cloning and DNA sequencing

2.9.1 Restriction enzyme digestions of PCR products and vectors

A restriction digest typically contained 100-200 ng DNA substrate, 1 μL of a restriction enzyme (typically 20 U/μL; New England Biolabs), 10 μL of the appropriate NEB buffer, 1 μL BSA (10 mg/mL; New England Biolabs) and sterile MilliQ water. For *in planta* expression of putative mature PIN proteins, the PCR products of full-length *Pina* and *Pinb* genes were re-amplified with primers containing added restriction sites (and additional tags) for directional cloning into various expression vectors (detailed in

sections 2.13.3 and 2.14.4). These second-round PCR products and the corresponding vectors were double-digested with two appropriate enzymes together to enable their ligations. All reactions were incubated at 37°C for 2 hours. An aliquot was tested on an agarose gel to check the success of digestions.

2.9.2 Ligation reactions

Ligations were typically performed in 10 µL volumes containing 1 µL ligase buffer (10x), 1 µL rapid T4-ligase (NEB), 50 ng digested plasmid DNA vector and 200 ng insert (e.g., the purified or restriction-digested PCR products). For an efficient ligation, the amount of plasmid vector should be one third of the insert, in terms of the number of molecules. The amount of insert was calculated as per Sambrook and Russell (2001):

$$\text{Insert (ng)} = \frac{\text{Vector (ng)} \times \text{Insert (Kb)}}{\text{Vector (Kb)}} \times \text{molar ratio } \frac{\text{Insert}}{\text{Vector}}.$$

Ligation reactions without insert were used as negative controls. The reactions were held at 4°C overnight and then transformed into chemically competent *E. coli* Mach1 cells.

2.9.3 Preparation of chemically competent cells of *E. coli* Mach1

Chemically competent *E. coli* Mach1 cells were prepared according to Inoue et al. (1990) with minor modifications. A single colony from a LB agar plate was inoculated into 5 mL LB medium and incubated overnight at 37°C on a shaker (200 rpm). This culture was used to inoculate 250 mL of SOB medium and incubated at 37°C with shaking until the cell density reached OD_{600} = 0.5. The culture was cooled on ice for 10 minutes then 40 mL of it was transferred into 50 mL tubes, followed by centrifugation at 2,500×g for 10 minutes at 4°C. The pellets were resuspended in 12 mL ice-cold TB buffer and incubated on ice for 10 minutes. The washing step was repeated and the cells were resuspended in 3 mL of TB buffer. This was followed by the addition of DMSO to a final concentration of 7% (v/v) with gentle mixing and incubation on ice for 10 minutes. The cell suspension was dispensed into 0.1 mL aliquots into prechilled tubes, which were then snap frozen in liquid nitrogen and stored at -80°C.

2.9.4 Transformation of *E. coli* Mach1 competent cells by heat shock

A tube of the above cells was thawed on ice for 5 minutes and 10 µL of a ligation reaction was added to it. The suspension was held on ice for 20 minutes, followed by heat-shock at 42°C for 50 seconds, then holding on ice for 2 minutes. The cells were transferred into 0.5 mL SOC medium and incubated at 37°C for 1 hour with shaking (200 rpm) then spread onto LB agar containing 100 µg/mL of carbenicillin and incubated for 16 hours at 37°C.

2.9.5 Screening of *E. coli* transformants containing recombinant plasmids by colony PCR

The recombinant colonies containing inserts in pICH-11599 or pNBV vectors cannot be distinguished from non-recombinant ones with blue/white selection, as the pICH vector does not carry the lacZ gene for the α-peptide of ß-galactosidase and the lacZ gene is also not active in pNBV. Hence colony PCR was used, wherein half each of many individual (all white) colonies from *E. coli* transformants were picked from the LB plates and transferred into 25 µL 2x Red PCR mix and the DNA amplified using gene specific primers (Table 2.7 and 2.11). The results were assessed using gel electrophoresis. For the colonies which were found positive for inserts, the remaining half colony was inoculated into 5 mL LB broth with the appropriate antibiotic and grown overnight at 37°C with shaking (200 rpm) and used for plasmid purification (Section 2.7.2).

2.9.6 Preparation of electro-competent *A. tumefaciens* cells

Agrobacterium strain GV3101 cells were prepared as per Mattanovich et al. (1989) with minor modifications. The stock culture was streaked onto a non-selective LB agar agar plate and grown for 1.5 days at 28°C with shaking (200 rpm) in 10 mL LB media containing 50 µg/mL rifampicin. One mL of this culture was used to inoculate 100 mL LB medium containing 50 µg/mL rifampicin and incubated at 28°C with shaking until the cell density reached OD_{600}=0.6. The culture was chilled before centrifugation of 25 mL of it at 2000×g for 20 minutes at 4°C. The supernatant was discarded and the cell pellet resuspended in 25 mL of ice cold 1 mM HEPES buffer (pH 7) and centrifuged. The cells were resuspended gently into 2 mL ice-cold glycerol (10%) and then a further

10 mL glycerol (10%). The cells were pelleted again and resuspended in 300 µL of glycerol (10%) with gentle mixing then aliquoted into 45 µL batches in pre-chilled tubes, which were stored at -80°C.

2.9.7 Electroporation of electro-competent *A. tumefaciens* cells

Electroporation was performed in 2 mm electroporation cuvettes using 1 µL of (non-recombinant or recombinant) plasmid DNA and 45 µL electro-competent *Agrobacterium* cells prepared as above. After mixing above, the cuvettes were incubated on ice for 5 minutes, then put into the electro holder of Gene Pulser (Bio-Rad, USA) and pulsed at 2.5kv (kilovolts), 200Ω (ohm), 25µF (Microfarad), 5.7msec (millisecond). One mL LB was immediately added into the cuvette. Cells were transferred into a culture tube and shaken at 28°C for 60 minutes. All non-recombinant magnICON® modules (extracted earlier from their *E. coli* XL1 Blue hosts) and all recombinant pICH11599 vectors were electroporated individually into *A. tumefaciens,* plated on plates with 100 µg/mL carbenicillin plus 50 µg/mL rifampicin selections and grown at 28°C for two days. Recombinant pMLBART vectors were also electroporated and grown on 50 µg/mL spectinomycin plus 50 µg/mL rifampicin selections at 28°C for two days.

2.9.8 Screening of *A. tumefaciens* transformants containing recombinant plasmids by colony PCR

Colony PCR was used to identify colonies of *A. tumefaciens* containing inserts. Half each of many individual colonies from *A. tumefaciens* transformants were picked from the LB plates and transferred into 25 µL 2x Red PCR mix volume and the DNA amplified using gene specific primers as above. The results were assessed using gel electrophoresis. The remaining half-colonies of interest were inoculated into 5 mL LB broth with the appropriate antibiotics and grown overnight at 28°C with shaking (200 rpm) for preparing the glycerol stock (750 µL of bacterial culture plus 750 µL LB glycerol) and processing for infiltration to the plant.

2.9.9 DNA sequencing

All plasmids from *E. coli* Mach1 were prepared using HiYield™ plasmid mini kit (RBC, Taiwan), as mentioned earlier. These were sequenced using the BigDye Terminator (BDT) version 3.1 (Applied Biosystems, USA) according to the instructions of the Australian Genome Research Facility (AGRF, Melbourne, Australia). The reactions contained 1 µL BDT reagent, 2 µL 5×BDT buffer, 200-500 ng plasmids DNA template and 3.2 pmol sequencing primer (*Pin* gene based primer), made up to 10 µL with sterile MilliQ water. The cycling conditions were as follows: initial denaturation at 96°C for 2 minutes then 35 cycles of denaturation at 96°C for 10 seconds, primer annealing at 50°C for 5 seconds and extension at 60°C for 4 minutes. Following this, the reactions were cleaned up by the addition of 75 µL of 0.2 mM $MgSO_4$ ethanol solution, incubated at RT for 15 minutes and centrifuged at 200×g for 20 minutes. The pelleted DNA was washed with 100 µL 70% ethanol followed by centrifugation using the same conditions. The pellets were air-dried and resuspended in 20 µL sterile MilliQ water. The solution was submitted to the AGRF (Melbourne) for capillary separation using an AB3730x/DNA Analyser. The resulting chromatograms were inspected visually using BioEdit (http://www.mbio.ncsu.edu/bioedit/bioedit.html) for quality checking. Generally, sequencing was done in both forward and reverse directions.

2.10 Bioinformatics methods

2.10.1 Sequence alignments

The putative amino acid sequences were translated from the nucleotide sequence data and aligned using Bioedit v 7.1.11 sequence alignment editor program. Bioedit also was used for analysis of gene sequences of *Pina-D1*, *Pinb-D1*. The alignments of DNA sequences were performed with homologous sequences found in Genbank (http://www.ncbi.nlm.nih.gov/genbank).

2.10.2 Plasmid vector maps

Vector maps of pNBV and pMLBART plasmids were created using A plasmid Editor (ApE) software v 8.5.2.0 (http://biologylabs.utah.edu/jorgensen/wayned/ape; last accessed March 2014) for sequence annotation, virtual digests and circular schematic sequence representation.

2.10.3 Predictions of the isoelectric point (pI) and molecular weight (Mw) of PIN proteins

The pI and Mw of the putative mature PINA and PINB sequences were determined using the 'compute pI/Mw tool' at the Expert Protein Analysis System (ExPAsy) (http://web.expasy.org/compute_pi/).

2.10.4 Prediction of protein subcellular localisation

The subcellular locations of mature PINA and PINB were predicted for plant systems using WoLF PSORT (http://www.genscript.com/psort/wolf_psort.html), which is an extension of the PSORT II program for converting protein amino acid sequences into numerical localisation features; based on sorting signals, amino acid composition and functional motifs (Horton et al., 2007).

2.10.5 Modeling and structure prediction of proteins

The putative amino acid sequences of wild type PIN proteins were submitted to the Iterative Threading Assembly Refinement (I-TASSER). Using this method, three dimensional (3D) atomic models were generated from multiple threading alignments and iterative structural assembly simulations (Roy et al., 2010; Zhang, 2008). The structures were visualized using molecular visualisation system and the final structural models with tryptophan-rich domain (TRD) and hydrophobic domain (HD) produced using PyMOL (http://www.pymol.org/; last accessed January 2014) (Delano, 2002). The output of the I-TASSER server included the following: five full length atomic models (ranked based on cluster density), the images of the predicted models and their estimated accuracy (including confidence score of all models and prediction of TM-score and RMSD for the first model), the predicted secondary structures, predicted solvent accessibility and 10 proteins in PDB (Protein Data Bank) which are structurally closest to the putative models (Roy et al., 2010). The 'C-score' is a confidence score for estimating the quality of the predicted models by I-TASSER and is calculated based on the significance of the threading template alignments and the convergence parameters of the structure assembly simulations and is highly correlated with the TM (template modelling)-score and RMSD (root-mean-square-deviation). The latter two are used as standards for measuring similarity between two structures, and are useful in

determining the accuracy of structure modelling when the native structure is unknown. A TM-score > 0.5 indicates a model of correct topology and TM-scores < 0.17 indicates random similarity (Roy et al., 2010).

2.10.6 Protein-Protein complexes structure prediction

Threading-recombination approach, (http://zhanglab.ccmb.med.umich.edu/COTH/) (CO-Threader: COTH) (Mukherjee and Zhang, 2011) is based on to fold-recognition and structural recombination of protein-protein complexes prediction by combining tertiary structure templates with complex alignments. The sequences are first aligned to complex templates using a modified dynamic programming algorithm. The monomer templates are then structurally superposed to the dimer template to generate the final models. The final protein-protein complex predictions for PINA+PINB and PINAΔHD+PINBΔHD were produced using PyMOL.

2.11 Biochemical methods for protein analysis

2.11.1 Protein concentration measurements

Protein concentrations were measured according to Bradford (1976) using the Bradford reagent (Bio-Rad, USA) for microtitre plate applications as described by the supplier. The Bio-Rad dye reagent concentrate was diluted 1:5 with sterile MilliQ water and filtered with Whatman filter paper 1. Bovine serum albumin (BSA) was used to generate the standard curve using the range of 0.1, 0.2, 0.3, 0.4 and 0.5 mg/mL. Protein samples (total soluble proteins or purified recombinant PIN proteins expressed in *N. benthamiana*; described later) were diluted 1:10 and/or 1:50 in PBS. To each well in a microtiter plate, 10 µL of each of the samples and standards (duplicates of each dilution) was added, followed by 200 µL of diluted dye regent, and incubated for 10 minutes. The absorbance was measured using a Microplate reader (Thermo Fisher, USA) at 595 nm wave length. The protein concentration of each unknown sample was calculated from the standard curve.

2.11.2 SDS-PAGE

Sodium dodecyl sulphate (SDS)-polyacrylamide gel electrophoresis (PAGE) was used to assess protein expression profiles, sizes of the (denatured) expressed PIN proteins and purity at various stages of purification. Samples were mixed with 5 µL of 5x protein loading dye and boiled for two minutes. The proteins of interest were separated using a 15% ReadyGel® Tris-HCl gel (Bio-Rad, USA) in running buffer at 20 mA for 1 to 2 hours. The gel was immersed in Coomassie Blue staining solution with gentle rocking for one hour then immersed overnight in de-staining solution. A molecular weight marker (250 kDa to 2 kDa) was used as size standards (Table 2.2).

2.11.3 Western blotting analysis for PIN proteins detection

Western blot analyses were carried out using the Durotest®S kit (R-Biopharm, Rhone Ltd., http://www.r-biopharm.com/wp-content/uploads/4173/DUROTEST-S-Follow-On-P10.pdf; last accessed February 2014). The kit has a monoclonal antibody raised against friabilin and it is highly specific for the PIN proteins, which are the two major components of friabilin (Greenwell et al., 1992; Rakszegi et al., 2009; Wiley et al., 2007). The kit is commonly used in the pasta industry for rapid detection of adulteration of durum wheat (semolina, which lacks PINs) with common wheat flour, which contains the friabilin (mostly PINs). The kit contains two standards for the test: (i) 100% durum flour, and (ii) durum flour containing 3% non-durum flour (i.e., common wheat flour). The epitope recognised by the Durotest antibody has not been mapped (Greenwell et al. 1992; Wiley et al., 2007).

The total soluble proteins or purified recombinant PINs expressed in *N. benthamiana* (described later) were identified through western blotting as described by Rakszegi et al. (2009) and Wiley et al. (2007) with modification. Proteins was fractionated by SDS-PAGE then transferred to polyvinylidene difluoride (PVDF) transfer membrane (Millipore, Australia) in transfer buffer. The membrane was blocked in 0.5% MPBST for one hour at 4°C on shaker. The Durotest antibody was used at a dilution of 1 in 1000 in 3 mL 0.3% MPBST and incubated for ten minutes at RT by using SNAP i.d.® protein detection system (Millipore, Australia). The membrane was washed three times with PBST, then incubated with the secondary antibody (the anti-mouse horseradish

peroxidise (HRP) conjugate produced in goat) at a dilution of 1 in 1000 in 3 mL 0.3% MPBST for ten minutes at RT by using SNAP id.® system. Following three washes with PBST, the membrane was incubated in chemiluminescent detection reagents (ECL) (Millipore, Australia) for five minutes and exposed to a Kodak, BioMax light film (Sigma, USA) for 30 seconds or 1 minute and developed by AGFA CP1000 processor.

2.11.4 Enzyme-linked immunosorbent assay (ELISA) for approximate quantitation of recombinant PIN proteins

Indirect ELISA involves two binding processes: binding of a primary antibody to the antigen of interest coated to the microtitre plate surface, and binding of a conjugated secondary antibody to the primary antibody, followed by assay of activity of the thus-activated enzyme linked to the secondary antibody (Figure 2.2). The ELISA protocol for PIN proteins was based on Zhang et al. (2010a) with modifications. The concentration of PIN proteins expressed in the total soluble protein (TSP) extracts from infiltrated *N. benthamiana* leaves (described later) were quantified approximately using extract of 3% non-durum wheat (Durotest kit; R-Biopharm Rhone Ltd) with different dilutions for developing a standard curve. The TSP samples were diluted 1/50, 1/100 and 1/200 in coating buffer. Each well (of a 96-well plate) was coated with 100 µL of the diluted protein samples and left overnight at 4°C. The plate was washed three times at RT with a phosphate buffered saline solution containing Tween-20 (PBST), then blocked with 300 µL PBS containing 1% (w/v) bovine serum albumin (PBS-BSA) and incubated for two hours at RT. Following three washes with PBST, 100 µL of the Durotest antibody (diluted 1:1000 in PBS-BSA) was added and the plate incubated overnight at 4°C. The plate was washed three times at RT with PBST. Then 100 µL solution containing goat anti-mouse horseradish peroxidase (HRP) conjugated antibody (Sigma, USA) was added (dilution 1:1000 in PBS-BSA) to the plate. The plate was incubated at RT for one hour and then wells washed five times with PBST. One hundred µL TMB (3, 3′, 5, 5′-Tetramethylbenzidine) (Sigma, USA) was added and plates incubated for 15 minutes at RT. The reactions were stopped by addition of 100 µL H_2SO_4 (0.18 M) and absorbance was measured at 450 nm using a microplate reader (Thermo Fisher, USA). The coating buffer and infiltrated leaf without *Pin* construct were used as negative controls.

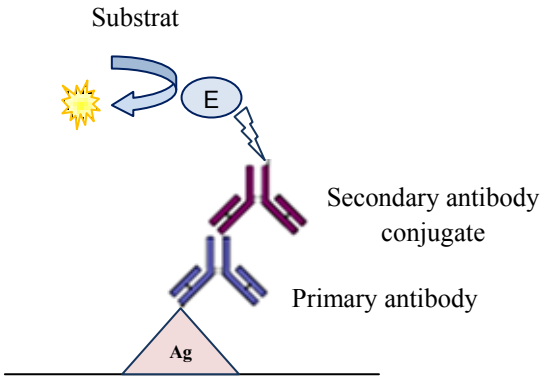

Figure 2.2 Diagram of indirect ELISA assay.
The antigen (Ag) of interest is coated directly to the assay plate and detection of the antigen performed using enzyme-conjugated (E) to the unlabeled primary and conjugated secondary antibodies.

2.12 Testing of antimicrobial properties of the *in planta* expressed PINs and a PIN-based synthetic peptide

2.12.1 Design of synthetic peptide based on PINA

The peptide PuroA (FPVTWRWWKWWKG-NH2) was modeled on the TRD of PINA and used as control for antimicrobial activity, as it had been tested previously (Jing et al., 2003; Phillips et al., 2011). The peptide was synthesised at >95% purity by Biomatik Corporation (Ontario, Canada) by solid-phase method using N-(9-flurenyl) methoxycarbonyl (Fmoc) chemistry, with C-terminal amidation (NH_2). Stock solution was prepared at 1 mg/mL in 0.01% glacial acetic and stored at -20°C.

2.12.2 Antibacterial activity assay

Escherichia coli (ATCC 25922) and *Staphylococcus aureus* (ATCC 25923) were used to test the antibacterial activity of the PIN proteins expressed in *N. benthamiana.* The minimum inhibitory concentration (MIC) was determined by the microtitre broth dilution method (Wiegand et al., 2008) with modifications. Bacterial suspension from an overnight culture was adjusted in Mueller-Hinton Broth (MHB; Oxoid, USA) to 1×10^{8} CFU/mL using a spectrophotometer (OD_{600}= 0.08-0.13). The suspension was diluted in MHB to 5×10^{5} CFU/mL. Recombinant purified PIN, from the elution steps of the His-tag purification and hydrophobic interaction systems (see later) in approximately 1 mg/mL stock concentrations (measured by Bradford assays) were added (25 µL) to the wells of sterile flat-bottomed 96-well plates (Corning, Australia)

and a two-fold serial dilution was carried out across each row with a starting concentration of 250 μg/mL and final concentration of 0.5 μg/mL. The wells were then inoculated with 75 μL of the bacterial suspension and incubated overnight at 37°C. The MIC values were determined by visual observation of bacterial growth as well as measuring absorbance at 595 nm using a microplate reader (Thermo Fisher, USA). All protein samples were tested in triplicate. The MIC was defined as 'the lowest concentration of antimicrobial agent that prevents visible growth of microorganism under defined conditions' (Wiegand et al., 2008).

2.12.3 Antifungal activity assay

The antifungal activity of PIN proteins was determined by microbroth assay (Broekaert et al., 1990) with modifications. Filamentous fungal cultures of *Colletotrichum graminicola, Drechslera brizae, Fusarium oxysporum, Rhizoctonia cerealis* and *Rhizoctonia solani* were grown in Potato Dextrose Broth (PDB; Difco-BD, USA) for seven days at 25°C with shaking (200 rpm). Mycelia were vortexed vigorously and the resulting suspension adjusted with PDB to a concentration of 0.8-5×10^6 mycelia fragments/mL (OD_{600} = 0.15-0.17). The suspension was diluted 1:50 with PDB to a final concentration 0.4-5×10^4 mycelia fragments/mL (Espinel-Ingroff and Cantón, 2007). Sterile water (~200 μL) was added to the outermost wells of plates when testing filamentous fungi, so as to reduce the effects of evaporation from the test sample wells during the longer incubation times. Recombinant purified PINs, from the elution steps of His-tag purification and hydrophobic interaction systems in approximately 1 mg/mL stock concentrations (measured by Bradford assays) in 25 μL volumes were added to the first empty well and a two-fold dilution was carried out across each row with a starting protein concentration of 500 μg/mL and a final of 2 μg/mL. Test wells were subsequently inoculated with 75 μL of the fungal mycelia and incubated at 25°C in the dark for 5-7 days. Then, MIC values were measured which is defined as the lowest value to completely inhibit fungal hyphal growth (Espinel-Ingroff and Cantón, 2007). All protein samples were tested in triplicate.

2.12.4 Stability testing of recombinant PIN proteins

Aliquots of the protein solutions (the same as those tested above) were stored at 37°C, RT (between 20°C-25°C), 4°C, -20°C and -80°C for one week. Activity against *E. coli* was then determined as above, each sample being tested in triplicate.

2.12.5 Haemolytic activity assay

The haemolytic activity of recombinant PINs, from the elution step of the His-tag purification system in approximately 1 mg/mL (measured by Bradford assays) stock concentrations was tested as described by Dathe et al. (1996) and Phillips et al. (2011). The sheep red blood cells (RBCs) were isolated from defibrinated blood (Amyl Media, Australia) by centrifugation of the whole blood at 1200×g at 4°C for 10 minutes. The pellets were washed three times with PBS (pH 7.4) and resuspended in 2 mL PBS. Then, 25 µL aliquots of the RBC suspension were mixed with different concentrations of the purified PIN proteins and or the PuroA peptide (500-16 µg/mL) then incubated for 1 hour at 37°C with gentle shaking. The samples were centrifuged at 3,000×g for 5 minutes and the absorbance of the supernatant measured at 540 nm. PBS-only (no haemolysis expected) and 1% Triton X-100 (Sigma, USA) in PBS (100% haemolysis expected) were included as negative control and positive control respectively. Haemolytic concentration was defined as the concentration of the protein/peptide required to haemolyse 50% of the RBCs (HD_{50}).

Methods specific to Chapter 3:

2.13 Expression of PIN proteins in *N. benthamiana* using magnICON® viral vector and characterisation of their biochemical and antimicrobial properties

2.13.1 Principles of the magnICON® viral vector systems for *in planta* expression

The magnICON® viral vectors system is based on tobacco mosaic virus (TMV) and designed for *in planta* assembly from separate pro-vector modules to produce the protein. The gene of interest is cloned in a 3' vector module. Various 5' modules are then used for targeting the expressed protein to different parts of the plant cell (cytosol, chloroplast or apoplast). An integrase module is used for recombination of 3' and 5' modules *in planta*. These modules recombine within the plant cell and the resulting DNA is transcribed and the recombination sites (integrase) are spliced out, to create an RNA replicon to produce the desired protein (Marillonnet et al., 2004) (Figure 2.3). The protein is thus expressed in the appropriate subcellular compartment in the plant cell (depending on the 5' module used).

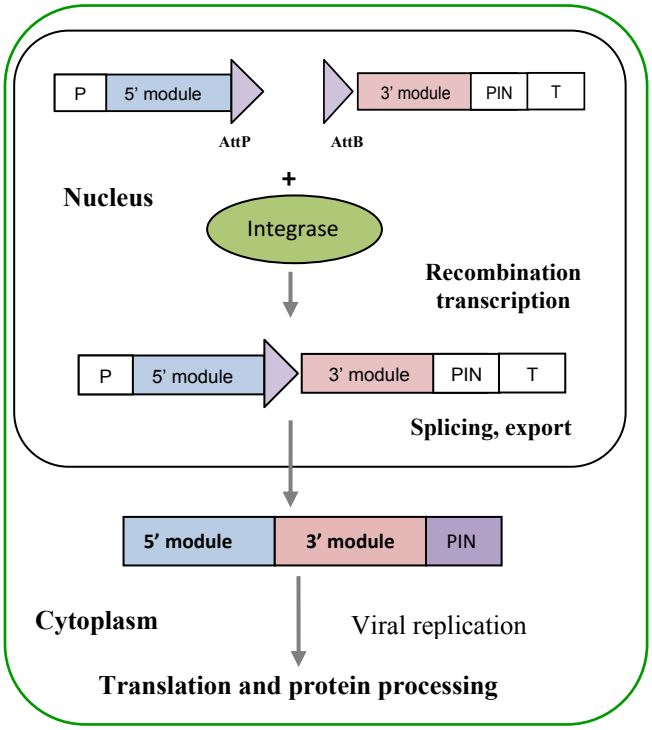

Figure 2.3 Schematic showing the assembly of the three viral vector modules and production of PIN proteins.
The 5' and 3' modules with integrase in the plant cell allow recombining via the AttP and AttB sites. The intron is then spliced out. Viral replication occurs and translation and PIN protein processing occurs. Source: modified from Marillonnet et al. (2004).

The vectors were obtained from ICON Genetics (Halle, Germany; http://www.icongenetics.com/html/home.htm; last accessed March 2014). The modules are ampicillin or carbenicillin resistance in *E. coli* and come as follows (Figure 2.4 and 2.5).

(i) Two 3' modules:

- [pICH11599]: 3' module for cloning the gene of interest at the multi-cloning site
- [pICH7410]: Green Fluorescent Protein (GFP)-expressing 3' module

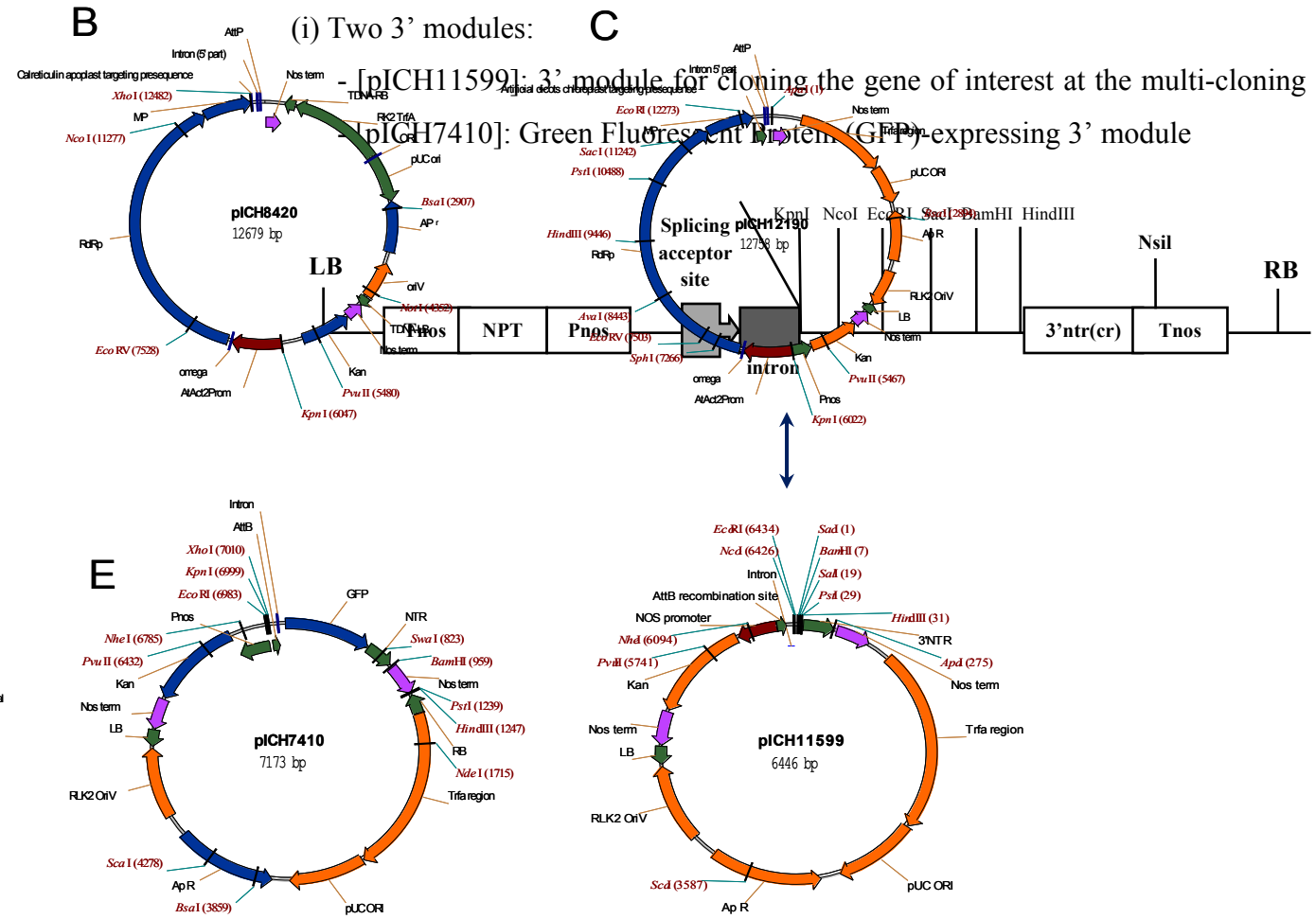

Figure 2.4 The 3' module pICH11599, for cloning in gene of interest at the multi-cloning site.

(ii) Various 5' modules for targeting the expressed protein to different compartments of the plant cell, including:

- [pICH15879]: untargeted (cytosol) 5' module
- [pICH8420]: apoplast-targeting 5' module
- [pICH12190]: chloroplast-targeting 5' module

(iii) [pICH14011]: the integrase module for recombination of the 3' and 5' modules within the plant cell

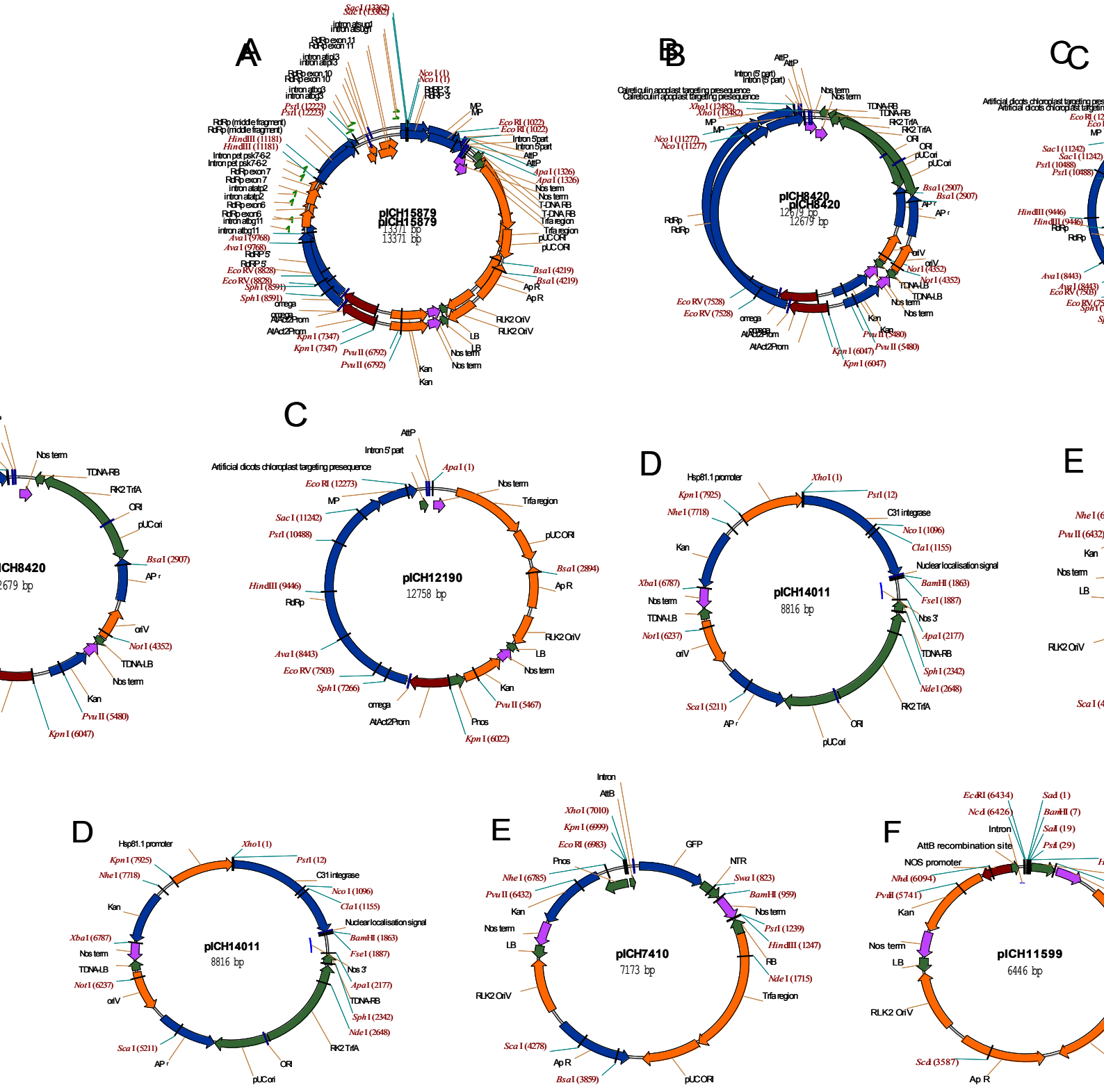

Figure 2.5 The other magnICON® viral vector modules.
Detailed vector maps for A: pICH15879, untargeted (cytosol) 5' module; B: pICH8420, apoplast-targeting 5' module; C: pICH12190, chloroplast-targeting 5' module; D: pICH14011, the integrase module; E: pICH7410, GFP expressing 3' module.

The above vector systems were used for the expression of the wheat *Pina* and *Pinb* genes in *N. benthamiana* to study the localisation of the PIN proteins and purify and characterise them. For this purpose, all above plasmids were extracted from their glycerol stock cultures in *E. coli* XL1 Blue (provided by Dr Diane Webster, Monash University) using the HiYield™ plasmid mini kit (Section 2.7.2). Four different 3' expression modules; pICH-PINA-His, pICH-PINB-His, pICH-PINA-His-SEKDEL and pICH-PINB-His-SEKDEL were then constructed in pICH-11599 such that they contained the gene sections encoding the putative mature PINA or PINB protein, with a C-terminal histidine tag (His-tag) or SEKDEL tag. The primer design and cloning processes for this purpose are detailed below.

2.13.2 Design of primers for directional cloning into the 3' module pICH11599

Primers were designed based on the open reading frame (ORF) encoding the mature proteins, i.e., without the 28 and 29 residue signal peptides of PINA and PINB, respectively (Gautier et al., 1994). For cloning of *Pina,* the nucleotide sequence encoding the restriction site for EcoRI was incorporated at the 5' end of the forward primer and the sequence for BamHI incorporated at the 5' end of the reverse primer. For cloning of *Pinb,* the restriction site for NcoI was incorporated in the forward primers and for SacI in the reverse primers. The reverse primer for both genes also contained a sequence that would encode a C-terminal six-histidine tag (His-tag) in the sense strand, to allow further protein purification. Further, another reverse primer was designed for each gene such that it also encoded a further C-terminal SEKDEL (Ser-Glu-Lys-Asp-Glu-Leu), the highly conserved eukaryotic endoplasmic reticulum (ER) retention signal (Munro and Pelham, 1987; Wang et al., 2008). A BamHI site was designed at the 5' end of both the pICH-PINA-His-SEKDEL and pICH-PINB-His-SEKDEL primers. A few extra spacer nucleotides were added to the primers before and after the restriction site to allow proper digestions. The primers are listed in Table 2.7. The expected PCR product sizes for both *Pin* genes with the His-tag and His-SEKDEL tag are shown in Table 2.8.

Table 2.7 Primers used in directional cloning into 3' viral module, pICH11599

Primer name	Sequence of primers used*	Cloning sites
Pina-His	**Forward:** 5'-GGTA*GAATTC*G*ATG*GAT GTTGCTGGCGGGGGTG-3'	EcoRI
	Reverse: 5'-CCG*GGATCCTCA***ATGGTGATGGTGATGGTG**CCAGTAATAGCCAATAGTGCC-3'	BamHI
Pinb-His	**Forward:** 5'-GAA*CCATG*GAA GTTGGCGGAGGAGGTGG-3'	NcoI
	Reverse: 5'-CCG*GAGCTCTCA***ATGGTGATGGTGATGGTG**CCAGTAATAGCCACTAGG-3'	SacI
Pina-His-SEKDEL	**Forward:** 5'-GGTA*GAATTC*G*ATG*GAT GTTGCTGGCGGGGGTG-3'	EcoRI
	Reverse: 5'CCG*GGATCCTCA***TAGCTCATCTTTCTCAGAATGGTGATGGTGATGGTG**CCAGTA3'	BamHI
Pinb-His-SEKDEL	**Forward:** 5'-GAA*GAATTC*G*ATG*GAA GTTGGCGGAGGAGGTGG-3'	EcoRI
	Reverse: 5'CCG*GGATCCTCA***TAGCTCATCTTTCTCAGAATGGTGATGGTGATGGTG**CCAGTA3'	BamHI

* Cloning sites to be incorporated for directional cloning are shown in italics and shaded. Nucleotides in bold and shade are sequences encoding the His-tag in the sense strand. Nucleotides in bold and underline are sequences encoding SEKDEL in the sense strand. Nucleotides in italics and wave underline encode start and stop codons. The first residue of mature PINs is boxed.

Table 2.8 Genes cloned with His-tag and His-SEKDEL tag into pICH11599

Clones	mature protein section of gene that was cloned into pICH11599	Final product size
pICH-PINA-His	PINA ORF from DVAGGG to stop (363 bp) +His-tag (18 bp)	381 bp
pICH- PINA-His-SEKDEL	PINA ORF from DVAGGG to stop (363 bp) +His-tag (18 bp)+SEKDEL(18 bp)	399 bp
pICH-PINB-His	PINB ORF from EVGGGG to stop (360 bp) +His-tag (18 bp)	378 bp
pICH-PINB-His-SEKDEL	PINB ORF from EVGGGG to stop (360 bp) +His-tag (18 bp)+SEKDEL (18 bp)	396 bp

2.13.3 Amplifications of *Pin* genes, restriction enzyme digestions, cloning into the 3' module pICH11599, and sequencing of clones

- The 447 bp full-length genes *Pina-D1* and *Pinb-D1* were amplified from the gDNA of *T. aestivum* cv. Rosella (with primers given in Table 2.6).
- These PCR products were then used as templates in second-round PCRs with the primer combinations given in Table 2.7, to amplify the gene sections encoding the mature PINs, with the His (and SEKDEL) tag(s) and the appropriate restriction sites.
- Both second-round PCR products were purified using HiYield™ gel/PCR fragments extraction kit (Section 2.8.6).

- The purified PINA PCR products (PINA-His and PINA-His-SEKDEL) were each double-digested with EcoRI and BamHI, as detailed in section (2.9.1).
- The empty vector pICH11599 was purified from the stock culture in *E. coli* XL-1 Blue using HiYield™ Plasmid Mini Kit (Section 2.7.2).
- An aliquot of pICH11599 was double-digested with EcoRI and BamHI.
- The two double-digests of PINA were ligated separately with the EcoRI-BamH1 digested pICH11599.
- Likewise, the purified PINB PCR product (PINB-His) and another aliquot of pICH11599 were each digested with NcoI and SacI and then ligated with each other.
- The purified PINB PCR product (PINB-His-SEKDEL) was double-digested with EcoRI and BamHI and then ligated with the double-digested pICH11599.
- The ligations were transformed into chemically competent cells of *E. coli* Mach1 (as detailed in Section 2.9.4), and plated on LB agar supplemented with carbenicillin.
- Several half-colonies per transformation were subjected to colony-PCR (Section 2.9.5) to identify those containing recombinant plasmids.
- The other half-colonies of interet were cultured and plasmids were prepared from these using HiYield™ plasmid mini kit (Section 2.7.2) and sequenced (Section 2.9.9)
- The steps are summarized in Figure 2.6.

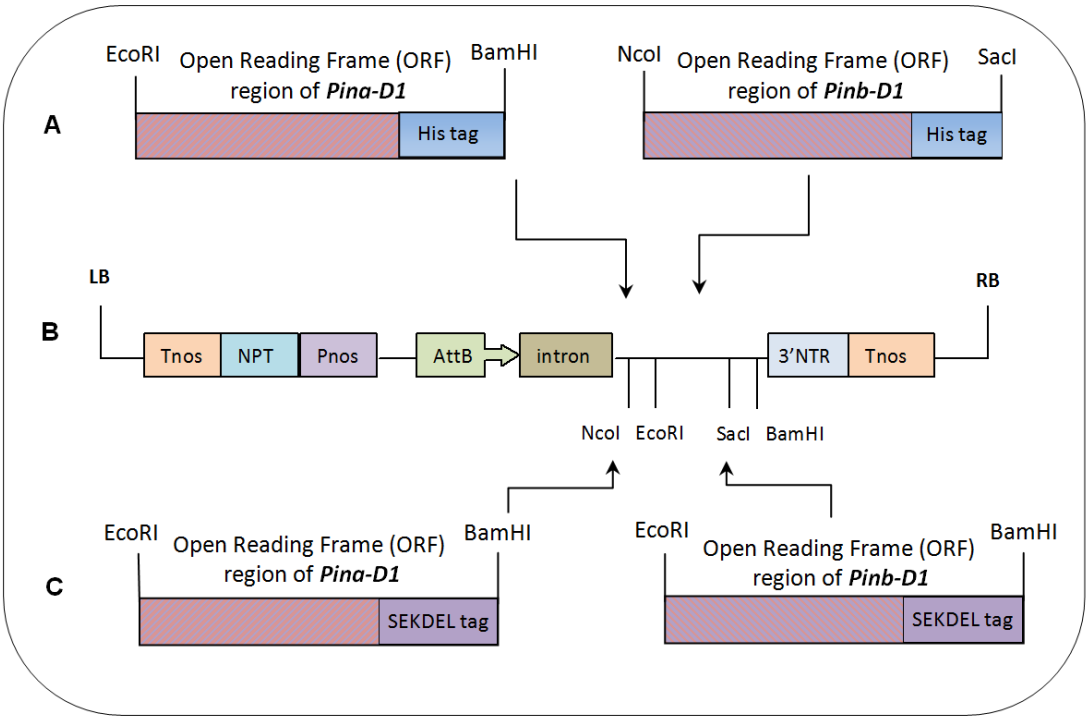

Figure 2.6 Generation of the *Pin* constructs in magnICON® viral vectors.
A: the open reading frame of *Pina* and *Pinb,* encoding the mature proteins, followed by the His-tag sequence, ligated into; B: the magnICON® viral vector 3' module; C: the open reading frame of *Pina* and *Pinb,* encoding the mature proteins, followed by the His-tag and SEKDEL sequence, ligated into magnICON® viral vector 3' module.

2.13.4 Electroporation of recombinant pICH11599 and other modules into *A. tumefaciens*

Following confirmation of correct DNA sequences encoding the mature PIN ORFs with the C-terminal His or His-SEKDEL tags, the recombinant pICH11599 vectors were electroporated into *A. tumefaciens* GV3101 (as described in section 2.9.7) and the bacteria grown on LB medium containing 100 µg/mL carbenicillin plus 50 µg/mL rifampicin selection at 28°C for two days. The colonies were screened by colony-PCR for recombinant plasmids using specific primers (Table 2.7). All non-recombinant vector modules were also electroporated individually into *A. tumefaciens*.

2.13.5 Agroinfiltration of *N. benthamiana* using the magnICON® viral vectors

Single colonies of *A. tumefaciens* cultures containing the different vectors were grown in LB medium supplemented with carbenicillin (100 µg/mL) and rifampicin (50 µg/mL) overnight at 28°C. Equal volumes (2.5 mL each) of three different cultures (Table 2.9) (OD_{600}=0.7 each) were mixed together in various combinations of (i) a 5'-module; (ii) a 3'-module; (iii) the integrase module. The mixture was then centrifuged at 600×g for ten minutes. The bacterial pellet was resuspended in 10 mL of infiltration buffer (Table 2.4) and infiltrated into leaves of 8 week old *N. benthamiana* plants using a 1 mL syringe without a needle (Figure 2.7). The injected area was marked with permanent marker pen for ease of identification. Plants were allowed to grow for a further 8 to 10 days in green house conditions before the leaves were harvested and frozen in liquid nitrogen then stored at -80°C.

Table 2.9 Tri-partatite infiltration of magnICON® constructs into *N. benthamiana*

Agrobacterium Culture / Infiltrated construct	**Integrase**	**Cytosol**	**Chloroplast**	**Apoplast**	**GFP**	**PINA Or PINB**	**PINA-SEKDEL Or PINB-SEKDEL**
Cytosol							
Chloroplast							
Apoplast							
ER							
GFPc							
GFPch							
Negative							

Columns show specific infiltrated constructs. Rows show the *Agrobacterium* cultures containing different viral vector modules. The colors show the mixture of *Agrobacterium* cultures for specific infiltrated constructs. GFPc: GFP cytosol targeting; GFPch: GFP chloroplast targeting.

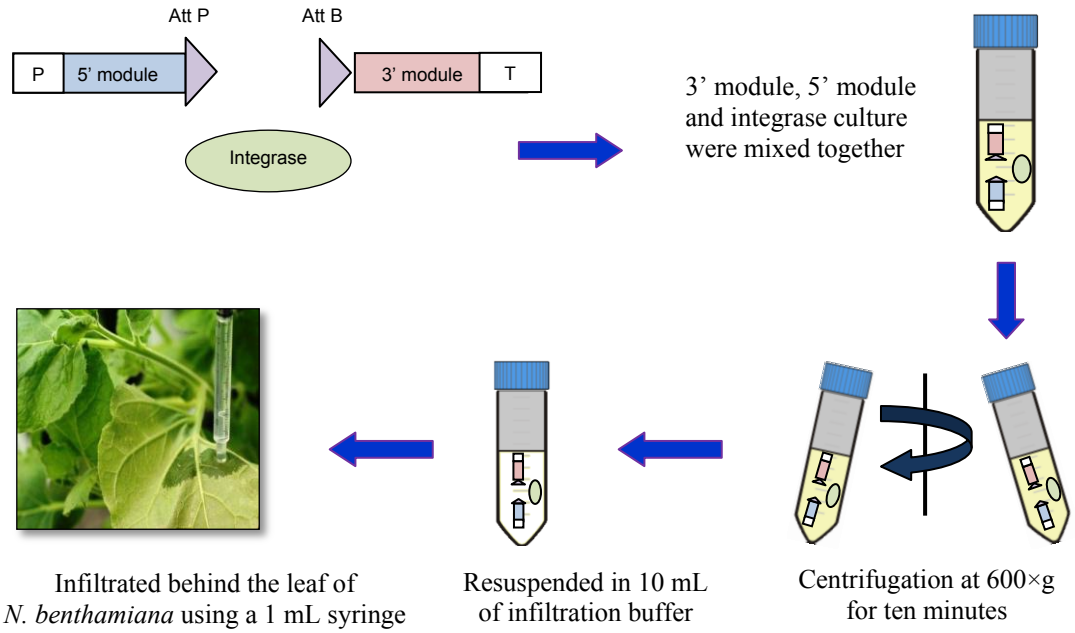

Figure 2.7 Agroinfiltration of *N. benthamiana* leaf.
Lower surface of leaf was infiltrated with *Agrobacterium* suspension in infiltration buffer.

2.13.6 GFP expression

The green fluorescent protein (GFP) is 238 amino acid long and has MW of 26.9 kDa. Shimomura et al. (1962) isolated GFP from the jelly fish *Aequorea victoria* and demonstrated that it could exhibit bright green fluorescence when exposed to light in the UltraViolet (UV) range. The gene for GFP was cloned by Prascher et al. (1992) and the protein was expressed in *E. coli* by Chalfie et al. (1994). A 3' viral vector containing the GFP gene (pICH7410) was infiltrated into *N. benthamiana* leaves side by side with the 5' module for cytosol or the 5' module for chloroplast. At 10 days post infiltration (dpi), GFP expression in leaves was checked under UV light (Spectroline UV transilluminator).

Protein methods

2.13.7 Extraction of total soluble protein (TSP) from *N. benthamiana* leaf

Pieces from the infiltrated area of the leaf (100 mg) were collected in pre-weighed two mL tubes and the tubes weighed again. Stainless steel beads of 5 mm diameter (Qiagen, USA) and 500 µL of extraction buffer [100 mM Ascorbic Acid, 0.1% Triton X-100, EDTA-free protease inhibitor cocktail tablets in PBS, pH 7.4] were added to each tube.

Leaf tissues were ground at 28 strokes per second for 1 minute using TissueLyserII (Qiagen, USA), then centrifuged at 4°C at 10,000×g for 10 minutes. The extract was filtered through Miracloth (Calbiochem, Australia) and centrifuged at 100×g for 5 minutes at 4°C. The clear supernatant was collected into a clean tube. The samples were either stored at -80ºC or used directly for western blot analysis. In further optimisations, different extraction buffers (Table 2.10) were used for TSP extraction before western blot analyses.

Table 2.10 Protein extraction buffers used in this study

No	Extraction buffers	References
1	PBS containing 100 mM Ascorbic Acid, 0.1% Triton X-100 or Triton X-114, protease inhibitor cocktail tablet	Webster et al. (unpublished)
2	PBS containing 100 mM Ascorbic Acid, 20 mM EDTA, 0.1% Triton X-100, protease inhibitor cocktail tablet	Webster et al. (2009)
3	50 mM Tris (pH 8.8), 50 mM NaCl, 10 mM EDTA, 1 µg/mL leupeptin, protease inhibitor cocktail tablet	Sorrentino et al. (2009)
4	PBS containing 50 mM Tris (pH 8.8), 50 mM NaCL, 10 mM EDTA, 1 µg/mL leupeptin,100 mM ascorbic acid, 0.1% TritonX-100, protease inhibitor cocktail tablet	Tremblay et al. (2011)

2.13.8 Protein concentration measurements, SDS-PAGE, western blotting for detection and ELISA for approximate quantitation of PINs

Protein concentrations of the TSP were measured by the Bradford assay (see section 2.11.1). SDS-PAGE was used to assess protein expression, the protein sizes and extent of purification (Section 2.11.2). The PIN components in the TSP, or the purified recombinant PINs from various methods described below, were identified through western blotting (Section 2.11.3). The PINs expressed in the TSPs were quantified approximately by ELISA (Section 2.11.4).

Methods for further PIN protein purification

2.13.9 His-tag purification under native conditions

The His-tagged recombinant PIN proteins expressed by the magnICON® viral vectors were purified from the TSP using the immobilized metal affinity chromatography (IMAC) system (Thermo Fisher, USA) which uses imidazole-containing buffers, according to the manufacturer's protocol with some modification. The Ni-NTA resin was equilibrated with equilibration buffer (Table 2.5). TSP samples (20 mL) were

mixed with an equal volume of equilibration buffer, applied to the centrifuged tube with pre-equilibrated resin and mixed on an end-over-end rotator for 30 minutes. The tube was centrifuged at 700×g for 5 minutes at 4°C. The resin with the assumed bound His-tagged protein was washed 3 times using two resin-bed volumes of wash buffer (Table 2.5) and centrifuged at 700×g for 2 minutes at 4°C. The bound proteins were eluted in one resin-bed volume of elution buffer (Table 2.5) by centrifuging at 700×g for 2 minutes at 4°C. The eluted products were removed carefully and stored at -80°C. Aliquots (50 µL) were taken at each step of purification for Bradford analysis, SDS-PAGE and western blot analysis (as above).

2.13.10 His-tag purification under denaturing conditions

Urea [$CO(NH_2)_2$] is a powerful protein denaturant, as it disrupts the noncovalent bonds in the proteins. Urea (6 M) was used for purification of the His-tagged recombinant PINs, to solubilise and make the proteins more accessible for interactions with the Ni-NTA resin. The TSP was purified using IMAC system (Nunc, Roskilde, Denmark) under denaturing conditions with urea. The binding, wash and elution buffers with 6 M urea and different concentration of imidazole were made up in PBS (pH 7.4) (Table 2.5). The TSP samples (20 mL) were applied to the pre-equilibrated nickel IMAC column and centrifuged at 150×g for 30 minutes at 4°C. The column was washed 3 times using wash buffer and centrifuged at 500×g for 3 minutes at 4°C. Elution buffer was added to the column and centrifuged at 500×g for 3 minutes at 4°C. The imidazole and urea were removed from the final eluted product by dialysis (Section 2.13.12) and stored at -80°C.

2.13.11 Hydrophobic interaction purification

The hydrophobic interaction purification method was used as described by Skosyrev et al. (2003) and Lee et al. (2011) with modifications. Saturated ammonium sulphate (pH 7.8) was added to a final concentration of 60%, 70% or 80% to the TSP extract. This suspension was then mixed vigorously with one-fourth the volume of ethanol (70%) for 2 minutes. The ethanol phase was separated by centrifugation at 2500×g at RT for 5 minutes and collected carefully to avoid disturbance of the interphase. Approximately 500 µL of 5 M sodium chloride (NaCl) solution was added to the ethanol phase and

mixed for 2 minutes with one-fourth volume of n-butanol (Sigma, USA). The solution was centrifuged at 2500×g for 2 minutes and the lower phase containing the fusion protein was carefully collected. The lower phase solution was adjusted to 20% ammonium sulphate and loaded directly on the pre-equilibrated column with Butyl-Toyopearl (Tosoh Corporation; Japan). The Butyl-Toyopearl were equilibrated and washed with equilibration buffer (Table 2.5). The protein was eluted with elution buffer (Table 2.5) and stored at -80°C for SDS-PAGE and western blot analysis.

2.13.12 Dialysis

The eluted proteins under native and denaturing conditions were exchanged into PBS (pH 7.5) to avoid precipitating the protein in imidazole and urea. The proteins purified under denaturing conditions (in 6 M urea) were dialyzed against buffers containing decreasing concentrations of the denaturing agent (urea) as follows: PBS, 6 M urea; PBS, 3 M urea; and PBS, 1 M urea. Samples were dialyzed at 4°C for more than 8 hours in each dialysis buffer. Following dialysis, the Amicon ultra 0.5 centrifugal filter device (3K-3,000 NMWL) were used to remove the rest of imidazole buffer by centrifugation at 4,000×g for 15 minutes at 4°C for eluted proteins under denaturing condition. The Amicon device was used for eluted proteins under native conditions to remove imidazole buffer and change the buffer into PBS.

2.13.13 Concentrate of dilute protein samples

All diluted purified proteins were concentrated using Amicon ultra 0.5 centrifugal filter device (3K-3,000 NMWL). Spin cycles were performed at 14,000×g for 500 µL of sample. To recover the concentrated protein, the device was placed upside down in a clean microcentrifuge tube and centrifuged at 1,000×g for 2 minutes at 4°C. The samples were applied and the column centrifuged until sufficient concentration was achieved.

2.13.14 Sodium phytate precipitation

Sodium phytate precipitation was performed as per Krishnan and Natarajan (2009), to remove Rubisco from samples purified with the hydrophobic interaction system. PINs purified with the hydrophobic interaction system were treated with 10 mM $CaCl_2$ and

10 mM sodium phytate (phytic acid sodium salt hydrate) for 10 minutes at 37°C, and then centrifuged at RT for 10 minutes at 10000×g. The supernatant was removed to a fresh tube for further analysis.

2.13.15 Testing of antimicrobial and haemolytic properties of the expressed PINs

The antibacterial and antifungal properties of the recombinant PINs purified with His-tag under native and denaturing conditions and the hydrophobic interaction purification system were tested as detailed above (Section 2.12).

Methods specific to Chapter 4:

2.14 Protein-protein interactions of PIN proteins using BiFC system

2.14.1 Principle of the Bimolecular Fluorescence Complementation (BiFC) system

The BiFC system is used to identify interactions between two proteins. The technique is based on the use of two candidate proteins that are translationally fused to the coding region fragments of two non-fluorescent fragments of the yellow fluorescent protein (YFP); YC (C-terminal half) and YN (N-terminal half). Therefore, in a BiFC assay, interaction of the candidate proteins leads to functional YFP reconstitution and fluorescence which can be detected by monitoring fluorescence via fluorescence microscopy techniques (Hu and Kerppola, 2003; Kerppola, 2006) (Figure 2.8). Initially, this technique was used to demonstrate protein-protein interactions in living mammalian cells (Hu et al., 2002; Hu and Kerppola, 2003) and then adapted for the use in plant systems (Bracha-Drori et al., 2004; Walter et al., 2004).

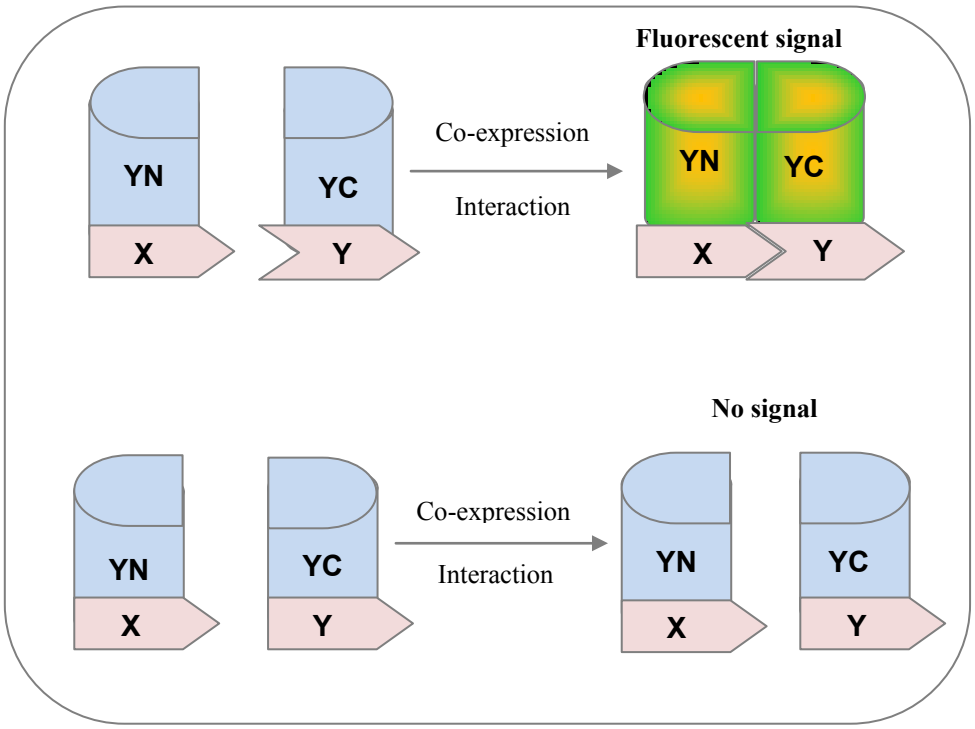

Figure 2.8 Principle of the BiFC assay.
X and Y were proteins that fused to N-(YN) or C-(YC) terminal of the fluorescent protein (YFP) fragments. If X and Y are interacting proteins the fluorescent protein will be reconstructed and fluorescent signal detected. But if X and Y are non-interacting proteins, the N-(YN) and C-(YC) terminals will not be fused to reconstruct the fluorescent protein and no signal will be detected.

The BiFC test was applied here to test and visualize the occurrence of any interactions between PINA and PINB proteins in living plant cells. The pNBV vectors used for this purpose are described below.

2.14.2 New BiFC Vector (pNBV)

The pNBV (Figure 2.9) were kindly provided by Professor David Smyth and Mr Tezz Quon (Monash University, Melbourne). The vectors (pNBV) contain the gene for ampicillin or carbenicillin resistance, a terminator of the *Nos* gene (NosT) and 35S promoter of the cauliflower mosaic virus. In each pNBV vector pair, the gene of interest fused either to the N-terminal 155 amino acid fragment (YN) or to the C-terminal 86 amino acid fragment (YC) of Yellow Fluorescent Protein (YFP) (Hu et al., 2002).

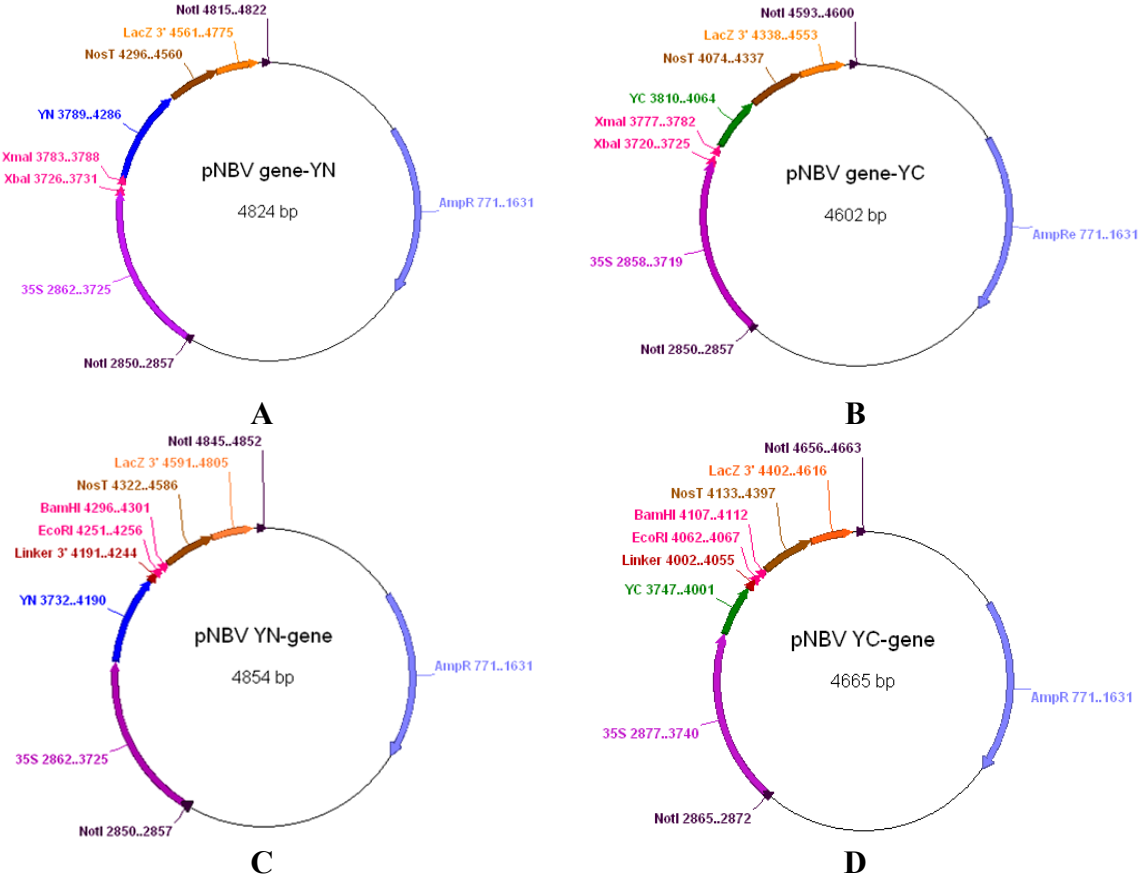

Figure 2.9 The pNBV (New BiFC Vector) modules.
Detailed vector maps for the, A: pNBV gene-YN; B: pNBV gene-YC; C: pNBV YN-gene; D: pNBV YC-gene. YN is the non-fluorescent N-terminal half and YC is the non-fluorescent C-terminal half of YFP. These need to come together for fluorescence to occur (see earlier section). Gene-YN refers to gene fused upstream of YN; YN-gene refers to gene fused downstream of YN. Gene-YC refers to gene fused upstream of YC; YC-gene refers to gene fused downstream of YC.

2.14.3 Design of primers for directional cloning into BiFC vectors (pNBVs)

Primers were designed based on the ORFs encoding mature PINA and PINB proteins (without the putative signal peptides) for directional cloning into pNBV vectors, in-frame and upstream or downstream of the YN and YC fragments. For cloning as gene-YN or gene-YC fusions, the restriction site for XbaI was incorporated at the 5' end of the forward primers and the site for XmaI at the 5' end of reverse primers. For cloning as YN-gene or YC-gene fusions, the site for EcoRI was incorporated into the forward primers and for BamHI into the reverse primers. For all forward primers the start codon was added to *Pin* sequence. The native stop codon was deleted in the reverse primers for cloning into two pNBV vectors (gene-YN and gene-YC). The primers listed in Table 2.11.

Table 2.11 Primers used in directional cloning into pNBV vectors

Primer name	Sequence of primers used *	Cloning sites
Pina-YN and *Pina*-YC	**Forward:** 5'- GGT*TCTAGAATG*GAT GTTGCTGGCGGGGGTG -3'	XbaI
	Reverse: 5'- CCG*CCCGGG*CCAGTAATAGCCAATAGTGCC -3'	XmaI
Pinb-YN and *Pinb*-YC	**Forward:** 5'- GAA*TCTAGAATG*GAA GTTGGCGGAGGAGGTGG -3'	XbaI
	Reverse: 5'- CCG*CCCGGG*CCAGTAATAGCCACTAGG -3'	XmaI
YN-*Pina* and YC-*Pina*	**Forward:** 5'- GGT*GAATTCATG*GAT GTTGCTGGCGGGGGTG -3'	EcoRI
	Reverse: 5'- CCG*GGATCCTCA*CCAGTAATAGCCAATAGTGCC -3'	BamHI
YN-*Pinb* and YC-*Pinb*	**Forward:** 5'- GAA*GAATTCATG*GAA GTTGGCGGAGGAGGTGG -3'	EcoRI
	Reverse: 5'- CCG*GGATCCTCA*CCAGTAATAGCCACTAGG -3'	BamHI

* Cloning sites to be incorporated for directional cloning are shown in italics and shaded. Nucleotides in italics and wave underline encode start and stop codons. The first residue of mature PINs is boxed.

2.14.4 Restriction enzyme digestion of PCR products

- The gene sections encoding the putative mature PINA and PINB, cloned previously into 3' viral module vector (pICH11599), were amplified with gene-specific primers with the appropriate restriction sites and start/stop codons (Table 2.11).
- An aliquot of the above *Pina* and *Pinb* PCR products was subjected to double-digestion with XbaI and XmaI.
- The four vectors pNBV (gene-YC and gene-YN) and pNBV (YC-gene and YN-gene) were prepared from their stocks in *E. coli* Mach1.
- The pNBV (gene-YN and gene-YC) were double-digested with XbaI and XmaI.
  Four separate ligations were set up, as (i) *Pina* with pNBV gene-YN vector; (ii) *Pina* with pNBV gene-YC; (iii) *Pinb* with pNBV gene-YN; (iv) *Pinb* with pNBV gene-YC.
- Another aliquot of the *Pina* and *Pinb* PCR products was double-digested with EcoRI and BamHI.
- The pNBV (YN-gene and YC-gene) were double-digested with EcoRI and BamHI.
- Four more ligations were set up, as (v) *Pina* with pNBV YN-gene; (vi) *Pina* with pNBV YC-gene; (vii) *Pinb* with pNBV YN-gene; (viii) *Pinb* with pNBV YC-gene.
- All ligations were transformed into chemically competent cells of *E. coli* Mach1, and plated on LB agar supplemented with carbenicillin.

- Several half-colonies per transformation were subjected to colony-PCR to identify those containing recombinant plasmids.
- The half-colonies of interest were cultured and plasmids were prepared from these using HiYield™ plasmid mini kit and sequenced.
- The eight BiFC constructs were sequenced and the correct ligations and ORFs (pNBV-YN-PINA, pNBV-YC-PINA, pNBV-PINA-YN, pNBV-PINA-YC, pNBV-YN-PINB, pNBV-YC-PINB, pNBV-PINB-YN and pNBV-PINB-YC) were confirmed.

2.14.5 Cloning of PIN-YFP fragments into pMLBART vector

The pMLBART vector (Figure 2.10) was kindly provided by Professor David Smyth and Mr Tezz Quon (Monash University, Melbourne). It is commonly used as a plant transformation vector for study of protein interactions, by using the NotI restriction site for cloning and spectinomycin resistance as the selection marker.

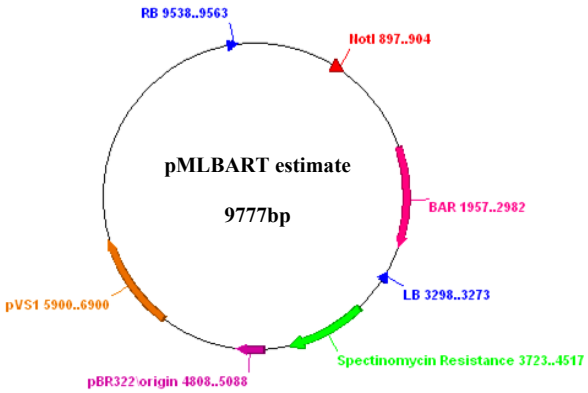

Figure 2.10 Plasmid map of pMLBART.
Plant transformation vector; NotI site show in red.

All eight BiFC constructs made as above were digested at the NotI site, to release the section containing the 35S promoter of CaMV, the non-fluorescent N-terminal half of YFP (YN) or the non-fluorescent C-terminal half of YFP (YC), PINA or PINB, terminator of the Nos gene (NosT) and LacZ (see Figure 2.9). The inserts were cloned at the NotI site of pMLBART, the ligation mixtures transformed into *E. coli* Mach1 and spread onto LB plates containing 50 µg/mL spectinomycin as well as 0.5 mM IPTG and

80 µg/mL X-gal for 'Blue-white screening', (based on the principle of α-complementation of the β-galactosidase (LacZ) gene) which were incubated at 37°C for 16 hours. The white colonies (potentially containing recombinant clones) were tested by colony PCR. The plasmids were prepared from cultures of insert using the HiYield™ plasmid mini kit, the inserts confirmed by PCR again and glycerol stocks of clones prepared and stored at -80°C. The pNBV vector without a *Pin* insert was also digested at the NotI site, transformed into *E. coli* Mach1 cell and the plasmid isolated (to be used as negative control).

2.14.6 Electroporation into *A. tumefaciens* GV3101

One µL each of the plasmid DNAs of all eight clones and the negative control in the pMLBART were each electroporated into *A. tumefaciens* GV3101 (Section 2.9.7) grown on LB plates supplemented with 50 µg/mL spectinomycin and 50 µg/mL rifampicin for two days at 28°C. The colonies were screened by PCR for the presence of the inserted gene.

2.14.7 Use of TBSV-P19 vector

TBSV-P19 is based on co-expression of a viral suppressor protein of the Tomato Bushy Stunt virus (TBSV-P19) called P19, that is able to prevent post-transcriptional gene silencing (PTGS); hence the vector allows high levels of transient gene expression (Voinnet et al., 2003) (Figure 2.11). It encodes kanamycin resistance and was transformed previously into *Agrobacterium* strain LB4404 and stored as a glycerol stock at -80°C (culture donated by Dr Diane Webster, Monash University).

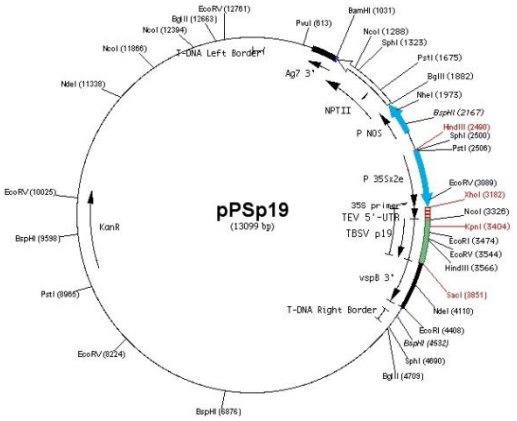

Figure 2.11 Plasmid map of the P19 vector.

2.14.8 Agroinfiltration of *N. benthamiana* using BiFC vectors

The cultures of the eight clones in pMLBART in *A. tumefaciens* were grown overnight at 28°C in LB supplemented with 50 µg/mL spectinomycin and 50 µg/mL rifampicin. *Agrobacterium tumefaciens* LB4404 containing the P19 vector (see above) was grown in LB medium supplemented with 50 µg/mL kanamycin and 50 µg/mL rifampicin. *Agrobacterium tumefaciens* cultures of various combinations of one pMLBART-YN, with one pMLBART-YC, and the P19 (all at OD_{600} of 1) were mixed in a ratio of 1:1:0.5 then the mixture centrifuged at 600×g for 10 minutes at RT. The mixed bacterial pellet was resuspended in 10 mL of infiltration buffer (Table 2.4) and allowed to stand for one hour at RT. The suspensions were infiltrated into leaves of 8 week old *N. benthamiana* plants using a 1 mL syringe (without a needle) until the entire leaf air space was filled with the *Agrobacterium* suspension. Plants were allowed to grow for a further 3 days under greenhouse conditions before the leaves were harvested and analysed by fluorescence microscopy.

2.14.9 Fluorescence microscope and imaging

Small sections from the infiltrated area of *N. benthamiana* leaves were removed and placed in distilled water on glass slides and covered with cover slips. The lower leaf epidermis was prepared for higher resolution of the intracellular distribution of any expressed fluorescence. The samples were examined using ZEISS fluorescence microscope equipped with AxioCam ICc3 (ZEISS) using a 460-480 nm excitation filter and a 495-540 nm barrier filter. Images were captured using the AxioVision LE software (ZEISS) and processed using Adobe Photoshop CS4 software.

2.14.10 Protein methods for detection of BiFC

Total soluble proteins (TSP) were isolated as described earlier (Section 2.13.7) from the *Agrobacterium*-infiltrated areas of *N. benthamiana* leaves potentially expressing the respective fusion proteins. Protein concentrations were measured by the Bradford assay. The TSP samples were ultra-filtered and concentrated using an Amicon ultra 0.5 centrifugal filter device (3K) (Millipore, Australia) at 13,000×g and used for western blots.

2.14.11 Native gel electrophoresis and detection of YFP fluorescence

The protocol followed Morell et al. (2007) with minor modifications. The TSP fractions were electrophoresed at 4°C using a 15% ReadyGel® Tris-HCl gel (Bio-Rad, USA) without SDS in any buffer. The gel was exposed to UV light using Spectroline UV transilluminator to detect YFP fluorescence.

The overall strategy for construction of BiFC vectors and infiltration into plant cells is summarized in Figure 2.12.

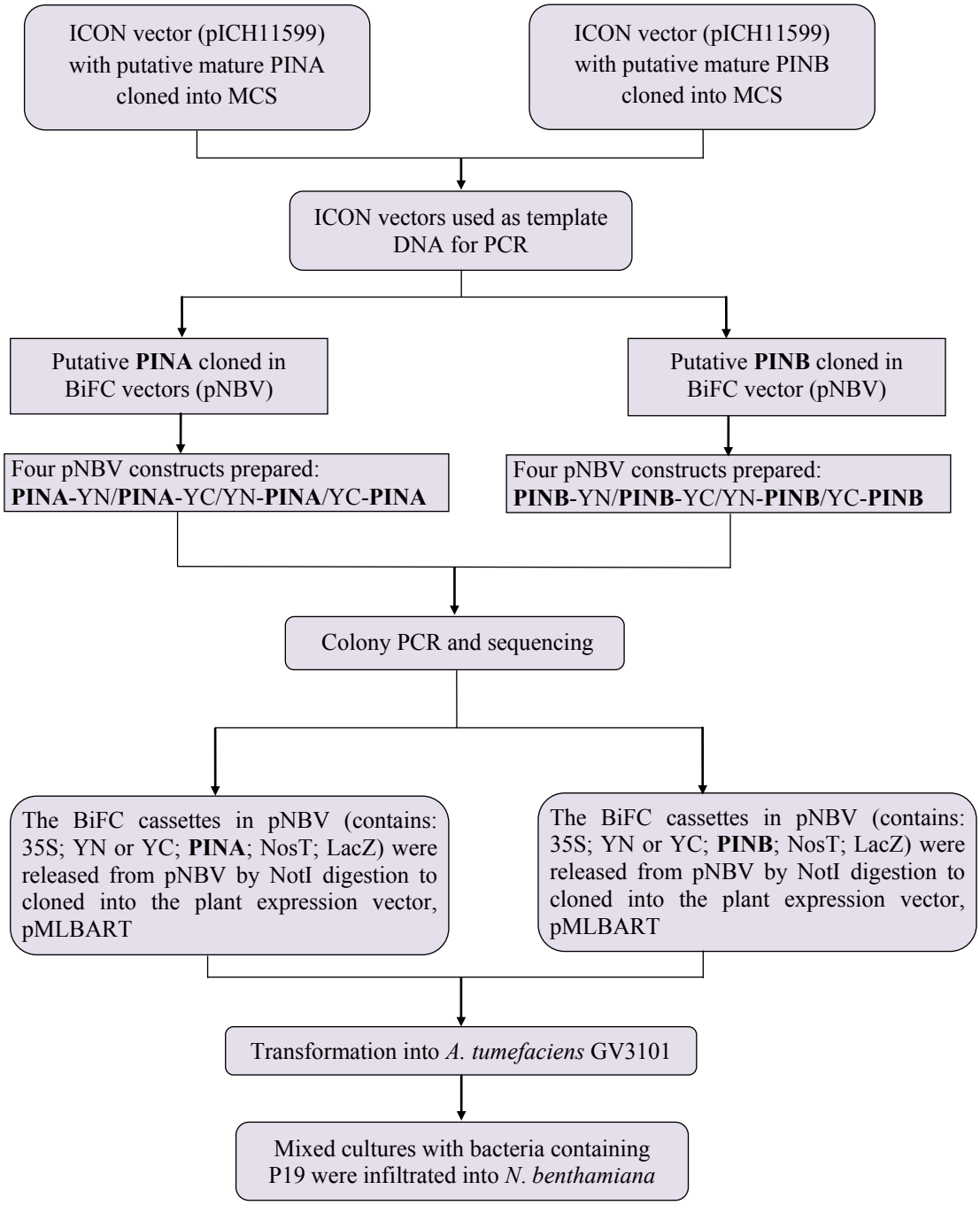

Figure 2.12 Strategy used to construction of BiFC vectors for investigating potential interactions of PIN proteins.

2.15 Identification of protein-protein interaction regions of PINs using BiFC

2.15.1 Gifts of gene construct containing deletions of the tryptophan-rich domain (TRD) of PINA and the hydrophobic domain (HD) of PINA and PINB

The clones designated PINAΔTRD (deletion of TRD at position 34-46 in the mature PINA protein; Figure 2.13A), PINAΔHD (deletion of HD at position 75-85 in the mature PINA protein; Figure 2.13B) and PINBΔHD (deletion of HD at position 75-83 in the mature PINB protein; Figure 2.13C) were constructed previously in the pGBK yeast 2-hybrid system vectors by Dr Rebecca Alfred using the QuikChange II site-directed mutagenesis kit (Stratagene, California, USA) to delete the above gene sections (Alfred, 2013 and Alfred et al., 2014). The primers used for introducing the above deletions are listed in Appendix I (Table I-1). These clones were kindly provided by Dr Alfred for the present *in planta* work.

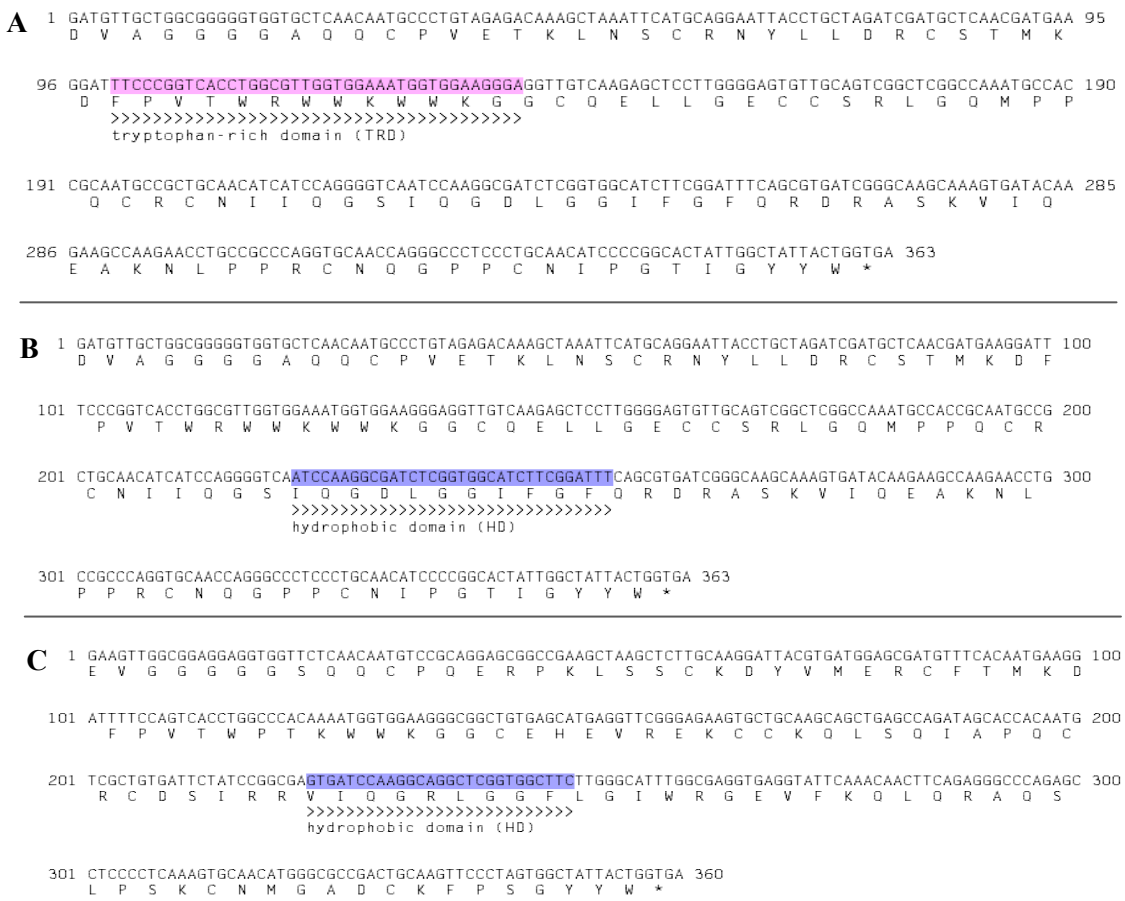

Figure 2.13 Alignment of putative PINA and PINB.
A: The tryptophan-rich domain (TRD) highlighted in pink (residues position 34-46) for PINA; B: The hydrophobic domain (HD) highlighted in blue (residues position 75-85) for PINA; C: The hydrophobic domain (HD) highlighted in blue (residues position 75-83) for PINB.

2.15.2 Cloning of PINAΔTRD and PINAΔHD and PINBΔHD into pNBV vectors

The PINAΔHD, PINBΔHD and PINAΔTRD-encoding genes cloned into pGBK were used as templates in a second-round PCR (with primers detailed in Table 2.11) to enable cloning into pNBV for interaction studies by BiFC assay.

- Second-round PCR products were sequenced and then purified using HiYield™ gel/PCR fragments extraction kit.
- The purified PCR products were double-digested with XbaI and XmaI.
- The vector pNBV (gene-YC) were double-digested with XbaI and XmaI.
- Two ligations were set up, as (i) PINA-ΔHD with pNBV gene-YC (ii) PINA-ΔTRD with pNBV gene-YC.
- The purified PCR product for PINBΔHD and the vector pNBV (YN-gene and YC-gene) were double-digested with EcoRI and BamHI.
- Two more ligations were set up, as (iii) PINB-ΔHD with pNBV YN-gene (iv) PINB-ΔHD with pNBV YC-gene.
- The ligations were transformed into *E. coli* Mach1 and plated on LB agar supplemented with carbenicillin.
- Several colonies per transformation were subjected to colony-PCR to identify those containing recombinant plasmids.
- The plasmids were prepared from cultures of this using HiYield™ plasmid mini kit and sequenced.
- The four PIN mutant BiFC constructs made as above were digested at the NotI site and cloned into the NotI site of pMLBART. The ligation mixtures were transformed into *E. coli* Mach1 and spread onto LB plates containing 50 µg/mL spectinomycin, 0.5 mM IPTG and 80 µg/mL X-gal for 'Blue-white screening'.
- The white colonies (containing recombinant clones) were tested by colony PCR.
- The plasmids were prepared from cultures of this using HiYield™ plasmid mini kit and the inserts were confirmed by PCR again and glycerol stock of clones were prepared and stored at -80°C. All further steps were as per the sections 2.14.6 and 2.14.8

2.15.3 Cloning of PINAΔTRD and PINAΔHD and PINBΔHD into the 3' module pICH11599

The above-made clones in pNBV (encoding PINAΔTRD, PINAΔHD and PINBΔHD) were used as template in a second-round PCR with gene specific primers with the appropriate restriction enzyme sites for pICH11599 (Table 2.7). Second-round PCR products were purified using HiYield™ gel/PCR fragments extraction kit, double-digested with appropriated restriction sites and ligated with the digested pICH11599 (Figure 2.14). The ligations were transformed into *E. coli* Mach1 and plated on LB agar supplemented with carbenicillin. Several colonies per transformation were subjected to colony-PCR to identify those containing recombinant plasmids. The plasmids were prepared from cultures of *E. coli* using HiYield™ plasmid mini kit and sequenced. All further steps were as per sections 2.13.4 and 2.13.5.

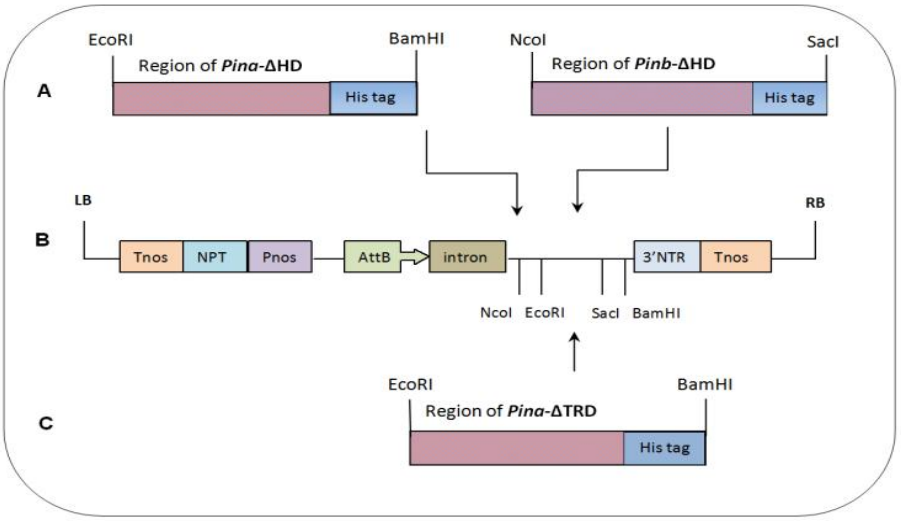

Figure 2.14 Generation of the mutant PIN constructs for magnICON® viral vectors.
A: the region of PINAΔHD and PINBΔHD, encoding the PIN proteins without HD, followed by the His-tag sequence, ligated into; B: the magnICON® viral vector 3' module; C: the region of PINAΔTRD encoding the PIN proteins without TRD ligated into magnICON® viral vector 3' module.

CHAPTER 3

Expression, purification and antimicrobial activity of PINA and PINB proteins in *Nicotiana benthamiana*

3.1 Introduction

Protein expression and purification is required in a number of biochemical investigations such as protein identifications, sequencing, testing of functionality including enzymatic activities and three dimensional structure determinations. Therefore, transgenic plant technology, followed by biochemical and techniques, were applied to PIN proteins to understand the roles they play in determining grain texture, protection against pathogens and the mechanisms of action in both aspects. For the past two decades, industrially and therapeutically important proteins have been successfully expressed in plant systems. However, low yield and lack of efficient purification methods are two major challenges for economical production of plant-made recombinant proteins (Conley et al., 2011). Further biochemical characterisation of the PIN proteins such as three-dimensional structure by X-ray crystallography is essential to better understand their properties and functions. PINs could be an alternative to conventional antibiotics to control plant and human diseases due to their antimicrobial properties. Despite several investigations, there are no reports of PIN proteins purified from wheat in high yield. However, a small number of studies have identified the lipid-binding nature of PIN extracted and purified directly from wheat flour (Clifton et al., 2007b; Clifton et al., 2008; Clifton et al., 2011b). Recombinant PINs have also been purified from *E. coli* based expression systems, with varying degrees of success (Capparelli et al., 2006; 2007; Miao et al., 2012). In addition, Sorrentino et al. (2009) showed that PINB can be produced in transgenic tobacco cells, targeted to chloroplast, with the maximum yield of only 0.35% of the total soluble proteins (TSP). In all these cases the purpose of producing the recombinant PINs was to assess their antimicrobial activity (detailed in Chapter 1).

The present work aimed to clone and transiently over-express PINA and PINB *in planta*, using expression systems based on plant viral vectors. The magnICON® system was used to produce C-terminal His-tagged fusion proteins in the cytosol, chloroplast, apoplast and ER. In addition, various strategies were tested for optimising the production of recombinant PIN within the TSP fraction, including the time of harvest and extraction buffers. It was necessary to subsequently purify the proteins to avoid effects of plant-based alkaloids during antimicrobial assays. Two purification systems

based on His-tag affinity and hydrophobic interactions, were used. To investigate the functionality of the *in planta* expressed PINs, antibacterial and antifungal assays were then performed.

The results in this chapter are divided into 3 sections: expression, purification and characterisation of the antimicrobial activity of the PINA and PINB.

3.2 Expression of PINs using magnICON® viral vectors

3.2.1 Cloning PINA and PINB into magnICON® viral vector system

The 447 bp genes encoding the full-length putative PINA and PINB proteins were first amplified from the gDNA of the soft wheat line *Triticum aestivum* cv. Rosella using the primers given in Table 2.6 (results not shown). For directional cloning into the 3' module of the magnICON® system, i.e., pICH11599, these products were used as templates in second-round PCR (using primers listed in Table 2.7) to amplify the gene sections encoding the putative mature PINA and PINB with C-terminal His-tags, or His-SEKDEL-tags, and appropriate restriction sites. PCR products of ~400 bp obtained for PINA-His and PINB-His (Figure 3.1) were consistent with sizes of the gene sections encoding start codon (3 bp), the putative mature PINA (363 bp) or PINB (360 bp), and the 6×His tag (18 bp) (Table 2.8). PCR products of ~400 bp were also obtained for mature PINA-His-SEKDEL and mature PINB-His-SEKDEL, consistent with the gene sections encoding mature PINA (363 bp) or PINB (360 bp) and the added start codon (3 bp) and tags (6×His, 18 bp; and SEKDEL, 18 bp) (data not shown).

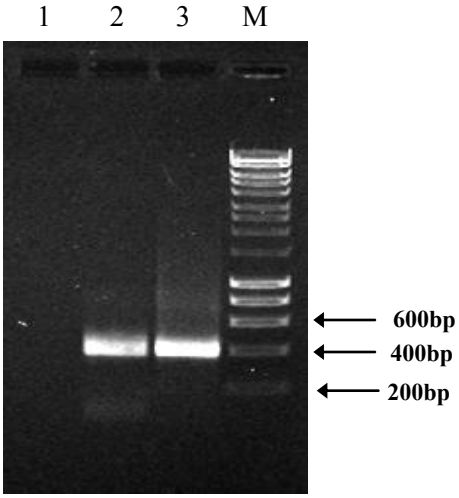

Figure 3.1 Second-round PCR of gene sections encoding mature PINs.
Lane 1: Negative control (no template); lane 2: PINA-His (mature protein-encoding section of *Pina-D1a* with His-tag); lane 3: PINB-His (mature protein-encoding section of *Pinb-D1a* with His-tag); lane M: DNA molecular weight marker, Hyperladder l.

As per the primer design (Section 2.13.2), the PINA-His and PINA-His-SEKDEL PCR products and the vector pICH11599 were double-digested with EcoRI+BamH1, for ligations. The PINB-His PCR products were double-digested with NcoI+SacI and PINB-His-SEKDEL PCR products with EcoRI+BamH1, and ligated with similarly-

digested pICH11599. The four ligations were transformed into *E. coli* Mach1 cells. Due to lack of blue/white colour-selection (lacZ) on pICH11599, colony PCR was carried out using PIN primers (Table 2.7) to test for inserts (approximately 400 bp), as exemplified in Figure 3.2. Plasmids were isolated from the above clones and double-digested with the appropriate enzyme combination, to also ensure the presence of correct-sized inserts. The results are exemplified in Figure 3.3.

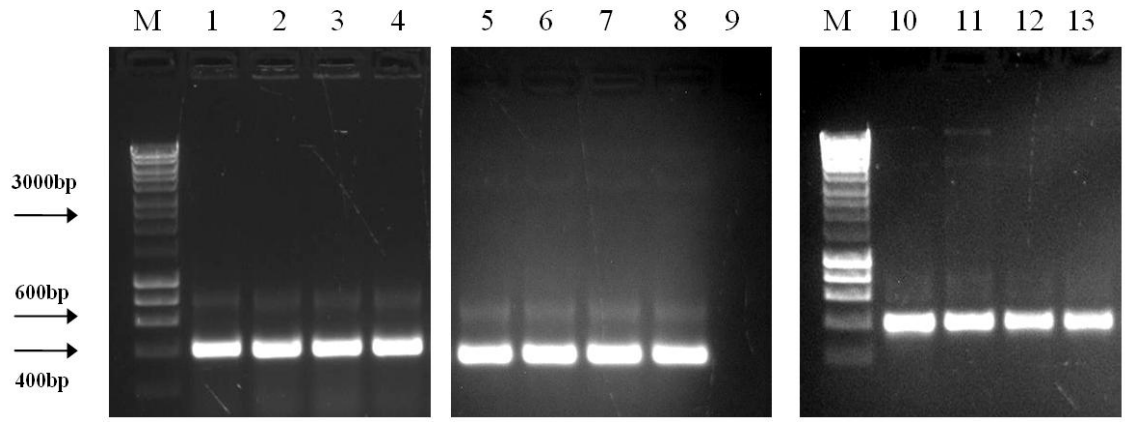

Figure 3.2 Colony PCR for preliminary selection of clones.
Lanes M: marker, Hyperladder 1; lanes 1-4: pICH-PINA-His products; lane 5-8: pICH-PINB-His products; lane 9: negative control (no template); lanes 10-11: pICH-PINA-His-SEKDEL products; lanes 12-13: pICH-PINB-His-SEKDEL.

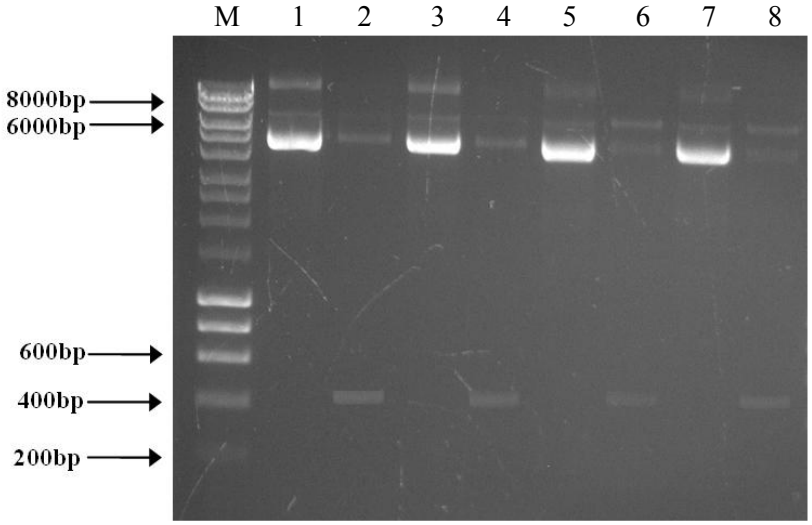

Figure 3.3 Example of double digests of clones in pICH11599.
Lane M: marker, Hyperladder 1; lanes 1, 2: undigested and EcoRI+BamHI digested pICH-PINA-His clone respectively; lanes 3, 4: undigested and NcoI+SacI digested pICH-PINB-His clone respectively; lanes 5, 6: undigested and EcoRI+BamHI digested pICH-PINA-His-SEKDEL clone respectively; lanes 7, 8: undigested and EcoRI+BamHI digested pICH-PINB-His-SEKDEL clone.

For each construct, four potential clones were sequenced using gene-specific primers and alignments of the data with the published sequences, *Pina-D1a* (DQ363911) and *Pinb-D1a* (DQ363913) showed high identity with the corresponding sections. The sequences are provided in Appendix II (Figure II-1 to II-4). The constructs were designated pICH-PINA-His; pICH-PINB-His; pICH-PINA-His-SEKDEL; pICH-PINB-His-SEKDEL (Figure 3.4). Each construct was electroporated into *A. tumefaciens* GV3101 (Section 2.13.4). Screenings of clones containing inserts were carried out using colony-PCR as above (data not shown). The various 5' modules, the 3' GFP module and the integrase module (Section 2.13.1) were also transformed individually into *A. tumefaciens*.

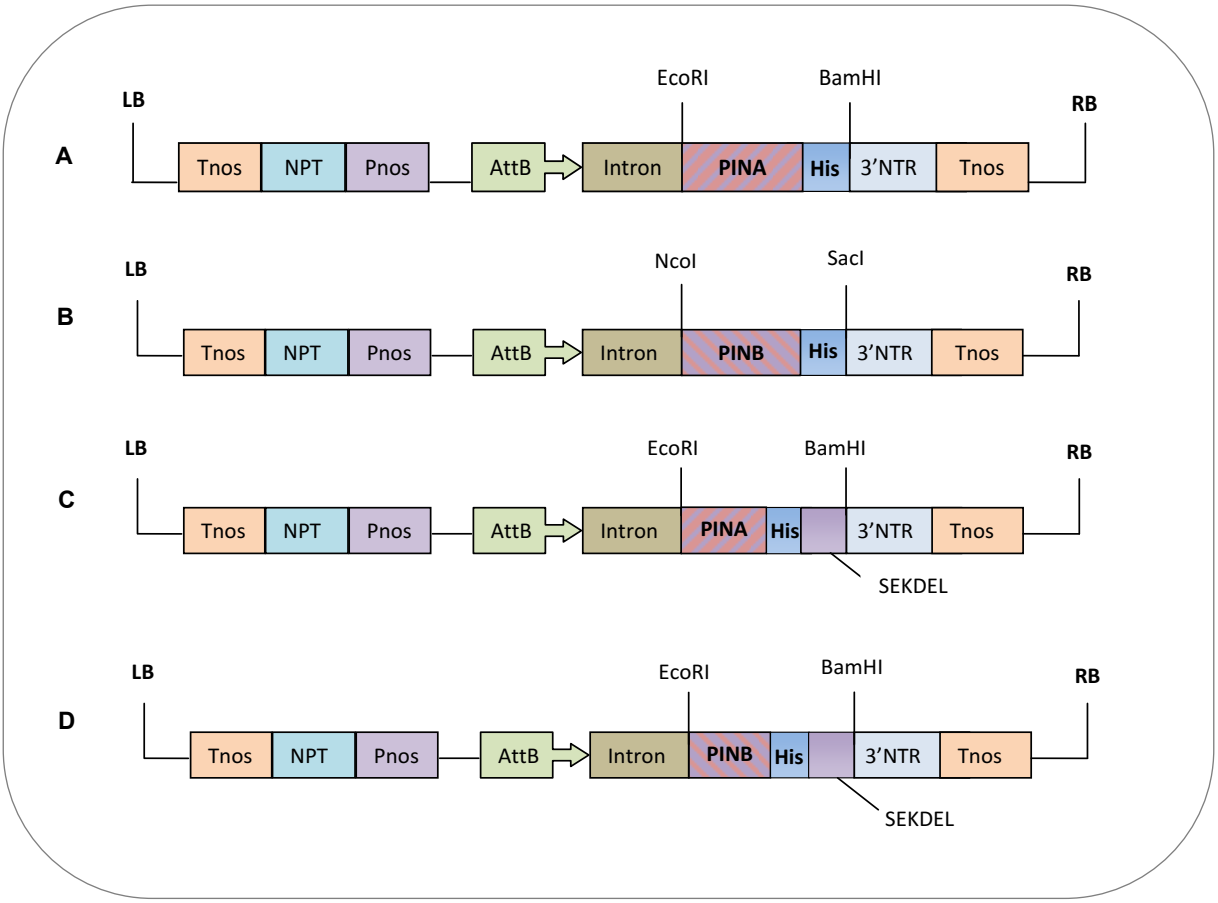

Figure 3.4 The 3' module constructs encoding mature PIN with His-tag and His/SEKDEL tags.
A: pICH-PINA-His; B: pICH-PINB-His; C: pICH-PINA-His-SEKDEL; D: pICH-PINB-His-SEKDEL.

3.2.2 Transient expression of PIN proteins in the viral vector system

The *A. tumefaciens* transformants were used in combinations of three cultures, one with a 5' module (for targeting the expressed protein to different cellular compartments), one with a 3' module (empty, or with PIN or GFP inserts), and one with the integrase module to allow recombination of the former two modules and hence recombinant protein expression. The cytosol and chloroplast targeting GFP served as positive control, while cultures of the 5' cytosol and the integrase modules (and no 3' module) served as negative control. The combinations are detailed in section 2.13.5 (Table 2.9). The cultures were mixed, pelleted, resuspended and infiltrated into the underside of *N. benthamiana* leaves for transiently expressing the encoded proteins. Leaves were harvested from three independent plants for each agro-infiltration, before and after necrosis developed in that area. The necrosis suggested protein production, as the negative control (5'+integrase modules only) developed marginal necrosis (Figure 3.5).

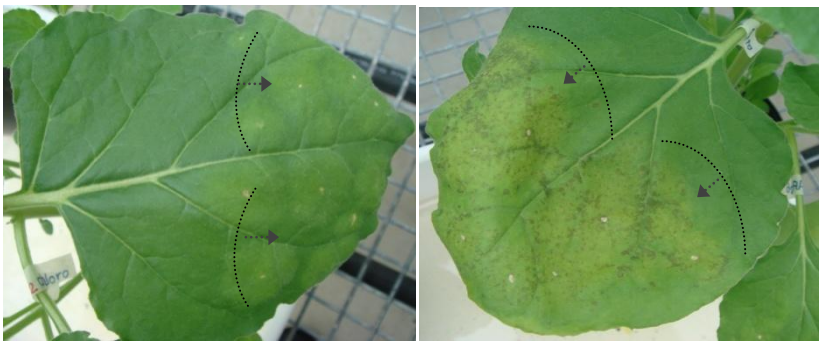

A **B**

Figure 3.5 *N. benthamiana* leaves 10 days post-infiltration (different leaves on one plant). A: agro-infiltration with the 5' cytosol+integrase modules only (negative control); B: agro-infiltration with 3' (pICH-PINB-His)+integrase+cytosol modules. Agro-infiltrated areas are shown by arrows and dotted lines.

The total soluble protein (TSP) was extracted (Section 2.13.7) from each infiltration area, GFP expression tested, and western blot and ELISA applied for PINs. Four different batches were tested and extracts with the highest amounts of PINA or PINB were preferentially used for further purification and test activity. The results are detailed below.

3.2.3 Expression of Green Fluorescent Protein (GFP) by the viral vector system

GFP is widely used as a reporter for gene expression and localisation (Ward, 2006), as an *in situ* tag for fusion proteins (Cremazy et al., 2005; Wang and Hazelrigg, 1994), a biosensor (Crone et al., 2013; Lalonde et al., 2005) or a probe for protein-protein interactions (Magliery and Regan, 2006; Ventura, 2011). It is 238 amino acids long (26.9 kDa) and forms a *ß*-barrel around one *α*-helix (Ormö et al., 1996; Yang et al., 1996). GFP expression (Section 2.13.6) was used as a positive control to ensure the viral vector-based heterologous expression was working correctly. In conjunction with the 3' GFP module and integrase, two separate 5' modules (for cytosol or chloroplast), were agro-infiltrated and production of GFP was observed over time, between 10-14 days post infiltration (dpi). Leaves were examined using UV light and GFP protein showed bright fluorescence (Figure 3.6).

A **Chloroplast** **B** **Cytosol**

Figure 3.6 GFP production using two different targeting modules, in *N. benthamiana* leaves (10 dpi). A: Agro-infiltrated leaves viewed under natural light; B: GFP production in chloroplast and cytosol viewed under UV.

The TSP extracted from infiltrated leaves using 3' GFP module and different 5' modules (cytosol or chloroplast) were quantified using Bradford assay. The absorbance of each sample was read at 595 nm and the TSP concentration determined from the standard curve (Figure 3.7), constructed using bovine serum albumin (BSA) standards ranging from 0.1 to 0.5 mg/mL (Section 2.11.1). Table 3.1 shows the concentration of TSP from leaves infiltrated with chloroplast-targeted GFP, cytosol-targeted GFP and also negative controls. Approximately 93 µg and 98 µg of the quantified TSP samples were run on a gel to analyse the GFP expression by SDS-PAGE gel (data not shown) and western blot. Western blot analysis using anti-GFP antibody (Section 2.3) confirmed the presence of GFP at approximately 25 kDa, at the expected size for GFP (Figure 3.8).

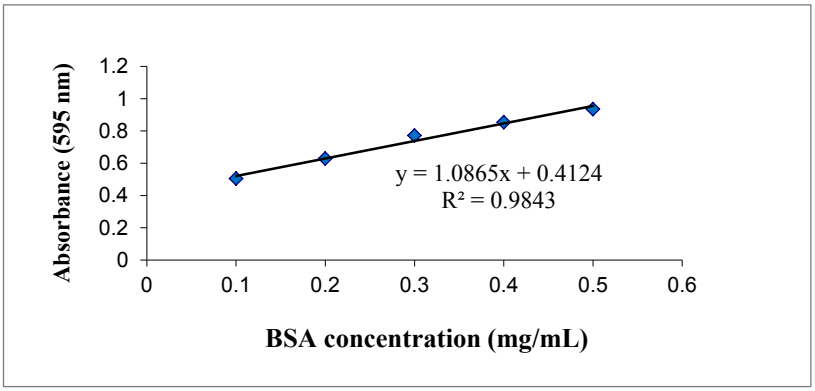

Figure 3.7 Standard curve of BSA concentration for Bradford assay.
The standard curve was prepared using BSA in PBS buffer, and absorbance measured at 595 nm.

Table 3.1 Quantification of TSP for targeted expression of GFP using Bradford assay

Protein Samples	Average of test OD_{595}	Protein calculation based on standard curve (mg/mL)	Dilution factor	Amount of TSP (mg/mL)	TSP loaded on SDS (µL)	Protein on gel (µg)
GFP Cytosol	0.698 ± 0.005	0.264	10	2.64	37	97.68
GFP Chloroplast	0.685 ± 0.004	0.252	10	2.52	37	93.24
Negative Cytosol	0.594 ± 0.007	0.168	10	1.68	37	62.16
Negative Chloroplast	0.577 ± 0.005	0.152	10	1.52	37	56.24

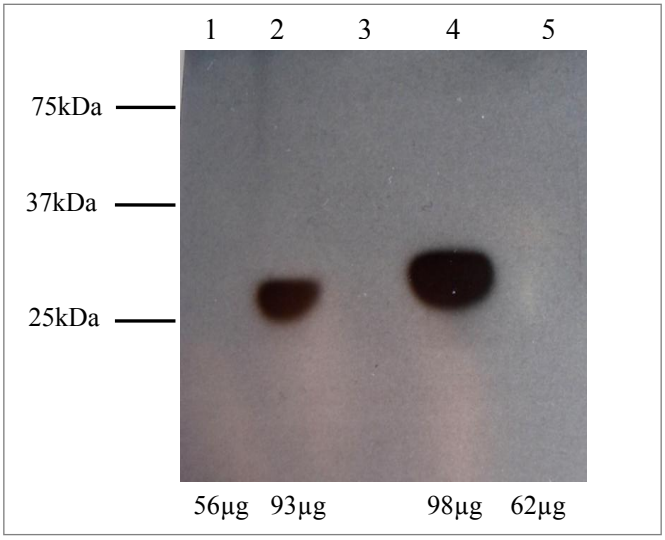

Figure 3.8 Western blot analysis to determine GFP expression using anti-GFP antibody.
Lane 1: TSP from leaf infiltrated with 5' chloroplast+integrase modules only (negative control); lane 2: TSP from leaf infiltrated with 5' chloroplast+integrase+3' GFP modules; lane 3: void lane (no sample loaded); lane 4: TSP from leaf infiltrated with 5' cytosol+integrase+3' GFP modules; lane 5: TSP from leaf infiltrated with 5' cytosol+integrase modules only (negative control).

3.2.4 Expression of the recombinant PINA protein by the viral vector system

Following agro-infiltration with pICH-PINA-His and pICH-PINA-His-SEKDEL using different 5' vector modules, leaves were harvested. The TSP extracted from these were quantitated by Bradford assay (Table 3.2), then analysed by SDS-PAGE and Coomassie Blue staining of gels (Figure 3.9). The results showed some major bands at ~50 kDa and ~15 kDa as well as some minor bands (e.g., 75 kDa, 37 kDa and 25 kDa). Since the GFP production showed the system was functioning as expected (Figure 3.6), PIN proteins were then detected by western blot using the Durotest, anti-friabilin monoclonal antibody (described in Section 2.11.3).

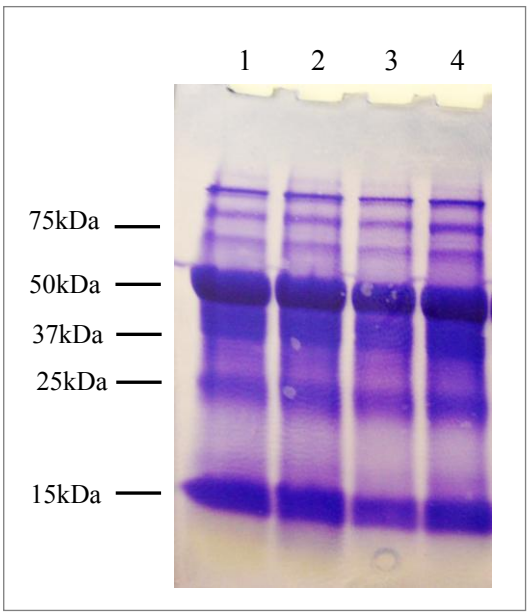

Figure 3.9 Coomassie Blue stained gel to analyse TSP from infiltrated leaves.
Lane 1: infiltration with chloroplast targeted PINA; lane 2: infiltration with cytosol targeted PINA; lane 3: infiltration with apoplast targeted PINA; lane 4: infiltration with ER targeted PINA.

The molecular weights of the C-terminally His-tagged PINA, with and without SEKDEL, were estimated at 14.97 kDa and 14.27 kDa respectively, using the 'compute pI/Mw tool' at the ExPASy (Section 2.10.3). The predicted subcellular localisation of PINA by WoLF PSORT (Section 2.10.4) showed the highest score for chloroplast targeting. The PIN proteins were detected by western blot using the Durotest antibody. The positive control supplied with the Durotest kit (3% non-durum wheat) exhibited a band at ~15 kDa (Figure 3.10; lane 1), the expected size for the friabilin protein mixture composed mainly of PINA and PINB, originating from the non-durum wheat.

Interestingly, the recombinant PINA was detected at the unexpected size of ~45 kDa (between 50 kDa and 37 kDa) when targeted to different parts of the plant cell, i.e., chloroplast, cytosol and ER, but not detected in the apoplast, probably due to limited protein delivery to this compartment. Further, the ~45 kDa bands were observed only when the TSP samples were not heated prior to the western blot, and could not be detected when the TSP samples were heated (as discussed later in section 3.2.6).

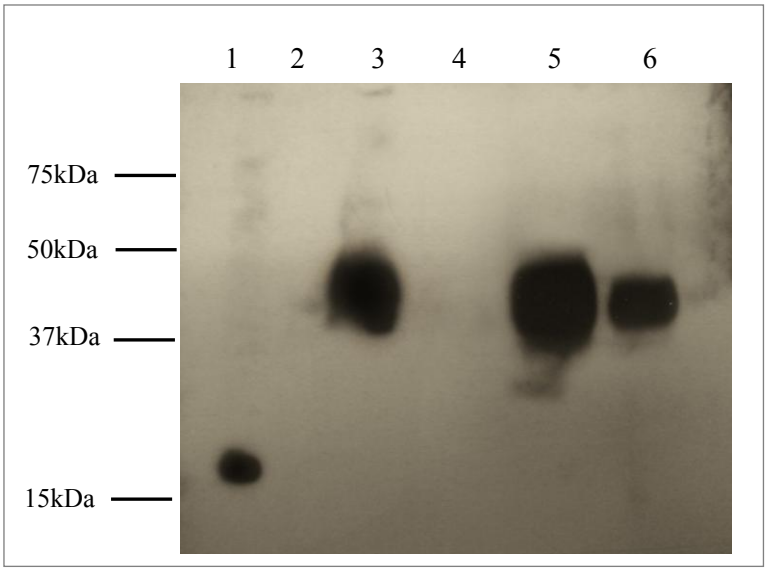

Figure 3.10 Determination of PINA expression by western blotting of TSP extracts from infiltrated leaves.
Lane 1: 3% non-durum wheat as positive control for antibody; lane 2: negative control (5'+ integrase modules only); lane 3: cytosol targeted PINA; lane 4: apoplast targeted PINA; lane 5: chloroplast targeted PINA; lane 6: ER targeted PINA.

The quantified TSP samples, as well as the negative controls, were used for enzyme-linked immunosorbent assay (ELISA) analysis (Section 2.11.4) to measure the yield of recombinant PINA in *N. benthamiana* leaves. High-binding ELISA plates were coated with 0.3 µg TSP/well. The assay tested protein samples in three different dilutions (1/50, 1/100 and 1/200). The absorbance of each sample was read at 450 nm, and the PINA concentration determined from the 3% non-durum wheat (supplied in the Durotest kit) standard curve, ranging from 0.0675-0.54 µg/mL (Figure 3.11).

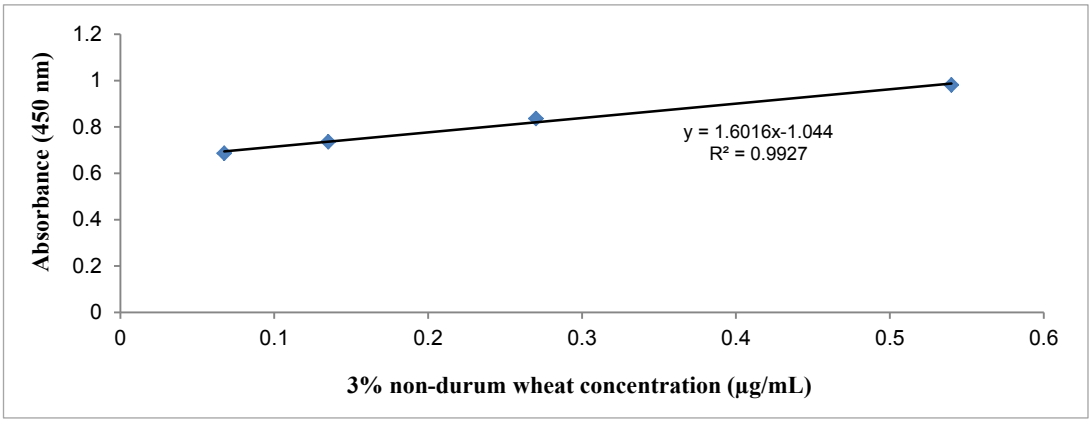

Figure 3.11 Standard curve of 3% non-durum wheat dilutions for ELISA assay.

Table 3.2 shows the concentration of the recombinant PINA (rPINA) in infiltrated leaves for the 1/200 dilution test. The maximum yield obtained for PINA was ~0.836% of TSP, or approximately ~51.7 µg/g of fresh weight using the 5' module for chloroplast (Figure 3.12). The PINA yields were ~0.642% TSP or ~40.5 µg/g of fresh weight using the 5' module for cytosol and ~0.63% TSP or ~39.7 µg/g of fresh weight for ER.

Table 3.2 ELISA data analysis for quantification of recombinant PINA (rPINA) protein

Sample name	OD_{450}[a]	rPINA (µg/mL)	rPINA (mg/mL)[b]	TSP (mg/mL)	FW[c] (µg/g)	Yield of rPINA (%)
PINA-Chloroplast	0.663 ± 0.0126	5.173	0.00517	0.702 ± 0.059	51.7	0.836 ± 0.033
PINA-Cytosol	0.658 ± 0.010	4.052	0.00405	0.602 ± 0.029	40.5	0.642 ± 0.032
PINA-ER	0.667 ± 0.012	3.972	0.00397	0.612 ± 0.044	39.7	0.63 ± 0.033
PINA-Apoplast[d]	0.10877 ± 0.003	-	-	-	-	-
Negative[d]	0.0547 ± 0.0015	-	-	-	-	-

[a] average of at least 4 independent tests; [b] different dilutions were tested, data show 200-fold dilution.
[c] FW: fresh weight; [d] data not applicable for apoplast and negative samples.

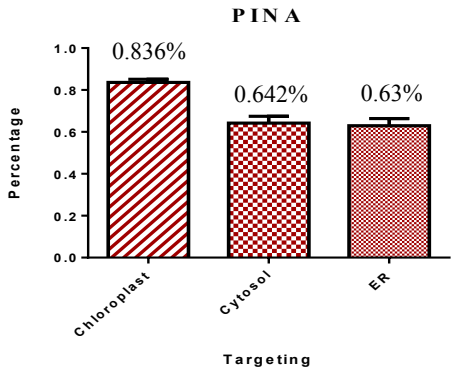

Figure 3.12 Quantification of PINA proteins targeted to chloroplast, cytosol and ER by ELISA.TSP extract from leaves harvested after infiltration was added to ELISA plate and PINA detected using the Durotest antibody. Bars show the mean percentage of protein extracts from four individual leaves and the error bars indicate the standard error of the mean (SEM).

3.2.5 Expression of the recombinant PINB protein by the viral vector system

The constructs pICH-PINB-His and pICH-PINB-His-SEKDEL made using different 5' vector modules were infiltrated into *N. benthamiana* leaves. The TSPs were extracted and analysed using SDS-PAGE (Figure 3.13) and quantitated by Bradford assay (Table 3.3).

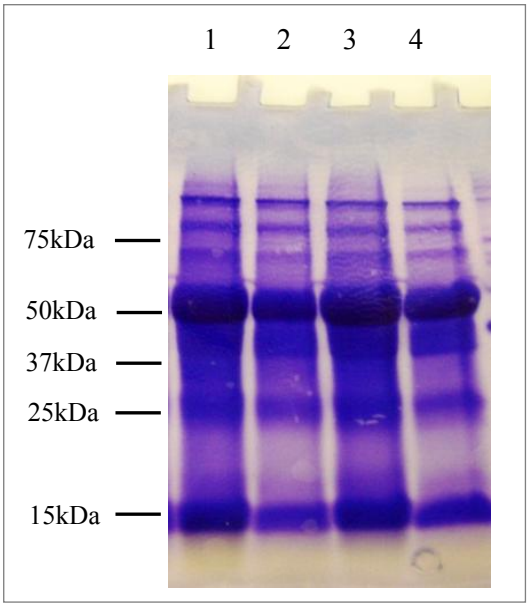

Figure 3.13 Coomassie Blue stained gel to analysis TSP from infiltrated leaves.
Lane 1: infiltration with chloroplast targeted PINB; lane 2: infiltration with cytosol targeted PINB; lane 3: infiltration with ER targeted PINB; lane 4: infiltration with apoplast targeted PINB.

The recombinant PINB (rPINB) was detected by western blot using the above antibody. The molecular weights for C-terminally His-tagged PINB with or without the SEKDEL were predicted, using the 'compute pI/Mw tool' at the ExPASy (Section 2.10.3) at 15.13 kDa and 14.43 kDa, respectively. The predicted subcellular localisation of PINB by WoLF PSORT (Section 2.10.4) showed the highest score for chloroplast targeting. The western blot showed the friabilin proteins at the expected size (~15 kDa), in the positive control, 3% non-durum wheat. The recombinant PINB with or without the SEKDEL was detected at the unexpected size of ~45 kDa bands (between 50 kDa and 37 kDa) (Figure 3.14), only when the TSP samples were not heated prior to western blot (as discussed in section 3.2.6). The ~45 kDa PINB was noted when targeted to the chloroplast, cytosol or ER, but not when targeted to apoplast.

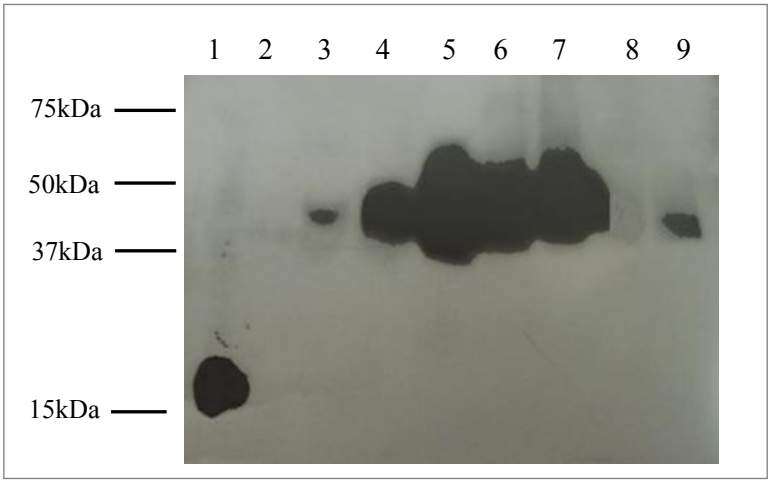

Figure 3.14 Determination of PINB expressions by western blotting of TSP extracts from infiltrated leaves.
Lane 1: 3% non-durum wheat as positive control for antibody; lane 2: negative control (5'+integrase modules only); lanes 3 and 9: ER targeted PINB; lanes 4 and 5: cytosol targeted PINB; lanes 6 and 7: chloroplast targeted PINB lane 8: apoplast targeted.

The TSP samples from freshly infiltrated leaves were quantified by Bradford assay and analysed by ELISA (Section 2.11.4) with Durotest antibody to measure the yield of recombinant PINB protein. ELISA plates were coated with 0.3 µg TSP/well. The assay tested protein samples in three dilutions (1/50, 1/100 and 1/200). The absorbance was read at 450 nm, and the PINB concentration determined from the 3% non-durum wheat standard curve as above (Figure 3.11). Table 3.3 shows the concentration of PINB in infiltrated leaves in 1/200 dilution test. As shown in Figure 3.15, the maximum yield for PINB was ~0.894% of TSP, or approximately ~70 µg/g of fresh weight using the 5' vector module for chloroplast. PINB yields of up to ~0.73% and ~0.68% TSP, or ~45 µg/g and ~40 µg/g of fresh weight were obtained for cytosol and ER targeting, respectively.

Table 3.3 ELISA data analysis for quantification of recombinant PINB (rPINB) protein

Sample name	OD_{450}[a]	rPINB (µg/mL)	rPINB (mg/mL)[b]	TSP (mg/mL)	FW[c] (µg/g)	Yield of rPINB (%)
PINB-Chloroplast	0.66 ± 0.011	6.294	0.00629	0.762 ± 0.045	62.9	0.894 ± 0.051
PINB-Cytosol	0.661 ± 0.012	4.533	0.00453	0.692 ± 0.060	45.3	0.734 ± 0.028
PINB-ER	0.66 ± 0.019	4.053	0.00405	0.615 ± 0.034	40.5	0.672 ± 0.023
PINB-Apoplast[d]	0.113 ± 0.0056	-	-	-	-	-
Negative[d]	0.0547 ± 0.001	-	-	-	-	-

[a] average of at least 4 independent test; [b] different dilutions were tested, data show 200-fold dilution;
[c] FW: fresh weight; [d] data not applicable for apoplast and negative samples.

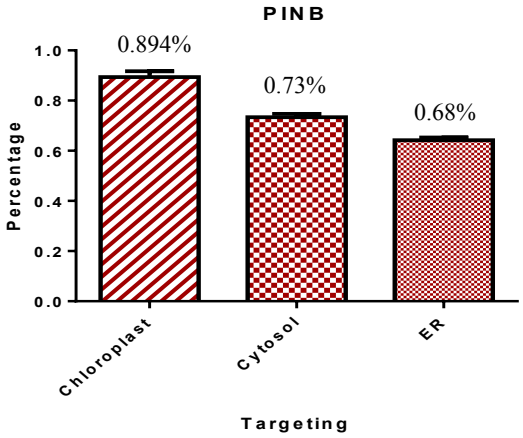

Figure 3.15 Quantification of PINB proteins targeted to chloroplast, cytosol and ER by ELISA.
TSP extract from leaves harvested after infiltration was added to ELISA plate and PINB detected using the Durotest antibody. Bars show the mean percentage of protein extracts from four individual leaves and the error bars indicate the standard error of the mean (SEM).

3.2.6 Optimisations of expression of His-tagged recombinant PINA and PINB

The optimal time of PIN harvest was investigated by infiltrating leaves with constructs for targeting to the chloroplast and cytosol and harvesting at 8, 10 or 12 days post-infiltration (dpi). One µg of TSP (as assayed by Bradford method) was used for ELISA in two dilutions (1/100 and 1/200). Total soluble protein (TSP) from the infiltrated leaves harvested at 10 dpi resulted in a slightly higher OD_{450} compared to 8 or 12 dpi (Figure 3.16). Overall, the maximal yields of PINs were achieved at 10 dpi, using these modules.

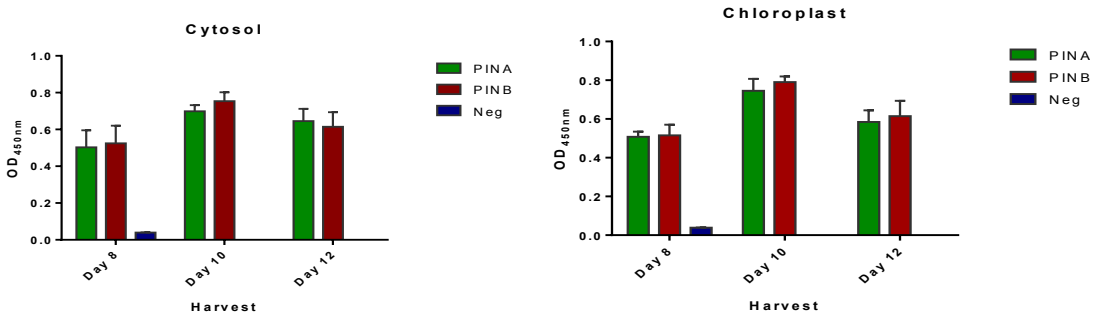

Figure 3.16 Detection of PIN proteins harvested at different times post-infiltration, by ELISA. Quantified TSP samples were added to ELISA plate and PINs detected using the Durotest antibody. The negative control was protein extracted from leaf material infiltrated with only the 5'+integrase modules. The bars indicate the mean OD_{450} of protein extracts from two individual leaves and the error bars indicate the standard error of the mean (SEM).

The quantified TSP samples (approximately 50 μg) were heated at 60°C, 65°C and 70°C for 15, 30 seconds and 1 minute to denature any recombinant PINs prior to western blotting. No bands were observed at 70°C for the tested proteins at all three time points (data not shown). The same result was observed for 60°C and 65°C as shown in Figure 3.17. Heating at 65°C for 30 seconds led to faint bands with size shift near 37 kDa compared to the unheated samples (Figure 3.17). No bands could be detected when the samples were heated at 65°C for 1 minute (Figure 3.17). This demonstrates that the plant-made recombinant PINs are heat-sensitive.

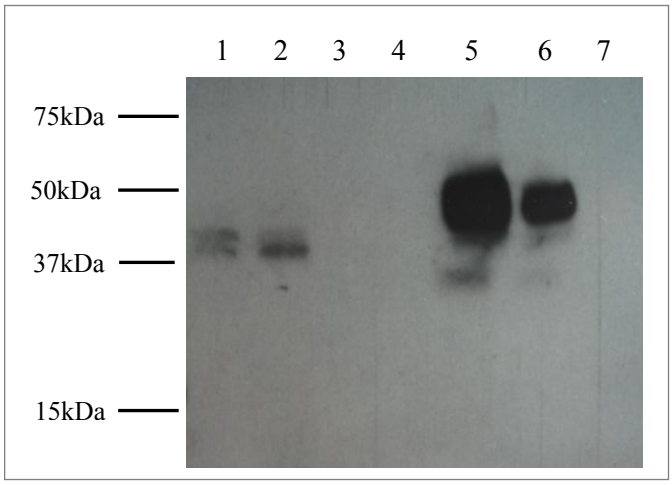

Figure 3.17 Heat sensitivity of plant-expressed PINA and PINB detected by western blot. Lane 1 and 2: chloroplast-targeted PINA and PINB, respectively, in TSP heated at 65°C for 30 seconds; lanes 3 and 4: these PINA and PINB in TSP heated at 65°C for one minute; lane 5 and 6: these PINA and PINB, in TSP not heated; lane 7: negative control (5'+integrase modules only).

A number of different extraction buffers (Section 2.13.7; Table 2.10) were then tested and the proteins detected by western blot. Extraction buffer 1 was used for all further analyses, as other buffers did not improve the yield or extent of denaturation of PINs. Further, in the optimisations, only one western blot confirmed the chloroplast-targeted PINA and PINB at ~15 kDa (Figure 3.18), expected for His-tagged PINA and PINB monomers, predicted to be 14.27 kDa and 14.43 kDa, respectively. These bands were obtained using extraction buffer 1 which was without EDTA, and without heating the TSP, and when approximately 90 µg of TSP samples were loaded on gels.

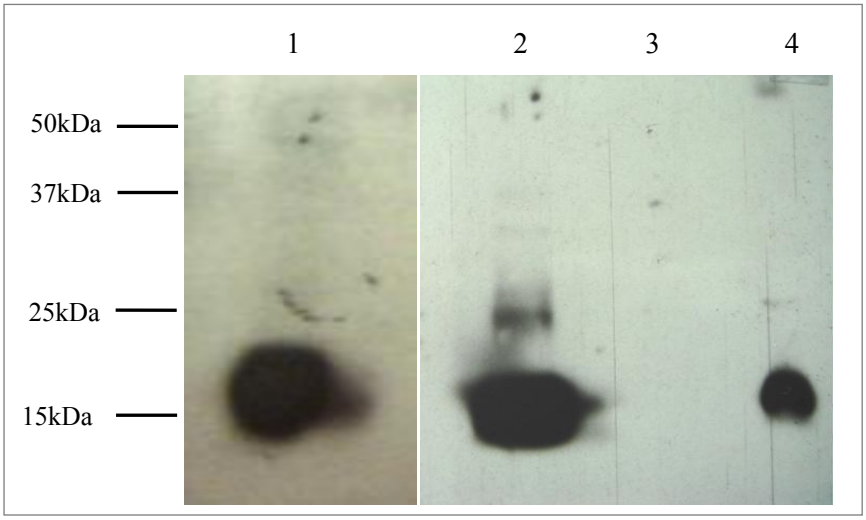

Figure 3.18 Determination of PINA and PINB protein expression in infiltrated leaves with viral vector module by western blot of TSP in expected size.
Lane 1: chloroplast targeted PINA (~15 kDa); lane 2: chloroplast targeted PINB (~15 kDa); lane 3: negative control (5'+integrase modules only); lane 4: 3% non-durum wheat as positive control.

3.3 Results for purification of PINA and PINB

3.3.1 His-tag purification under native conditions

The PINs were purified from TSP of leaf infiltrated with pICH-PINA-His or pICH-PINB-His, in combination with the chloroplast 5' module, due to the high yield of recombinant PINs when targeted to the chloroplast. Purification was performed using Ni-NTA resin column (Section 2.13.9). In order to increase the chances of C-terminal His-tag being correctly folded and functional, the soluble PIN-His proteins were purified under native conditions (without denaturing buffer) and at 4°C to minimize protein degradation. Samples (approximately 50 µg) that had indicated chloroplast-expressed PINs by western blots before purification, and the fractions passed over a Ni-NTA resin column with wash buffer (Table 2.5), were run on 15% SDS-PAGE and visualized by Coomassie Blue staining (Figure 3.19). The washed fractions with imidazole (25 mM) in the wash buffer showed faint bands at 50 kDa. However, the 37 kDa and 15 kDa bands were absent on gel (Figure 3.19; lane 4, 5).

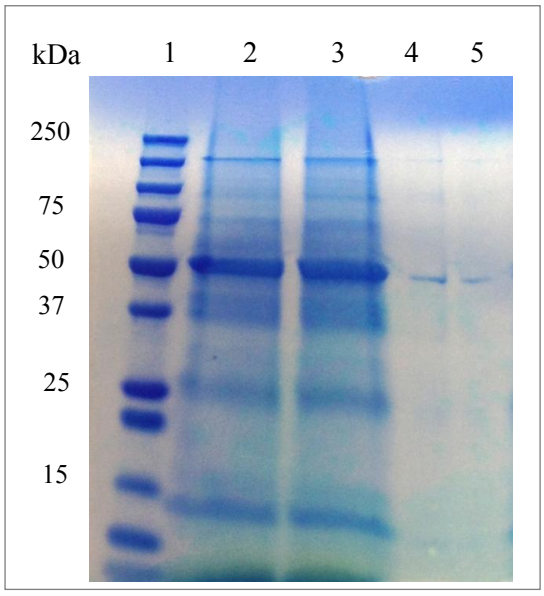

Figure 3.19 SDS-PAGE of TSP and wash steps of His-tag purification under native conditions.
Lane 1: Dual Xtra standards (Bio-Rad); lane 2 and 3: TSP of chloroplast-expressed PINA and PINB respectively; lane 4 and 5: fractions from Ni-NTA column with imidazole (25 mM) in wash buffer for PINA and PINB purification respectively.

His-tagged PINs were eluted with an elution buffer containing 250 mM imidazole (Table 2.5) and then dialysed to remove imidazole, then concentrated (Sections 2.13.12 and 2.13.13) and quantitated using Bradford assays. This was followed by SDS-PAGE and western blot analysis with ~48 µg and ~52 µg for PINA and PINB, respectively (Figure 3.20). The fractions exhibited a few faint bands and strong bands at 37 kDa and 15 kDa for both PINs in the stained gel (lanes 2, 3) which may correspond to the multimer and monomer sizes of His-tagged PINs, respectively. The results indicate that the target proteins were retained on the resin and were only visible after elution with high imidazole (250 mM) in the elution buffer. The western blot of the eluted fractions (42 µg, 48 µg and 52 µg protein for negative control, PINA and PINB, respectively) indicated a broad band at ~37 kDa, confirming the identity of 37 kDa bands as PIN proteins (Figure 3.20; lanes 6, 7). However, the 15 kDa band not shown signal with antibody which may not just detected with Durotest. The faint band above ~37 kDa reacted with the Durotest antibody in PINA and PINB samples (lane 6 and 7) which was probably observed as 45 kDa protein when TSP samples were analysed.

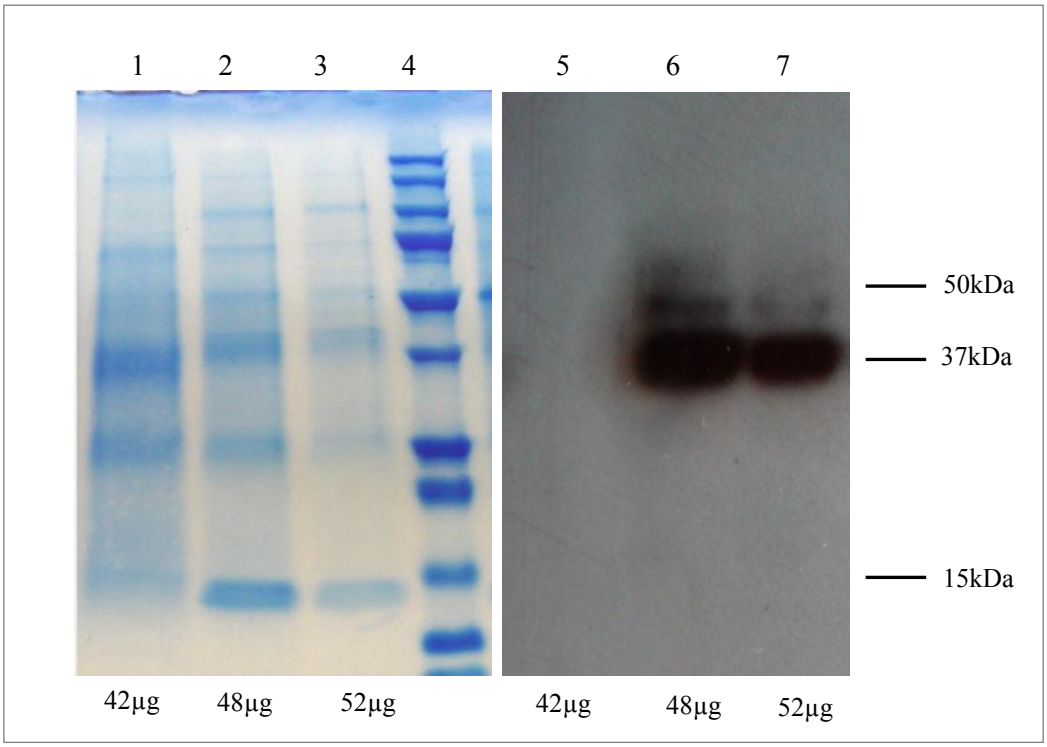

Figure 3.20 SDS-PAGE and western blot analysis with Durotest antibody for eluted fraction on Ni-NTA resin columns based on His-tag purification under native conditions. Lane 1 and 5: eluted fraction of negative control (5'+integrase modules only); lane 2 and 6: eluted fraction of PINA on SDS-PAGE and western blot respectively; lane 3 and 7: eluted fraction of PINB on SDS-PAGE and western blot respectively; lane 4: Dual Xtra standards (Bio-Rad).

3.3.2 His-tag purification under denaturing conditions

His-tag purification was performed using the refolding method (Section 2.13.10) to observe the effect of a protein denaturant such as urea, which disrupts the non-covalent bonds and increases protein solubility. His-tag purification generally works well under denaturing conditions (Waugh, 2005). Purification steps were typically performed at 4°C to minimize degradation. PINs were eluted from the Ni-NTA column with a buffer containing 250 mM imidazole and 6 M urea (Table 2.5) then dialysed (Section 2.13.12) to remove imidazole and urea, and protein concentrations measured by Bradford assays. This was followed by SDS-PAGE and western blotting with ~32 µg and ~35 µg for eluted samples of PINA and PINB, respectively, and 30 µg for negative control. A single band was observed for PINA and PINB at approximately 15 kDa on the gel (Figure 3.21; lanes 2 and 3) which could be their putative monomer. The same amounts of protein samples were analysed by western blot, however the denatured monomeric forms of both PINs were not detected (lanes 6 and 7).

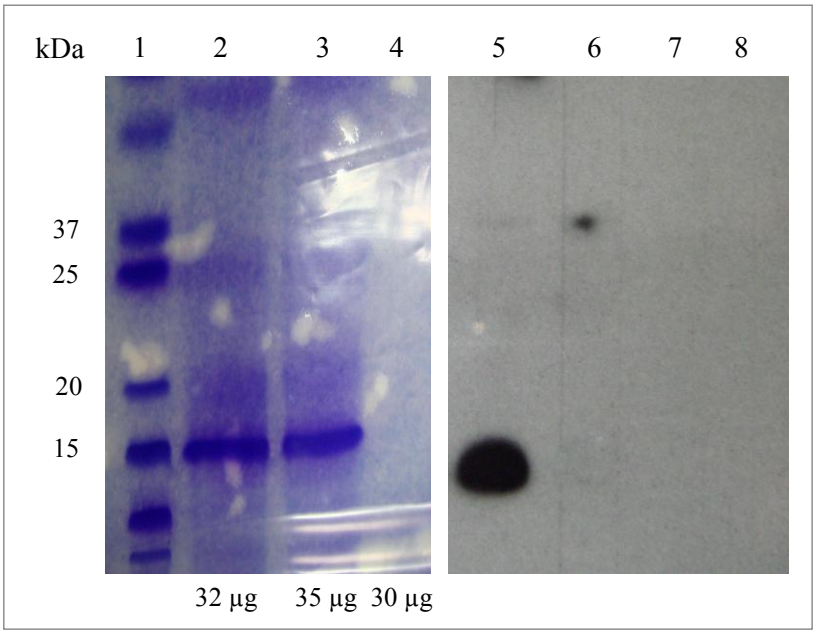

Figure 3.21 SDS-PAGE and western blot analysis with Durotest antibody for eluted fraction on columns with 6M urea in elution buffer.
Lane 1: Dual Xtra standards (Bio-Rad); lane 2 and 6: eluted fraction of PINA on SDS-PAGE and western blot respectively; lane 3 and 7: eluted fraction of PINB on SDS-PAGE and western blot respectively; lane 4 and 8: eluted fraction of negative control (5'+integrase modules only) lane 5: 3% non-durum wheat as a positive control for antibody.

3.3.3 Hydrophobic interaction purification

In a previous attempt to purify the PINs using His-tag, the proteins had not shown a dominant band on SDS-PAGE (results in section 3.3.1). This may be due to the other plant proteins binding to the Ni-NTA resin. Therefore, hydrophobic interaction purification, a separation technique that uses the properties of hydrophobicity to separate proteins from one another, was applied (Section 2.13.11). Proteins passing through the column with hydrophobic amino acid side chains on their surfaces are able to bind to the hydrophobic groups on the column. The interactions are too weak in water (a polar solvent), however the additions of salts such as ammonium sulfate [$(NH_4)_2SO_4$] to the buffer result in stronger hydrophobic interactions. Ammonium sulfate concentrations of 60%, 70% and 80% saturation were used for phase separation by ethanol extraction (Figure 3.22).

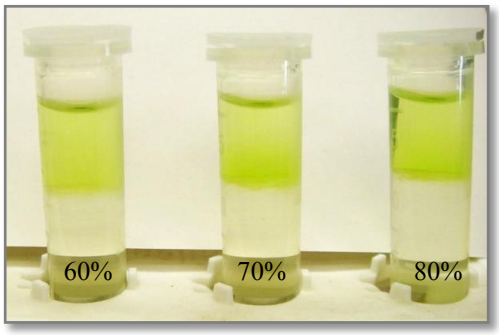

Figure 3.22 Fractions in the course of extraction procedure.
Protein was extracted into upper phase (ethanol) after addition of ammonium sulfate (60%, 70% and 80% saturation) and ethanol.

The proteins were eluted from Butyl-Toyopearl column, quantified by Bradford assay and ~40 µg of each preparation was run on SDS–PAGE gel and visualized by Coomassie Blue staining. 70% and 80% ammonium sulfate did not show clear bands of PINs (data not shown). However, elution with reduced (60%) ammonium sulfate led to pure proteins, seen as two bands at ~37 kDa and ~15 kDa, assumed to be a multimeric and monomeric forms of PINs (Figure 3.23; lanes 2 and 3). It is notable that these bands were only recovered by hydrophobic interaction purification. Further, strong bands at about 50 kDa were observed on the gel for chloroplast PIN proteins and also negative control (Figure 3.23; lanes 2, 3, 5). This band may represent the ribulose 1, 5-

bisphosphate carboxylase/oxygenase (RuBisCO) large subunit, which is the most abundant protein in leaves (Bally et al., 2009).

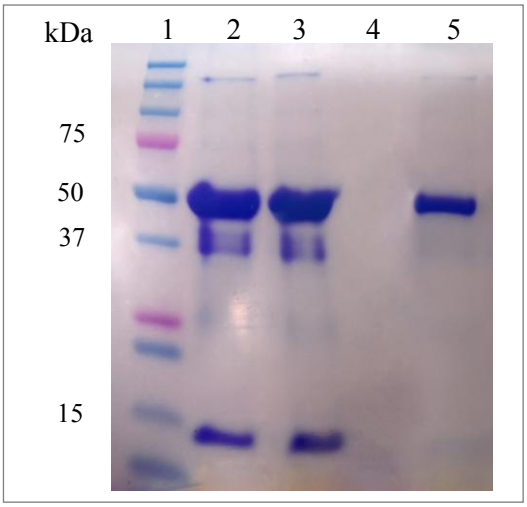

Figure 3.23 SDS-PAGE for fractions eluted from the Butyl-Toyopearl column based on hydrophobic interaction system.
Lane 1: Dual Xtra standards (Bio-Rad); lane 2 and 3: eluted fractions of PINA and PINB respectively; lane 4: no sample; lane 5: eluted fraction of negative control (5'+integrase modules only).

Further purification was attempted in order to remove Rubisco. TSP fractions were prepared as per previous purifications and passed over a Butyl-Toyopearl column. After this, RuBisCO was removed using sodium phytate precipitation (Section 2.13.14). The stained gel showed successful removal of Rubisco, but the bands of interest (37 kDa and 15 kDa) were also very faint (Figure 3.24; lanes 2 and 3).

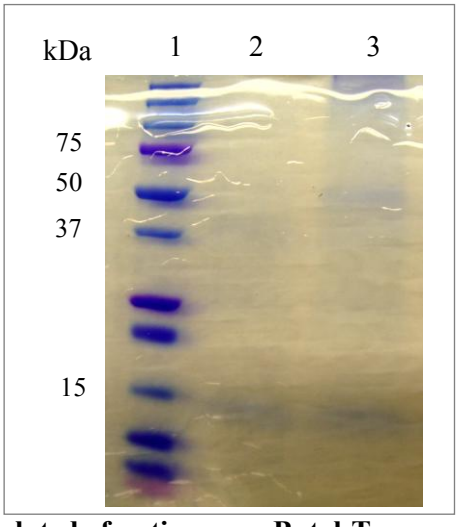

Figure 3.24 SDS-PAGE of eluted fraction on Butyl-Toyopearl column based on hydrophobic interaction system and sodium phytate precipitation.
Lane 1: Dual Xtra standards (Bio-Rad); lane 2 and 3: eluted fractions of PINA and PINB with sodium phytate precipitation respectively.

Western blot analysis using the Durotest antibody resulted in a broad band at ~37 kDa, confirming this as the multimer form of PINA and PINB (Figure 3.25; lanes 1 and 2). The result confirmed that this antibody is specific for both PINs, but also suggest that it is most likely not able to recognize the monomer forms of PINA or PINB, as seen earlier (Figure 3.20).

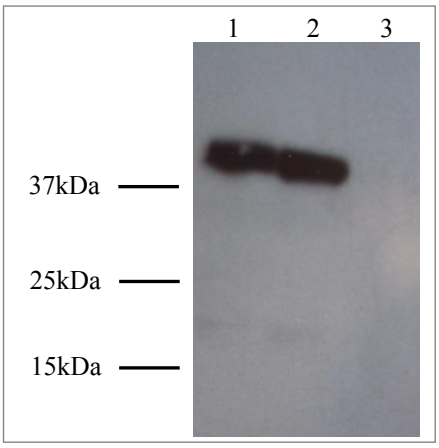

Figure 3.25 Western blot of eluted fractions on Butyl-Toyopearl column based on hydrophobic interaction system. Lane 1 and 2: eluted fractions of PINA and PINB, respectively; lane 3: eluted fractions of negative control (5'+integrase modules only).

3.3.4 Western blot analysis using anti His-tag for PIN proteins

The TSP of infiltrated leaves using 3' PINA and PINB modules and different 5' vector modules (cytosol or chloroplast) were subjected to western blot analysis with Durotest antibody. The samples which showed a signal with this antibody were used for western blot with anti-His antibody (Table 2.3). Different concentrations of proteins and anti-His antibody were tested, but no signals detected. Further, after purification with two different systems, i.e., His-tag purification under native conditions, and hydrophobic interaction purification, purified PINs were used for western blots. Following His-tag purification under native conditions, no bands for C-terminally His-tagged PINs were observed (Figure 3.26; lanes 3 and 4), while the samples after hydrophobic purification showed two bands, corresponding to the PIN multimer of ~37 kDa and monomer size of ~15 kDa (lanes 1 and 2).

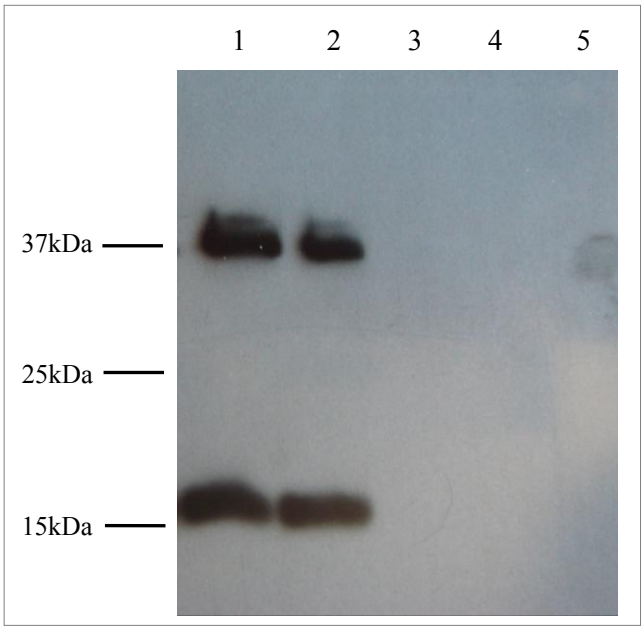

Figure 3.26 Western blot analysis of PIN proteins purified with two different systems.
Lane 1 and 2: eluted fractions of PINA and PINB from Butyl-Toyopearl columns respectively; lane 3 and 4: eluted fractions of PINA and PINB on Ni-NTA resin columns respectively; lane 5: eluted fraction of negative control (5'+integrase modules only).

After purification the recombinant PIN proteins, to obtain an accurate mass PINs the preliminary analysis has been done using Maldi-TOF MS (detailed in Appendix III). However, the results were inconclusive as sequences of the peptide were determined to be unknown.

3.4 Results of antimicrobial activity tests

3.4.1 Antibacterial activity

The chloroplast-expressed purified PINs with different purification systems were tested for antibacterial activity (as detailed in Chapter 2), using the protein stock (~1 mg/mL). The synthetic peptide PuroA (FPVTWRWWKWWKG-NH_2) was used as positive control (Section 2.12.1). The negative control used was the TSP of *N. benthamiana* infiltrated by 5' and integrase modules that was purified based on affinity and hydrophobic purifications. The activities were tested against *Escherichia coli* (ATCC 25922; a Gram negative bacterium) and *Staphylococcus aureus* (ATCC 25923; a Gram positive bacterium); the strains of both can cause a range of illnesses in humans. The minimum inhibitory concentration (MIC) was defined 'the lowest concentration of an antimicrobial agent which will inhibit the growth of a microorganism after overnight incubation' (Wiegand et al., 2008). The MIC results were observed by eye and by measuring the optical density at 595 nm (OD_{595}) of each well after 18 hours incubation of cells with the peptide/protein. Activity of PuroA was consistent with previous work in our laboratory (Phillips et al., 2011) (Table 3.4). The results confirmed *in vitro* antibacterial abilities of plant-made recombinant PINs purified by His-tag purification under native conditions and also by hydrophobic interaction purification. The PINs purified under denaturing conditions had no observable activity. Both PINA and PINB His-tag purified under native conditions showed activity against *E. coli* (MIC 64 µg/mL) which was less than that of the PuroA peptide (MIC 16 µg/µL) (Table 3.4; Figure 3.27). PINA was observed to be active against *S. aureus* (MIC 64 µg/mL), however, PINB showed higher activity (MIC 125 µg/mL). With hydrophobic purification, both PINA and PINB showed better activity against *E. coli* (32 µg/mL), and PINA showed the same activity (MIC 32 µg/mL) against *S. aureus* while PINB was less active against it (64 µg/mL). These observations confirm the *in vitro* antimicrobial abilities of recombinant PINs. Further, the PINs purified based on hydrophobic interaction had better activity compared to both the His-tag purification systems. The antibacterial activity of mixed PINA and PINB (1:1) (~1 mg/mL stock) were also tested against both bacteria. The result observed same activities for both purification systems (32 µg/mL and 64 µg/mL) (Table 3.4).

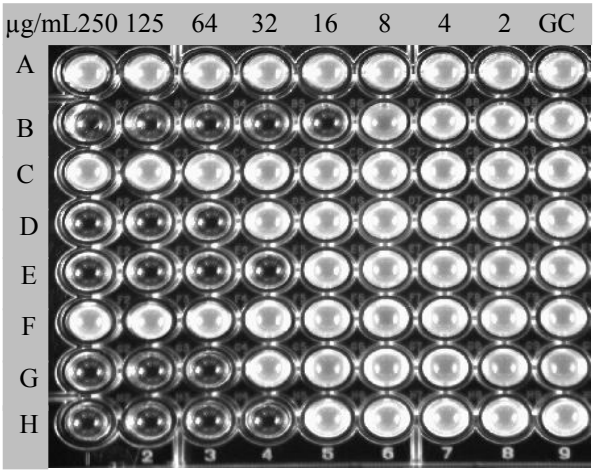

Figure 3.27 Example of Minimum Inhibitory Concentration (MIC) assay for PuroA peptide and plant-made recombinant PIN proteins against *E. coli.*
Peptide/protein dilution series from column 1 to 8; A: negative control (extract of leaf infiltrated with 5'+integrase modules only); B: positive control (PuroA peptide); C: rPINA (His-tag purification under denaturing conditions); D: rPINA (His-tag purification under native conditions); E: rPINA (hydrophobic purification); F: rPINB (His-tag purification under denaturing conditions); G: rPINB (His-tag purification under native conditions); H: rPINB (hydrophobic purification). Wells were inoculated with *E. coli* (ATCC 25922) and MIC recorded as the lowest concentration to completely inhibit growth. GC column= growth control of *E. coli.*

Table 3.4 Antibacterial activity of plant made recombinant PINA and PINB

Protein/peptide name	Purification method	MIC (µg/mL)[a]	
		E. coli	***S. aureus***
PuroA Positive control	Synthetic peptide FPVTWRWWKWWKG-NH_2	16 (±0)	16 (±0)
rPINA	His-tag purification under denaturing conditions	>250	>250
rPINA	His-tag purification under native conditions	64 (±0)	64 (±0)
rPINA	Hydrophobic interaction purification	32 (±0)	32 (±0)
rPINB	His-tag purification under denaturing conditions	>250	>250
rPINB	His-tag purification under native conditions	64 (±0)	125 (±0)
rPINB	Hydrophobic interaction purification	32 (±0)	64 (±0)
PINA+PINB	His-tag purification under native conditions	32 (±0)	64 (±0)
PINA+PINB	Hydrophobic interaction purification	32 (±0)	64 (±0)
Negative control[b]	His-tag purification under native conditions	>250	>250
Negative control[b]	Hydrophobic interaction purification	>250	>250

[a]Defined as the lowest concentration that completely inhibited bacterial growth/ the mean of triplicate assays. [b]TSP of *N. benthamiana* infiltrated by 5' and integrase modules only.

3.4.2 Antifungal activity

The purified recombinant PINs were also tested for activity against five common phyto-pathogenic fungi (Section 2.12.3). *Rhizoctonia cerealis* and *Rhizoctonia solani* are responsible for sharp eye spot in wheat and sheath blight in rice, respectively (Hamada et al., 2011; Taheri and Tarighi, 2011). *Colletotrichum graminicola* is responsible for anthracnose in many cereals including wheat and maize (Dean et al., 2012). *Drechslera brizae* is a fungus that causes post-harvest rot in crops (Naureen et al., 2009). Negative control wells contained purified TSP of *N. benthamiana* infiltrated by 5' and integrase modules, and positive control wells contained PuroA. The MIC was defined as the lowest concentration of the protein/peptide to inhibit fungal growth (Espinel-Ingroff and Cantón, 2007), which was observed visually only. The results are presented in Table 3.5. The PIN proteins purified under both the native condition of His-tag purification and the hydrophobic interaction purification showed activity against *R. solani* (250 µg/mL and 125 µg/mL) but were less active than the PuroA peptide (32 µg/mL) (Table 3.5; Figure 3.28). Proteins purified under denaturing conditions had no observable antifungal activity.

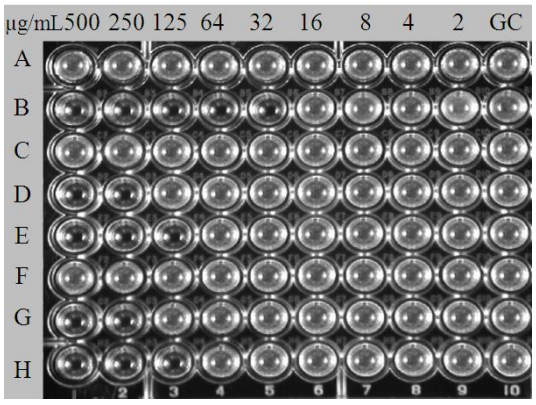

Figure 3.28 Example of microdilution plate Minimum Inhibitory Concentration (MIC) assay for filamentous fungi against *R. solani.*
Peptide/protein dilution series from column 1 to 9; A: negative control (extract of leaf infiltrated with 5'+integrase modules only); B: positive control (PuroA peptide); C: rPINA (His-tag purification under denaturing conditions); D: rPINA (His-tag purification under native conditions); E: rPINA (hydrophobic interaction purification); F: rPINB (His-tag purification under denaturing conditions); G: rPINB (His-tag purification under native conditions); H: rPINB (hydrophobic interaction purification). GC column=growth control of *R. solani*.

Table 3.5 Antifungal activity of plant made recombinant PINA and PINB

Protein/ peptide name	Purification method	MIC (µg/mL)[a]				
		C.Gramini cola	*D.brizae*	*F. oxy-sporum*	*R. solani*	*R. cerealis*
PuroA Positive control	Synthetic peptides FPVTWRWWKWWKG-NH_2	250 (±0)	250 (±0)	>500	32 (±0)	125 (±0)
PINA	His-tag purification under denaturing conditions	>500	>500	>500	>500	>500
PINA	His-tag purification under native conditions	500(±0)	500(±0)	>500	250(±0)	250(±0)
PINA	Hydrophobic interaction purification	500(±0)	500(±0)	>500	125(±0)	250(±0)
PINB	His-tag purification under denaturing conditions	>500	>500	>500	>500	>500
PINB	His-tag purification under native conditions	500(±0)	500(±0)	>500	250(±0)	250(±0)
PINB	Hydrophobic interaction purification	500(±0)	500(±0)	>500	125(±0)	125(±0)
PINA+PINB	His-tag purification under native conditions	500(±0)	500(±0)	>500	125(±0)	125(±0)
PINA+PINB	Hydrophobic interaction purification	500(±0)	500(±0)	>500	125(±0)	125(±0)
Negative control[b]	His-tag purification under native conditions	>500	>500	>500	>500	>500
Negative control[b]	Hydrophobic interaction purification	>500	>500	>500	>500	>500

[a]Defined as the lowest concentration of the peptide or protein to inhibit fungal growth/ the mean of triplicate assays. [b]TSP of *N. benthamiana* infiltrated by 5' and integrase modules only.

3.4.3 Protein stability at different temperature

The effect of temperature on the activity and stability of PIN proteins purified by His-tag purification under native conditions were tested against *E. coli* and determined by MIC assay. PIN proteins were stored at 37°C, RT (between 20°C-25°C), 4°C, -20°C and -80°C for one week, then tested against *E. coli.* The results showed stable activity against *E. coli* when stored at -20°C and -80°C. PIN proteins showed better activity against *E. coli* at day one (MIC 64 μg/mL) compared to when stored at 4°C (MIC 250 μg/mL). The PuroA peptides retained with their original activity after one week of incubation at room temperature (between 20°C-25°C), 4°C, -20°C and -80°C for one week (Table 3.6).

Table 3.6 Stability of recombinant PINs at different incubation temperature

Peptide/Protein name	Incubation Temperature	MIC (μg/mL)[a] against *E. coli* at day 1	MIC (μg/mL)* against *E. coli* at day 7
PuroA	All[b]	16 (±0)	16 (±0)
rPINA/rPINB	-80°C	64 (±0)	64 (±0)
rPINA/rPINB	-20°C	64 (±0)	64 (±0)
rPINA/rPINB	4°C	64 (±0)	250(±5)
rPINA/rPINB	20°C-25°C	64 (±0)	>250
rPINA/rPINB	37°C	64 (±0)	>250

[a] The mean of triplicate assays, [b] PuroA not tested at 37°C.

3.4.4 Haemolytic activity

The haemolytic activity of the purified PINs against sheep RBCs was determined as a measure of toxicity to eukaryotic cells (Section 2.12.5). Positive haemolytic activity was defined as the recombinant protein/peptide dose required to lyse 50% of the RBCs (HD50). PBS (pH 7.4) and 1% Triton X-100 were included as a negative (zero% haemolysis) and positive (100% haemolysis) controls, respectively. The recombinant PINs purified with His-purification system under native condition at 125 µg/mL, 64 µg/mL, 32 µg/mL and 16 µg/mL did not show any notable activity (Figure 3.29, Table 3.7), confirming their non-lysis of mammalian cells and specificity against microbial membranes. However, the PINs at 500 µg/mL and 250 µg/mL appeared to show higher haemolytic activity than the peptide PuroA.

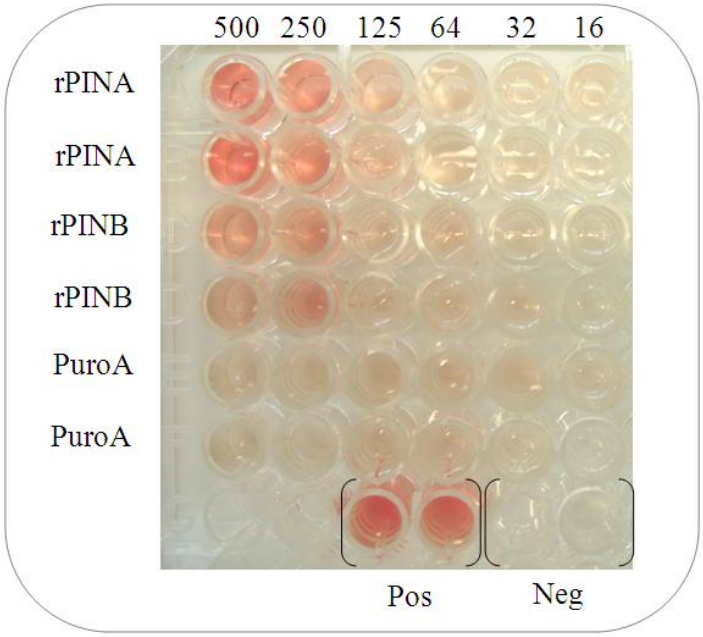

Figure 3.29 Haemolytic activity assays against sheep red blood cells (RBCs).
Dilution series from column 1 to 6: 500 µg/mL, 250 µg/mL, 125 µg/mL, 64 µg/mL, 32 µg/mL and 16 µg/mL. rPINA: recombinant plant made PINA; rPINB: recombinant plant made PINB; Pos: Positive control 100% RBC lysis (1% Triton X-100); Neg: Negative control 0% RBC lysis (PBS, pH 7.4).

Table 3.7 Haemolytic activity of plant-made recombinant PINs

Protein/ Peptide	Percent haemolysis of sheep RBCs by recombinant PINs						Haemolysis (HD_{50})[a]
	500 (µg/mL)	250 (µg/mL)	125 (µg/mL)	64 (µg/mL)	32 (µg/mL)	16 (µg/mL)	
PuroA	15	10	6	4	0	0	>500
rPINA	32	22	10	6	0	0	>125
rPINB	20	20	8	6	0	0	>125

[a] Results represent the average of three separate experiments conducted in duplicate.

3.5 Discussion

3.5.1 Expression

A number of studies with transgenic *Pin* genes have reported, the purpose being to test their causative roles of PIN proteins in altering grain texture (Beecher et al., 2002a; Hogg et al. 2004; Krishnamurthy and Giroux, 2001; Wada et al., 2010; Xia et al., 2008) or testing whether they can impart *in vivo* antimicrobial activity (Faize et al., 2004; Kim et al., 2012a; Krishnamurthy et al., 2001; Luo et al., 2008; Zhang et al., 2011) as detailed in Chapter 1 (Sections 1.4.2 and 1.5.1). Further, mature full-length PINA and PINB have been reported to be over-expressed in bacterial expression systems (Capparelli et al., 2006; Capparelli et al., 2007) and in BY-2 *Nicotiana tabacum* cell suspension culture (Sorrentino et al., 2009). In the BY-2 culture, only the recombinant PINB targeted to the chloroplast was observed with an apparent size of 20 kDa and yield of 0.35% of TSP but no signal were observed using two constructs for apoplast targeting for both PINs (Sorrentino et al., 2009). Further, peptides similar to the PINs in terms of being cysteine-rich and antimicrobial, but smaller, expressed in transgenic tobacco lines represented only 0.1% of the TSP, and their expression either intra- or extra-cellularly did not result in increased fungal resistance (De Bolle et al., 1996).

Plants as an alternative production platform for active recombinant therapeutic proteins offers several advantages including lower production costs and high biomass volume. In this study we used a transient transformation technology, the magnICON® for production of PINs using *N. benthamiana*. This system is based on the deconstructed tobacco mosaic virus (TMV) and is distinguished by the use of independent modules harboring binary vectors, encoding different virus components, and allowing for DNA delivery into plant cells by *A. tumefaciens*. The *in vivo* recombination, mediated by the integrase (pICH14011) is accompanied with assembly of various pro-vectors, followed by intron splicing, rendering an active viral replicon capable of producing the protein of interest, and yields of up to 40% of TSP (Gleba et al. 2007). The replicon can move systemically through the plant (Gleba et al. 2005; Marillonnet et al. 2004). The assembly of recombinant proteins in plant tissues is critical for viability the plant systems as bioreactors for therapeutic proteins (Streatfield 2007). The magnICON® system is considered to be fast, requiring approximately 10 days for transformation and

less than a month for the recovery of the expressed protein. This is highly desirable compared to other systems such as chloroplast transformation which requires more than two months, and nuclear stable transformation that requires several months (Patiño-Rodríguez et al., 2013).

The successful expression of GFP proteins was visualized by examination under UV light and in western blot using the anti-GFP antibody. Different constructs were used to produce the PIN proteins in leaves of *N. benthamiana*. Both PIN proteins produced the highest amount 10 days post infiltration when targeted to the chloroplast and cytosol. As a commercial standard is not available for PINs, the 3% non-durum wheat in Durotest kit for standard in ELISA assay was used to quantify PIN proteins; hence the quantify estimates for PINs are approximate. The results demonstrate PINA and PINB were transiently expressed in *N. benthamiana* and accumulated to ~0.83% and ~0.89% of the TSP, respectively, following targeting to chloroplast. Western blot analysis by Durotest antibody confirmed the size at approximately 45 kDa when the chloroplast and cytosol targeting 5' modules were used, and also with C-terminal SEKDEL added for retention of the expressed protein in the ER. This finding suggests the formation of aggregates not only inside chloroplasts but also in the cytosol and ER compartments of the plant cell.

PINA is known to form aggregates in solutions with high ionic strength and low pH (Le Bihan et al., 1996), correct folding being dependent on pH and a contributor to low protein solubility (Issaly et al., 2001). Further, an earlier study has noted the importance of protein aggregates of recombinant soybean agglutinin (rSBA) in *N. benthamiana* necessary for its biological activity (Tremblay et al., 2011). Similar folding pattern has also been observed, when proteins containing multiple disulphide bonds were expressed in chloroplasts, including CTB-proinsulin (Ruhlman et al., 2007) and interferon-a2b (Arlen et al., 2007) RC101 and PG1 (Lee et al., 2011b).

3.5.2 Purification

Both PINA and PINB are disulphide-bonded proteins with unique TRD. PINs contain 10-Cys backbone proposed to form five disulphide bonds that have an important role in protein stability and activity (detailed in Chapter 1). PINA and PINB have been expressed in bacterial systems using His-tag (Capparelli et al., 2006) and GST-tag (Capparelli et al., 2006; Capparelli et al., 2007). Furthermore, 3×FLAG N-terminal tag was added for western blot analysis using mouse anti-flag monoclonal antibody which detected recombinant PINB at ~20 kDa (Sorrentino et al., 2009).

Affinity tags can have role for promoting the solubility of the expressed fusion proteins (Hearn and Acosta, 2001; Terpe, 2003; Waugh, 2005). Ideally, the tags should not affect the structure and stability of the proteins. On the other hand, they may affect proteins advantageously by increasing expression, solubility and stability (Arnau et al., 2006; Hearn and Acosta 2001; Smyth et al., 2003; Terpe, 2003) and promote proper folding (Smyth et al., 2003; Waugh, 2005). The His-tag with metal IMAC systems is currently the most commonly used affinity tag (Listwan et al., 2004; Waugh, 2005). Generally His-tag can interact with a chromatographic matrix like Ni-NTA resin as it is most attracted to immobilized metal ions, such as cobalt, nickel and copper (Terpe, 2003; Waugh, 2005) the selectivity being based on the fact that the density of His residues in this tag is higher than that on the surface of many proteins (Gaberc-Porekar and Menart 2001) and other potential electron donor side chains include tryptophan and cysteine (Scopes, 1993). Since both PINs contain tryptophan and cysteine, they may be capable of binding to metal-chelate columns, hence both were fused translationally to a small His-tag.

After affinity purification using the His-tag for PINs expressed in the chloroplast, western blot analysis confirmed two bands at 45 kDa and 37 kDa. However the ~45 kDa proteins were observed as faint bands (Figure 3.20; lanes 6 and 7). In addition, for the PINs protein sample infiltrated using the chloroplast 5'-module, the western blot detected the small and faint band at ~30 kDa before purification (Figure 3.10 and 3.17; lane 5). The expected sizes of the PIN monomers with His-tag were ~15 kDa. Thus, the bands may correspond to multimers. Further, the His-tag could have affected the

folding of the recombinant PIN proteins or incomplete cleavage of the chloroplast transit peptide (Bruce, 2000; Emanuelsson et al., 1999), resulting in the size discrepancy. The incomplete cleavage of the chloroplast transit peptide has also been reported for the PyMSP4/5 antigen expressed in plants using the magnICON® system chloroplast 5'-module (Webster et al., 2009). The artificial dicot chloroplast targeting presequence for pICH12190 chlorolast targeted 5' module coding for [massmlssaavvatrasaaqasmvapftglksaasfpvtrkqnnlditsiasnggrvqca] (Marillonnet et al., 2004; Dr. S. Marillonnet, personal commincation, April 2014) with estimated size of 6 kDa using the 'compute pI/Mw tool' at the ExPASy.

The hydrophobic purification system was attempted for C-terminally His-tagged PINs, as this is widely used for the isolation of hydrophobic membrane proteins and antimicrobial cationic peptides (Skosyrev et al., 2003). Hydrophobic patches of proteins interact with a hydrophobic stationary phase. Ammonium sulfate decreases solubility of most proteins, due to the salting-out effect, hence ethanol was used, being less polar. The organic solvents, i.e., ethanol or n-butanol, enable protein precipitation by electrostatic aggregations. Protein solubility during extraction is affected by a complex mechanism using organic solvents. The salt promotes solubility of proteins by preventing their electrostatic aggregation in the organic solvent (Samarkina et al., 2009). However, the ethanol phase is also saturated with ammonium sulfate. It is important to add ethanol as soon as possible after ammonium sulfate so as to avoid nonspecific precipitation of target protein with other proteins. The two phases were formed within three to five minutes after addition of ethanol and vigorous shaking, and centrifugation was started as soon as the phases began to form. The n-butanol, a less polar and more hydrophobic organic solvent than water was added to the ethanol phase to recover the PINs in the lower aqueous phase. The hydrophobic interaction purification thus allowed fast processing and ability to concentrate the sample. Butyl-Toyopearl column was used for removing any compounds that were not visible in Coomassie Blue stained gels. Both PINs were detected at ~37 kDa with the Durotest antibody, and this was the only technique that showed the PINs with anti-His antibody in both multimer (~37 kDa) and monomer (~15 kDa) bands. This finding is most significant and suggests that hydrophobic purification affected the folding of PINs. Further, the results confirmed

that the Durotest antibody is likely not able to detect monomeric forms of PINs. However this antibody detected the positive at ~15 kDa which is protein complex of friabilin with PINs as major part (detailed in section 1.2.1). Prior studies (Greenwell, 1992; Wiley et al., 2007) noted that the Durotest antibody probably did not react with PINs after reduction of disulphide bonds or denaturation during fixation for immunocytochemical analyses. The protein extracts from grain of a bread wheat line and two transgenic lines of durum wheat expressing PINA and PINB were tested by western blot using this antibody and unreduced PIN detected at 15 kDa (Wiley et al., 2007). Recently, this antibody was used for immunolocalisation of PIN proteins in the endosperm cell of transgenic rice (Fujiwara et al., 2014).

3.5.3 Characterisation of bioactivity

PINA and PINB have potent activities against a broad spectrum of microorganisms (detailed in section 1.5). The recombinant PINA and PINB have been expressed in *E. coli* and affinity-purified using His and GST tags, and tested against *E. coli* (MIC 30 μg/mL) and *S. aureus* (MIC 30 μg/mL) (Capparelli et al., 2006). The activity of recombinant PINA expressed in *E. coli* and purified by affinity purification using NusA fusion tag was reported to be active against *E. coli* (MIC 90 μg/mL) and *S. aureus* (MIC 150 μg/mL) (Miao et al., 2012). Furthermore, chloroplast targeted PINB in *N. tabacum* cells has activity against *E. coli* (91% growth inhibition) (Sorrentino et al., 2009). Several studies have revealed the successful production of low-cost and functional antimicrobial peptides and proteins in transgenic tobacco (Jacob and Zasloff, 1994; Lee et al., 2011b; Oey et al., 2009). Previously the ability of the Potato Virus X (PVX) vector to produce an antimicrobial protein in *N. benthamiana* leaves has been reported (Saioth et al. 2001). The human lactoferrin (hLfN) expressed in *N. benthamiana* using a PVX is also active against *E. coli* and *S. aureus* (Li et al., 2004). The magnICON® technology was also used in *N. tabacum* for producing the antimicrobial peptide protegrin-1 (PG-1), which inhibited the growth of several bacterial and fungal pathogens of humans (Patiño-Rodríguez et al., 2013). Hence the goal of this study was to produce and purify functional PINs *in planta*.

In the current study, purified soluble protein extracts from transiently-transformed *N. benthamiana* leaves with magnICON® system, have been used for biological activity assays of PIN proteins and sharp decrease observed in the viability of different pathogens. Purified extracts of leaves infiltrated with PIN transgenes were added to *in vitro* bioassays and showed successful expression of bioactive proteins. The antibacterial activity of the His-tag purified PINA under native conditions showed a similar activity against *S. aureus* and *E. coli* (MIC 64 µg/mL), however the purified PINA using hydrophobic interaction system was more active against both *S. aureus* and *E. coli* (MIC 32 µg/mL). His-tag purified PINB under native conditions had similar activity as PINA against *E. coli* (MIC 64 µg/mL) but not against *S. aureus* (MIC 125 µg/mL). The activity results indicate that the hydrophobic interaction purified proteins displayed 2-fold more activity against *E. coli* for both recombinant PINs. No inhibition of microbial growth was detected with extracts from infiltrated leaves without PINs, purified with both systems. The peptide PuroA (based on the TRD of wild type PINA) used as positive control in the assays showed strong activity towards *E. coli* and *S. aureus* (MIC 16 µg/mL), supporting previous reports (Jing et al., 2003; Phillips at al., 2011). It is particularly noteworthy that the growth inhibition of both Gram-positive and Gram-negative bacteria by recombinant PINs was high for both affinity and hydrophobic systems, suggesting correct formation of disulphide bonds in the plant-made PINs. The PIN proteins lose antimicrobial activity in the presence of 6 M urea. Many proteins require a particular three-dimensional structure and disulphide bonds to function. If the disulphide bonds are not formed correctly, the protein can degrade or accumulate as insoluble inclusion bodies (Lesk, 2010). PINs, with their 10-Cys backbone that forms five disulphide bonds may require these bonds for protein stability and activity.

The antifungal activity of PIN proteins has been shown *in vitro* (Dubreil et al., 1998) and *in planta* when *Pin* genes have been introduced transgenically, e.g., in rice (Krishnamurthy et al., 2001), apple (Faize et al., 2004), durum wheat (Luo et al., 2008) and wheat seeds overexpressing *Pins* (Kim et al., 2012a). This work further examined the activity of the recombinant PINs against the five common fungi. Recombinant plant-made PINs purified under His-tag and hydrophobic purification showed activity

against *R. solani* and *R. cerealis*. PINA and PINB, when purified by hydrophobic interactions, showed better activity against most organisms tested, in comparison with the His-tag purification under native conditions. A possible reason might be related to the presence of more monomer forms of PINs in these preparations, or better protein folding. Initially, the assay was carried out, which showed no activity against *C. graminicola*, *D. brizae* and *F. oxysporum* at MIC 250 µg/mL. Hence, the assay was repeated at a higher MIC (500 µg/mL) for both recombinant PINs. Activity was observed only against *C. graminicola* and *D. brizae* (not for *F. oxysporum*) for PINA and PINB purified with His-tag under native conditions and hydrophobic purification systems. A possible explanation may be the stability of PINs and the time of incubation (at 25°C in dark for 7 days). The results of stability testing indicate that the plant-made PINs are not stable at 25°C or 37°C for 7 days. However, prior study in our laboratory has noted the thermal stability of PuroA and PuroB peptides (Alfred et al., 2013a). Previously *in vitro* studies indicated that the two proteins work synergistically with enhanced activity against fungal pathogens (Capparelli et al., 2005). In this work when PINA and PINB were mixed for the antimicrobial assay shown the inhibition against bacteria and fungi and have shown synergy between the two proteins against fungi and bacteria. The haemolytic activity assay displayed in PuroA at >500 µg/mL, however the haemolytic activity of the recombinant PINs showed at >125 µg/mL. This variation between PuroA and PIN proteins may be related to plant alkaloids in the preparations, such as nicotine most abundant alkaloid in the genus *Nicotiana* and recently found to exhibit haemolytic activity *in vitro* against human erythrocytes (Jasiewicz et al., 2014).

The findings in this chapter are highly promising in providing a methodology for production of PINs as potential therapeutic agents against various mammalian and plant pathogens as well as for use in hygiene and food industries. The two wild type PINs are reported act in a co-operative manner when binding to the surface of starch granules. The following chapter investigates PIN interaction in a plant system using the BiFC system.

CHAPTER 4

Determination of the protein-protein interactions (PPI) of PIN proteins using Bimolecular Fluorescence Complementation (BiFC) *in planta*

4.1 Introduction

The wild type PIN proteins (PINA and PINB) are causatively associated with soft wheat, while mutations in one or both *Puroindoline* genes result in hard textures, as summarised in Chapter 1 (Sections 1.3 and 1.4). Both PINA and PINB associate with biological membranes through their lipid-binding properties, which are also likely involved in grain hardness determinants (Gautier et al., 1994; reviewed in Bhave and Morris, 2008b; Morris, 2002; Nadolska-Orczyk et al., 2009). Transgenic studies (Hogg et al., 2004; Martin et al., 2006; Swan et al., 2006, Wanjugi et al., 2007) have shown that the PINs undergo some interaction or act in an inter-dependent manner in their effects on grain texture. The two wild type PINs were found to act co-operatively to prevent break-down of lipids in soft grains, mutations in either gene leading to higher polar lipid degradation (Kim et al., 2012a). Furthermore, the tryptophan-rich domain (TRD) has been considered the most important domain for the membrane-active nature of PIN proteins. Despite the above literature on PINs, the nature of the interdependence of the two proteins, interactions of PINs and any role of the TRD in these are unclear. Addressing these important questions could help to improve wheat quality. Previous work in our laboratory using the yeast 2-hybrid system provided evidence of *in vivo* protein-protein interactions (PPI) in PIN proteins expressed in yeast cells (Ziemann et al., 2008). The bimolecular fluorescence complementation (BiFC) assay is based on complementation approaches to detect protein associations occurring *in-vivo*, and allows visualisation of PPI in living cells by fluorescent signal (Gell et al., 2012; Hu et al., 2002). This chapter investigates (i) whether any physical interactions occur in PINA and PINB *in planta* using BiFC system; (ii) the effect of deletions of the hydrophobic domain (HD) domains from both PINs and the TRD of PINA on any interactions, and expression based on magnICON® system. The aims have been addressed using the methodologies explained in section 2.14.

4.2A Interaction studies for wild type PINA and PINB

4.2.1 Cloning of wild type PINA and PINB into pNBV vectors of the BiFC system

The ORF regions of the wild type alleles *Pina-D1a* (Genbank DQ363911), and *Pinb-D1a* (Genbank DQ363913) encoding the mature PIN protein sections (lacking the N-terminal signal peptide sequences) were amplified from the pICH-PINA-His and pICH-PINB-His clones (detailed in Chapter 3). Gene-specific primers with the appropriate restriction sites (Table 2.11) were used to introduce specific restriction sites at the 5' and 3' ends of the PCR fragments for cloning into the pNBV vectors (Section 2.14.2). The start codon was added to all forward primers and the native stop codon was removed for cloning into two pNBV vectors (gene-YN and gene-YC). The resulting PCR fragments were 400 bp (Figure 4.1; lanes 1 and 2). These were double-digested and cloned into four sets of double-digested pNBV vectors (gene-YN, gene-YC, YN-gene and YC-gene), which allowed for fusions of each gene with the N-terminal 155 amino acids of YFP (the YN fragment) or the 84 amino acids of the C-terminal end of YFP (the YC fragment). Empty pNBV vector DNAs were used to confirm the vector size consistent with promoter, terminator and YFP fragments (~4 kb) (Figure 4.1; lanes 4 to 7). More details for pNBV vectors are shown in Figure 4.3.

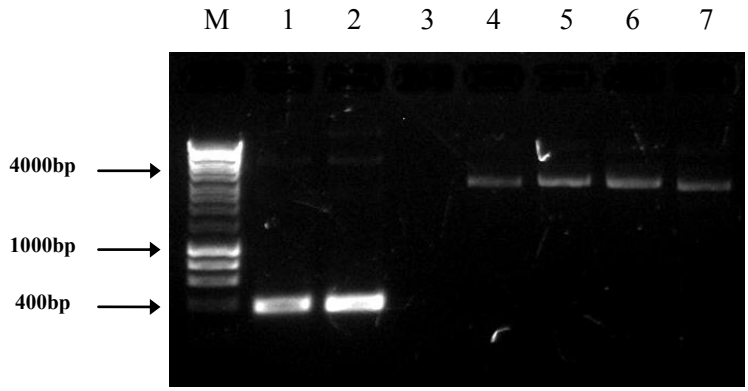

Figure 4.1 Second-round PCR of gene sections encoding mature PINs and DNA plasmids of empty pNBV vectors.
Lane M: DNA molecular weight marker, Hyperladder 1; lane 1: PINA (mature protein section of *Pina-D1a* with restriction sites); lane 2: PINB (mature protein section of *Pinb-D1a* with restriction sites); lane 3: negative control (no template); lane 4: DNA plasmid of pNBV vector (gene-YC); lane 5: DNA plasmid of pNBV vector (gene-YN); lane 6: DNA plasmid of pNBV vector (YN-gene); lane 7: DNA plasmid of pNBV (YC-gene).

The ligation mixtures of pNBV were transformed into *E. coli* Mach1 cells and grown on LB plates with carbenicillin. Empty vectors were also transformed to be used as controls. The presence of inserts was confirmed by colony-PCR (Figure 4.2) using insert-specific primers (Table 2.11). Positive colonies (clones with inserts) were grown in LB media containing carbenicillin. Plasmids were isolated from the positive clones and used for PCR and double-digestion with restriction sites at the 5' and 3' ends of the PINA and PINB fragments to confirm that the vectors contained the insert (data not shown).

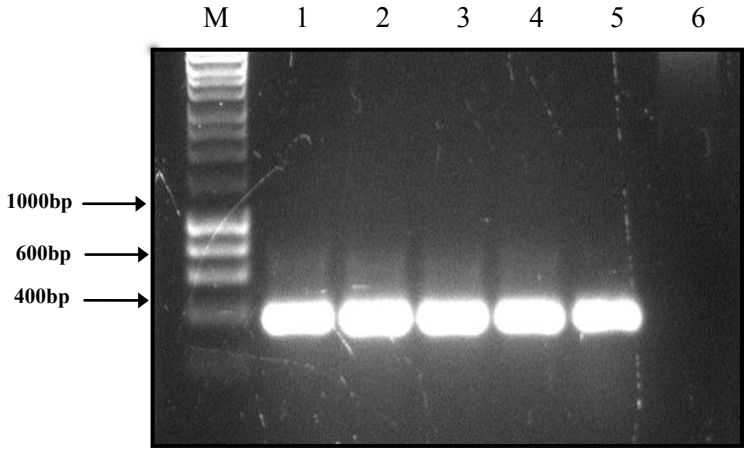

Figure 4.2 Colony PCR for preliminary selection of clones.
Lane M: DNA molecular weight marker, Hyperladder 1; lane 1-3: pNBV-PINA product; lane 4 and 5: pNBV-PINB product; lane 6: negative control (no template).

The above BiFC constructs were designated as pNBV-PINA-YN, pNBV-PINA-YC, pNBV-YN-PINA and pNBV-YC-PINA for PINA and pNBV-PINB-YN, pNBV-PINB-YC, pNBV-YN-PINB and pNBV-YC-PINB for PINB (Figure 4.3). They contain the 35S promoter of the cauliflower mosaic virus (862 bp), terminator of the *Nos* gene (NosT: 264 bp), lacZ gene (215 bp), a linker between YN or YC and the gene (54 bp), and yellow fluorescent protein (YFP) (**YN**=N-terminal fragment, amino acids 1 to 155 (465 bp), or **YC**=C-terminal fragment, amino acids 156 to 238 (249 bp)). The BiFC cassettes in pNBV were released from pNBV by NotI digestion and inserted into the plant expression vector (pMLBART; Figure 2.10). The full sequences of pNBV cassettes without PINs are shown in Appendix IV.

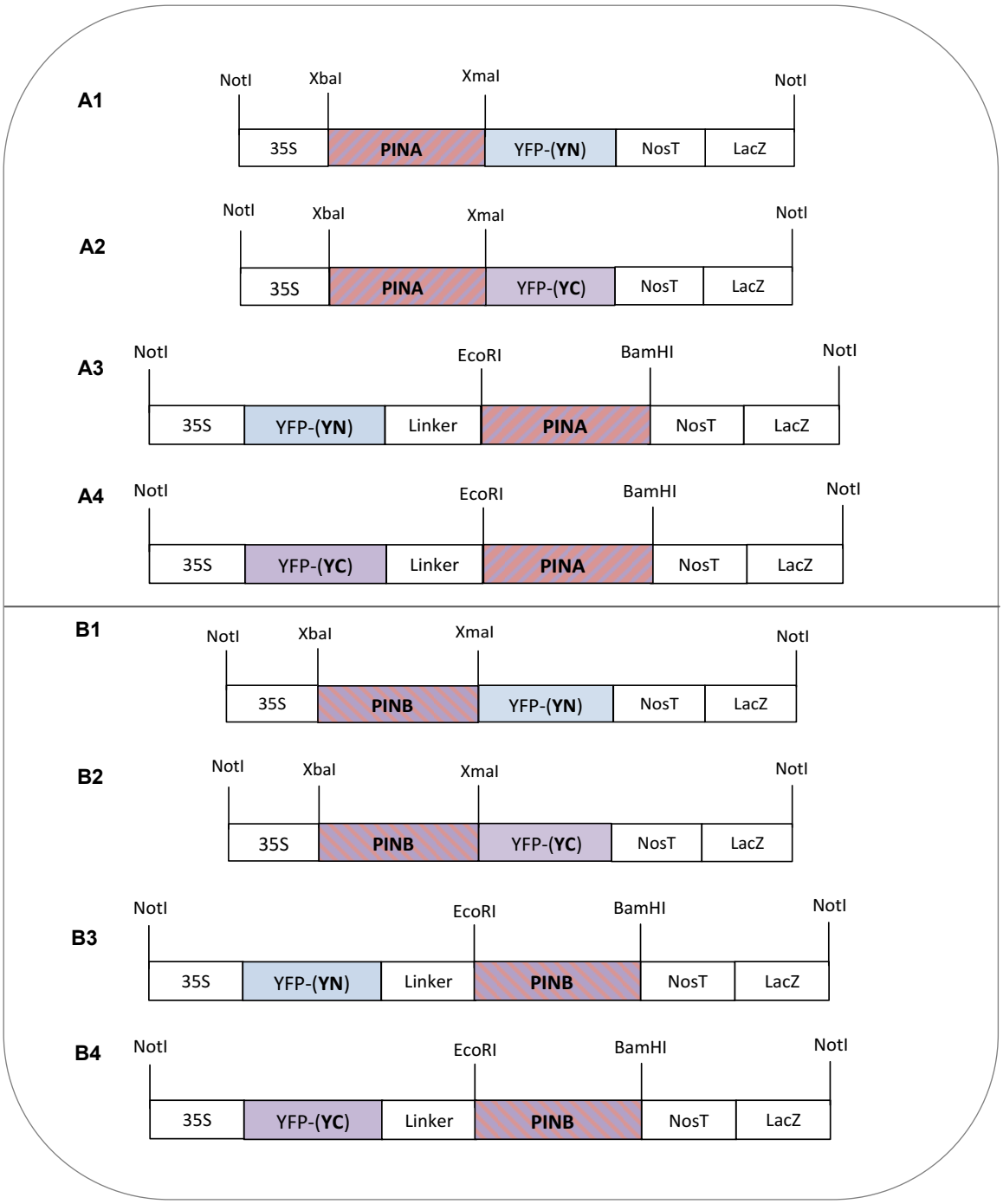

Figure 4.3 The pNBV module constructs encoding mature PINA and PINB proteins.
35S: promoter of the cauliflower mosaic virus; NosT: terminator of the *Nos* gene; YFP: yellow fluorescent protein (**YN**=N-terminal fragment 1 to 155 amino acid/**YC**=C-terminal fragment 156 to 238 amino acid). A1: pNBV-PINA-YN; A2: pNBV-PINA-YC; A3: pNBV-YN-PINA; A4: pNBV-YC-PINA; B1: pNBV-PINB-YN; B2: pNBV-PINB-YC; B3: pNBV-YN-PINB; B4: pNBV-YC-PINB.

The constructs were transformed into *E. coli* strain cells and screened by colony PCR with insert-specific primers (Table 2.11) followed by DNA sequencing. Alignment with the reference sequences; *Pina-D1a* (DQ363911) (Figure 4.4) and *Pinb-D1a* (DQ363913) (Figure 4.5) showed 100% identity.

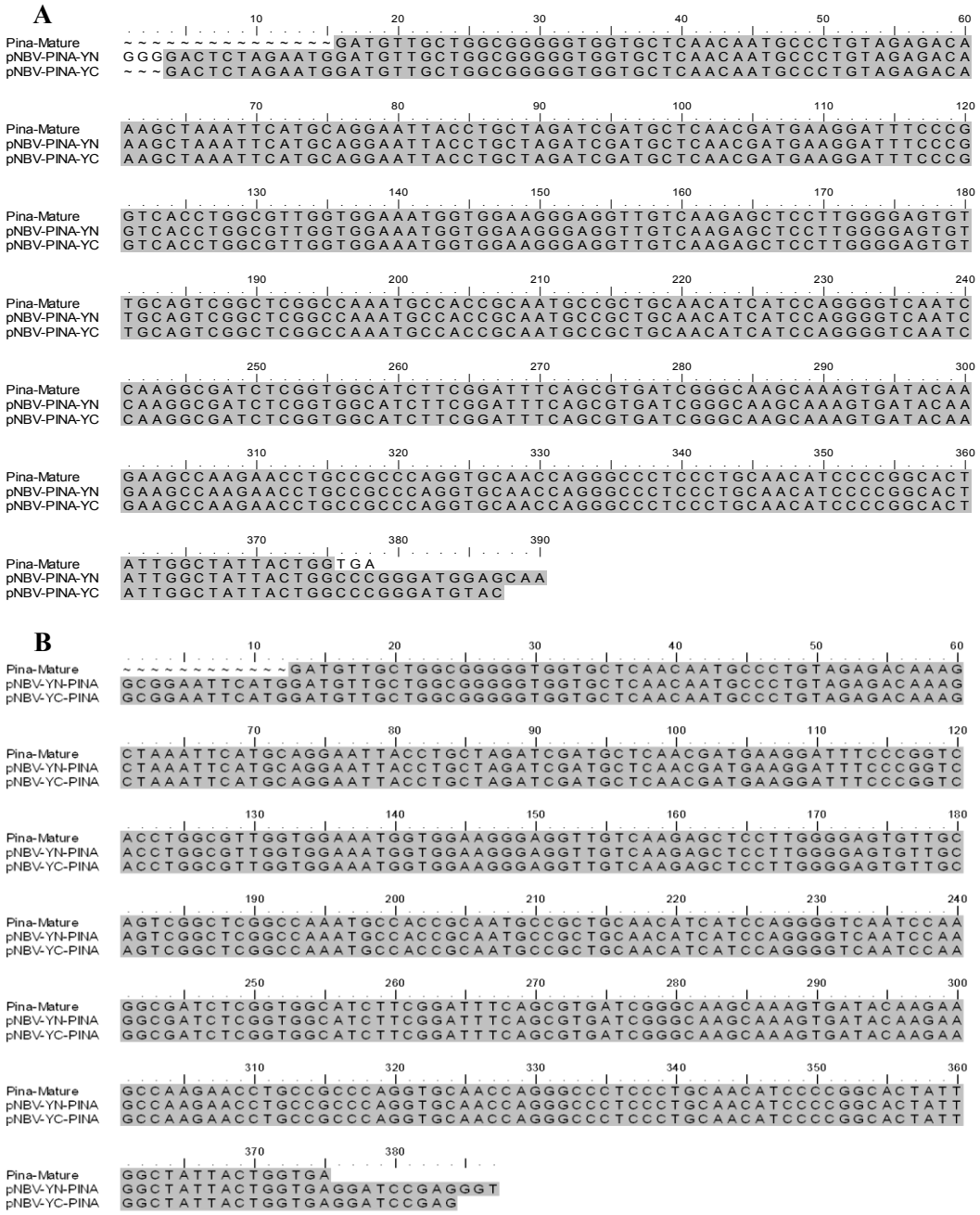

Figure 4.4 Alignments sequence of PINA in pNBV construct.
A: DNA sequence of mature putative *Pina-D1a* genes cloned in the pNBV (gene-YN) and pNBV (gene-YC) vectors. B: DNA sequence of mature putative *Pina-D1a* genes cloned in the pNBV (YN-gene) and pNBV (YC-gene) vectors. In both A and B, the line 1 is sequence of the reported WT *Pina-D1a* gene (DQ363911).

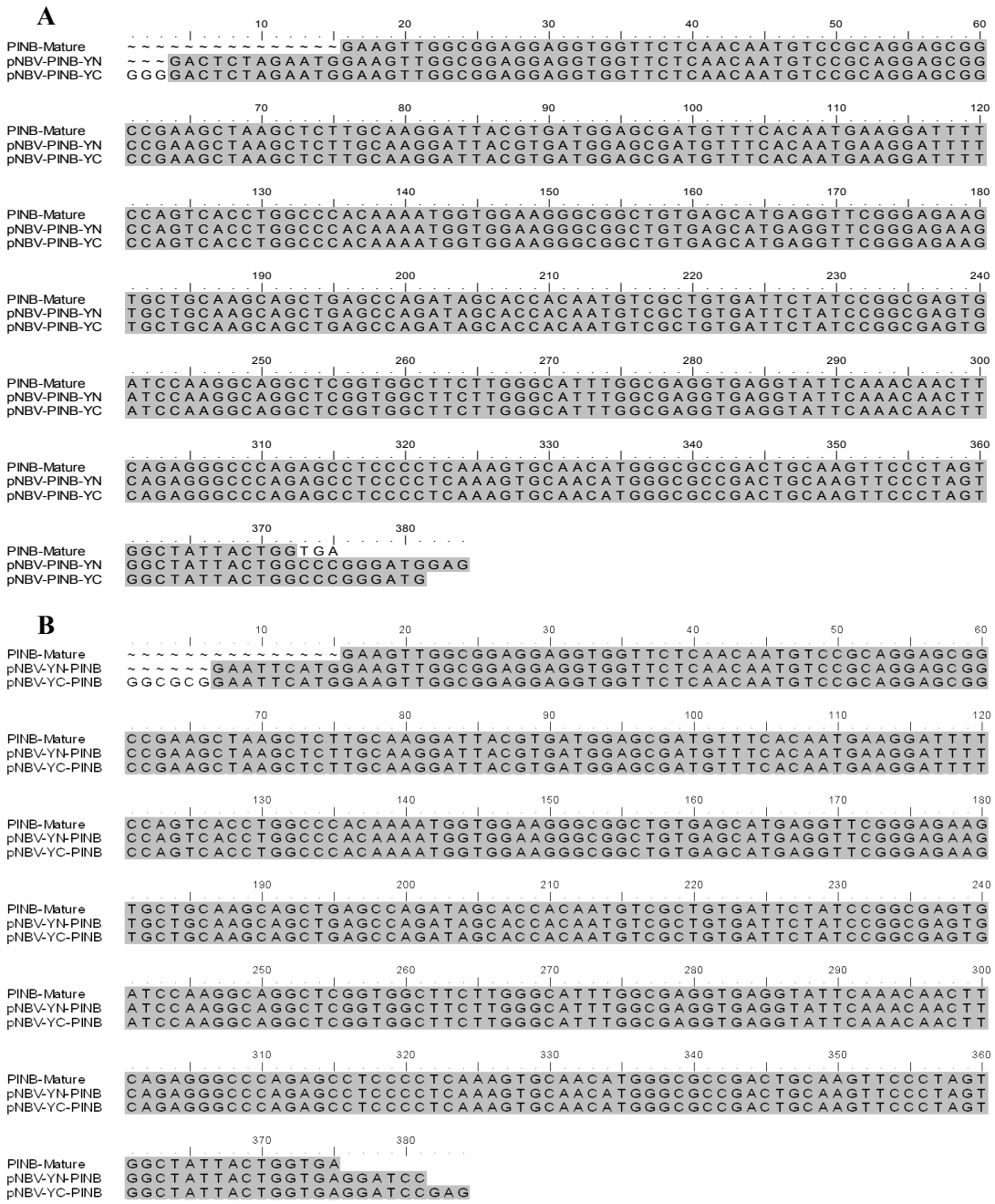

Figure 4.5 Alignments sequence of PINB in pNBV construct.
A: DNA sequence of mature putative *Pinb-D1a* genes cloned in the pNBV (gene-YN) and pNBV (gene-YC) vectors. B: DNA sequence of mature putative *Pinb-D1a* genes cloned in the pNBV (YN-gene) and pNBV (YC-gene) vectors. In both A and B, the line 1 is sequence of the reported WT *Pinb-D1a* gene (DQ363913).

One each of the eight pMLBART constructs was individually transformed into the *Agrobacterium* strain GV3101. Screening of the clones containing inserts was carried out by colony-PCR using primer listed in Table 2.11 (data not shown).

4.2.2 BiFC system for transient expression in *N. bethamiana* leaves

Agrobacterium harbouring BiFC constructs were infiltrated into eight week old *N. benthamiana* leaves. The fluorescence started to appear 3-4 days post infiltration (dpi). In general, the best observation time for BiFC fluorescence was 3 dpi, after which the signal began to fade. The expression of the fusion proteins was observed using a highly active promoter i.e., the CaMV 35S promoter. In order to ensure that the fluorescence resulted from the specific PIN protein-protein interactions and not from non-specific binding of the two YFP fragments, or from background or autofluorescence, infiltrations with buffer only, or with just one PIN-YFP construct, or YN and YC construct without PIN ligation, were used as negative controls. Any fluorescence obtained with such constructs would reflect non-specific interactions of the expressed proteins. In addition, non-treated leaves were used to detect background fluorescence.

4.2.3 Post-transcriptional gene silencing (PTGS) in transient system

N. benthamiana plants were transiently co-transformed with the desired construct and p19. The p19 protein from tomato bushy stunt virus (TBSV) (Section 2.14.7), by co-expression of a viral-encoded suppressor of gene silencing can prevent post-transcriptional gene silencing (PTGS) in a transient assay system (Voinnet et al., 2003). This strategy has been used in a number of transient assays to enhance transgene expression (Grefen et al., 2008; Hellens et al., 2005; Wroblewski et al., 2005), including BiFC analyses (Schütze et al., 2009; Walter et al., 2004; Waadt et al., 2008). To determine if co-expression of BiFC constructs and the p19 could enhance PIN expressions, an *Agrobacterium* LB4404 containing the p19 was co-infiltrated with BiFC constructs into *N. benthamiana* leaves. This led to a strong increase in fluorescence signal, as observed in individual cells. This improvement in signal and experimental reliability was the reason for the p19 to be included in the subsequent transient BiFC analyses.

4.2.4 Fluorescence detection for the wild type PIN protein-protein interactions

The infiltration experiments were carried out in at least three replicates. The lower epidermal layers of infiltrated leaves were examined by fluorescence microscopy 3 dpi. No fluorescence signal was detected in non-treated leaves and in leaves infiltrated with negative controls (Figure 4.6A and 4.6B). Background fluorescence was often observed in cells surrounding wounded tissues of leaves, probably caused by the infiltration procedure. These areas became yellowish 3 dpi.

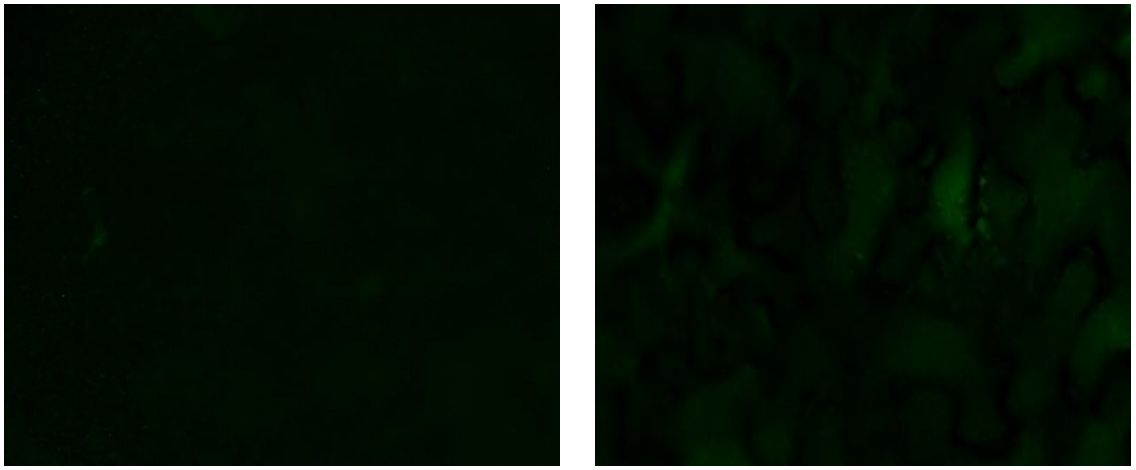

A **B**

Figure 4.6 BiFC visualisation in *N. benthamiana* leaves.
A and B: negative control (YC+YN without PINs) (20×magnification) and (200×magnification) respectively.

Leaves co-infiltrated with a 1:1 volume ratio of *Agrobacteria* harbouring PINA-YC and YN-PINB constructs showed fluorescence, which was stronger than the background (Figure 4.7A-D) thus indicating an interaction between the fusion proteins. Remarkably, the strong fluorescence was only observed in the PINA-YC+YN-PINB. In contrast, leaves infiltrated with combinations of other PIN-BiFC constructs led to a weak fluorescence in a small number of leaf cells, lack of fluorescence. This finding suggests that the orientation of the PIN proteins is important for the interactions.

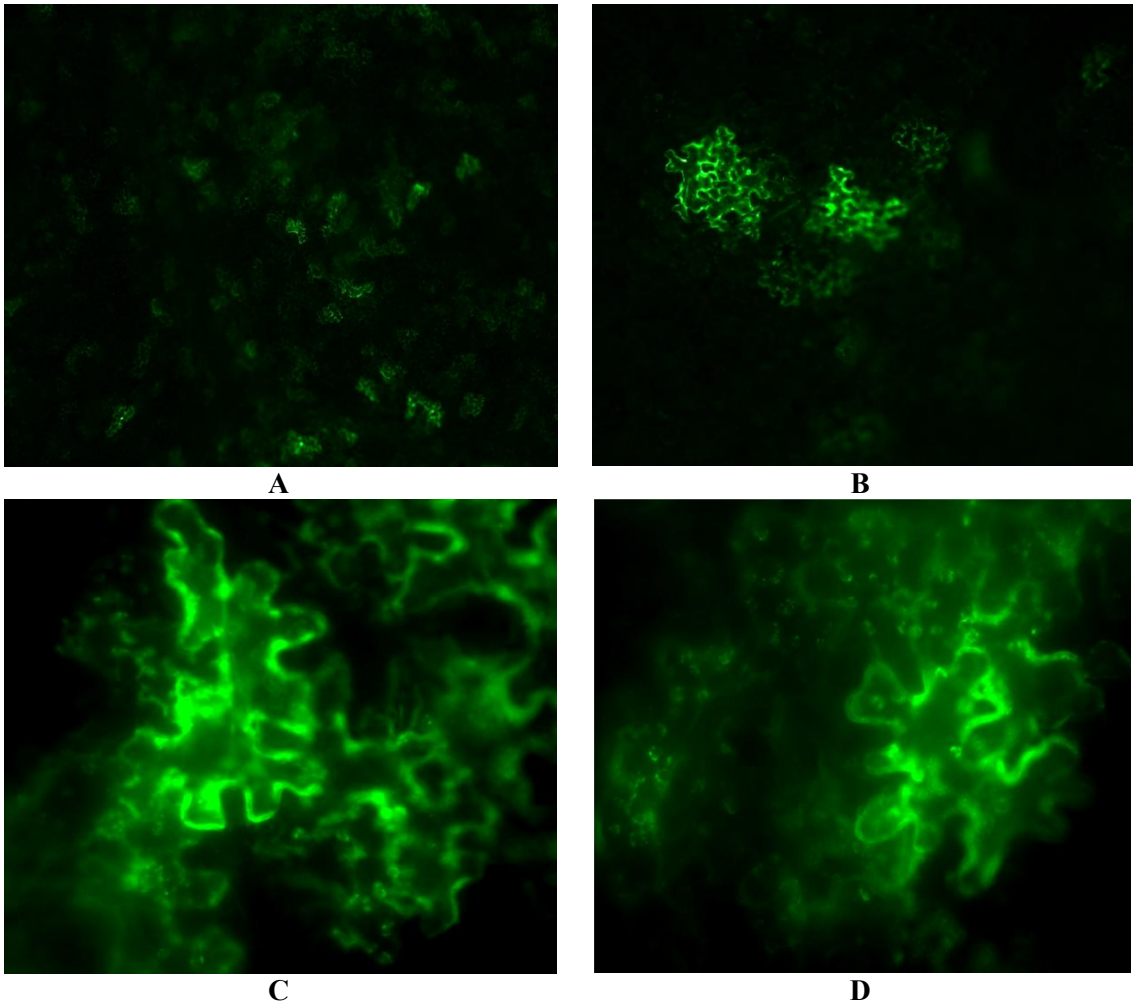

Figure 4.7 BiFC visualisation of PINA-PINB interactions in *N. benthamiana* leaves.
A and B: interaction of PINA-PINB, in direction of PINA-YC+YN-PINB (20×magnification); C and D: interaction of PINA-PINB, in direction of PINA-YC+YN-PINB (200×magnification).

Since the structural basis of complex formations for PIN proteins is not clear, the two interacting proteins were fused N- and C-terminally to the C- and N- terminal part of YFP. Furthermore, potential homodimerisation was also investigated. Notably, the fluorescence signals were observed in YN-PINB and YC-PINB constructs (Figure 4.8A and 4.8B). However, no fluorescence was detected for homodimerisation in wild type of PINA (Figure 4.8C and 4.8D) tested in different orientations (Table 4.1). From images of fluorescence microscopy it seemed that PINA and PINB most likely presented interactions in the cytoplasm. The small fluorescence dots illustrated likely location in the chloroplast, and the small rings as Golgi compartments, for PINA-PINB (Figure 4.7A-D) and especially for PINB-PINB (Figure 4.8A and B) interactions.

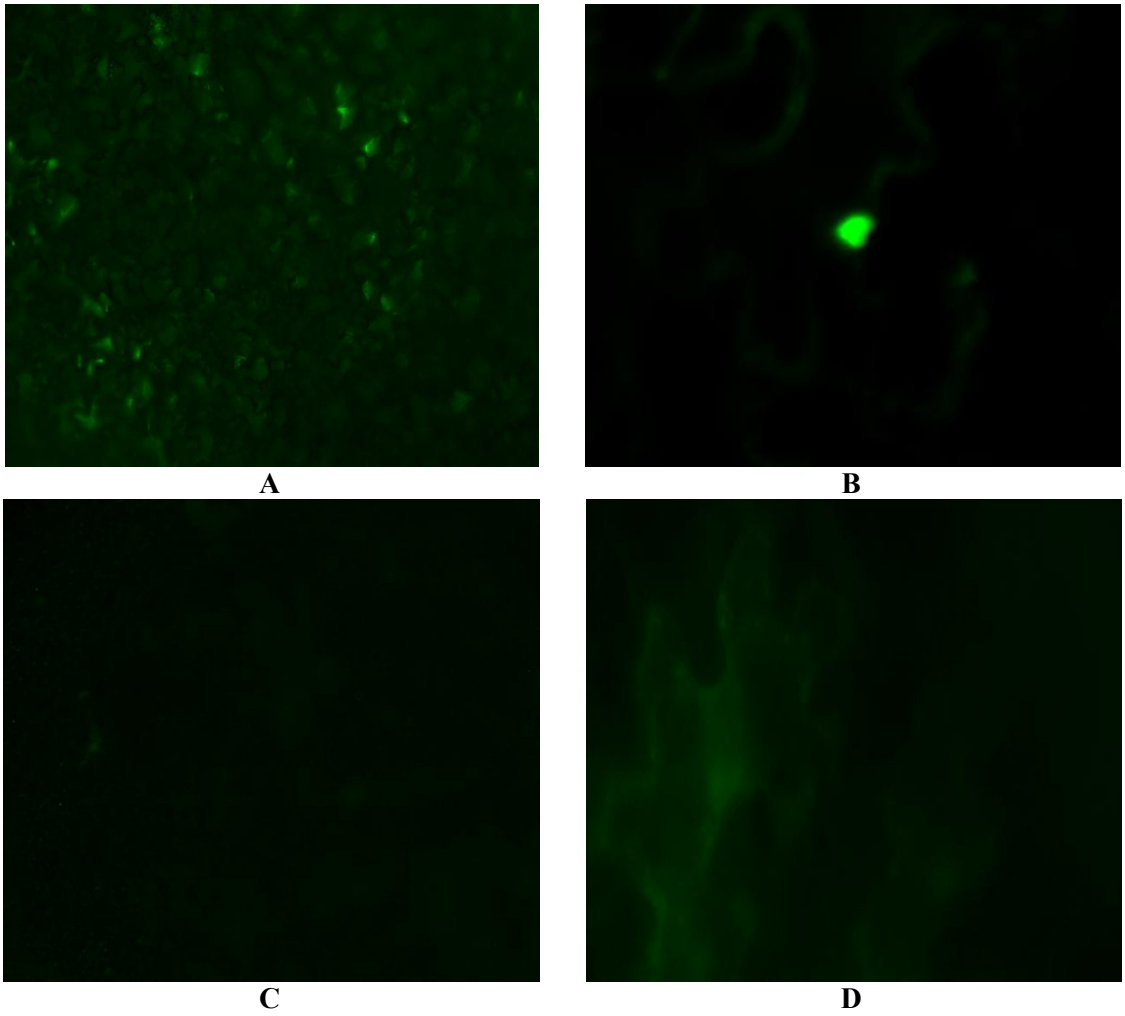

Figure 4.8 BiFC visualisation of PINA-PINA and PINB-PINB interactions in *N. benthamiana* leaves.
A: interaction of PINB-PINB, in direction of YN-PINB+YC-PINB (20× magnification); B: interaction of PINB-PINB, in direction of YN-PINB+YC-PINB (200× magnification); C: interaction of PINA-PINA (20×magnification); D: interaction of PINA-PINA (200× magnification).

4.2.5 Western blot analysis of wild type PIN protein-protein interactions

Western blot analysis using the Durotest antibody was used to verify the co-expression of the interacting forms of PINs. The leaves were harvested after 3 dpi and used for microscopy. The total soluble protein (TSP) was extracted from leaves with the fluorescence signal. The amounts of TSP were quantified using Bradford assay and about 40 µg of TSP were loaded on 15% gel for further analysis by western blot. One intense band at approximately 45 kDa was detected by western blot from the TSP of infiltrated leaf with the PINA-YC+YN-PINB constructs (Figure 4.9; lanes 4 and 5).

The western blot also detected YN-PINB+YC-PINB interacting forms (Figure 4.9; lane 2); however the band size appeared to be slightly higher than PINA+PINB interactions.

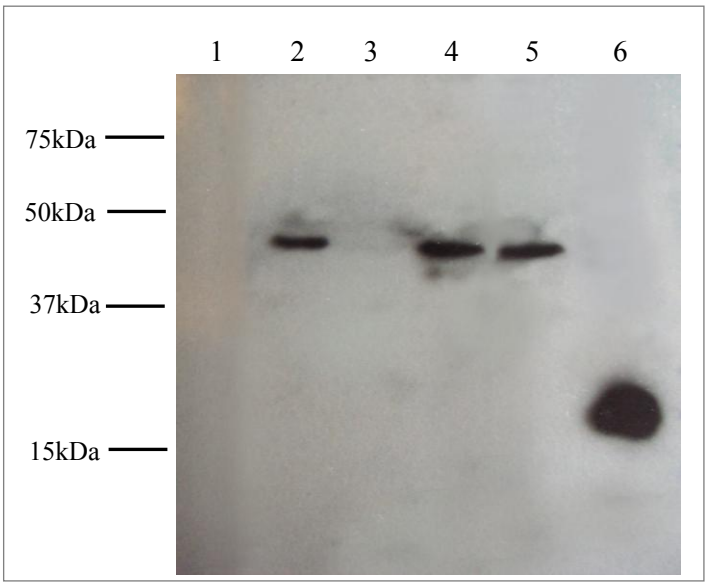

Figure 4.9 Determination of interacting form of PINA+PINB and PINB+PINB by western blot analysis from TSP extract.
Lane 1: YFP construct without PIN (negative control); lane 2: interacting form of recombinant PINB and PINB (YN-PINB+YC-PINB); lane 3: void lane (no sample loaded); lanes 4 and 5: interacting form of recombinant PINA and PINB (PINA-YC+YN-PINB); lane 6: 3% non-durum wheat as positive for antibody.

4.2.6 Gel detection of YFP fluorescence for wild type PIN protein-protein interactions

In order to confirm the protein complexes, native electrophoresis was used on the same samples as those used for western blot, for subsequent imaging of in-gel YFP fluorescent under UV light. Fluorescent bands were detected for PINA-YC+YN-PINB and for YN-PINB+YC-PINB interactions (Figure 4.10; lanes 1 and 2) which was also confirming the above results of fluorescent microscopy and western blot. No bands were detected for the negative controls (lanes 3 and 4).

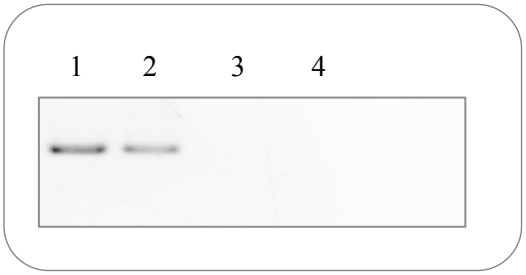

Figure 4.10 Native gel electrophoresis and UV imaging of YFP fluorescence of PIN protein complexes.
Lane 1: interacting form of recombinant PINA and PINB (PINA-YC+YN-PINB); lane 2: interacting form of recombinant PINB and PINB (YN-PINB+YC-PINB); lanes 3 and 4: YFP construct without PIN (negative).

4.2B Interaction studies of mutagenised PINA and PINB

4.2.7 Cloning of the previously made constructs PINAΔHD and PINBΔHD into pNBV vectors

Site-Directed Mutagenesis (SDM) PCR had been earlier carried out by Dr R. Alfred (Swinburne University of Technology) to delete the predicted hydrophobic domain (HD) at positions 75-85 in the putative mature PINA (PINAΔHD) and at positions 75-83 in the putative mature PINB (PINBΔHD) in yeast 2-hybrid system vectors pGBK (details in section 2.15.1). These clones kindly provided by Dr R. Alfred, were used in the present work as templates for PCR (Figure 4.11) to clone into pNBV vectors, so as to see whether these deletions significantly affect the likely PPI of PINs. The primers PIN-Forward and PIN-Reverse (Section 2.14.3) were used to introduce specific restriction sites (XbaI and XmaI for PINAΔHD and EcoRI and BamHI for PINBΔHD) at the 5' and 3' ends of the PCR fragments. PCR products of ~400 bp were obtained for PINAΔHD and PINBΔHD (Figure 4.11), consistent with sizes of the gene sections encoding putative mature PINA without HD (330 bp) or PINB without HD (333 bp) and the added specific restriction sites (12 bp).

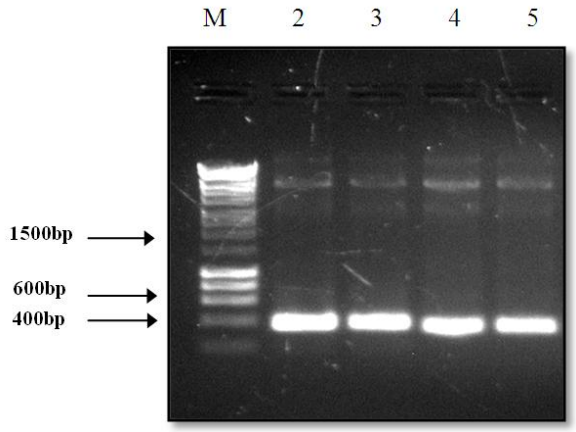

Figure 4.11 Amplification of inserts from PINAΔHD and PINBΔHD constructs.
PCR products from clones in pGBK vectors using insert-specific primers. Lane 1: DNA molecular weight marker, Hyperladder l; lanes 2 and 3: PINAΔHD; lanes 4 and 5: PINBΔHD.

The PCR fragments were digested at restriction sites and cloned into cloning site of pNBV vector to allow for translational fusions with the YN or YC fragments of YFP, as above. The BiFC constructs were designated: pNBV-PINAΔHD-YC, pNBV-YN-PINBΔHD and pNBV-YC-PINBΔHD (Figure 4.12). The cassettes in pNBV were released from pNBV by NotI digestion, inserted into pMLBART transformed into *E. coli* cells and screened by colony PCR with insert-specific primers (Table 2.11) followed by DNA sequencing. Alignment with the reference sequences; *Pina-D1a* (DQ363911) and *Pinb-D1a* (DQ363913) that showed 100% identity with the corresponding sections (Figures 4.13 and 4.14).

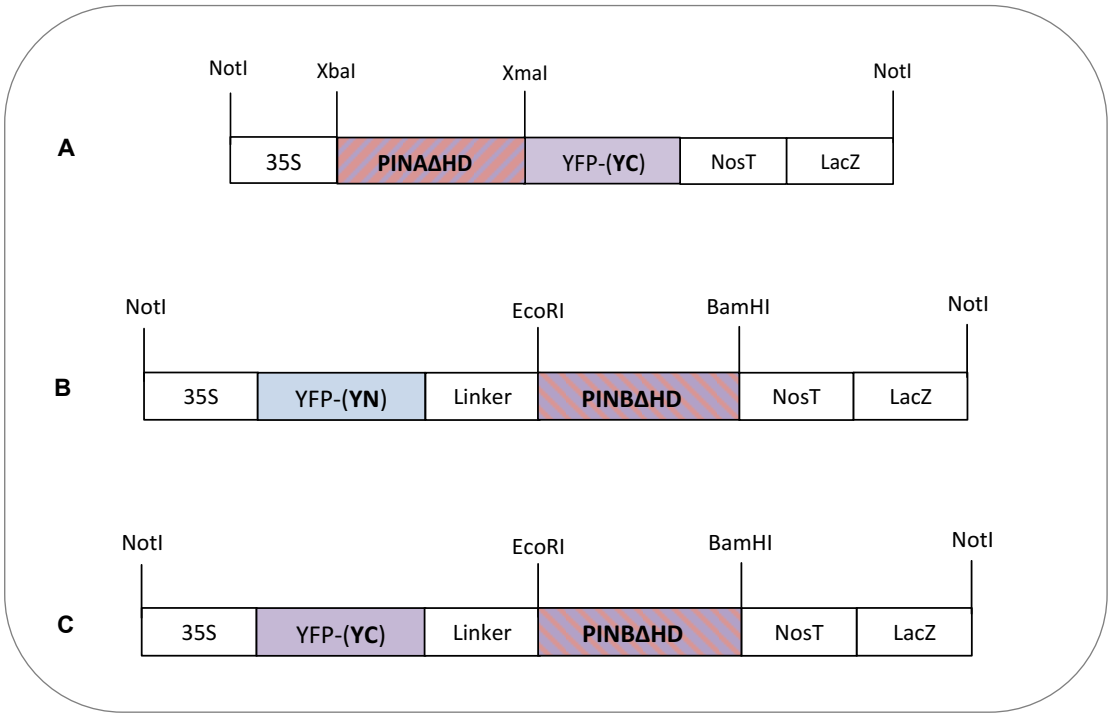

Figure 4.12 The pNBV module constructs generated encoding mutant PIN proteins.
35S: promoter of the cauliflower mosaic virus; NosT: terminator of the *Nos* gene; YFP: yellow fluorescent protein (**YN**=N-terminal fragment 1 to 155 amino acid/**YC**=C-terminal fragment 156 to 238 amino acid). A: pNBV-PINAΔHD-YC; B: pNBV-YN-PINBΔHD; C: pNBV-YC-PINBΔHD.

```
                    10        20        30        40        50        60        70
                    |....|....|....|....|....|....|....|....|....|....|....|....|
PINA                                    D  V  A  G  G  G  G  A  Q  Q  C  P  V  E  T  K  L  N
Pina-D1a            ~~~~~~~~~~~~~~~~GATGTTGCTGGCGGGGGTGGTGCTCAACAATGCCCTGTAGAGACAAAGCTAAATT
pNBV-PINAΔHD-YC     ~~~GACTCTAGAATGGATGTTGCTGGCGGGGGTGGTGCTCAACAATGCCCTGTAGAGACAAAGCTAAATT

                    80        90        100       110       120       130       140
                    |....|....|....|....|....|....|....|....|....|....|....|....|....|
PINA                S  C  R  N  Y  L  L  D  R  C  S  T  M  K  D  F  P  V  T  W  R  W  W  K
Pina-D1a            CATGCAGGAATTACCTGCTAGATCGATGCTCAACGATGAAGGATTTCCCGGTCACCTGGCGTTGGTGGAA
pNBV-PINAΔHD-YC     CATGCAGGAATTACCTGCTAGATCGATGCTCAACGATGAAGGATTTCCCGGTCACCTGGCGTTGGTGGAA

                    150       160       170       180       190       200       210
                    |....|....|....|....|....|....|....|....|....|....|....|....|....|
PINA                W  W  K  G  G  C  Q  E  L  L  G  E  C  C  S  R  L  G  Q  M  P  P  Q
Pina-D1a            ATGGTGGAAGGGAGGTTGTCAAGAGCTCCTTGGGGAGTGTTGCAGTCGGCTCGGCCAAATGCCACCGCAA
pNBV-PINAΔHD-YC     ATGGTGGAAGGGAGGTTGTCAAGAGCTCCTTGGGGAGTGTTGCAGTCGGCTCGGCCAAATGCCACCGCAA

                    220       230       240       250       260       270       280
                    |....|....|....|....|....|....|....|....|....|....|....|....|....|
PINA                C  R  C  N  I  I  Q  G  S  I  Q  G  D  L  G  G  I  F  G  F  Q  R  D
Pina-D1a            TGCCGCTGCAACATCATCCAGGGGTCAATCCAAGGCGATCTCGGTGGCATCTTCGGATTTCAGCGTGATC
pNBV-PINAΔHD-YC     TGCCGCTGCAACATCATCCAGGGGTCA~~~~~~~~~~~~~~~~~~~~~~~~~~~~~~~~TCAGCGTGATC

                    290       300       310       320       330       340       350
                    |....|....|....|....|....|....|....|....|....|....|....|....|....|
PINA                R  A  S  K  V  I  Q  E  A  K  N  L  P  P  R  C  N  Q  G  P  P  C  N  I
Pina-D1a            GGGCAAGCAAAGTGATACAAGAAGCCAAGAACCTGCCGCCCAGGTGCAACCAGGGCCCTCCCTGCAACAT
pNBV-PINAΔHD-YC     GGGCAAGCAAAGTGATACAAGAAGCCAAGAACCTGCCGCCCAGGTGCAACCAGGGCCCTCCCTGCAACAT

                    360       370       380
                    |....|....|....|....|....|..
PINA                P  G  T  I  G  Y  Y  W  *
Pina-D1a            CCCCGGCACTATTGGCTATTACTGGTGA
pNBV-PINAΔHD-YC     CCCCGGCACTATTGGCTATTACTGGCCCGGGATGTAC
```

Figure 4.13 Sequences of PINAΔHD in pNBV construct.
DNA sequences of the mutated *Pina-D1a* genes cloned in pNBV vector. The top line (PINA) is the deduced protein sequence of the reported WT *Pina-D1a* (Genbank ABD72477, mature protein), line 2 is the DNA sequence of the reported *Pina-D1a* gene (DQ363911) and line 3 is the DNA sequence of PINAΔHD in pNBV (gene-YC) vector. The HD (IQGDLGGIFGF) is underlined.

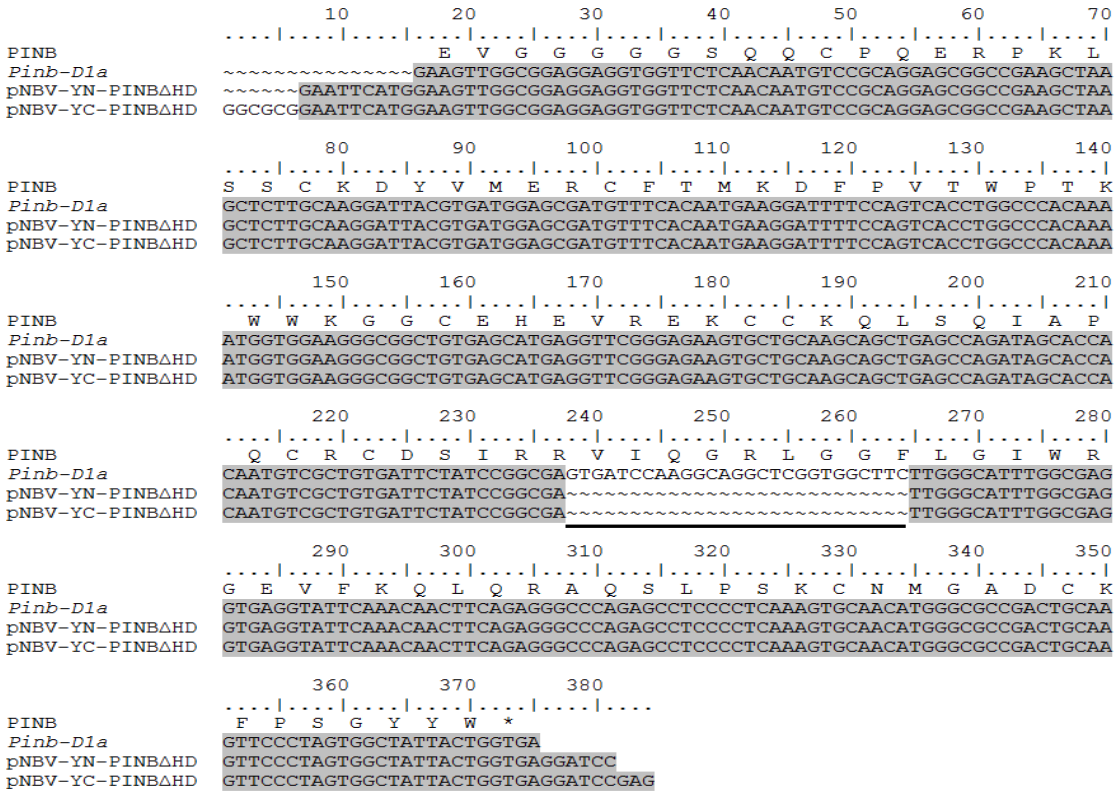

Figure 4.14 Sequences of PINBΔHD in pNBV construct.
DNA sequences of the mutated *Pinb-D1a* genes cloned in pNBV vector. The top line (PINB) is the deduced protein sequence of the reported WT *Pinb-D1a* (Genbank ABD72479, mature protein), line 2 is the DNA sequence of the reported *Pinb-D1a* gene (DQ363913), line 3 is the DNA sequence of PINBΔHD in pNBV-YN-gene vector, line 4 is the DNA sequence of PINBΔHD in pNBV-YC-gene. The HD (VIQGRLGGF) is underlined.

Each pMLBART construct was transformed into the *Agrobacterium* strain GV3101. Screening of the clones containing inserts was confirmed by antibiotic (spectinomycin plus rifampicin) selection and colony PCR using primer listed in Table 2.11 (data not shown).

4.2.8 Detection of mutant PINAΔHD and PINBΔHD protein-protein interactions by fluorescence and western blot

The potential role of the hydrophobic domain (HD) in any PPI of PINA and PINB was investigated through infiltration of the above constructs into *N. benthamiana* leaves side by side on the same leaf (Figure 4.15), with the wild type PIN construct which had shown the fluorescent signal for interactions (Figure 4.7). Since the PINs had shown fluorescent signal in one orientation (PINA-YC+YN-PINB), the mutant PINs were tested as same orientation, i.e., PINAΔHD-YC+YN-PINBΔHD. However the results showed no fluorescence. The interaction between PINAΔHD and wild type PINB (PINAΔHD-YC+YN-PINB) and also wild type PINA and PINBΔHD (PINA-YC+YN-PINBΔHD) led to no fluorescence.

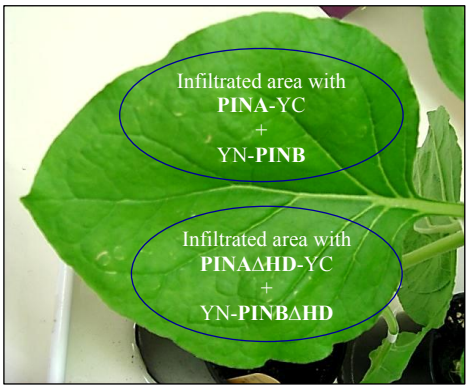

Figure 4.15 Infiltrated mixtures of constructs into *N. benthamiana* leaves side by side for detect and compare the interaction of wild type and mutant form of PIN proteins.

Further, TSP were extracted from infiltrated areas, quantified using Bradford assay and about 40 µg of TSP electrophoresed. Western blot analysis resulted in very faint bands at ~45 kDa (Figure 4.16; lanes 2, 3, 4) compared to the wild type controls (lanes 5, 7). The results suggest that the HD deletion in the direction led to significant reduction in interactions of PINAΔHD-YC with YN-PINBΔHD and also of the self-interacting PINB (YN-PINBΔHD+YC-PINBΔHD) (Figure 4.16; lane 4).

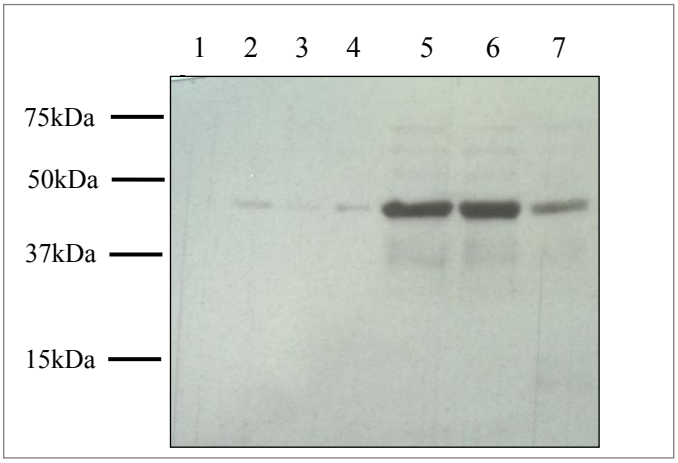

Figure 4.16 Western blot analysis to determine the interacting forms of wild type and mutant PIN proteins.
Lane 1: YFP construct without insert (negative control); lanes 2 and 3: interacting form of recombinant PINAΔHD-YC+YN-PINBΔHD; lane 4: interacting form of recombinant YN-PINBΔHD+YC-PINBΔHD; lane 5 and 6: interacting form of recombinant PINA-YC+YN-PINB; lane 7: interacting form of recombinant YN-PINB+YC-PINB.

4.2.9 Cloning of PINAΔTRD into pNBV vectors

PCR was also conducted by Dr R. Alfred to delete the TRD at positions 34-46 in the mature PINA protein (PINAΔTRD) in the yeast 2-hybrid system vectors pGBK (details in section 2.15.1). The clone (kindly donated by Dr R. Alfred) was also used in the present work as template for PCR (data not shown) to clone in pNBV. The primers PIN-Forward and PIN-Reverse (Section 2.14.3) were used to insert restriction sites (XbaI and XmaI) at the 5' and 3' ends of the PCR fragment. The resulting PCR fragments were ~400 bp for PINAΔTRD was consistent with the gene sections encoding putative mature PINA without the TRD (324 bp). The PCR fragments were digested and cloned into pNBV as above to obtain the construct pNBV-PINAΔTRD-YC with the translational fusion with the YC fragment of YFP (Figure 4.17). The BiFC cassette in pNBV was released by NotI digestion, inserted into pMLBART transformed into *E. coli* which cells and screened by colony PCR with insert-specific primers (Table 2.11), followed by DNA sequencing. Alignment with *Pina-D1a* (DQ363911) showed 100% identity (Figure 4.18). The pMLBART construct was then transformed into the *Agrobacterium* strain GV3101.

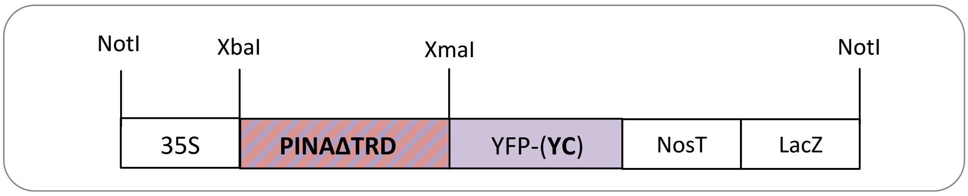

Figure 4.17 The pNBV module construct generated encoding PINAΔTRD protein.
35S: promoter of the cauliflower mosaic virus; NosT: terminator of the *Nos* gene; YFP: yellow fluorescent protein (**YC**=C-terminal fragment 156 to 238 amino acid); pNBV-PINAΔTRD-YC.

```
                            10        20        30        40        50        60        70
                   ....|....|....|....|....|....|....|....|....|....|....|....|....|....|
PINA                                D  V  A  G  G  G  A  Q  Q  C  P  V  E  T  K  L  N
Pina-D1a           ~~~~~~~~~~~~~~~GATGTTGCTGGCGGGGGTGGTGCTCAACAATGCCCTGTAGAGACAAAGCTAAATT
pNBV-PINAΔTRD-YC   ~~~GACTCTAGAATGGATGTTGCTGGCGGGGGTGGTGCTCAACAATGCCCTGTAGAGACAAAGCTAAATT

                            80        90       100       110       120       130       140
                   ....|....|....|....|....|....|....|....|....|....|....|....|....|....|
PINA               S  C  R  N  Y  L  L  D  R  C  S  T  M  K  D  F  P  V  T  W  R  W  W  K
Pina-D1a           CATGCAGGAATTACCTGCTAGATCGATGCTCAACGATGAAGGATTTCCCGGTCACCTGGCGTTGGTGGAA
pNBV-PINAΔTRD-YC   CATGCAGGAATTACCTGCTAGATCGATGCTCAACGATGAAGGAT~~~~~~~~~~~~~~~~~~~~~~~~~~

                           150       160       170       180       190       200       210
                   ....|....|....|....|....|....|....|....|....|....|....|....|....|....|
PINA                 W  W  K  G  G  C  Q  E  L  L  G  E  C  C  S  R  L  G  Q  M  P  P  Q
Pina-D1a           ATGGTGGAAGGAGGTTGTCAAGAGCTCCTTGGGGAGTGTTGCAGTCGGCTCGGCCAAATGCCACCGCAA
pNBV-PINAΔTRD-YC   ~~~~~~~~~~~~GGTTGTCAAGAGCTCCTTGGGGAGTGTTGCAGTCGGCTCGGCCAAATGCCACCGCAA

                           220       230       240       250       260       270       280
                   ....|....|....|....|....|....|....|....|....|....|....|....|....|....|
PINA                 C  R  C  N  I  I  Q  G  S  I  Q  G  D  L  G  G  I  F  G  F  Q  R  D
Pina-D1a           TGCCGCTGCAACATCATCCAGGGGTCAATCCAAGGCGATCTCGGTGGCATCTTCGGATTTCAGCGTGATC
pNBV-PINAΔTRD-YC   TGCCGCTGCAACATCATCCAGGGGTCAATCCAAGGCGATCTCGGTGGCATCTTCGGATTTCAGCGTGATC

                           290       300       310       320       330       340       350
                   ....|....|....|....|....|....|....|....|....|....|....|....|....|....|
PINA               R  A  S  K  V  I  Q  E  A  K  N  L  P  P  R  C  N  Q  G  P  P  C  N  I
Pina-D1a           GGGCAAGCAAAGTGATACAAGAAGCCAAGAACCTGCCGCCCAGGTGCAACCAGGGCCCTCCCTGCAACAT
pNBV-PINAΔTRD-YC   GGGCAAGCAAAGTGATACAAGAAGCCAAGAACCTGCCGCCCAGGTGCAACCAGGGCCCTCCCTGCAACAT

                           360       370       380
                   ....|....|....|....|....|....|....|
PINA                 P  G  T  I  G  Y  Y  W  *
Pina-D1a           CCCCGGCACTATTGGCTATTACTGGTGA
pNBV-PINAΔTRD-YC   CCCCGGCACTATTGGCTATTACTGGCCCGGGATGTA
```

Figure 4.18 Sequences of PINAΔTRD in pNBV construct.
DNA sequences of the mutated *Pina-D1a* genes cloned in pNBV vector. The top line (PINA) is the deduced protein sequence of the reported WT *Pina-D1a* (Genbank ABD72477, mature protein), line 2 is the DNA sequence of the reported *Pina-D1a* gene (DQ363911), and line 3 is the DNA sequence of PINAΔTRD in pNBV (gene-YC) vector. The TRD (FPVTWRWWKWWKG) is underlined.

4.2.10 Fluorescence detection for mutant PINAΔTRD protein-protein interactions

Infiltration of the relevant constructs into *N. benthamiana* leaves showed no fluorescence or only background fluorescence for PINAΔTRD-YC+YN-PINB. Further, no fluorescence signal was detected for interaction between PINAΔTRD-YC+YN-PINBΔHD. These results suggest that the TRD deletion in PINA leads to significant change in the interactions of PIN. The full set of PIN interactions tested by the BiFC assay is shown in Table 4.1.

Table 4.1 BiFC constructs for PIN proteins (wild type and mutant) to detect fluorescence signal

No	Construct 1	Construct 2	Heterodimerisation wild type PIN proteins	Fluorescence signal
1	PINA-YC	YN-PINB	PINA+PINB	**Yes**
2	PINA-YC	PINB-YN	PINA+PINB	No
3	PINA-YN	YC-PINB	PINA+PINB	No
4	PINA-YN	PINB-YC	PINA+PINB	No
5	YC-PINA	PINB-YN	PINA+PINB	No
6	YC-PINA	YN-PINB	PINA+PINB	No
7	YN-PINA	PINB-YC	PINA+PINB	No
8	YN-PINA	YC-PINB	PINA+PINB	No
No	Construct 1	Construct 2	Homodimerisation wild type PINA proteins	Fluorescence signal
1	YN-PINA	PINA-YC	PINA+PINA	No
2	YN-PINA	YC-PINA	PINA+PINA	No
3	PINA-YN	YC-PINA	PINA+PINA	No
4	PINA-YN	PINA-YC	PINA+PINA	No
No	Construct 1	Construct 2	Homodimerisation wild type PINB proteins	Fluorescence signal
1	YN-PINB	PINB-YC	PINB+PINB	No
2	YN-PINB	YC-PINB	PINB+PINB	**Yes**
3	PINB-YN	YC-PINB	PINB+PINB	No
4	PINB-YN	PINB-YC	PINB+PINB	No
No	Construct 1	Construct 2	Heterodimerisation of mutant PIN proteins	Fluorescence signal
1	PINAΔHD-YC	YN-PINBΔHD	PINAΔHD+PINBΔHD	No
2	PINAΔHD-YC	YN-PINB	PINAΔHD+PINB	No
3	PINA-YC	YN-PINBΔHD	PINA+PINBΔHD	No
4	PINAΔTRD-YC	YN-PINBΔHD	PINAΔTRD+PINBΔHD	No
5	PINAΔTRD-YC	YN-PINB	PINAΔTRD+PINB	No
No	Construct 1	Construct 2	Homodimerisation of mutant PINB proteins	Fluorescence signal
1	YN-PINB	YC-PINBΔHD	PINB+PINBΔHD	No
2	YN-PINBΔHD	YC-PINBΔHD	PINBΔHD+PINBΔHD	No

PINAΔTRD=Deletion of the tryptophan-rich domain (TRD), location at 34-46 amino acid in PINA
PINAΔHD=Deletion of a hydrophobic domain (HD), location at 75-85 amino acid in PINA
PINBΔHD=Deletion of a hydrophobic domain (HD), location at 75-85 amino acid in PINA

4.2.11 Expression of mutant PIN proteins in magnICON® system

To determine the roles of the HD in both PINA and PINB and the TRD in PINA on expression of PIN proteins *in planta*, the magnICON® system was also used. The 3' modules pICH11599 containing PINAΔHD, PINBΔHD and PINAΔTRD were constructed as detailed in Chapter 2 (Figure 4.19). This was followed by transformation of the plasmids into *E. coli* Mach1 cells and purification of plasmids. Sequencing confirmed the correct deletions and 100% identity of the rest of the sequence with the wild type alleles (Figures 4.20 and 4.21).

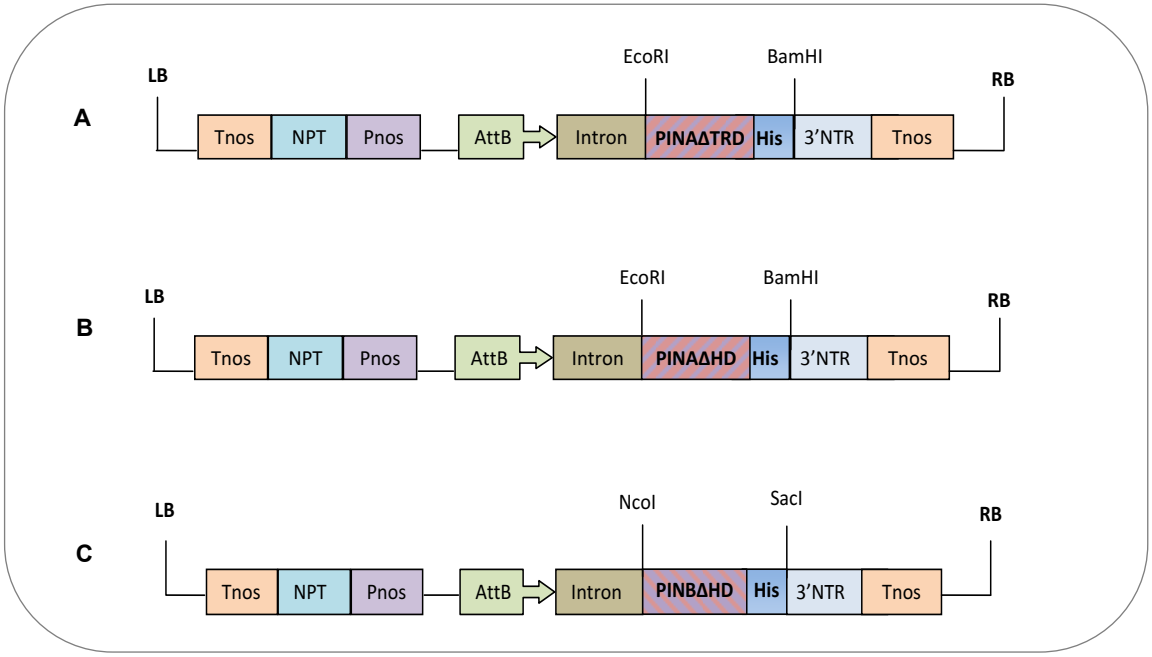

Figure 4.19 The 3' module constructs encoding mutant PIN proteins with His-tag.
A: pICH-PINAΔTRD-His; B: pICH-PINAΔHD-His C: pICH-PINBΔHD-His

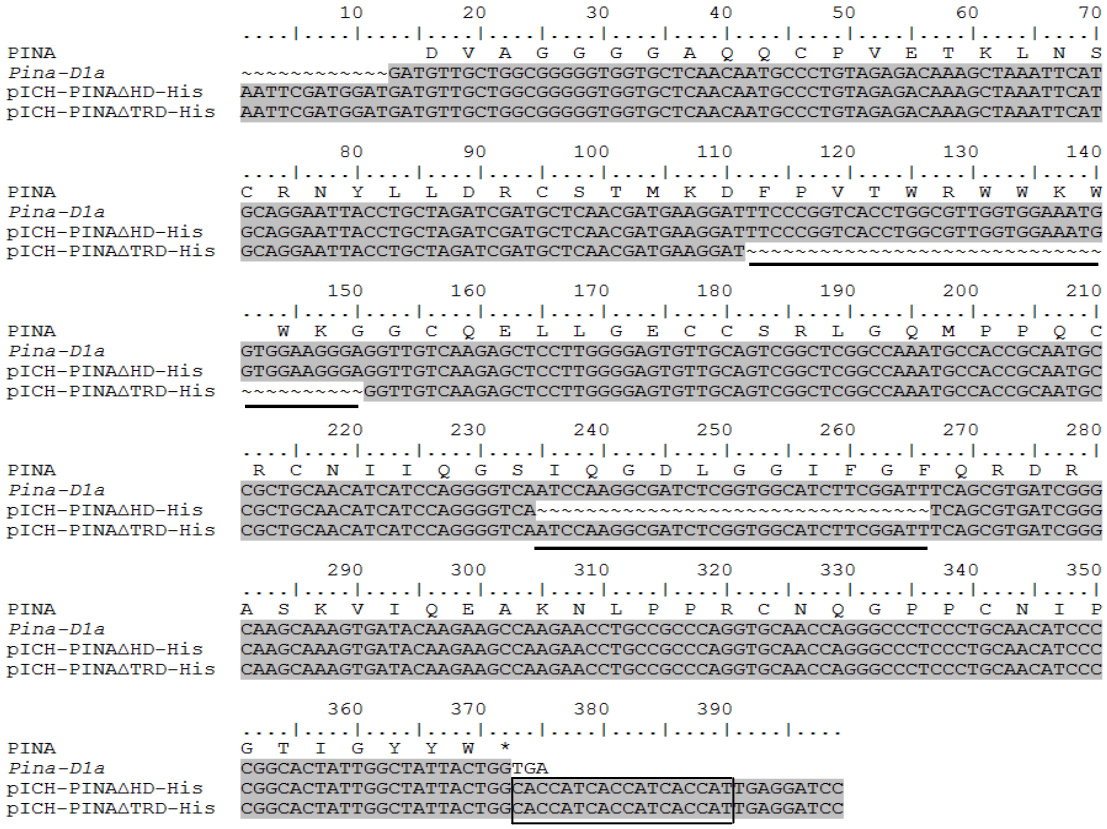

Figure 4.20 Sequences of PINAΔHD-His and PINAΔTRD-His in the 3' module pICH11599.

The top line (PINA) is the deduced protein sequence of the reported WT *Pina-D1a* (Genbank ABD72477, mature protein), line 2 is the DNA sequence of the reported *Pina-D1a* gene (DQ363911), line 3 is the DNA sequence of PINAΔHD-His, line 4 is the DNA sequence of PINAΔTRD-His. The HD (VIQGRLGGF) and TRD (FPVTWRWWKWWKG) are underlined. His-tag sequences are in box.

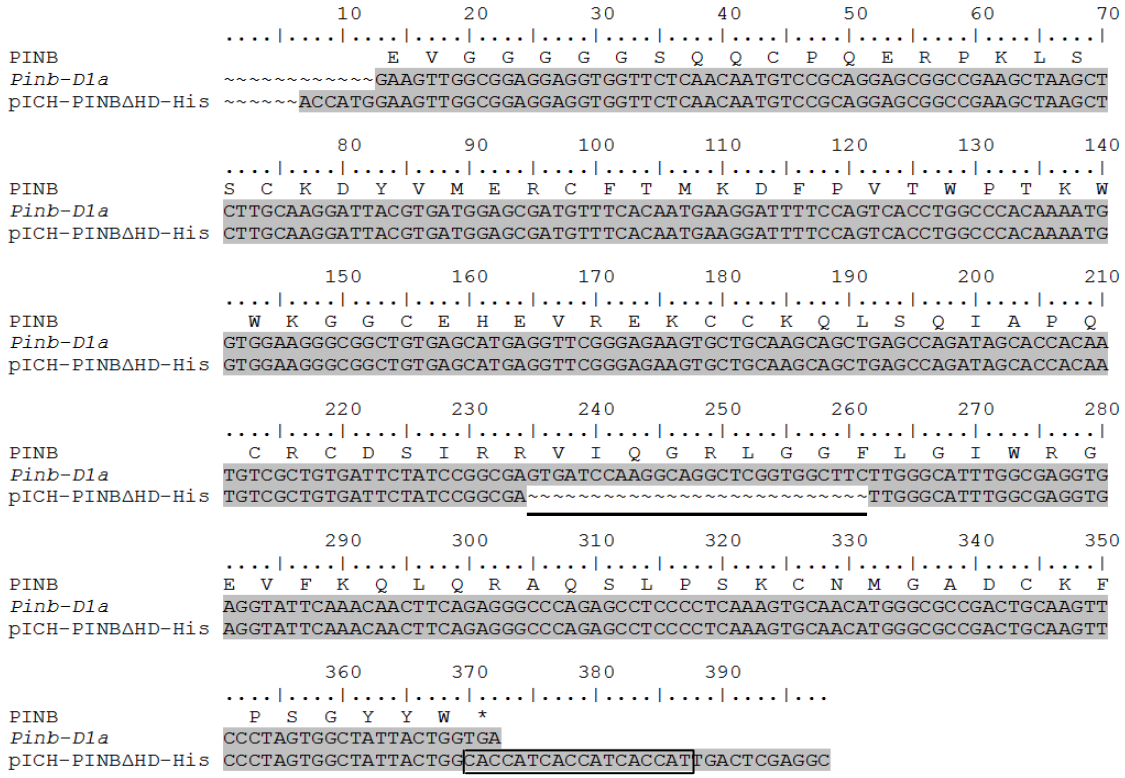

Figure 4.21 Sequences of PINBΔHD-His in 3' module pICH11599.
The top line (PINB) is the deduced protein sequence of the reported WT *Pinb-D1a* (Genbank ABD72479, mature protein), line 2 is the DNA sequence of the reported *Pinb-D1a* gene (DQ363913), line 3 is the DNA sequence of PINBΔHD-His. The HD (VIQGRLGGF) is underlined. His-tag sequence is in box.

The plasmids were electroporated into *Agrobacterium* GV3101 and infiltrated in *N. benthamiana* leaves side by side with wild type of PINA and PINB. Approximately ~40 µg of TSP was loaded in each lane, followed by western blot. Interestingly, bands were detected at ~45 kDa for expressions of chloroplast targeted PINAΔHD and PINBΔHD, suggesting aggregate forms (Figure 4.22; lanes 1 and 2) similar to wild type PINA and PINB (lanes 3 and 4), but PINAΔTRD was not detected (lane 5). The results suggest that PINA with deletion of TRD may be degraded, or the Durotest antibody was not able to detect it. The cytosol targeted PINs indicated the same result (data not shown).

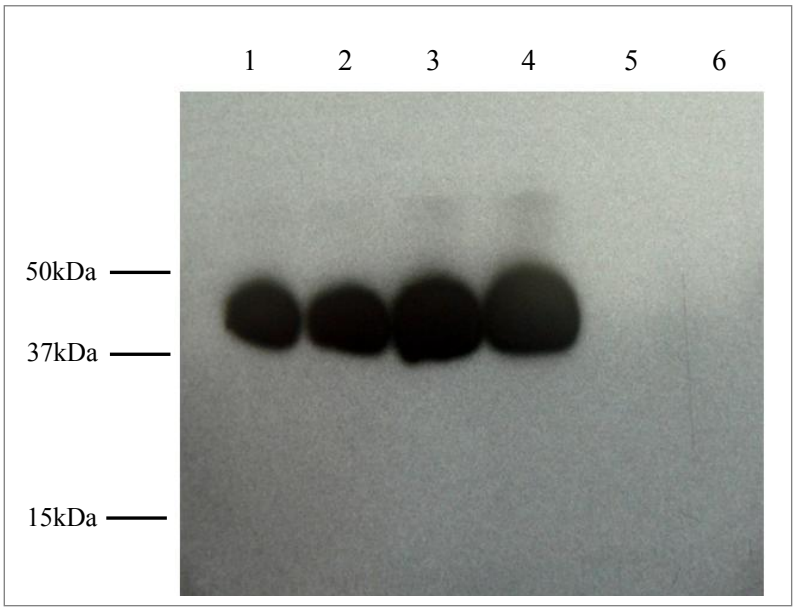

Figure 4.22 Determination of wild type and mutant PIN proteins expressions in infiltrated leaves with chloroplast viral vector module by western blotting of TSP extract.
Lane1: chloroplast targeted PINAΔHD; lane 2: chloroplast targeted PINBΔHD; lane 3: chloroplast targeted PINA; lane 4: chloroplast targeted PINB; lane 5: chloroplast targeted PINAΔTRD; lane 6: negative control (5'+integrase modules only).

4.2.12 Bioinformatics analysis of PIN sequences for potential interaction domain(s)

In order to gain more insights into any particular residues/domains that could be involved in the interaction of PIN proteins, predictive modelling was conducted using I-TASSER (Section 2.10.5) and the outputs analysed in PyMOL for viewing the 3D structure and predicted functional domains such as the TRD and HD of the PINA and PINB. Modelling of wild type PINA (Figure 4.23) showed very similar structures to that predicted by Lesage et al. (2011) (Figure 1.5). The model showed homology to the 2S albumin storage protein and exhibited four alpha helices, with the TRD located as an extended loop between α-helices 1 and 2, as reported previously by Marion et al. (1994). The five tryptophan residues (W) in PINA and three in PINB with their indole-ring are shown in blue (Figures 4.23 and 4.24).

An earlier prediction by using Kyte-Doolittle Hydropathy plot had shown strong hydrophobic properties for the sequence at position 75-80 in the mature PINA protein, this distinct hydrophobic domain (HD) formed a separate loop between α-helices 3 and 4 (Alfred, 2013). These HDs for PINA and PINB are shown in purple (Figures 4.23 and 4.24) and the phenylalanine residues (F) are marked. The C-score is a confidence score for estimating the quality of predicted models by I-TASSER (Roy et al., 2010; Zhang, 2008) (Section 2.10.5). The calculated C-score was 0.28 for PINA and 0.37 for PINB, signifying a model with a high confidence.

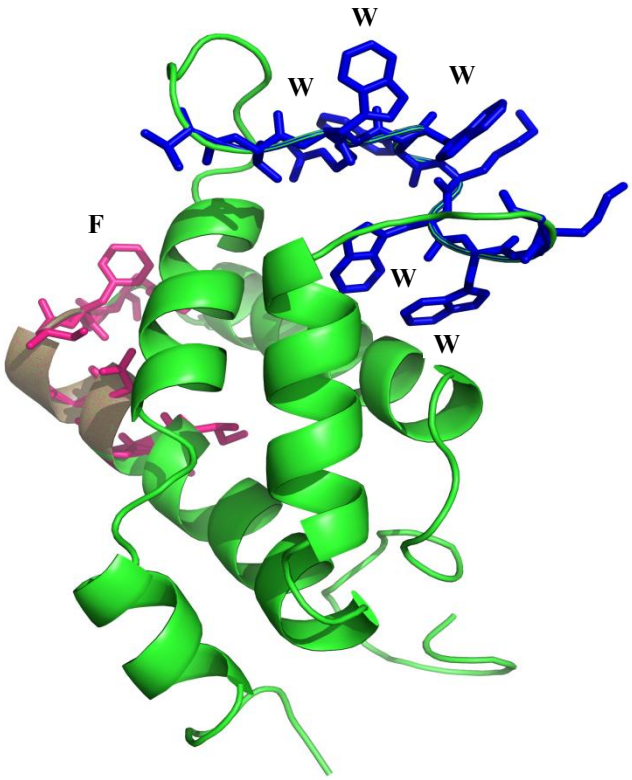


```
                    20        40        60        80        100       120
                    |         |         |         |         |         |
Sequence    DVAGGGGAQQCPVETKLNSCRNYLLDRCSTMKDFPVTWRWWKWWKGGCQELLGECCSRLGQMPPQCRCNIIQGSIQGDLGGIFGFQRDRASKVIQEAKNLPPRCNQGPPCNIPGTIGYYW
Prediction  CCCCCCCCCCCCHHHHHCHHHHHHHHHCCCCCCCCCCCCCCCCCCCCCHHHHHHHHHHHHHHCCHHHHHHHHHHHHHHHHHHHHCCCCCHHHHHHHHHCCCHCCCCCCCCCCCCCCCCCC
Conf.Score  98776654588366665079999999674311365333451125341699999999988838887735999999999998775014007999999986562102999888778877777 9
```

Figure 4.23 Structure prediction using PyMOL and prediction secondary structure for PINA.
Prediction line, elements are shown as H for Alpha helix and C for Coil) using I-TASSER for PINA.
Structure displaying TRD (blue) and HD (purple) domains are enclosed.

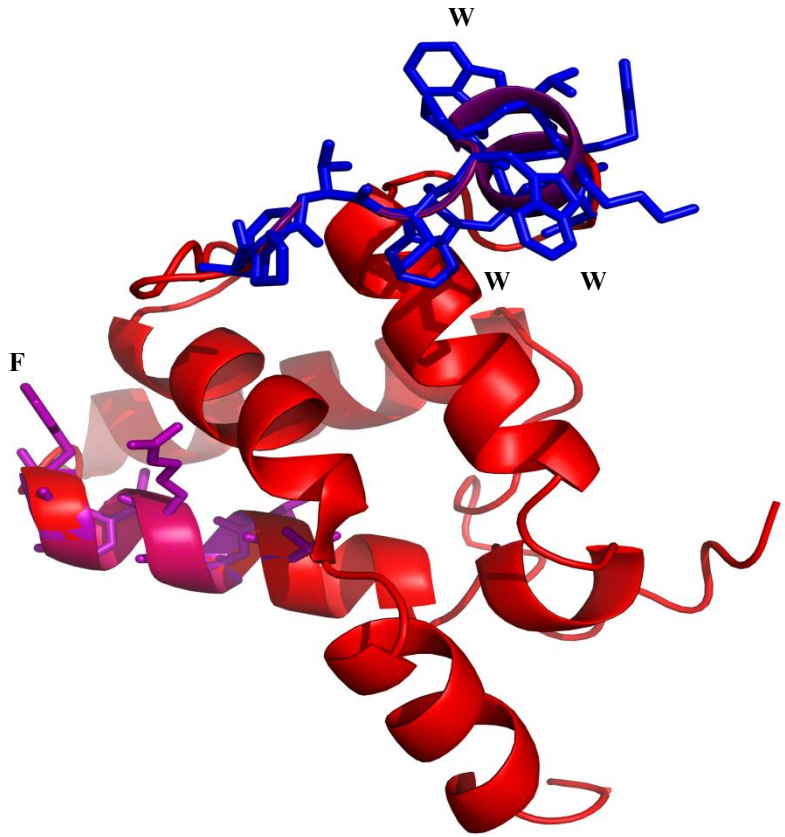


```
                    20        40        60        80        100
                    |         |         |         |         |
Sequence    EVGGGGGSQQCPQERPKLSSCKDYVMERCFTMKDFPVTWPTKWWKGGCEHEVREKCCKQLSQIAPQCRCDSIRRVIQGRLGGFLGIWRGEVFKQLQRAQSLPSKCNMGADCKFPSGYYW
Prediction  CCCCCCCCCCCCHHCHCCCHHHHHHHHHCCCCCCCCCCHHHHHHHCCCHHHHHHHHHHHHHHCCHHHCHHHHHHHHHHHHHHHCCCCCHHHHHHHHHHCCCCCCCCCCCCCCCCCCCC
Conf.Score  98776743248053010038999999977433357510347874152179999999999985766346299999999998735054303899999998647510299999988888779
```

Figure 4.24 Structure prediction using PyMOL and prediction secondary structure for PINB.
Prediction line, elements are shown as H for Alpha helix and C for Coil) using I-TASSER for PINB.
Structure displaying TRD (blue) and HD (purple) domains are enclosed.

The COTH (Threading-recombination approach) software (Section 2.10.6) was also used to predict the possible structure of PINA and PINB protein-protein complex. The quality of the complex template was detected by TM-score, alignment coverage, and complex root mean-square deviation (Mukherjee and Zhang, 2011). TM-score was used for quality assessment of PIN structure predictions, since it has ability in combining alignment accuracy and coverage. First rank of the template for PIN proteins was selected when TM-score was determined as individual protein; templates >0.5 but the complex TM-score was <0.4. The prediction complex model for wild type PINA and PINB with coverage of alignment, 0.816 is given in Figure 4.25. These models were determined also for PINAΔHD and PINBΔHD with coverage of alignment, 0.795 (Figure 4.26). Interestingly, coverage of the alignment which is based on dividing the length of the alignment by the total length of the query complex is higher for interaction of wild type PINs than for mutant proteins. The top models predicted by COTH for interaction of PINAΔHD+PINBΔHD showed change in protein folding that can lead to aggregation. PIN proteins without HD were folded somehow differently and the TRD locations in both PIN proteins were changed (Figure 4.26). The complex structure when the HD was removed exhibited a change in position of the two tryptophan residues (W40 and W41) (shown in blue) in PINA and proline and valine residues (P36 and V37) (shown in blue) in PINB. The change in position of the TRD in predicted PINAΔHD and PINBΔHD complexes may explain the results of lack of protein-protein interactions in plant cells when the HD is removed. The result shows that both the TRD and HD regions may have roles in the interactions of PIN proteins, but may contribute in different ways to the stability of the protein complexes.

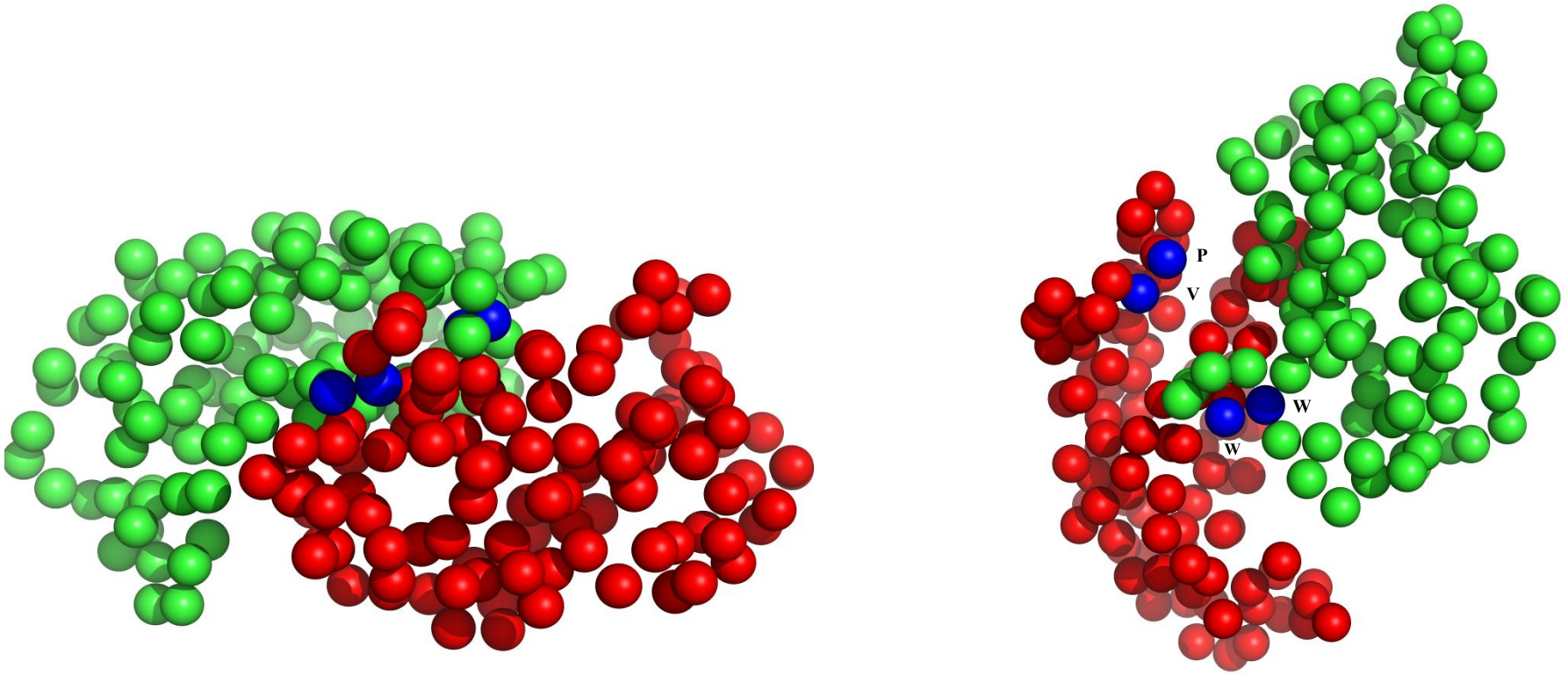

DVAGGGGAQQCPVETKLNSCRNYLLDRCSTMKDFPVTWRWWKWWKGGCQELLGECCSRLGQMPPQCRCNIIQGSIQGDLGGIFGFQRDRASKVIQEAKNLPPRCNQ
GPPCNIPGTIGYYWEVGGGGGSQQCPQERPKLSSCKDYVMERCFTMKDFPVTWPTKWWKGGCEHEVREKCCKQLSQIAPQCRCDSIRRVIQGRLGGFLGIWRGEVFK
QLQRAQSLPSKCNMGADCKFPSGYYW

Figure 4.25 Modeling result of COTH for PINA and PINB Complex in horizontal and vertical direction.

Wild type **PINA** (green) and **PINB** (red) complex; two residues of TRD domain for both proteins are positioned in blue; HD domains for both PINA and PINB proteins are bordered of protein sequences.

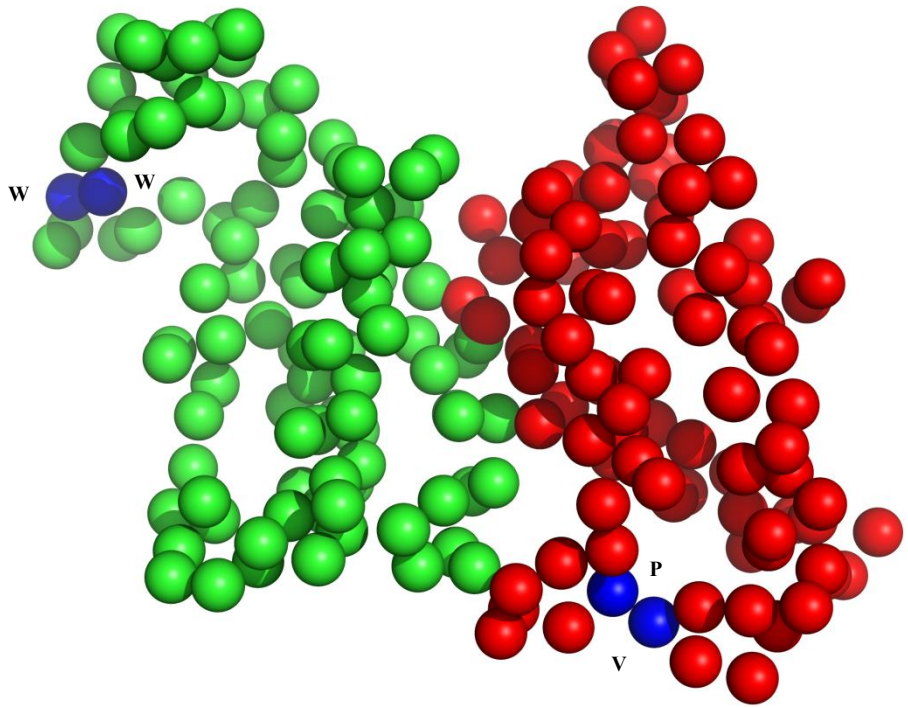

DVAGGGGAQQCPVETKLNSCRNYLLDRCSTMKDFPVTWRWWKWWKGGCQELLGECCSRLGQMPPQCRCNIIQGSQRDRASKVIQEAKNLPPRCNQGPPCNIPGTIG
YYWEVGGGGGSQQCPQERPKLSSCKDYVMERCFTMKDFPVTWPTKWWKGGCEHEVREKCCKQLSQIAPQCRCDSIRRLGIWRGEVFKQLQRAQSLPSKCNMGADC
KFPSGYYW

Figure 4.26 Modeling result of COTH for PINAΔHD and PINBΔHD Complex.
HD deletion mutation **PINAΔHD** (green) and **PINBΔHD** (red) complex; two residues of TRD domain are positioned in blue

4.3 Discussion

Previously PIN proteins have been expressed successfully in maize with the 27 kDa γ-Zein promoter and the 35S polyadenylation region terminator (Zhang et al., 2009). RNA-mediated silencing (RNAi) of the *Pin* genes in transgenic wheat reported with stable transformation via *A. tumefaciens* under control of 35S promoter (Gasparis et al., 2011). Moreover recently overexpression of *Pina* gene in transgenic durum wheat was conducted under the control of the maize Ubiquitin promoter and also under the control of 35S promoter (Li et al., 2014). In the present work, the PIN proteins for BiFC assay have been expressed successfully under the control of 35S promoter.

Protein-protein interaction is one of the most important considerations for the function of many proteins. The present work is the first investigation of *in vivo* interaction for PIN proteins based on the BiFC assay in a plant system. Defining protein interactions can be assisted by BiFC assays in live plant cells such as *N. benthamiana* (Goodin et al., 2008; Ohad et al., 2007; Waadt et al., 2008). This approach is based on the complementation between two non-fluorescent fragments of the yellow fluorescent protein (YFP) when they are brought together by interactions between proteins fused to each fragment resulting in fluorescence (Hu and Kerppola, 2003; Kerppola, 2006). Since the induction of the fluorescence signal is dependent on the physical association between the two terminal parts of YFP, it is dependent not only on their presence but also their orientation. Overall, when the structural basis of a protein complex is not clear, as in the present case, the two interacting proteins should be fused N- and also C-terminally to the C- and N- terminal parts of YFP and all eight combinations tested for fluorescence complementation (Kerppola, 2006). Table 4.1, shows interactions results in different directions for heterodimersations and homodimersations, for both PINA and PINB. Strong interactions were observed only in one direction: PINA-YC+YN-PINB, i.e., co-expression of the C-terminal half of YFP fused to PINA and the N-terminal half of YFP fused to PINB. The finding suggests that the orientation of the PIN proteins is important for their interactions. Previous work by Ziemann et al. (2008) using the yeast two-hybrid system (Fields and Song, 1989) showed physical interactions between wild type of PINA and PINB, and also PINB interacting with itself while PINA showed weaker self interaction. Further, the important role of direction for PIN proteins in the

yeast two-hybrid system confirmed in studies of wild type as well as the mutated (TRD and HD domain-deleted) proteins (Alfred, 2013; Alfred et al., 2014).

Using BiFC, leaf cells of *N. benthamiana* showed fluorescence signal due to PINB homo-dimerisation (YN-PINB+YC-PINB). The presence of three tryptophan residues in the TRD of PINB may explain the result. However, most interestingly, no interactions were detected for PINA homo-dimerisation, suggesting the domain alone or its tryptophans (five in PINA) may not be directly relevant to the interactions. Fluorescence complementation can occur when the YFP fragments are fused to positions that are separated by an average distance of greater than 100A°, which provides enough flexibility to allow reconstitution of the split-YFP fragments (Hu et al., 2002). The lack of fluorescence of PINA homo-dimerisation may result from insufficient flexibility compared to that of PINB complexes.

The region or amino acid residues involved in the PIN proteins interactions still remains elusive. The TRD is the most important region for lipid interactions (Kooijman et al., 1997; Kooijman et al., 1998; Jing et al., 2003), therefore one strong candidate is the TRD in both proteins, at residues 34-46 in mature PINA and 35-47 in mature PINB. The other candidate is the little-studied hydrophobic domain (HD) at position of residue 75-85 of the mature PINA (Le Bihan et al., 1996), and the corresponding residues 75-83 of the mature PINB. Clones created previously (Alfred, 2013; Alfred et al., 2014) by site-directed mutagenesis (SDM) PCR to delete the TRD within PINA and the HD within PINA and PINB were therefore used in the present work. The PINAΔHD interactions with PINBΔHD showed no fluorescence signal based on BiFC assays, in contrast to interaction of a specific orientation of the wild type PINA and PINB. The interactions for PINA and PINB without HD tested in the same orientation were unsuccessful in inducing fluorescence. Furthermore, no fluorescence signal was observed with itself or between PINBΔHD and wild type PINB. The results indicate that the HD domains are important for co-expression and/or stability and/or interaction between PINA and PINB and among PINB and PINB in *N. benthamiana* leaf cells. There is one possible explanation for the non-interaction of PINAΔHD+PINBΔHD; aggregation of mutant proteins, due to the change in the protein folding.

Deletion of the HD may also have an effect on the refolding of the PINs. Dimerisation and/or oligomerisations can have different structural and functional advantages for proteins, such as improved stability, control over accessibility and specificity of active sites, and increased complexity (Marianayagam et al., 2004). Protein complexes are stabilized by the burial of hydrophobic complementary occluding surfaces, covalent bonds such as disulphide bridges, and hydrogen bonding (Lesk, 2010). The disulphide bonds are indeed necessary to stabilize the α-helical structure and maintain the native structure and solubility of PINA and PINB (Le Bihan et al, 1996). The formation of α-helices at membrane surfaces is also an important point for binding to membrane (Seelig, 2004). The preliminary protein-protein complex predictions based on the COTH have shown refolding and a shift in the rotation of structure of the mutant PINs, which may affect their functionality.

No protein-protein interactions were noted for PINAΔTRD with wild type PINB. Thus the TRD of PINA may be important for expression *in planta* and protein-protein interactions. Previous studies have emphasized that the TRD region has important role in binding to the membranes polar lipids on the surface of starch (Blochet et al., 1993; Kooijman et al., 1997; Giroux and Morris, 1997), direct binding to surface of starch granules (Wall et al., 2010) and the activity of PINs (Capparelli et al., 2005; Dubreil et al., 1998; Jing et al., 2003). The TRD has also been shown to be important for the antibacterial and antifungal activities of PINs (Jing et al., 2003; Miao et al., 2012; Phillips et al., 2011). The self-assembly of PINA micelle in solution has been shown by hydrophobic forces that involve intermolecular interactions between the tryptophan residues in the TRD (Clifton et al., 2011a). However no such self-assembly has been observed for PINB, possibly due to fewer hydrophobic tryptophan residues in its TRD (Clifton et al., 2011a; Pauly et al., 2013). There is evidence that PINA forms aggregates, and TRD has been implicated in the formation of PINA aggregates (Le Bihan et al., 1996). Thus, PINA-PINB interaction may explain the reported change to hard grain when there is a mutation or a lack in either PIN protein (Giroux and Morris, 1997, 1998). Transgenic wheat work has provided further insights into the roles of PINA and PINB together and individually in influencing grain texture (Giroux and Morris, 1998; Morris et al., 2001; Wanjugi et al., 2007) (reviewed in Section 1.5.4).

Two tryptophan residues (W41 and W44) at the TRD have shown essential role for interaction of PINA with the yeast plasma membranes, while the lysine in the TRD of PINB seems to be more important (Evrard et al., 2008). *In planta* mutagenesis studies had found that mutations within the TRD of PINA and PINB resulted significantly increased the grain hardness, and PINB function was likely to be more critical to overall *Ha locus* effects (Feiz et al., 2009a). The TRD has a role in stabilizing the structure of both PIN proteins (Pauly et al., 2013).

The present work has shown that the PINA and PINB proteins do interact physically *in planta*, and PINB can also self-associate, indicating that its function may more considerable despite having a TRD with fewer tryptophan residues. A more detailed understanding of the mechanisms for protein-protein interaction between the PIN proteins is required to explain many of their co-operative and inter-dependant properties involved in starch binding and weather these are also relevant to their bioactivity against microbial pathogen.

CHAPTER 5

General discussion and future directions

5.1 General discussion

Wheat is the third most widely consumed cereals in the world after maize and rice. The quality of wheat is critical in the food industry owing to its nutritional value and health benefits. The hardness or texture of the wheat grain is a major determinant of the quality, as it affects milling and end use properties.

The first chapter of this thesis presented a comprehensive review of literature on structure of the wheat grain, grain hardness and its effects on the end-use of wheat and the discoveries of friabilin and puroindoline proteins. Friabilin is a 15 kDa protein complex that consists of two structurally similar proteins, puroindoline-a (PINA) and puroindoline-b (PINB). It was originally suggested that friabilin act as a non-stick surface between the starch granules and the protein matrix to determine wheat grain hardness. The PINs are unique small proteins with a highly conserved 10 cysteine-backbone and a tryptophan-rich domain (TRD), the latter most likely involved in the binding to the phospholipids on the surface of starch granules. The soft grain texture in wheat encoded by the wild type *Pin* alleles (*Pina-D1a* and *Pinb-D1a*), while the hard texture occurs as a result of mutation in one or both of the *Pin* genes, and deletions of both genes result in the 'very hard' texture of durum wheat. Chapter 1 also described evidence of transgenic *Pin* genes altering grain texture, as well as plant-based expression systems for production of valuable recombinant proteins such as anti-microbial peptides (AMPs). The review also presented several predicted homology models of PIN proteins due to the lack of an absolute three dimensional structure. Another limitation in structural analysis of PINs is their strong aggregation properties at high protein concentration. Several other gaps in literature were also identified, such as the *in vivo* roles of PIN proteins within the wheat seed and the exact mode of actions of PINs in grain hardness and their co-operative activity at membranes. Hence, characterisation of PIN proteins is critical to exploit the potential benefits of PIN proteins and PIN-based peptides in agricultural or medical applications. Therefore, the major objectives of this research were as follows:

1. To clone the *Pin* genes encoding the putative mature PINA and PINB in magnICON® viral vector system and *A. tumefaciens* infiltrations, to express and optimize their transient expression for high yield in the leaves of *Nicotiana benthamiana*.

2. To test the antibacterial and antifungal activities of recombinant PIN proteins purified with affinity purification using His-tag and hydrophobic interactions systems.

3. To analyse the protein-protein interactions among the PIN proteins *in planta* using the BiFC system based on pNBV vectors and co-expression of the silencing suppressor protein p19.

4. To test the significance of the tryptophan-rich domain (TRD) of PINA and the hydrophobic domain (HD) of both PINs in any interactions between the PINs using the BiFC system.

The above aims were addressed using a number of experimental approaches as set out in Chapter 2. In brief, these included molecular and biochemical methodologies such as, DNA extractions, PCRs, cloning into viral vectors, plasmid purifications, DNA sequencing, electroporation of *A. tumefaciens* cells, agroinfiltration, *in planta* protein expression, protein purification and quantitation, SDS-PAGE, western blot and ELISA analyses, fluorescence microscopy, microbiological techniques and also bioinformatics tools (e.g., DNA and protein sequence alignments, primer design, BLAST searches, 3D modeling and protein-protein complex structure predications).

The aims 1 and 2 were addressed in Chapter 3. In brief, this chapter investigated the plant expression system as a platform to produce recombinant PINA and PINB proteins in sufficient yield for antimicrobial activities. The study focussed on the rapid transient expression of PINs using the deconstructed tobacco mosaic virus-based 'magnICON®' for subcellular localisation of PINs in different compartments of *N. benthamiana.* The results have shown: (i) the presence of recombinant PINA and PINB in both monomeric and oligomeric forms when targeted to the chloroplast, cytosol and ER as shown by western blot and ELISA analyses (ii) PIN A and PINB yields of up to 0.8% TSP or 51.7

µg/g of fresh weight for PINA, and 70 µg/g of fresh weight for PINB when proteins targeted to the chloroplast (iii) the achievement of maximum yields of recombinant PIN proteins at 10 dpi (iv) heat-sensitivity of recombinant PIN proteins (v) establishment of the most efficient purification method for recombinant PINs based on hydrophobic interaction (vi) antimicrobial activity for recombinant PINA and PINB against *Escherichia coli* (a Gram negative bacterium) and *Staphylococcus aureus* (a Gram positive bacterium) and four phytopathogenic fungal strains and low haemolytic activity towards mammalian cells. Overall, the work has led to successful expression, purification and characterisation methodology for obtaining PIN proteins with appropriate quality that is essential for potential infection control and therapeutic applications.

Aims 3 and 4 were addressed in Chapter 4. There is evidence that PINs may interact co-operatively or interdependently to confer the soft grain texture. The present work showed interactions between PINA and PINB proteins using BiFC system in *N. benthamiana* leaves, just in one direction; PINA-YC+YN-PINB, based on the fluorescence intensity visualised in living plant cells. The finding suggests that the orientation of the PIN proteins is important for their interactions. In addition, homodimerisation was noted for PINB (YN-PINB+YC-PINB) but not PINA. Moreover the chapter investigated the key regions/residues essential for protein-protein interaction. Site-directed mutagenesis (SDM) PCR had been conducted previously to deletions in PINA at the TRD and in both PINs at the hydrophobic domain (HD). These inserts were subcloned into the BiFC vectors in the present work. The results indicate that no interaction occurred between PINA and PINB, or between PINB and PINB, without their HD. The HD domain may affect the folding of PIN proteins and rotation possibilities of the structure. Predictions of the 3D models of the possible structure for PINs further corroborated this hypothesis. The deletion of the TRD in PINA also showed no interaction with wild type PINB. Overall, the result shows that both the TRD and HD regions may have roles in the *in planta* interactions of PIN proteins, but the two domains may contribute in different ways to stability of the protein complexes. The mutant PIN proteins were also expressed *in planta* based on magnICON® system to test their expression. The result showed that PINs without the HD were successfully

expressed, while the PINA without TRD was not detected. The results suggest that PINA with deletion of TRD may be degraded, or the Durotest antibody was not able to detect this mutant protein, suggesting the TRD is among the epitopes for this antibody.

5.2 Future directions

The significance of the PIN proteins in the wheat industry has led to a considerable amount of research focus on their structures and mechanisms. The worldwide research has led to over 150 publications that outline their lipid-binding properties, the mutant alleles as well as orthlogs in other monocot crop species, also the antimicrobial properties of the proteins and the peptides based on these. However, the exact mechanisms of action for PINs are not completely clear yet. The results of the present study led to successful expression of bioactive proteins in a plant systems and also establishe PINA-PINB and PINB-PINB associations *in planta*, as summarized above. However further in-depth research is required on nature and mechanisms for their functionality. The identity of the active protein can be established using peptide mapping of the trypsinized protein, sizing using MALDI-TOF MS methods and identity through LC–MS/MS (Klimyuk et al., 2014). Additionally, it would be important to use circular dichroism (CD) tools (Greenfield, 2007) to determine the secondary structure and folding properties of recombinant proteins to assess how the different mutations affects their structure and stability.

Designing more strategies for increased production of soluble PIN proteins, such as plant-codon optimisation would be important, as effected on increasing yield of protein in plant system (Webster et al., 2009). The choice of expression systems such as cell-free system (Endo and Sawasaki, 2006; Sawasaki et al., 2002), or vectors with fusion tag, for instance, Halo-tag (Los et al., 2008) would be important. Furthermore, several fusion strategies have been developed recently to significantly enhance the production yield of plant-made recombinant proteins, as reviewed by Conley et al. (2011).

The exact mechanism of membrane activity for PIN-based peptides and proteins still is unclear. Hence it would be useful to design chloroplast transformation vector with the PIN-based peptide fused with GFP to confer stability to the peptide (Lee et al., 2011b).

PIN-based peptides can be obtained with the tag to help their purification for further analysis of direct interactions with biological membranes. Expression and characterisation of antimicrobial peptides in chloroplasts to control viral and bacterial infections has been successfully utilised (Daniell et al., 2009a; Lee et al., 2011b; Nadai et al., 2009; Ruhlman et al., 2007; Sanz-Barrio et al., 2011). Further work is needed to explore these applications for PINs, especially for activity against pathogens of relevance to the food and agriculture industries.

This study has shown protein-protein interaction of PIN proteins *in planta*. The knowledge gained will be invaluable for future work for more detailed understanding of the mechanisms interactions, which is required to explain their co-operative or interdependent properties in starch binding. Site-directed mutagenesis of residues that may have a role in the hardness phenotype would be important for exploring their effects on protein interaction. Further, the GSP-1 and PINB-2v1 proteins may be additional factors that interact with the PINs, contribute to further variation in wheat grain hardness, and therefore would be important for exploring their effects on protein interaction. Flow cytometry techniques (Berendzen et al., 2012; Morell et al., 2008) and multicolour BiFC analysis may allows simultaneous visualisation of multiple protein complexes in the same cell (Hu and Kerppola, 2003; Kerppola, 2008) and enable subcellular localisation of the interaction (Kerppola, 2013). Furthermore, quantification of BiFC fluorescence can be measured by analytical flow cytometry (Berendzen et al., 2012).

The PIN proteins were discovered more than twenty years ago and numerous studies so far have already revealed a number of their fundamental biochemical and functional aspects. Further investigations building on this wealth of knowledge will one day explain the unique activities and effects of these small proteins.

References

Adam Z, Clarke AK (2002) Cutting edge of chloroplast proteolysis. Trends in Plant Science, 7: 451-456.

Alfred RL, Palombo EA, Panozzo JF, Bhave M (2014) The co-operative interaction of puroindolines in wheat grain texture may involve the hydrophobic domain. Journal of Cereal Science, In Press.

Alfred RL (2013) Biochemical analysis of the functionality of puroindoline peptides and proteins. PhD Thesis, Swinburne University of Technology, http://hdl.handle.net/1959.3/368064.

Alfred RL, Palombo EA, Panozzo JF, Bariana H, Bhave M (2013a) Stability of puroindoline peptides and effects on wheat rust. World Journal of Microbiology and Biotechnology, 29: 1409-1419.

Alfred RL, Palombo EA, Panozzo JF, Bhave M (2013b) The antimicrobial domains of wheat puroindolines are cell-penetrating peptides with possible intracellular mechanisms of action. PLoS ONE, 8, e75488.

Amoroso MG, Longobardo L, Capparelli R (2004) Real Time RT-PCR and flow cytometry to investigate wheat kernel hardness: Role of puroindoline genes and proteins. Biotechnology Letters, 26: 1731-1737.

Arlen PA, Falconer R, Cherukumilli S, Cole A, Cole AM, Oishi KK, Daniell H (2007) Field production and functional evaluation of chloroplast-derived interferon-α2b. Plant Biotechnology Journal, 5: 511-525.

Arnau J, Lauritzen C, Petersen GE, Pedersen J (2006) Current strategies for the use of affinity tags and tag removal for the purification of recombinant proteins. Protein Expression and Purification, 48: 1-13.

Bakó A, Gárdonyi M, Tamás L (2007) *In vitro* starch binding experiments: Study of the proteins related to grain hardness of Wheat. In: Buck HT, Nisi JE and Salomón N (eds.) Wheat Production in Stressed Environments. Springer Netherlands. pp 685-691.

Bally J, Nadai M, Vitel M, Rolland A, Dumain R, Dubald M (2009) Plant physiological adaptations to the massive foreign protein synthesis occurring in recombinant chloroplasts. Plant Physiology, 150: 1474-1481.

Barampuram S, Zhang ZJ (2011) Recent advances in plant transformation. Methods in Molecular Biology (Clifton, N.J.), 701: 1-35.

Barlow K, Buttrose M, Simmonds D, Vesk M (1973) Nature of starch-protein interface in wheat endosperm. Cereal Chemistry, 50: 443-454.

Basaran P, Rodriguez-Cerezo E (2008) Plant molecular farming: Opportunities and challenges. Critical Reviews in Biotechnology, 28: 153-172.

Beecher B, Bettge A, Smidansky E, Giroux MJ (2002a) Expression of wild-type pinB sequence in transgenic wheat complements a hard phenotype. Theoretical and Applied Genetics, 105: 870-877.

Beecher B, Bowman J, Martin JM, Bettge AD, Morris CF, Blake TK, Giroux MJ (2002b) Hordoindolines are associated with a major endosperm-texture QTL in Barley (*Hordeum vulgare*). Genome, 45: 584-591.

Benchabane M, Goulet C, Rivard D, Faye L, Gomord V, Michaud D (2008) Preventing unintended proteolysis in plant protein biofactories. Plant Biotechnology Journal, 6: 633-648.

Benko-Iseppon AM, Galdino SL, Calsa Jr T, Kido EA, Tossi A, Belarmino LC, Crovella S (2010) Overview on plant antimicrobial peptides. Current Protein and Peptide Science, 11: 181-188.

Berendzen KW, Böhmer M, Wallmeroth N, Peter S, Vesić M, Zhou Y, Tiesler FKE, Schleifenbaum F, Harter K (2012) Screening for in planta protein-protein interactions combining bimolecular fluorescence complementation with flow cytometry. Plant Methods, 8: 25-40.

Bettge AD, Morris CF, Greenblatt GA (1995) Assessing genotypic softness in single wheat kernels using starch granule-associated friabilin as a biochemical marker. Euphytica, 86: 65-72.

Bhave M, Morris CF (2008a) Molecular genetics of puroindolines and related genes: Allelic diversity in wheat and other grasses. Plant Molecular Biology, 66: 205-219.

Bhave M, Morris CF (2008b) Molecular genetics of puroindolines and related genes: Regulation of expression, membrane binding properties and applications. Plant Molecular Biology, 66: 221-231.

Bi X, Wang C, Ma L, Sun Y, Shang D (2013) Investigation of the role of tryptophan residues in cationic antimicrobial peptides to determine the mechanism of antimicrobial action. Journal of Applied Microbiology, 115: 663-672.

Blochet JE, Chevalier C, Forest E, Pebay-Peyroula E, Gautier MF, Joudrier P, Pezolet M, Marion D (1993) Complete amino acid sequence of puroindoline, a new basic and cystine-rich protein with a unique tryptophan-rich domain, isolated from wheat endosperm by Triton x-114 phase partitioning. FEBS Letters, 329: 336-340.

Bracha-Drori K, Shichrur K, Katz A, Oliva M, Angelovici R, Yalovsky S, Ohad N (2004) Detection of protein-protein interactions in plants using bimolecular fluorescence complementation. The Plant Journal, 40: 419-427.

Bradford MM (1976) A rapid and sensitive method for the quantitation of microgram quantities of protein utilizing the principle of protein-dye binding. Analytical Biochemistry, 72: 248-254.

Branlard G, Amiour N, Igrejas G, Gaborit T, Herbette S, Dardevet M, Marion D (2003) Diversity of puroindolines as revealed by two-dimensional electrophoresis. Proteomics, 3: 168-174.

Broekaert WF, Cammue BPA, De Bolle MFC, Thevissen K, De Samblanx GW, Osborn RW (1997) Antimicrobial peptides from plants. Critical Reviews in Plant Sciences, 16: 297-323.

Broekaert WF, Terras FRG, Cammue BPA, Vanderleyden J (1990) An automated quantitative assay for fungal growth inhibition. FEMS Microbiology Letters, 69: 55-60.

Bruce BD (2000) Chloroplast transit peptides: Structure, function and evolution. Trends in Cell Biology, 10: 440-447.

Capparelli R, Amoroso MG, Palumbo D, Iannaccone M, Faleri C, Cresti M (2005) Two plant puroindolines colocalize in wheat seed and *in vitro* synergistically fight against pathogens. Plant Molecular Biology, 58: 857-867.

Capparelli R, Borriello G, Giroux MJ, Amoroso MG (2003) Puroindoline A-gene expression is involved in association of puroindolines to starch. Theoretical and Applied Genetics, 107: 1463-1468.

Capparelli R, Palumbo D, Iannaccone M, Ventimiglia I, Di Salle E, Capuano F, Salvatore P, Amoroso M (2006) Cloning and expression of two plant proteins: similar antimicrobial activity of native and recombinant form. Biotechnology Letters, 28: 943-949.

Capparelli R, Ventimiglia I, Palumbo D, Nicodemo D, Salvatore P, Amoroso MG, Iannaccone M (2007) Expression of recombinant puroindolines for the treatment of staphylococcal skin infections (acne vulgaris). Journal of Biotechnology, 128: 606-614.

Chalfie M, Tu Y, Euskirchen G, Ward WW, Prasher DC (1994) Green fluorescent protein as a marker for gene expression. Science, 263: 802-805.

Chan DI, Prenner EJ, Vogel HJ (2006) Tryptophan- and arginine-rich antimicrobial peptides: Structures and mechanisms of action. Biochimica et Biophysica Acta - Biomembranes, 1758: 1184-1202.

Chang C, Zhang H, Xu J, Li W, Liu G, You M, Li B (2006) Identification of allelic variations of puroindoline genes controlling grain hardness in wheat using a modified denaturing PAGE. Euphytica, 152: 225-234.

Chantret N, Cenci A, Sabot F, Anderson O, Dubcovsky J (2004) Sequencing of the *Triticum monococcum Hardness* locus reveals good microcolinearity with rice. Molecular Genetics and Genomics, 271: 377-386.

Chantret N, Salse J, Sabot F, Rahman S, Bellec A, Laubin B, Dubois I, Dossat C, Sourdille P, Joudrier P, Gautier MF, Cattolico L, Beckert M, Aubourg S, Weissenbach J, Caboche M, Bernard M, Leroy P, Chalhoub B (2005) Molecular basis of evolutionary events that shaped the *Hardness* locus in diploid and polyploid wheat species (Triticum and Aegilops). The Plant Cell, 17: 1033-1045.

Charnet P, Molle G, Marion D, Rousset M, Lullien-Pellerin V (2003) Puroindolines form ion channels in biological membranes. Biophysical Journal, 84: 2416-2426.

Chase MW, Knapp S, Cox AV, Clarkson JJ, Butsko Y, Joseph J, Savolainen V, Parokonny AS (2003) Molecular systematics, GISH and the origin of hybrid taxa in *Nicotiana* (Solanaceae). Annals of Botany, 92: 107-127.

Chen F, He Z, Xia X, Lillemo M, Morris C (2005) A new puroindoline b mutation present in Chinese winter wheat cultivar Jingdong 11. Journal of Cereal Science, 42: 267-269.

Chen F, He ZH, Xia XC, Xia LQ, Zhang XY, Lillemo M, Morris CF (2006) Molecular and biochemical characterization of puroindoline a and b alleles in Chinese landraces and historical cultivars. Theoretical and Applied Genetics, 112: 400-409.

Chen F, Yu Y, Xia X, He Z (2007) Prevalence of a novel puroindoline b allele in Yunnan endemic wheats (*Triticum aestivum* ssp. *yunnanense* King). Euphytica, 156: 39-46.

Chen F, Beecher B, Morris C (2010a) Physical mapping and a new variant of *Puroindoline b-2* genes in wheat. Theoretical and Applied Genetics, 120: 745-751.

Chen F, Xu HX, Zhang FY, Xia XC, He ZH, Wang DW, Dong ZD, Zhan KH, Cheng XY, Cui DQ (2010b) Physical mapping of *puroindoline b-2* genes and molecular characterization of a novel variant in durum wheat (*Triticum turgidum* L.). Molecular Breeding, 28: 153-161.

Chen F, Zhang F, Cheng X, Morris C, Xu H, Dong Z, Zhan K, Cui D (2010c) Association of *Puroindoline b-B2* variants with grain traits, yield components and flag leaf size in bread wheat (*Triticum aestivum* L.) varieties of the Yellow and Huai Valleys of China. Journal of Cereal Science, 52: 247-253.

Chevreau E, Dupuis F, Ortolan C, Parisi L (2001) Transformation of apple for durable scab resistance: Expression of a puroindoline gene in susceptible and resistant (Vf) genotypes. Acta Horticulturae, 560: 323-327.

Christou P, Stoger E, Twyman RM (2004) Monocot expression systems for molecular farming. In: Fischer R and Schillberg S (eds.) Molecular Farming. Wiley-VCH Verlag GmbH & Co. KGaA,Weinheim. pp 55-67.

Clifton LA, Green RJ, Frazier RA (2007a) Puroindoline-b mutations control the lipid binding interactions in mixed puroindoline-a:puroindoline-b systems. Biochemistry, 46: 13929-13937.

Clifton LA, Green RJ, Hughes AV, Frazier RA (2008) Interfacial structure of wild-type and mutant forms of puroindoline-b bound to DPPG monolayers. Journal of Physical Chemistry B, 112: 15907-15913.

Clifton LA, Lad MD, Green RJ, Frazier RA (2007b) Single amino acid substitutions in puroindoline-b mutants influence lipid binding properties. Biochemistry, 46: 2260-2266.

Clifton LA, Sanders MR, Castelletto V, Rogers SE, Heenan RK, Neylon C, Frazier RA, Green RJ (2011a) Puroindoline-a, a lipid binding protein from common wheat, spontaneously forms prolate protein micelles in solution. Physical Chemistry Chemical Physics, 13: 8881-8888.

Clifton LA, Sanders MR, Hughes AV, Neylon C, Frazier RA, Green RJ (2011b) Lipid binding interactions of antimicrobial plant seed defence proteins: Puroindoline-a and β-purothionin. Physical Chemistry Chemical Physics, 13: 17153-17162.

Conley AJ, Joensuu JJ, Richman A, Menassa R (2011) Protein body-inducing fusions for high-level production and purification of recombinant proteins in plants. Plant Biotechnology Journal, 9: 419-433.

Conrad U, Fiedler U (1998) Compartment-specific accumulation of recombinant immunoglobulins in plant cells: An essential tool for antibody production and immunomodulation of physiological functions and pathogen activity. Plant Molecular Biology, 38: 101-109.

Cornell H (2003) The chemistry and biochemistry of wheat. In: Cauvain S (ed.) Bread Making: Improving Quality. Woodhead Publishing. Cambridge, United Kingdom. pp 31-70.

Corona V, Gazza L, Boggini G, Pogna NE (2001) Variation in friabilin composition as determined by A-PAGE fractionation and PCR amplification, and its relationship to grain hardness in bread wheat. Journal of Cereal Science, 34: 243-250.

Cremazy FGE, Manders EMM, Bastiaens PIH, Kramer G, Hager GL, Van Munster EB, Verschure PJ, Gadella Jr TWJ, Van Driel R (2005) Imaging in situ protein-DNA interactions in the cell nucleus using FRET-FLIM. Experimental Cell Research, 309: 390-396.

Crone DE, Huang Y-M, Pitman DJ, Schenkelberg C, Fraser K, Macari S, Bystroff C (2013) GFP-Based Biosensors. In: Rinken T (ed.) State of the Art in Biosensors - General Aspects. Rijeka, croatia: InTech. pp 3-36.

Daniell H (2006) Production of biopharmaceuticals and vaccines in plants via the chloroplast genome. Biotechnology Journal, 1: 1071-1079.

Daniell H, Cohill PR, Kumar S, Dufourmantel N (2004) Chloroplast genetic engineering. In: Daniell H and Chase CD (eds.) Molecular Biology and Biotechnology of Plant Organelles. Springer, Netherlands. pp 443-490.

Daniell H, Ruiz G, Denes B, Sandberg L, Langridge W (2009a) Optimization of codon composition and regulatory elements for expression of human insulin like growth factor-1 in transgenic chloroplasts and evaluation of structural identity and function. BMC Biotechnology, 9: 33-48.

Daniell H, Singh ND, Mason H, Streatfield SJ (2009b) Plant-made vaccine antigens and biopharmaceuticals. Trends in Plant Science, 14: 669-679.

Daniell H, Streatfield SJ, Wycoff K (2001) Medical molecular farming: Production of antibodies, biopharmaceuticals and edible vaccines in plants. Trends in Plant Science, 6: 219-226.

Dathe M, Schumann M, Wieprecht T, Winkler A, Beyermann M, Krause E, Matsuzaki K, Murase O, Bienert M (1996) Peptide helicity and membrane surface charge modulate the balance of electrostatic and hydrophobic interactions with lipid bilayers and biological membranes. Biochemistry, 35: 12612-12622.

Davies HM (2010) Review article: Commercialization of whole-plant systems for biomanufacturing of protein products: evolution and prospects. Plant Biotechnology Journal, 8: 845-861.

Day L, Bhandari DG, Greenwell P, Leonard SA, Schofield JD (2006) Characterization of wheat puroindoline proteins. FEBS Journal, 273: 5358-5373.

De Bolle MFC, Osborn RW, Goderis IJ, Noe L, Acland D, Hart CA, Torrekens S, Van Leuven F, Broekaert WF (1996) Antimicrobial peptides from Mirabilis jalapa and Amaranthus caudatus: Expression, processing, localization and biological activity in transgenic tobacco. Plant Molecular Biology, 31: 993-1008.

De Jaeger G, Buys E, Eeckhout D, De Wilde C, Jacobs A, Kapila J, Angenon G, Van Montagu M, Gerats T, Depicker A (1999) High level accumulation of single-chain variable fragments in the cytosol of transgenic Petunia hybrida. European Journal of Biochemistry, 259: 426-434.

Dean R, Van Kan JaL, Pretorius ZA, Hammond-Kosack KE, Di Pietro A, Spanu PD, Rudd JJ, Dickman M, Kahmann R, Ellis J, Foster GD (2012) The Top 10 fungal pathogens in molecular plant pathology. Molecular Plant Pathology, 13: 414-430.

Delano WL (2002) PyMOL: An Open-Source Molecular Graphics Tool. DeLano Scientific, San Carlos, CA, USA, 40.

Delcour JA, Hoseney RC (2010) Principles of cereal science and technology authors provide insight into the current state of cereal processing. Cereal Foods World, 55: 21-22.

Desai PN, Shrivastava N, Padh H (2010) Production of heterologous proteins in plants: Strategies for optimal expression. Biotechnology Advances, 28: 427-435.

Digeon JF, Guiderdoni E, Alary R, Michaux-Ferrière N, Joudrier P, Gautier MF (1999) Cloning of a wheat puroindoline gene promoter by IPCR and analysis of promoter regions required for tissue-specific expression in transgenic rice seeds. Plant Molecular Biology, 39: 1101-1112.

Doekes GJ, Belderok B (1976) Kernel hardness and baking quality of wheat - A genetic analysis using chromosome substitution lines. Euphytica, 25: 565-576.

Doran PM (2006) Foreign protein degradation and instability in plants and plant tissue cultures. Trends in Biotechnology, 24: 426-432.

Doran PM (2013) Therapeutically important proteins from *in vitro* plant tissue culture systems. Current Medicinal Chemistry, 20: 1047-1055.

Douliez JP, Michon T, Elmorjani K, Marion D (2000) Structure, biological and technological functions of lipid transfer proteins and indolines, the major lipid binding proteins from cereal kernels. Journal of Cereal Science, 32: 1-20.

Dubcovsky J, Dvorak J (2007) Genome plasticity a key factor in the success of polyploid wheat under domestication. Science, 316: 1862-1866.

Dubovskii PV, Vassilevski AA, Slavokhotova AA, Odintsova TI, Grishin EV, Egorov TA, Arseniev AS (2011) Solution structure of a defense peptide from wheat with a 10-cysteine motif. Biochemical and Biophysical Research Communications, 411: 14-18.

Dubreil L, Compoint JP, Marion D (1997) Interaction of puroindolines with wheat flour polar lipids determines their foaming properties. Journal of Agricultural and Food Chemistry, 45: 108-116.

Dubreil L, Gaborit T, Bouchet B, Gallant DJ, Broekaert WF, Quillien L, Marion D (1998) Spatial and temporal distribution of the major isoforms of puroindolines (puroindoline-a and puroindoline-b) and non specific lipid transfer protein (ns-LTPle1) of *Triticum aestivum* seeds. Relationships with their *in vitro* antifungal properties. Plant Science, 138: 121-135.

Eckardt NA (2001) A sense of self: the role of DNA sequence elimination in allopolyploidization. The Plant Cell, 13: 1699-1704.

Egelkrout E, Rajan V, Howard JA (2012) Overproduction of recombinant proteins in plants. Plant Science, 184: 83-101.

Egorov TA, Odintsova TI, Pukhalsky VA, Grishin EV (2005) Diversity of wheat anti-microbial peptides. Peptides, 26: 2064-2073.

Elmorjani K, Geneix N, Dalgalarrondo M, Branlard G, Marion D (2013) Wheat grain softness protein (Gsp1) is a puroindoline-like protein that displays a specific post-translational maturation and does not interact with lipids. Journal of Cereal Science, 58: 117-122.

Emanuelsson O, Nielsen H, Von Heijne G (1999) ChloroP, a neural network-based method for predicting chloroplast transit peptides and their cleavage sites. Protein Science, 8: 978-984.

Endo Y, Sawasaki T (2006) Cell-free expression systems for eukaryotic protein production. Current Opinion in Biotechnology, 17: 373-380.

Espinel-Ingroff A, Cantón E (2007) Antifungal susceptibility testing of filamentous fungi. In: Schwalbe R, Steele-Moore L and Goodwin AC (eds.) Antimicrobial Susceptibility Testing Protocols. Hoboken: CRC Press. pp 209-241.

Evrard A, Lagarde V, Joudrier P, Gautier MF (2008) Puroindoline-a and puroindoline-b interact with the *Saccharomyces cerevisiae* plasma membrane through different amino acids present in their tryptophan-rich domain. Journal of Cereal Science, 48: 379-386.

Faize M, Sourice S, Dupuis F, Parisi L, Gautier MF, Chevreau E (2004) Expression of wheat puroindoline-b reduces scab susceptibility in transgenic apple (*Malus* × *domestica* Borkh). Plant Science, 167: 347-354.

Faye L, Boulaflous A, Benchabane M, Gomord V, Michaud D (2005) Protein modifications in the plant secretory pathway: Current status and practical implications in molecular pharming. Vaccine, 23: 1770-1778.

Feiz L, Beecher BS, Martin JM, Giroux MJ (2009a) *In planta* mutagenesis determines the functional regions of the wheat puroindoline proteins. Genetics, 183: 853-860.

Feiz L, Martin JM, Giroux MJ (2009b) Creation and functional analysis of new *puroindoline* alleles in *Triticum aestivum*. Theoretical and Applied Genetics, 118: 247-257.

Feiz L, Wanjugi HW, Melnyk CW, Altosaar I, Martin JM, Giroux MJ (2009c) Puroindolines co-localize to the starch granule surface and increase seed bound polar lipid content. Journal of Cereal Science, 50: 91-98.

Feldman M (1995) Wheats. In: Smartt. J and Simmonds. NW (eds.) Evolution of Crop Plants. Longman Scientific and Technical. Harlow, UK. pp 184-192.

Feldman M (2001) Origin of cultivated wheat. In: Bonjean AP and Angus WJ (eds.) The world wheat book: a history of wheat breeding. Lavoisier Publishing. France. pp 3-56.

Fischer R, Emans N (2000) Molecular farming of pharmaceutical proteins. Transgenic Research, 9: 279-299.

Fischer R, Schillberg S, Buyel JF, Twyman RM (2013) Commercial aspects of pharmaceutical protein production in plants. Current Pharmaceutical Design, 19: 5471-5477.

Fischer R, Stoger E, Schillberg S, Christou P, Twyman RM (2004) Plant-based production of biopharmaceuticals. Current Opinion in Plant Biology, 7: 152-158.

Fischer R, Twyman RM, Schillberg S (2003) Production of antibodies in plants and their use for global health. Vaccine, 21: 820-825.

Fujiwara M, Suzuki G, Kudo D, Oba H, Wada Y, Wada H, Wada N, Rahman S, Fukui K, Mukai Y (2014) Localization of transgene-derived friabilins in rice endosperm cells. Plant Biotechnology, 31: 67-70.

Gaberc-Porekar V, Menart V (2001) Perspectives of immobilized-metal affinity chromatography. Journal of Biochemical and Biophysical Methods, 49: 335-360.

Gao AG, Hakimi SM, Mittanck CA, Wu Y, Woerner BM, Stark DM, Shah DM, Liang J, Rommens CMT (2000) Fungal pathogen protection in potato by expression of a plant defensin peptide. Nature Biotechnology, 18: 1307-1310.

García-Olmedo F, Molina A, Alamillo JM, Rodríguez-Palenzuéla P (1998) Plant defense peptides. Peptide Science, 47: 479-491.

Gasparis S, Orczyk W, Nadolska-Orczyk A (2013) *Sina* and *Sinb* genes in triticale do not determine grain hardness contrary to their orthologs *Pina* and *Pinb* in wheat. BMC Plant Biology, 13: 190-201.

Gasparis S, Orczyk W, Zalewski W, Nadolska-Orczyk A (2011) The RNA-mediated silencing of one of the *Pin* genes in allohexaploid wheat simultaneously decreases the expression of the other, and increases grain hardness. Journal of Experimental Botany, 62: 4025-4036.

Gautier MF, Aleman ME, Guirao A, Marion D, Joudrier P (1994) *Triticum aestivum* puroindolines, two basic cystine-rich seed proteins: cDNA sequence analysis and developmental gene expression. Plant Molecular Biology, 25: 43-57.

Gautier MF, Cosson P, Guirao A, Alary R, Joudrier P (2000) Puroindoline genes are highly conserved in diploid ancestor wheats and related species but absent in tetraploid *Triticum* species. Plant Science, 153: 81-91.

Gazza L, Nocente F, Ng PKW, Pogna NE (2005) Genetic and biochemical analysis of common wheat cultivars lacking puroindoline a. Theoretical and Applied Genetics, 110: 470-478.

Gazza L, Zanella L, Pogna N (2008) Development of durum wheat (*Triticum turgidum* ssp durum) lines with soft kernel texture by chromosome engineering In*:* Appels R, Eastwood R, Lagudah E, Langridge P, Mackay M, Mcintyre L and Sharp P (eds.) Proceedings of the 11th International, Wheat Genetics Symposium. Sydney, Australia: Sydney University. pp 339-41.

Gell DA, Grant RP, Mackay JP (2012) The detection and quantitation of protein oligomerzation In: Matthews JM (ed.) Protein Dimerization and Oligomerization in Biology. Springer Science+Business Media, LLC. New York, USA. pp 19-37.

Gelvin SB (2003) Agrobacterium-mediated plant transformation: The biology behind the "gene-jockeying" tool. Microbiology and Molecular Biology Reviews, 67: 16-37.

Giddings G, Allison G, Brooks D, Carter A (2000) Transgenic plants as factories for biopharmaceuticals. Nature Biotechnology, 18: 1151-1155.

Gill BS, Appels R, Botha-Oberholster AM, Buell CR, Bennetzen JL, Chalhoub B, Chumley F, Dvořák J, Iwanaga M, Keller B, Li W, Mccombie WR, Ogihara Y, Quetier F, Sasaki T (2004) A workshop report on wheat genome sequencing: International genome research on wheat consortium. Genetics, 168: 1087-1096.

Gillies SA, Futardo A, Henry RJ (2012) Gene expression in the developing aleurone and starchy endosperm of wheat. Plant Biotechnology Journal, 10: 668-679.

Gils M, Kandzia R, Marillonnet S, Klimyuk V, Gleba Y (2005) High-yield production of authentic human growth hormone using a plant virus-based expression system. Plant Biotechnology Journal, 3: 613-620.

Giritch A, Marillonnet S, Engler C, Van Eldik G, Botterman J, Klimyuk V, Gleba Y (2006) Rapid high-yield expression of full-size IgG antibodies in plants coinfected with noncompeting viral vectros. Proceedings of the National Academy of Sciences of the United States of America, 103: 14701-14706.

Giroux MJ, Kim KH, Hogg AC, Martin JM, Beecher B (2013) The *Puroindoline b-2* variants are expressed at low levels relative to the *Puroindoline D1* genes in wheat seeds. Crop Science, 53: 833-841.

Giroux MJ, Morris CF (1997) A glycine to serine change in puroindoline b is associated with wheat grain hardness and low levels of starch-surface friabilin. Theoretical and Applied Genetics, 95: 857-864.

Giroux MJ, Morris CF (1998) Wheat grain hardness results from highly conserved mutations in the friabilin components puroindoline a and b. Proceedings of the National Academy of Sciences of the United States of America, 95: 6262-6266.

Gleba Y, Giritch A (2012) Vaccines, antibodies, and pharmaceutical proteins. In: Altman A and Hasegawa PM (eds.) Plant Biotechnology and Agriculture. Elsevier Inc, USA. pp 465-479.

Gleba Y, Klimyuk V, Marillonnet S (2005) Magnifection - A new platform for expressing recombinant vaccines in plants. Vaccine, 23: 2042-2048.

Gleba Y, Klimyuk V, Marillonnet S (2007) Viral vectors for the expression of proteins in plants. Current Opinion in Biotechnology, 18: 134-141.

Gleba Y, Marillonnet S, Klimyuk V (2004) Engineering viral expression vectors for plants: The 'full virus' and the 'deconstructed virus' strategies. Current Opinion in Plant Biology, 7: 182-188.

Gleba Y, Tusé D, Giritch A (2014) Plant viral vectors for delivery by *Agrobacterium*. In: Palmer K and Gleba Y (eds.) Current Topics in Microbiology and Immunology; Plant Viral Vectors. Springer, Berlin Heidelberg, Germany. pp 155-192.

Gomord V, Faye L (2004) Posttranslational modification of therapeutic proteins in plants. Current Opinion in Plant Biology, 7: 171-181.

Goodin MM, Zaitlin D, Naidu RA, Lommel SA (2008) *Nicotiana benthamiana*: Its history and future as a model for plant-pathogen interactions. Molecular Plant-Microbe Interactions, 21: 1015-1026.

Goodspeed TH (1954) The genus *Nicotiana*. Journal of the American Pharmaceutical Association, 45: 193-193.

Greenblatt GA, Bettge AD, Morris CF (1995) Relationship between endosperm texture and the occurrence of friabilin and bound polar lipids on wheat starch. Cereal Chemistry, 72: 172-176.

Greenfield NJ (2007) Using circular dichroism spectra to estimate protein secondary structure. Nature Protocols, 1: 2876-2890.

Greenwell P, Schofield J (1986) A starch Granule protein associated with endosperm softness in wheat. Cereal Chemistry, 63: 379-380.

Greenwell P, Stimson W, Mackay E (1992) Durotest-rapid purity control for pasta semolina. Chorleywood Dig, 121: 115-116.

Grefen C, Städele K, Růžička K, Obrdlik P, Harter K, Horák J (2008) Subcellular localization and *in vivo* interactions of the *Arabidopsis thaliana* ethylene receptor family members. Molecular Plant, 1: 308-320.

Haider N (2013) The origin of the B-genome of bread wheat (*Triticum aestivum* L.). Russian Journal of Genetics, 49: 263-274.

Hamada MS, Yin Y, Chen H, Ma Z (2011) The escalating threat of *Rhizoctonia cerealis*, the causal agent of sharp eyespot in wheat. Pest Management Science, 67: 1411-1419.

Hancock REW, Chapple DS (1999) Peptide antibiotics. Antimicrobial Agents and Chemotherapy, 43: 1317-1323.

Haney EF, Petersen AP, Lau CK, Jing W, Storey DG, Vogel HJ (2013) Mechanism of action of puroindoline derived tryptophan-rich antimicrobial peptides. Biochimica et Biophysica Acta - Biomembranes, 1828: 1802-1813.

Hearn MTW, Acosta D (2001) Applications of novel affinity cassette methods: Use of peptide fusion handles for the purification of recombinant proteins. Journal of Molecular Recognition, 14: 323-369.

Hellens R, Allan A, Friel E, Bolitho K, Grafton K, Templeton M, Karunairetnam S, Gleave A, Laing W (2005) Transient expression vectors for functional genomics, quantification of promoter activity and RNA silencing in plants. Plant Methods, 1: 13-27.

Hogg AC, Sripo T, Beecher B, Martin JM, Giroux MJ (2004) Wheat puroindolines interact to form friabilin and control wheat grain hardness. Theoretical and Applied Genetics, 108: 1089-1097.

Horn ME, Woodard SL, Howard JA (2004) Plant molecular farming: Systems and products. Plant Cell Reports, 22: 711-720.

Horton P, Park KJ, Obayashi T, Fujita N, Harada H, Adams-Collier CJ, Nakai K (2007) WoLF PSORT: Protein localization predictor. Nucleic Acids Research, 35: W585-W587.

Hoseney R, Seib P (1973) Structural differences in hard and soft wheat. Bakers Dig, 47 (6): 26.

Howard JA, Hood E (2005) Bioindustrial and biopharmaceutical products produced in plants. Advances in Agronomy, 85: 91-124.

Hu CD, Chinenov Y, Kerppola TK (2002) Visualization of interactions among bZIP and Rel family proteins in living cells using bimolecular fluorescence complementation. Molecular Cell, 9: 789-798.

Hu CD, Kerppola TK (2003) Simultaneous visualization of multiple protein interactions in living cells using multicolor fluorescence complementation analysis. Nature Biotechnology, 21: 539-545.

Huang FC, Studart-Witkowski C, Schwab W (2010) Overexpression of hydroperoxide lyase gene in *Nicotiana benthamiana* using a viral vector system. Plant Biotechnology Journal, 8: 783-795.

Hyunjong B, Lee DS, Hwang I (2006) Dual targeting of xylanase to chloroplasts and peroxisomes as a means to increase protein accumulation in plant cells. Journal of Experimental Botany, 57: 161-169.

Ikeda TM, Cong H, Suzuki T, Takata K (2010) Identification of new *Pina* null mutations among Asian common wheat cultivars. Journal of Cereal Science, 51: 235-237.

Ikeda TM, Ohnishi N, Nagamine T, Oda S, Hisatomi T, Yano H (2005) Identification of new puroindoline genotypes and their relationship to flour texture among wheat cultivars. Journal of Cereal Science, 41: 1-6.

Inoue H, Nojima H, Okayama H (1990) High efficiency transformation of *Escherichia coli* with plasmids. Gene, 96: 23-28.

Issaly N, Solsona O, Joudrier P, Gautier MF, Moulin G, Boze H (2001) Optimization of the wheat puroindoline-a production in *Pichia pastoris*. Journal of Applied Microbiology, 90: 397-406.

Jacob L, Zasloff M (1994) Potential therapeutic applications of magainins and other antimicrobial agents of animal origin. Ciba Foundation symposium, 186: 197-216.

Jasiewicz B, Mrówczyńska L, Malczewska-Jaskóła K (2014) Synthesis and haemolytic activity of novel salts made of nicotine alkaloids and bile acids. Bioorganic and Medicinal Chemistry Letters, 24: 1104-1107.

Jenssen H, Hamill P, Hancock REW (2006) Peptide antimicrobial agents. Clinical Microbiology Reviews, 19: 491-511.

Jerkovic A, Kriegel AM, Bradner JR, Atwell BJ, Roberts TH, Willows RD (2010) Strategic distribution of protective proteins within bran layers of wheat protects the nutrient-rich endosperm. Plant Physiology, 152: 1459-1470.

Jing W, Demcoe AR, Vogel HJ (2003) Conformation of a bactericidal domain of puroindoline a: Structure and mechanism of action of a 13-residue antimicrobial peptide. Journal of Bacteriology, 185: 4938-4947.

Jolly CJ, Glenn GM, Rahman S (1996) GSP-1 genes are linked to the grain hardness locus (*Ha*) on wheat chromosome 5D. Proceedings of the National Academy of Sciences of the United States of America, 93: 2408-2413.

Jolly CJ, Rahman S, Kortt AA, Higgins TJV (1993) Characterisation of the wheat Mr 15000 "grain-softness protein" and analysis of the relationship between its accumulation in the whole seed and grain softness. Theoretical and Applied Genetics, 86: 589-597.

José-Estanyol M, Gomis-Rüth FX, Puigdomènech P (2004) The eight-cysteine motif, a versatile structure in plant proteins. Plant Physiology and Biochemistry, 42: 355-365.

Kerppola TK (2006) Design and implementation of bimolecular fluorescence complementation (BiFC) assays for the visualization of protein interactions in living cells. Nature Protocols, 1: 1278-1286.

Kerppola TK (2008) Bimolecular fluorescence complementation (BiFC) analysis as a probe of protein interactions in living cells. Annual Review of Biophysics, 37: 465-487.

Kerppola TK (2013) Multicolor bimolecular fluorescence complementation (BiFC) analysis of protein interactions with alternative partners. Cold Spring Harbor Protocols, 798-803.

Kim KH, Feiz L, Dyer AT, Grey W, Hogg AC, Martin JM, Giroux MJ (2012a) Increased resistance to *Penicillium* seed rot in transgenic wheat over-expressing puroindolines. Journal of Phytopathology, 160: 243-247.

Kim KH, Feiz L, Martin JM, Giroux MJ (2012b) Puroindolines are associated with decreased polar lipid breakdown during wheat seed development. Journal of Cereal Science, 56: 142-146.

Kitamura S, Inoue M, Shikazono N, Tanaka A (2001) Relationships among *Nicotiana* species revealed by the 5S rDNA spacer sequence and fluorescence in situ hybridization. Theoretical and Applied Genetics, 103: 678-686.

Klimyuk V, Marillonnet S, Knäblein J, Mccaman M, Gleba Y (2008) Production of recombinant proteins in plants. In: Knaeblein J (eds.) Modern Biopharmaceuticals, Wiley-VCH Verlag GmbH & Co, Weinheim, Germany. 3: pp 893-917.

Klimyuk V, Pogue G, Herz S, Butler J, Haydon H (2014) Production of recombinant antigens and antibodies in *Nicotiana benthamiana* using 'Magnifection' technology: GMP-compliant facilities for small- and large-scale manufacturing. In: Palmer K and Gleba Y (eds.) Current Topics in Microbiology and Immunology; Plant Viral Vectors. Springer, Berlin Heidelberg, Germany. pp 127-154.

Knapp S, Chase MW, Clarkson JJ (2004) Nomenclatural changes and a new sectional classification in *Nicotiana* (Solanaceae). Taxon, 53: 73-82.

Konopka I, Kozirok W, Tańska M (2005) Wheat endosperm hardness. Part I. Relationships to colour of kernel cross-section. European Food Research and Technology, 220: 11-19.

Kooijman M, Orsel R, Hamer RJ, Bekkers ACaPA (1998) The insertion behaviour of wheat puroindoline-a into diacylgalactosylglycerol films. Journal of Cereal Science, 28: 43-51.

Kooijman M, Orsel R, Hessing M, Hamer RJ, Bekkers ACaPA (1997) Spectroscopic characterisation of the lipid-binding properties of wheat puroindolines. Journal of Cereal Science, 26: 145-159.

Krishnamurthy K, Balconi C, Sherwood JE, Giroux MJ (2001) Wheat puroindolines enhance fungal disease resistance in transgenic rice. Molecular Plant-Microbe Interactions, 14: 1255-1260.

Krishnamurthy K, Giroux MJ (2001) Expression of wheat puroindoline genes in transgenic rice enhances grain softness. Nature Biotechnology, 19: 162-166.

Krishnan HB, Natarajan SS (2009) A rapid method for depletion of Rubisco from soybean (Glycine max) leaf for proteomic analysis of lower abundance proteins. Phytochemistry, 70: 1958-1964.

Lalonde S, Ehrhardt DW, Frommer WB (2005) Shining light on signaling and metabolic networks by genetically encoded biosensors. Current Opinion in Plant Biology, 8: 574-581.

Law C, Young C, Brown J, Snape J, Worland A. (1978) The study of grain protein control in wheat using whole chromosome substitution lines. Seed protein improvement by nuclear techniques, Conference Vienna, Austria. International Atomic Energy Agency. pp 483-502.

Le Bihan T, Blochet JÉ, Désormeaux A, Marion D, Pézolet M (1996) Determination of the secondary structure and conformation of puroindolines by infrared and Raman spectroscopy. Biochemistry, 35: 12712-12722.

Le Guernevé C, Seigneuret M, Marion D (1998) Interaction of the wheat endosperm lipid-binding protein puroindoline-a with phospholipids. Archives of Biochemistry and Biophysics, 360: 179-186.

Leckie BM, Stewart J, C. N. (2011) Agroinfiltration as a technique for rapid assays for evaluating candidate insect resistance transgenes in plants. Plant Cell Reports, 30: 325-334.

Lee LY, Gelvin SB (2008) T-DNA binary vectors and systems. Plant Physiology, 146: 325-332.

Lee S-H, Kim S-J, Lee Y-S, Song M-D, Kim I-H, Won H-S (2011a) De novo generation of short antimicrobial peptides with simple amino acid composition. Regulatory Peptides, 166: 36-41.

Lee S, Li B, Jin S, Daniell H (2011b) Expression and characterization of antimicrobial peptides Retrocyclin-101 and Protegrin-1 in chloroplasts to control viral and bacterial infections. Plant Biotechnology Journal, 9: 100-115.

Lesage VS, Bouchet B, Rhazi L, Elmorjani K, Branlard G, Marion D (2011) New insight into puroindoline function inferred from their subcellular localization in developing hard and soft near-isogenic endosperm and their relationship with polymer size of storage proteins. Journal of Cereal Science, 53: 231-238.

Lesk AM (2010) Introduction to Protein Science: Architecture, Function, and Genomics., Oxford University Press New York, ISBN: 9780199541300.

Leuzinger K, Dent M, Hurtado J, Stahnke J, Lai H, Zhou X, Chen Q (2013) Efficient agroinfiltration of plants for high-level transient expression of recombinant proteins. Journal of Visualized Experiments, 77: 50521.

Lewis R (2011) *Nicotiana*. In: Kole C (ed.) Wild Crop Relatives: Genomic and Breeding Resources. Springer Berlin Heidelberg, Germany. pp 185-208.

Li G, He Z, Lillemo M, Sun Q, Xia X (2008) Molecular characterization of allelic variations at *Pina* and *Pinb* loci in Shandong wheat landraces, historical and current cultivars. Journal of Cereal Science, 47: 510-517.

Li G, He Z, Peña RJ, Xia X, Lillemo M, Sun Q (2006) Identification of novel secaloindoline-a and secaloindoline-b alleles in CIMMYT hexaploid triticale lines. Journal of Cereal Science, 43: 378-386.

Li Y, Geng Y, Song H, Zheng G, Huan L, Qiu B (2004) Expression of a human lactoferrin N-lobe in *Nicotiana benthmiana* with potato virus X-based agroinfection. Biotechnology letters, 26: 953-957.

Li Y, Mao X, Wang Q, Zhang J, Li X, Ma F, Sun F, Chang J, Chen M, Wang Y, Li K, Yang G, He G (2014) Overexpression of *Puroindoline a* gene in transgenic durum wheat (*Triticum turgidum* ssp. *durum*) leads to a medium-hard kernel texture. Molecular Breeding, 33: 545-554.

Li Y, Wang Q, Li X, Xiao X, Sun F, Wang C, Hu W, Feng Z, Chang J, Chen M, Wang Y, Li K, Yang G, He G (2012a) Coexpression of the high molecular weight glutenin subunit 1Ax1 and puroindoline improves dough mixing properties in Durum Wheat (*Triticum turgidum* L. ssp. durum). PLoS ONE, 7.

Li Y, Xiang Q, Zhang Q, Huang Y, Su Z (2012b) Overview on the recent study of antimicrobial peptides: Origins, functions, relative mechanisms and application. Peptides, 37: 207-215.

Lillemo M, Chen F, Xia X, William M, Peña RJ, Trethowan R, He Z (2006) Puroindoline grain hardness alleles in CIMMYT bread wheat germplasm. Journal of Cereal Science, 44: 86-92.

Lillemo M, Morris CF (2000) A leucine to proline mutation in puroindoline B is frequently present in hard wheats from Northern Europe. Theoretical and Applied Genetics, 100: 1100-1107.

Ling HY, Pelosi A, Walmsley AM (2010) Current status of plant-made vaccines for veterinary purposes. Expert Review of Vaccines, 9: 971-982.

Listwan P, Martin JL, Kobe B, Cowieson NP (2004) Methods for high-throughput protein expression, purification and structure determination adapted for structural genomics. Australian Biochemist, 35: 43-46.

Los GV, Encell LP, Mcdougall MG, Hartzell DD, Karassina N, Zimprich C, Wood MG, Learish R, Ohana RF, Urh M, Simpson D, Mendez J, Zimmerman K, Otto P, Vidugiris G, Zhu J, Darzins A, Klaubert DH, Bulleit RF, Wood KV (2008) HaloTag: A novel protein labeling technology for cell imaging and protein analysis. ACS Chemical Biology, 3: 373-382.

Ludevid D, Torrent M, Lasserre-Ramassamy S (2005) Production of peptides and proteins by accumulation in plant endoplasmic reticulumderived protein bodies. Patent EP1523558.

Luo L, Zhang J, Yang G, Li Y, Li K, He G (2008) Expression of puroindoline a enhances leaf rust resistance in transgenic tetraploid wheat. Molecular Biology Reports, 35: 195-200.

Luo Y, Zhang DD, Dong XW, Zhao PB, Chen LL, Song XY, Wang XJ, Chen XL, Shi M, Zhang YZ (2010) Antimicrobial peptaibols induce defense responses and systemic resistance in tobacco against tobacco mosaic virus. FEMS Microbiology Letters, 313: 120-126.

Ma JKC, Barros E, Bock R, Christou P, Dale PJ, Dix PJ, Fischer R, Irwin J, Mahoney R, Pezzotti M, Schillberg S, Sparrow P, Stoger E, Twyman RM (2005) Molecular farming for new drugs and vaccines. Current perspectives on the production of pharmaceuticals in transgenic plants. EMBO Reports, 6: 593-599.

Ma JKC, Drake PMW, Christou P (2003) The production of recombinant pharmaceutical proteins in plants. Nature Reviews Genetics, 4: 794-805.

Ma JKC, Hiatt A, Hein M, Vine ND, Wang F, Stabila P, Van Dolleweerd C, Mostov K, Lehner T (1995) Generation and assembly of secretory antibodies in plants. Science, 268: 716-719.

Ma JKC, Hikmat BY, Wycoff K, Vine ND, Chargelegue D, Yu L, Hein MB, Lehner T (1998) Characterization of a recombinant plant monoclonal secretory antibody and preventive immunotherapy in humans. Nature Medicine, 4: 601-606.

Magliery TJ, Regan L (2006) Reassembled GFP: Detecting protein-protein interactions and protein expression patterns. In: Chalfie M and Kain S (eds.) Green Fluorescent Protein: Properties, Applications, and Protocols. John Wiley & Sons, Inc. Toronto, Canada. pp 391-405.

Mainieri D, Rossi M, Archinti M, Bellucci M, De Marchis F, Vavassori S, Pompa A, Arcioni S, Vitale A (2004) Zeolin. A new recombinant storage protein constructed using maize γ-zein and bean phaseolin. Plant Physiology, 136: 3447-3456.

Marianayagam NJ, Sunde M, Matthews JM (2004) The power of two: Protein dimerization in biology. Trends in Biochemical Sciences, 29: 618-625.

Marillonnet S, Giritch A, Gils M, Kandzia R, Klimyuk V, Gleba Y (2004) *In planta* engineering of viral RNA replicons: Efficient assembly by recombination of DNA modules delivered by *Agrobacterium*. Proceedings of the National Academy of Sciences of the United States of America, 101: 6852-6857.

Marillonnet S, Thoeringer C, Kandzia R, Klimyuk V, Gleba Y (2005) Systemic *Agrobacterium tumefaciens*-mediated transfection of viral replicons for efficient transient expression in plants. Nature Biotechnology, 23: 718-723.

Marion D, Bakan B, Elmorjani K (2007) Plant lipid binding proteins: Properties and applications. Biotechnology Advances, 25: 195-197.

Marion D, Gautier MF, Joudrier P, Ptak M, Pezolet M, Forest E, Clark DC, Broekaert W (1994) Structure and function of wheat lipid binding proteins. In: Wheat kernel proteins: molecular and functional aspects. Universitá Degli Studi Della. Tuscia - Consiglio Nazionale Delle Ricerche, Viterbo. pp 175-180.

Martin JM, Frohberg RC, Morris CF, Talbert LE, Giroux MJ (2001) Milling and bread baking traits associated with puroindoline sequence type in hard red spring wheat. Crop Science, 41: 228-234.

Martin JM, Meyer FD, Smidansky ED, Wanjugi H, Blechl AE, Giroux MJ (2006) Complementation of the pina (null) allele with the wild type Pina sequence restores a soft phenotype in transgenic wheat. Theoretical and Applied Genetics, 113: 1563-1570.

Marusic C, Nuttall J, Buriani G, Lico C, Lombardi R, Baschieri S, Benvenuto E, Frigerio L (2007) Expression, intracellular targeting and purification of HIV Nef variants in tobacco cells. BMC Biotechnology, 7: 1-12.

Massa AN, Morris CF, Gill BS (2004) Sequence diversity of Puroindoline-a, Puroindoline-b, and the grain softness protein genes in *Aegilops tauschii* Coss. Crop Science, 44: 1808-1816.

Matsuoka Y (2011) Evolution of polyploid *Triticum* Wheats under cultivation: the role of domestication, natural hybridization and allopolyploid speciation in their diversification. Plant and Cell Physiology, 52: 750-64.

Mattanovich D, Rüker F, Da Cämara Machado A, Laimer M, Regner F, Steinkeliner H, Himmler G, Katinger H (1989) Efficient transformation of *Agrobacterium* spp. by eletroporation. Nucleic Acids Research, 17: 6747.

Mattern P, Morris R, Schmidt J, Johnson V. (1973) Location of genes for kernel properties in the wheat variety 'Cheyenne' using chromosome substitution lines. the 4th International Wheat Genetics Symposium, Conference Columbia. pp 703-708.

Melnik S, Stoger E (2013) Green factories for biopharmaceuticals. Current Medicinal Chemistry, 20: 1038-1046.

Melo MN, Ferre R, Castanho MaRB (2009) Antimicrobial peptides: Linking partition, activity and high membrane-bound concentrations. Nature Reviews Microbiology, 7: 245-250.

Mett V, Farrance CE, Green BJ, Yusibov V (2008) Plants as biofactories. Biologicals, 36: 354-358.

Miao Y, Chen L, Wang C, Wang Y, Zheng Q, Gao C, Yang G, He G (2012) Expression, purification and antimicrobial activity of puroindoline A protein and its mutants. Amino Acids, 43: 1689-1696.

Michaud D, Vrain T, Gomord V, Faye L (1998) Stability of recombinant proteins in plants. In: Cunningham C and Porter AR (eds.) Recombinant Proteins from Plants. Humana Press. New York, USA. pp 177-188.

Mikulíková D (2007) The effect of friabilin on wheat grain hardness. Czech Journal of Genetics and Plant Breeding, 43: 35-43.

Mohammadi M, Zaidi MA, Ochalski A, Tanchak M, Altosaar I (2007) Immunodetection and immunolocalization of tryptophanins in oat (*Avena sativa* L.) seeds. Plant Science, 172: 579-587.

Morell M, Espargaro A, Aviles FX, Ventura S (2008) Study and selection of *in vivo* protein interactions by coupling bimolecular fluorescence complementation and flow cytometry. Nature Protocols, 3: 22-33.

Morell M, Espargaró A, Avilés FX, Ventura S (2007) Detection of transient protein-protein interactions by bimolecular fluorescence complementation: The Abl-SH3 case. Proteomics, 7: 1023-1036.

Morris CF (2002) Puroindolines: the molecular genetic basis of wheat grain hardness. Plant Molecular Biology, 48: 633-647.

Morris CF, Greenblatt GA, Bettge AD, Malkawi HI (1994) Isolation and characterization of multiple forms of friabilin. Journal of Cereal Science, 20: 167-174.

Morris CF, Lillemo M, Simeone MC, Giroux MJ, Babb SL, Kidwell KK (2001) Prevalence of puroindoline grain hardness genotypes among historically significant North American spring and winter wheats. Crop Science, 41: 218-228.

Morris CF, Simeone MC, King GE, Lafiandra D (2011) Transfer of soft kernel texture from *Triticum aestivum* to durum wheat, *Triticum turgidum* ssp. durum. Crop Science, 51: 114-122.

Morrison WR, Greenwell P, Law CN, Sulaiman BD (1992) Occurrence of friabilin, a low molecular weight protein associated with grain softness, on starch granules isolated from some wheats and related species. Journal of Cereal Science, 15: 143-149.

Mukherjee S, Zhang Y (2011) Protein-protein complex structure predictions by multimeric threading and template recombination. Structure, 19: 955-966.

Munro S, Pelham HRB (1987) A C-terminal signal prevents secretion of luminal ER proteins. Cell, 48: 899-907.

Nadai M, Bally J, Vitel M, Job C, Tissot G, Botterman J, Dubald M (2009) High-level expression of active human alpha1-antitrypsin in transgenic tobacco chloroplasts. Transgenic Research, 18: 173-183.

Nadolska-Orczyk A, Gasparis S, Orczyk W (2009) The determinants of grain texture in cereals. Journal of Applied Genetics, 50: 185-197.

Nagpal S, Gupta V, Kaur KJ, Salunke DM (1999) Structure-function analysis of tritrypticin, an antibacterial peptide of innate immune origin. Journal of Biological Chemistry, 274: 23296-23304.

Naureen F, Humaira B, Viqar S, Ara J, Ehteshamul-Haque S (2009) Prevalance of post-harvest rot of vegetables and fruits in Karachi, Pakistan. Pakistan Journal of Botany, 41: 3185-3190.

Nawrot R, Barylski J, Nowicki G, Broniarczyk J, Buchwald W, Goździcka-Józefiak A (2014) Plant antimicrobial peptides. Folia Microbiologica, 59: 181-196.

Nebenfuhr A, Frohlick JA, Staehelin LA (2000) Redistribution of Golgi stacks and other organelles during mitosis and cytokinesis in plant cells. Plant Physiology, 124: 135-151.

Oda S, Schofield JD (1997) Characterisation of friabilin polypeptides. Journal of Cereal Science, 26: 29-36.

Odintsova TI, Vassilevski AA, Slavokhotova AA, Musolyamov AK, Finkina EI, Khadeeva NV, Rogozhin EA, Korostyleva TV, Pukhalsky VA, Grishin EV, Egorov TA (2009) A novel antifungal hevein-type peptide from *Triticum kiharae* seeds with a unique 10-cysteine motif. FEBS Journal, 276: 4266-4275.

Oey M, Lohse M, Scharff LB, Kreikemeyer B, Bock R (2009) Plastid production of protein antibiotics against pneumonia via a new strategy for high-level expression of antimicrobial proteins. Proceedings of the National Academy of Sciences of the United States of America, 106: 6579-6584.

Ohad N, Shichrur K, Yalovsky S (2007) The analysis of protein-protein interactions in plants by bimolecular fluorescence complementation. Plant Physiology, 145: 1090-1099.

Ormö M, Cubitt AB, Kallio K, Gross LA, Tsien RY, Remington SJ (1996) Crystal structure of the *Aequorea victoria* green fluorescent protein. Science, 273: 1392-1395.

Painter J, Rah JH, Lee YK (2002) Comparison of international food guide pictorial representations. Journal of the American Dietetic Association, 102: 483-489.

Palumbo D, Iannaccone M, Porta A, Capparelli R (2010) Experimental antibacterial therapy with puroindolines, lactoferrin and lysozyme in Listeria monocytogenes-infected mice. Microbes and Infection, 12: 538-545.

Pan Z, Song W, Meng F (2004) Characterization of genes encoding wheat grain hardness from Chinese cultivar Gaocheng 8901. Cereal Chemistry, 82: 38-43.

Parachin NS, Mulder KC, Viana AaB, Dias SC, Franco OL (2012) Expression systems for heterologous production of antimicrobial peptides. Peptides, 38: 446-456.

Patiño-Rodríguez O, Ortega-Berlanga B, Llamas-González YY, Flores-Valdez MA, Herrera-Díaz A, Montes-De-Oca-Luna R, Korban SS, Alpuche-Solís ÁG (2013) Transient expression and characterization of the antimicrobial peptide protegrin-1 in *Nicotiana tabacum* for control of bacterial and fungal mammalian pathogens. Plant Cell, Tissue and Organ Culture, 115: 99-106.

Pauly A, Pareyt B, Fierens E, Delcour JA (2013) Wheat (*Triticum aestivum* L. and *T. turgidum* L. ssp. durum) Kernel Hardness: I. Current view on the role of puroindolines and polar lipids. Comprehensive Reviews in Food Science and Food Safety, 12: 413-426.

Peña RJ, Trethowan R, Pfeiffer WH, Van Ginkel M (2002) Quality (end-use) improvement in wheat: Compositional, genetic, and environmental factors. Journal of Crop Production, 5: 1-37.

Phillips RL, Palombo EA, Panozzo JF, Bhave M (2011) Puroindolines, Pin alleles, hordoindolines and grain softness proteins are sources of bactericidal and fungicidal peptides. Journal of Cereal Science, 53: 112-117.

Pickering PA, Bhave M (2007) Comprehensive analysis of Australian hard wheat cultivars shows limited puroindoline allele diversity. Plant Science, 172: 371-379.

Pogue GP, Lindbo JA, Garger SJ, Fitzmaurice WP (2002) Making an ally from an enemy: Plant virology and the new agriculture. Annual Review of Phytopatology, 40: 45-74.

Portieles R, Ayra C, Gonzalez E, Gallo A, Rodriguez R, Chacón O, López Y, Rodriguez M, Castillo J, Pujol M, Enriquez G, Borroto C, Trujillo L, Thomma BPHJ, Borrás-Hidalgo O (2010) *NmDef02*, a novel antimicrobial gene isolated from *Nicotiana megalosiphon* confers high-level pathogen resistance under greenhouse and field conditions. Plant Biotechnology Journal, 8: 678-690.

Prasher DC, Eckenrode VK, Ward WW, Prendergast FG, Cormier MJ (1992) Primary structure of the *Aequorea victoria* green-fluorescent protein. Gene, 111: 229-233.

Ragupathy R, Cloutier S (2008) Genome organisation and retrotransposon driven molecular evolution of the endosperm *Hardness* (*Ha*) locus in *Triticum aestivum* cv Glenlea. Molecular Genetics and Genomics, 280: 467-481.

Rahman S, Jolly CJ, Skerritt JH, Wallosheck A (1994) Cloning of a wheat 15-kDa grain softness protein (GSP). GSP is a mixture of puroindoline-like polypeptides. European Journal of Biochemistry, 223: 917-925.

Rakszegi M, Wilkinson MD, Tosi P, Lovegrove A, Kovacs G, Bedo Z, Shewry PR (2009) Puroindoline genes and proteins in tetraploid and hexaploid species of *Triticum*. Journal of Cereal Science, 49: 202-211.

Ram S, Jain N, Shoran J, Singh R (2005) New frame shift mutation in puroindoline B in Indian wheat cultivars Hyb65 and Nl5439. Journal of Plant Biochemistry and Biotechnology, 14: 45-48.

Ramalingam A, Palombo EA, Bhave M (2012) The *Pinb-2* genes in wheat comprise a multigene family with great sequence diversity and important variants. Journal of Cereal Science, 56: 171-180.

Rao AQ, Bakhsh A, Kiani S, Shahzad K, Shahid AA, Husnain T, Riazuddin S (2009) The myth of plant transformation. Biotechnology Advances, 27: 753-763.

Rochelle JC (2001) Bread for the wilderness: Baking as spiritual craft, Xulon Press, ISBN: 9781931232524.

Roy A, Kucukural A, Zhang Y (2010) I-TASSER: a unified platform for automated protein structure and function prediction. Nature Protocols, 5: 725-738.

Rubio-Infante N, Govea-Alonso DO, Alpuche-Solís AG, García-Hernández AL, Soria-Guerra RE, Paz-Maldonado LMT, Ilhuicatzi-Alvarado D, Varona-Santos JT, Verdín-Terán L, Korban SS, Moreno-Fierros L, Rosales-Mendoza S (2012) A chloroplast-derived C4V3 polypeptide from the human immunodeficiency virus (HIV) is orally immunogenic in mice. Plant Molecular Biology, 78: 337-349.

Ruhlman T, Ahangari R, Devine A, Samsam M, Daniell H (2007) Expression of cholera toxin B-proinsulin fusion protein in lettuce and tobacco chloroplasts - Oral administration protects against development of insulitis in non-obese diabetic mice. Plant Biotechnology Journal, 5: 495-510.

Rybicki EP (2009) Plant-produced vaccines: promise and reality. Drug Discovery Today, 14: 16-24.

Saitoh H, Kiba A, Nishihara M, Yamamura S, Suzuki K, Terauchi R (2001) Production of antimicrobial defensin in *Nicotiana benthamiana* with a potato virus X vector. Molecular Plant-Microbe Interactions, 14: 111-115.

Samarkina ON, Popova AG, Gvozdik EY, Chkalina AV, Zvyagin IV, Rylova YV, Rudenko NV, Lusta KA, Kelmanson IV, Gorokhovatsky AY, Vinokurov LM (2009) Universal and rapid method for purification of GFP-like proteins by the ethanol extraction. Protein Expression and Purification, 65: 108-113.

Sambrook J, Russell DW (2001) Molecular cloning: a laboratory manual (3rd ed) Cold Spring Harbor Laboratory Press N.Y, ISBN: 10 0-87969-577-3.

Sanders MR, Clifton LA, Neylon C, Frazier RA, Green RJ (2013) Selected wheat seed defense proteins exhibit competitive binding to model microbial lipid interfaces. Journal of Agricultural and Food Chemistry, 61: 6890-6900.

Santi L, Batchelor L, Huang Z, Hjelm B, Kilbourne J, Arntzen CJ, Chen Q, Mason HS (2008) An efficient plant viral expression system generating orally immunogenic Norwalk virus-like particles. Vaccine, 26: 1846-1854.

Santi L, Giritch A, Roy CJ, Marillonnet S, Klimyuk V, Gleba Y, Webb R, Arntzen CJ, Mason HS (2006) Protection conferred by recombinant Yersinia pestis antigens produced by a rapid and highly scalable plant expression system. Proceedings of the National Academy of Sciences of the United States of America, 103: 861-866.

Sanz-Barrio R, Millán AFS, Corral-Martínez P, Seguí-Simarro JM, Farran I (2011) Tobacco plastidial thioredoxins as modulators of recombinant protein production in transgenic chloroplasts. Plant Biotechnology Journal, 9: 639-650.

Sathish K, Sriraman R, Subramanian BM, Rao NH, Balaji K, Narasu ML, Srinivasan VA (2011) Plant expressed EtMIC2 is an effective immunogen in conferring protection against chicken coccidiosis. Vaccine, 29: 9201-9208.

Sawasaki T, Ogasawara T, Morishita R, Endo Y (2002) A cell-free protein synthesis system for high-throughput proteomics. Proceedings of the National Academy of Sciences of the United States of America, 99: 14652-14657.

Scheller J, Conrad U (2004) Production of spider silk proteins in transgenic tobacco and potato. In: Fischer R and Schillberg S (eds.) Molecular Farming. Wiley-VCH Verlag GmbH & Co. KGaA,Weinheim, Germany. pp 171-181.

Schibli DJ, Epand RF, Vogel HJ, Epand RM (2002) Tryptophan-rich antimicrobial peptides: Comparative properties and membrane interactions. Biochemistry and Cell Biology, 80: 667-677.

Schiermeyer A, Dorfmüller S, Schinke H (2004) Production of pharmaceutical proteins in plants and plant cell suspension cultures. In: Fischer R and Stefan S (eds.) Molecular Farming. Wiley-VCH Verlag GmbH & Co. KGaA,Weinheim, Germany. pp 91-112.

Schiffer M, Chang CH, Stevens FJ (1992) The functions of tryptophan residues in membrane proteins. Protein Engineering, 5: 213-214.

Schmidt FR (2004) Recombinant expression systems in the pharmaceutical industry. Applied Microbiology and Biotechnology, 65: 363-372.

Scholthof HB, Scholthof KBG, Jackson AO (1996) Plant virus gene vectors for transient expression of foreign proteins in plants. Annual Review of Phytopatology, 34: 299-323.

Schütze K, Harter K, Chaban C (2009) Bimolecular fluorescence complementation (BiFC) to study protein-protein interactions in living plant cells. Methods in Molecular Biology, 479: 189-202.

Scopes RK (1993) Protein Purification: Principles and Practice, Springer New York, ISBN: 978-1-4419-2833-7.

Seelig J (2004) Thermodynamics of lipid-peptide interactions. Biochimica et Biophysica Acta - Biomembranes, 1666: 40-50.

Shai Y (2002) Mode of action of membrane active antimicrobial peptides. Biopolymers - Peptide Science Section, 66: 236-248.

Sharma KK, Bhatnagar-Mathur P, Thorpe TA (2005) Genetic transformation technology: Status and problems. In Vitro Cellular and Developmental Biology - Plant, 41: 102-112.

Shevchenko A, Tomas H, Havliš J, Olsen JV, Mann M (2007) In-gel digestion for mass spectrometric characterization of proteins and proteomes. Nature Protocols, 1: 2856-2860.

Shewry PR (2009) Wheat. Journal of Experimental Botany, 60: 1537-1553.

Shewry PR (2013) Improving grain quality: Wheat. In: Becraft PW (ed.) Seed Genomics. John Wiley & Sons, Inc. Toronto, Canada. pp 159-178.

Shimomura O, Johnson FH, Saiga Y (1962) Extraction, purification and properties of Aequorin, a bioluminescent protein from the Luminous Hydromedusan, *Aequorea*. Journal of Cellular and Comparative Physiology, 59: 223-239.

Silva ON, Mulder KCL, Barbosa AEaD, Otero-Gonzalez AJ, Lopez-Abarrategui C, Rezende TMB, Dias SC, Franco OL (2011) Exploring the pharmacological potential of promiscuous host-defense peptides: From natural screenings to biotechnological applications. Frontiers in Microbiology, 2: 1-14.

Simeone MC, Lafiandra D (2005) Isolation and characterisation of friabilin genes in rye. Journal of Cereal Science, 41: 115-122.

Simmonds D, Barlow K, Wrigley C (1973) Biochemical basis of grain hardness in wheat. Cereal Chemistry, 50: 553-562.

Skosyrev VS, Rudenko NV, Yakhnin AV, Zagranichny VE, Popova LI, Zakharov MV, Gorokhovatsky AY, Vinokurov LM (2003) EGFP as a fusion partner for the expression and organic extraction of small polypeptides. Protein Expression and Purification, 27: 55-62.

Slavin J (2003) Why whole grains are protective: Biological mechanisms. Proceedings of the Nutrition Society, 62: 129-134.

Smyth DR, Mrozkiewicz MK, Mcgrath WJ, Listwan P, Kobe B (2003) Crystal structures of fusion proteins with large-affinity tags. Protein Science, 12: 1313-1322.

Sorrentino A, Iannaccone M, Palumbo D, Capparelli R, Porta R, Mariniello L (2009) Tobacco (*Nicotiana tabacum* cv. Bright Yellow 2) cells as an effective bioreactor for the production of puroindolines. Biotechnology and Applied Biochemistry, 53: 193-199.

Stoger E, Sack M, Nicholson L, Fischer R, Christou P (2005) Recent progress in plantibody technology. Current Pharmaceutical Design, 11: 2439-2457.

Stulemeijer IJE, Joosten MHJ (2008) Post-translational modification of host proteins in pathogen-triggered defence signalling in plants. Molecular Plant Pathology, 9: 545-560.

Swan CG, Bowman JGP, Martin JM, Giroux MJ (2006a) Increased puroindoline levels slow ruminal digestion of wheat (*Triticum aestivum* L.) starch by cattle. Journal of Animal Science, 84: 641-650.

Swan CG, Meyer FD, Hogg AC, Martin JM, Giroux MJ (2006b) Puroindoline B limits binding of puroindoline A to starch and grain softness. Crop Science, 46: 1656-1665.

Symes KJ (1965) The inheritance of grain hardness in wheat as measured by the particle size index. Australian Journal of Agricultural Research, 16: 113-123.

Symes KJ (1969) Influence of a gene causing hardness on the milling and baking quality of two wheats. Australian Journal of Agricultural Research, 20: 971-979.

Taheri P, Tarighi S (2011) Cytomolecular aspects of rice sheath blight caused by *Rhizoctonia solani*. European Journal of Plant Pathology, 129: 511-528.

Tanaka H, Morris CF, Haruna M, Tsujimoto H (2008) Prevalence of puroindoline alleles in wheat varieties from eastern Asia including the discovery of a new SNP in puroindoline b. Plant Genetic Resources: Characterisation and Utilisation, 6: 142-152.

Terpe K (2003) Overview of tag protein fusions: From molecular and biochemical fundamentals to commercial systems. Applied Microbiology and Biotechnology, 60: 523-533.

Terras FRG, Eggermont K, Kovaleva V, Raikhel NV, Osborn RW, Kester A, Rees SB, Torrekens S, Van Leuven F, Vanderleyden J, Cammue BPA, Broekaert WF (1995) Small cysteine-rich antifungal proteins from radish: Their role in host defense. The Plant Cell, 7: 573-588.

Thomas DR, Penney CA, Majumder A, Walmsley AM (2011) Evolution of plant-made pharmaceuticals. International Journal of Molecular Sciences, 12: 3220-3236.

Tranquilli G, Heaton J, Chicaiza O, Dubcovsky J (2002) Substitutions and deletions of genes related to grain hardness in wheat and their effect on grain texture. Crop Science, 42: 1812-1817.

Tremblay R, Feng M, Menassa R, Huner NPA, Jevnikar AM, Ma S (2011) High-yield expression of recombinant soybean agglutinin in plants using transient and stable systems. Transgenic Research, 20: 345-356.

Turnbull KM, Rahman S (2002) Endosperm texture in wheat. Journal of Cereal Science, 36: 327-337.

Turnbull KM, Turner M, Mukai Y, Yamamoto M, Morell MK, Rahman S, Appels R (2003) The organization of genes tightly linked to the *Ha* locus in *Aegilops tauschii*, the D-genome donor to wheat. Genome, 46: 330-338.

Twyman RM (2004) Host plants, systems and expression strategies for molecular farming. In: Fischer R and Schillberg S (eds.) Molecular Farming. Wiley-VCH Verlag GmbH & Co. KGaA,Weinheim, Germany. pp 191-216.

Twyman RM, Stoger E, Schillberg S, Christou P, Fischer R (2003) Molecular farming in plants: Host systems and expression technology. Trends in Biotechnology, 21: 570-578.

Vaghchhipawala Z, Rojas CM, Senthil-Kumar M, Mysore KS (2011) Agroinoculation and agroinfiltration: simple tools for complex gene function analyses. Methods in Molecular Biology. 678: 65-76.

Ventura S (2011) Bimolecular fluorescence complementation: illuminating cellular protein interactions. Current Molecular Medicine, 11: 582-598.

Vitale A, Pedrazzini E (2005) Recombinant pharmaceuticals from plants: The plant endomembrane system as bioreactor. Molecular Interventions, 5: 216-225.

Voinnet O, Rivas S, Mestre P, Baulcombe D (2003) An enhanced transient expression system in plants based on suppression of gene silencing by the p19 protein of tomato bushy stunt virus. The Plant Journal, 33: 949-956.

Waadt R, Schlücking K, Schroeder JI, Kudla J (2014) Protein fragment bimolecular fluorescence complementation analyses for the *in vivo* study of protein-protein interactions and cellular protein complex localizations. In: Jose J. Sanchez-Serrano and Julio Salinas (eds.) Arabidopsis Protocols, Methods in Molecular Biology. Springer Science, New York, USA. pp 629-658.

Waadt R, Schmidt LK, Lohse M, Hashimoto K, Bock R, Kudla J (2008) Multicolor bimolecular fluorescence complementation reveals simultaneous formation of alternative CBL/CIPK complexes *in planta*. The Plant Journal, 56: 505-516.

Wada N, Kajiyama S, Cartagena JA, Lin L, Akiyama Y, Otani M, Suzuki G, Mukai Y, Aoki N, Fukui K (2010) The effects of puroindoline b on the ultrastructure of endosperm cells and physicochemical properties of transgenic rice plant. Journal of Cereal Science, 51: 182-188.

Wall ML, Wheeler HL, Huebsch MP, Smith JC, Figeys D, Altosaar I (2010) The tryptophan-rich domain of puroindoline is directly associated with the starch granule surface as judged by tryptic shaving and mass spectrometry. Journal of Cereal Science, 52: 115-120.

Walter M, Chaban C, Schütze K, Batistic O, Weckermann K, Näke C, Blazevic D, Grafen C, Schumacher K, Oecking C, Harter K, Kudla J (2004) Visualization of protein interactions in living plant cells using bimolecular fluorescence complementation. The Plant Journal, 40: 428-438.

Wandelt CI, Khan MRI, Craig S, Schroeder HE, Spencer D, Higgins TJV (1992) Vicilin with carboxy-terminal KDEL is retained in the endoplasmic reticulum and accumulates to high levels in the leaves of transgenic plants. The Plant Journal, 2: 181-192.

Wang L, Webster DE, Campbell AE, Dry IB, Wesselingh SL, Coppel RL (2008) Immunogenicity of *Plasmodium yoelii* merozoite surface protein 4/5 produced in transgenic plants. International Journal for Parasitology, 38: 103-110.

Wang S, Hazelrigg T (1994) Implications for bcd mRNA localization from spatial distribution of exu protein in Drosophila oogenesis. Nature, 369: 400-403.

Wanjugi HW, Hogg AC, Martin JM, Giroux MJ (2007) The role of puroindoline A and B individually and in combination on grain hardness and starch association. Crop Science, 47: 67-76.

Ward TH (2006) The uses of green fluorescent protein in mammalian cells. In: Chalfie M and Kain SR (eds.) Green Fluorescent Protein: Properties, Applications, and Protocols. Second ed. John Wiley & Sons, Inc. Toronto, Canada. pp 305-337.

Waugh DS (2005) Making the most of affinity tags. Trends in Biotechnology, 23: 316-320.

Webster DE, Thomas MC (2012) Post-translational modification of plant-made foreign proteins; glycosylation and beyond. Biotechnology Advances, 30: 410-418.

Webster DE, Wang L, Mulcair M, Ma C, Santi L, Mason HS, Wesselingh SL, Coppel RL (2009) Production and characterization of an orally immunogenic *Plasmodium* antigen in plants using a virus-based expression system. Plant Biotechnology Journal, 7: 846-855.

Werner S, Breus O, Symonenko Y, Marillonnet S, Gleba Y (2011) High-level recombinant protein expression in transgenic plants by using a double-inducible viral vector. Proceedings of the National Academy of Sciences of the United States of America, 108: 14061-14066.

Wiegand I, Hilpert K, Hancock REW (2008) Agar and broth dilution methods to determine the minimal inhibitory concentration (MIC) of antimicrobial substances. Nature Protocols, 3: 163-175.

Wiley PR, Tosi P, Evrard A, Lovegrove A, Jones HD, Shewry PR (2007) Promoter analysis and immunolocalisation show that puroindoline genes are exclusively expressed in starchy endosperm cells of wheat grain. Plant Molecular Biology, 64: 125-136.

Wilken LR, Nikolov ZL (2012) Recovery and purification of plant-made recombinant proteins. Biotechnology Advances, 30: 419-433.

Wilkinson M, Wan Y, Tosi P, Leverington M, Snape J, Mitchell RaC, Shewry PR (2008) Identification and genetic mapping of variant forms of puroindoline b expressed in developing wheat grain. Journal of Cereal Science, 48: 722-728.

Wimley WC (2010) Describing the mechanism of antimicrobial peptide action with the interfacial activity model. ACS Chemical Biology, 5: 905-917.

Witzel K, Shahzad M, Matros A, Mock HP, Mühling KH (2011) Comparative evaluation of extraction methods for apoplastic proteins from maize leaves. Plant Methods, 7: 48-58.

Wrigley C, Corke H, C.E. W (2004) Encyclopedia of grain science, Elsevier Academic Press, Massachusetts, USA. ISBN: 978-0-12-765490-4.

Wrigley CW (2009) Wheat: A unique grain for the world. In: Khan K and Shewry PR (eds.) Wheat Chemistry and Technology. 4th ed. AACC International, Inc, St. Paul, Minnesota, USA. pp 1-17.

Wroblewski T, Tomczak A, Michelmore R (2005) Optimization of *Agrobacterium*-mediated transient assays of gene expression in lettuce, tomato and *Arabidopsis*. Plant Biotechnology Journal, 3: 259-273.

Xia L, Chen F, He Z, Chen X, Morris CF (2005) Occurrence of puroindoline alleles in Chinese winter wheats. Cereal Chemistry, 82: 38-43.

Xia L, Geng H, Chen X, He Z, Lillemo M, Morris CF (2008) Silencing of puroindoline a alters the kernel texture in transgenic bread wheat. Journal of Cereal Science, 47: 331-338.

Yang F, Moss LG, Phillips Jr GN (1996) The molecular structure of green fluorescent protein. Nature Biotechnology, 14: 1246-1251.

Yang SJ, Carter SA, Cole AB, Cheng NH, Nelson RS (2004) A natural variant of a host RNA-dependent RNA polymerase is associated with increased susceptibility to viruses by *Nicotiana benthamiana*. Proceedings of the National Academy of Sciences of the United States of America, 101: 6297-6302.

Yevtushenko DP, Misra S (2007) Comparison of pathogen-induced expression and efficacy of two amphibian antimicrobial peptides, MsrA2 and temporin A, for engineering wide-spectrum disease resistance in tobacco. Plant Biotechnology Journal, 5: 720-734.

Zhang J, Martin JM, Balint-Kurti P, Huang L, Giroux MJ (2011) The wheat puroindoline genes confer fungal resistance in transgenic corn. Journal of Phytopathology, 159: 188-190.

Zhang J, Martin JM, Beecher B, Lu C, Hannah LC, Wall ML, Altosaar I, Giroux MJ (2010a) The ectopic expression of the wheat Puroindoline genes increase germ size and seed oil content in transgenic corn. Plant Molecular Biology, 74: 353-365.

Zhang J, Martin JM, Beecher B, Morris CF, Curtis Hannah L, Giroux MJ (2009) Seed-specific expression of the wheat puroindoline genes improves maize wet milling yields. Plant Biotechnology Journal, 7: 733-743.

Zhang R, Cao Y, Wang X, Feng Y, Chen P (2010b) Development and characterization of a *Triticum aestivum*-H. villosa T5VS-5DL translocation line with soft grain texture. Journal of Cereal Science, 51: 220-225.

Zhang Y (2008) I-TASSER server for protein 3D structure prediction. BMC Bioinformatics, 9: 40-47.

Ziemann M, Ramalingam A, Bhave M (2008) Evidence of physical interactions of puroindoline proteins using the yeast two-hybrid system. Plant Science, 175: 307-311.

Appendices

Appendix I

Table I.1 Primer used for deletion of HD in PINA and PINB; TRD in PINA

Primer*	Sequence (5' to 3')	Application
PINAΔTRD-F	5'-*atgaaggat*GGTTGTCAAGAGCTCCTTGG-3'	Deletion of TRD in PINA (position 34-46)
PINAΔTRD-R	5'-*ttgacaacc*ATCCTTCATCGTTGAGCATC-3'	
PINAΔHD-F	5'-*caggggtca*CAGCGTGATCGGGCAAGCAA-3'	Deletion of hydrophobic domain (HD) in PINA (position 75-85)
PINAΔHD-R	5'-*atcacgctg*TGACCCCTGGATGATGTTGC-3'	
PINBΔHD-F	5'-*atccggcga*TTGGGCATTTGGCGAGGTGA-3'	Deletion of hydrophobic domain (HD) in PINB (position 75-83)
PINBΔHD-R	5'-*aatgcccaa*TCGCCGGATAGAATCACAGC-3'	

* F: Forward primer; R: Reverse primer

Appendix II

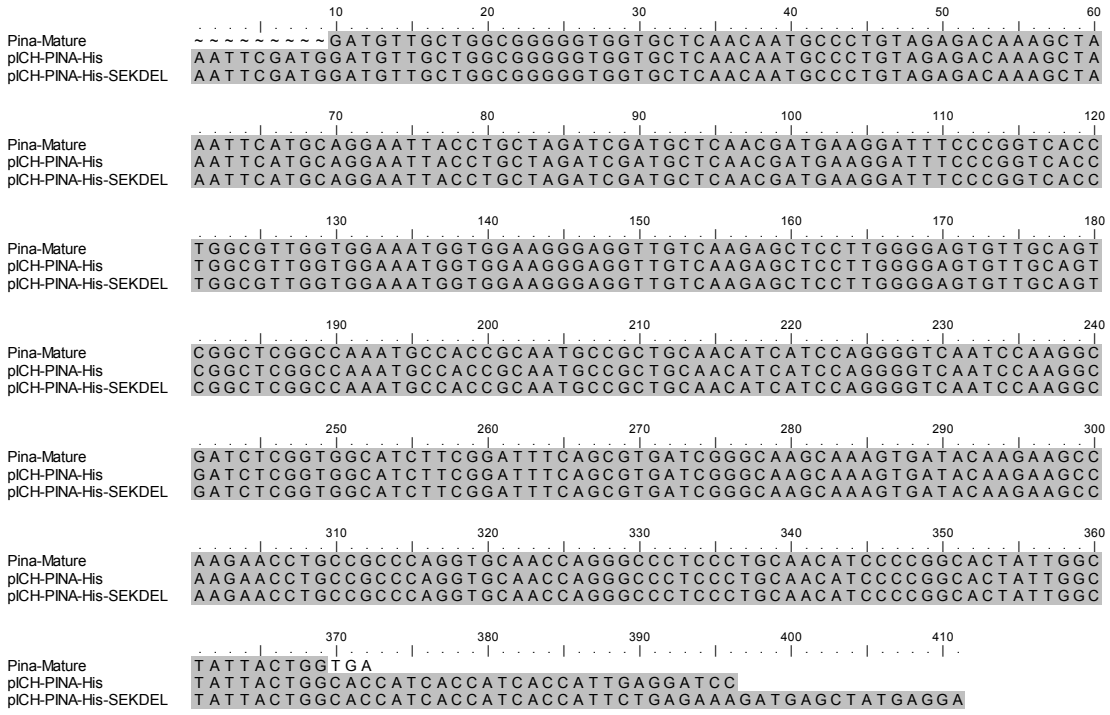

Figure II.1 pICH-PINA expressions constructs.
DNA sequence of mature putative *Pina-D1a* (DQ363911, line1) aligned with the sequence of pICH-PINA-His clone (line 2) and with the sequence of pICH-PINA-His-SEKDEL clone (line 3). His-tag and SEKDEL site underlined.

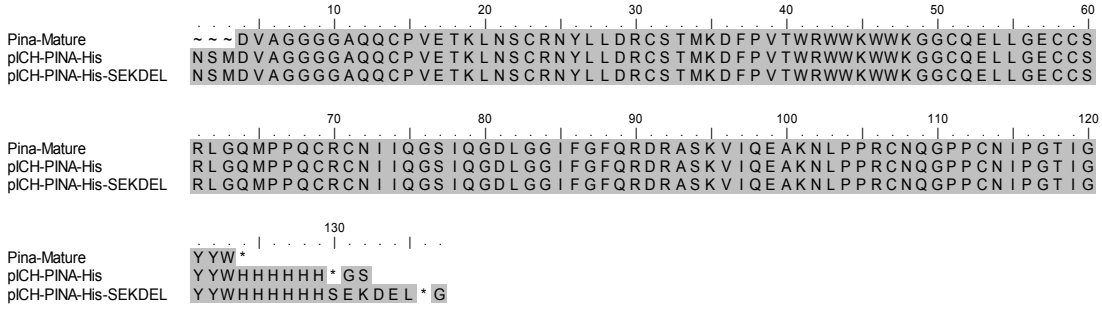

Figure II.2 pICH-PINA expressions construct.
Amino acid sequence of mature putative PINA (line1) aligned with the sequence of pICH-PINA-His clone (line 2) with sequence of pICH-PINA-His-SEKDEL clone (line 3).

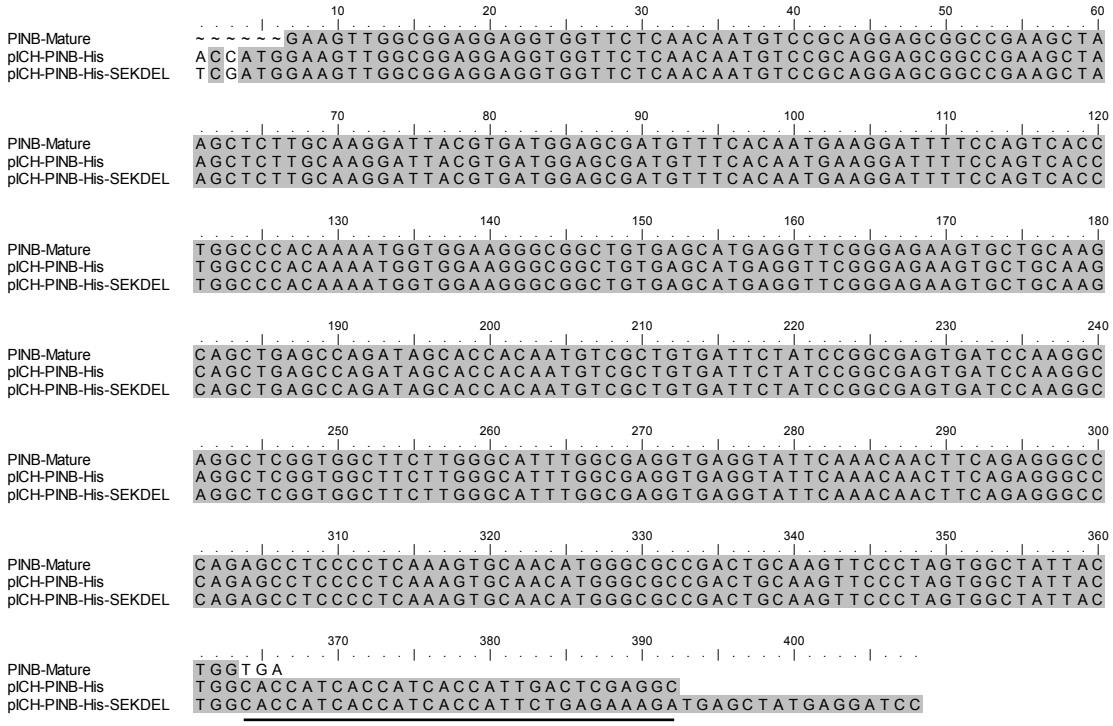

Figure II.3 pICH-PINB expressions construct.
DNA sequence of mature putative PINB aligned with the sequence of pICH-PINB-His clone (line 2) and with sequence of pICH-PINB-His-SEKDEL clone (line 3). His-tag and SEKDEL site underlined.

Figure II.4 pICH-PINB-His expressions construct.
Amino acid sequence of mature putative PINB (line1) aligned with the sequence of pICH-PINB-His clone (line 2) with sequence of pICH-PINB-His-SEKDEL clone (line 3).

Appendix III

Protein identification using MALDI-TOF

To obtain an accurate mass for recombinant PINs, and further investigate multimer formation, MALDI-TOF analysis was done. The result was inconclusive as data provide unknown peptides sequence.

The protocol for MALDI-TOF was based on Shevchenko et al. (2007) with minor modification and was applied to SDS-PAGE bands of interest at various stages of purification. Coommassie stained gels were used for protein identification. Protein bands of PINs resolved on SDS-PAGE were excised from the gel using a sterile scalpel and transferred into microcentrifuge tubes. The gel plugs were first added in 500 µL of neat acetonitrile by incubating at 37°C for 10 minutes until the gel pieces shrank. The gel plug solution was removed after centrifugation at 10,000×g, then 100 µL DTT was added to cover the gel pieces and incubated for 30 minutes at 56°C. The tubes were allowed to cool down to room temperature for 10 minutes and solution was removed. 50 µL of iodoacetamide solution added to tubes and incubated for 20 minutes at RT in dark. Then 500 µL of acetonitrile were added and incubated for 10 minutes. Then 100 µL of solution (50% v/v acetonitrile and 50% v/v 100 mM ammonium bicarbonate) was added and tubes incubated at RT with occasional vortex for 2 hours. 50 µL of the trypsin solution (Biolabs, Australia) was added to each sample then added 20 µL ammonium bicarbonate buffer (100mM) and incubate at 37°C for overnight. The next day tubes were incubated at room temperature and the gel pieces spun down. Then 100 µL extraction buffer (5% formic acid: acetonitrile 1:1 (v/v)) was added to each tube and incubated for 15 minutes at 37°C on a shaker. The supernatant was collected into new tube and dried down in vacuum centrifuge for 2 hours at 50°C. Samples were resuspended in trifluoroacetic acid and then with equal volume of saturated α-Cyano-4-hydroxycinnamic acid (CHCA) matrix was spotted onto target plate of Axima MALDI-TOF mass spectrometer (Shimadzu-Biotech, Japan). Samples were analysed using the Shimadzu MALDI-MS software. A total of four sample spots (1 µL each) were analysed for each aliquot taken.

Appendix IV

A

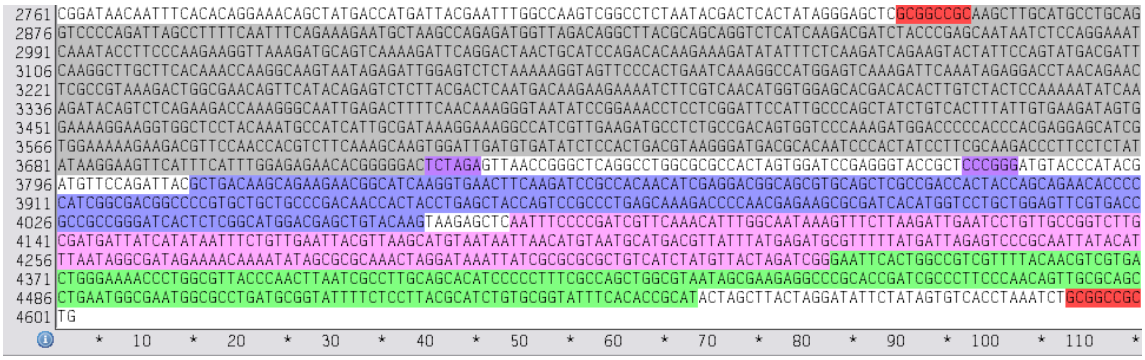

B

Figure III.1 Partial sequence of pNBV constructs.
A: pNBV-gene-YC; B: pNBV-gene-YN
35S promoter highlighted in gray. The two NotI (GCGGCCGC) site highlighted in red; XbaI site [TCTAGA] and XmaI [CCCGGG] highlighted; DNA sequence of YC and YN highlighted in blue. Sequence of NosT and LacZ highlighted.

A

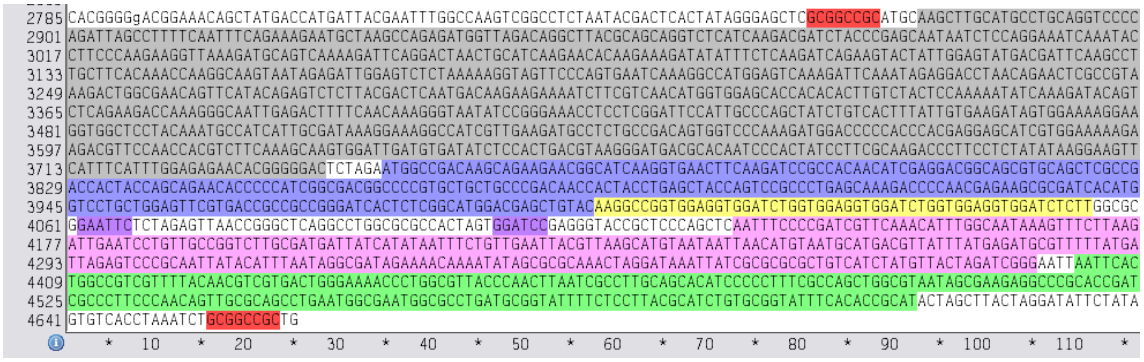

B

Figure III.2 Partial Sequence of pNBV constructs.
A: pNBV-YC-gene; B: pNBV-YN-gene
35S promoter highlighted in gary. The two NotI (GCGGCCGC) site highlighted in red; EcoRI site [GAATTC] and BamHI [GGATCC] highlighted; DNA sequence of YC and YN highlighted in blue. Sequence of NosT and LacZ highlighted.

Appendix V

Record of Proposed Notifiable Low Risk Dealing(s) (NLRDs):

(Regulation 13A (1) (a) - Gene Technology Regulations 2001 (as amended))

INSTRUCTIONS: Under r.13A(1)(c) of the Gene Technology Regulations 2001 (as amended), the Institutional Biosafety Committee (IBC) must provide a copy of this record to (i) the person or accredited organisation that requested the IBC to assess the proposed dealing; and (ii) the project supervisor for the proposed dealing. Under r.13A (2)(a)(i) an accredited organisation that proposed the dealing must include a copy of the IBC's record with the Accredited Organisation Annual Report to the Gene Technology Regulator. Under r.13A (2)(a)(ii) non-accredited organisations must provide a copy of this record to the Regulator at the end of the financial year.

NOTE: This form also captures information required by the Gene Technology Regulator to meet the requirements of r. 39 for NLRDs in maintaining a record of GMO and GM product dealings.

IBC NLRD Identifier (number)	PC2-N26/10
Date of IBC Assessment	18 November 2010
Name of IBC	Monash University IBC #309
Name of Organisation Conducting Dealing	Monash University
Project Title	Production, characterisation and evaluation of recombinant puroindolines in plants
PC1 NLRD TYPE (*a*) – (*c*)*	
PC2 NLRD TYPE (*a*) – (*i*)*	(b) (ba) (c) (d)
Name(s) of Project Supervisor(s)	Dr Diane Webster, Prof Mrinal Bhave
Has the IBC assessed the proposed dealing to be an NLRD?	Yes

* References to NLRD types are the paragraph numbers relating to the kinds of dealing detailed in Parts 1 and 2 in Schedule 3 of the Gene Technology Regulations 2001 (as amended). These Regulations are available on the OGTR website <www.ogtr.gov.au>.

Publications arising from this work

Poster presentations:

- Azadeh Niknejad, Diane Webster, Mrinal Bhave. (10^{th}-14^{th} February 2013); Recombinant plant-made puroindolines exhibit anti-microbial activity and interaction in plant system. 38th Lorne conference on protein structure and function, Lorne, Victoria, Australia.

- Azadeh Niknejad, Diane Webster, Mrinal Bhave. (11^{th} July 2013); Investigating PIN proteins interactions in a plant system using Bimolecular Fluorescence Complementation (BiFC). 12^{th} Melbourne protein group student symposium, La Trobe University, Melbourne, Victoria, Australia.

Manuscripts:

- Azadeh Niknejad, Diane Webster, Mrinal Bhave. Transient expression and characterization of puroindoline proteins in *Nicotiana benthamiana* using a virus-based expression system. (in preparation)

- Azadeh Niknejad, Diane Webster, Mrinal Bhave. Evidence of physical interactions of puroindoline proteins in living plant cells using bimolecular fluorescence complementation (BiFC) analysis. (in preparation)